

Title	Structural relaxations and crystallization in amorphous food model formulations
Authors	Fanghui, Fan
Publication date	2017
Original Citation	Fanghui, F. 2017. Structural relaxations and crystallization in amorphous food model formulations. PhD Thesis, University College Cork.
Type of publication	Doctoral thesis
Rights	© 2017, Fanghui Fan. - <a href="http://creativecommons.org/licenses/by-nc-nd/3.0/">http://creativecommons.org/licenses/by-nc-nd/3.0/</a>
Download date	2024-04-20 11:12:16
Item downloaded from	<a href="https://hdl.handle.net/10468/4425">https://hdl.handle.net/10468/4425</a>

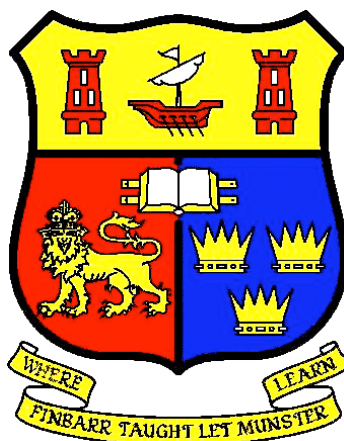
*Ollscoil na hÉireann*

**THE NATIONAL UNIVERSITY OF IRELAND**

*Coláiste na hOllscoile, Corcaigh*

**UNIVERSITY COLLEGE, CORK**

**SCHOOL OF FOOD AND NUTRITIONAL SCIENCES**



**STRUCTURAL RELAXATIONS AND CRYSTALLIZATION IN  
AMORPHOUS FOOD MODEL FORMULATIONS**

Thesis presented by

**FANGHUI FAN**

*M.Sc. Food Engineering (Jinan University)*

*B.Sc. Food Science and Engineering (Gansu Agricultural University)*

For the degree of

**DOCTOR OF PHILOSOPHY**

**(Food Science and Technology)**

Under the Supervision of

**Professor Yrjö H. Roos**

*June 2017*

# *DEDICATION*

---

*To My Parents and All of My Family Members  
with Love, Respect, and Gratitude*

# *ACKNOWLEDGEMENT*

---

I wish to give my deepest gratitude to my supervisor Prof. Yrjö H. Roos, who introduces me to the world of food material science. It is a great honour for being his student and study in his laboratory. It was only due to his valuable guidance, cheerful enthusiasm, and ever-friendly nature that I was able to complete my research work in a respectable manner. Also, I would like to give special thanks to Prof. Shuze Tang for recommending me to study in UCC. I appreciate for his invaluable advices, comments, and suggestions.

I wish to express gratitude and appreciation to Dr. Ourania Gouseti for being the external examiner and Dr. John Fitzpatrick for acting as internal examiner of my thesis examination. It was a great honour and pleasure for me to have such a wonderful and enjoyable time during the scientific discussion in my viva.

I would like to thank Chinese Scholarship Council for grant me a scholarship (Chinese Scholarship Council/Irish Universities Association Joint Scholarship, No. 201306780016) for the last four years. I am very honour to be chosen as a scholarship awardee and, I hope, I could do something contribution in future to my beloved country - China. Also, I would like to thank Mr. Xiaochuang Wu, who is the Second Secretary in Chinese Embassy (Dublin), for his kindly support during my stay in Ireland.

Many thanks to the technicians and staffs, in particular Mr. Dave Waldron, Mr. Eddie Beatty, Mr. Donal Humphreys, Mr. Jim McNamara, Ms. Avril McCord, and Ms. Anne Cahalane in the School of Food and Nutritional Sciences and Dr. Graham Eugene O'Mahony in the School of Pharmacy as well as Dr. Humphrey Moynihan and Dr. Danielle Elizabeth Horgan in Department of Chemistry, for their kind help with the accesses to instruments and the guidance in operations.

I appreciate all of my friends who make my PhD journey easier and unforgettable. Many thanks to my lab mates and friends, Dr. Naritchaya Potes, Dr. Bambang Nurhadi, Dr. Aaron Lim, Mr. Valentyn Maidannyk, Ms. Sarah Al-Jassar, Ms. Qiao Ma, Mr. Pieter Dekker, Ms. Sandy Abidh, Mr. César Palomino, Dr.



Mingquan Huang, and Dr. Xiuting Li, for their helping and making me happy during doing my PhD study. Also, I would like to thank Dr. Jian Huang, Mrs. Libin Zhang, Prof. Finbarr O’Sullivan, and Mrs. Janet O’Sullivan, for bring me happiness and making me feel part of family in Ireland. Please allow me to give my gratitude to all other friends that I could not mention one by one. I wish you all the best.

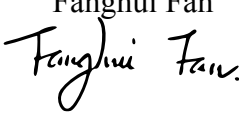
I would like to thank my girlfriend Tian Mou. We met each other almost the same time as I started my PhD journey in UCC. She has witnessed and also been involved in my mental and psychological growth during the last four years. Her patient and supportive help me overcome every difficult period when I lost my motivation and confidence in a four-year journey.

Finally, millions thanks to my parents and all my family members, especially my grandfather in heaven, for their unconditional love, absolute understanding, and selfless supporting that come across ten thousand miles to me. They made my life beautiful and full of possible. I feel happy and grateful of having their company.

Thank you very much to all the people who have walked with me and wish you all the best!

*“If a man withdraws his mind from the love of beauty, and applies it as sincerely to the love of the virtuous; if, in serving his parents, he can exert his utmost strength; if, in serving his country, he can devote his life; if, in his intercourse with his friends, his words are sincere: - although men say that he has not learned, I will certainly say that he has.” ---- <Confucian Analects, Hsio R >, Translated by James Legge*

子夏曰：“賢賢易色；事父母，能竭其力；事君，能致其身；與朋友交，言而有信。雖曰未學，吾必謂之學矣。” ——《論語，學而》

Fanghui Fan  


July 2, 2017 in Western Gateway Building

# ABSTRACT

---

Formulation and design of amorphous food solids structures for improved dehydration properties, stabilization of active components, and controlled structure deterioration require materials science characterization of components and mixtures. However, understanding phase transitions associated with structural relaxations and their coupling with properties of food materials is still a challenging and developing area of food materials science. Our laboratory has developed a new approach for the use of  $\alpha$ -relaxation times ( $\tau$ ) and introduced a “*Strength, S*” concept, which is the temperature difference between the material temperature and its calorimetric onset glass transition temperature ( $T_g$ ) that gives rise to a  $10^4$  reduction in  $\tau$  (or viscosity), for characterization of noncrystalline food materials, their properties and performance in typical processing and storage conditions where a component or miscible components within food structure may undergo phase and state transitions. Besides the *S* concept of amorphous food solids, the *Deborah* number (*De*) was applied to provide a useful translation of measured  $\tau$  to real experimental timescales.

Our systems were composed of crystalline and amorphous lactose, trehalose, and whey protein isolates (WPI) at various water activities ( $0 \leq a_w \leq 0.76$ ) at 25 °C to 45 °C. Differential scanning calorimetry (DSC), dynamic-mechanical (DMA) and dielectric (DEA) analysis, static sorption measurement (SSM) and dynamic dewpoint isotherm (DDI) analysis, and powder X-ray diffractometry (XRD) were used in material characterization and determination of glass transition temperatures ( $T_g$ ),  $\alpha$ -relaxation temperatures ( $T_\alpha$ ) and corresponding  $\tau$  ( $a_w \leq 0.44$ ), water sorption ( $0.11 \leq a_w \leq 0.76$ ), time-dependent crystallization ( $0.65 \leq a_w \leq 0.76$ ) and crystalline forms of components. The static water sorption data and calorimetric  $T_g$  were modeled by using Guggenheim-Anderson-de Boer (GAB) and Gordon-Taylor (GT) relationships, respectively. Moreover, the William-Landel-Ferry (WLF) relationship was used to model the  $\tau$  and  $T_\alpha - T_g$  relationships of amorphous solids systems, where

material-specific constants  $C_1$  and  $C_2$  were used to obtain  $S$  values.

Both SSM and DDI measurements were part of fractional water sorption analysis of sugars/WPI mixtures at  $a_w \leq 0.44$  which allowed quantification of water in specific components within solids mixtures from 25 °C to 45 °C. Such quantification of water in component fractions was required for the use of  $T_g$  data in solids characterization. DDI data also showed that the critical  $a_w$  for water sorption-related crystallization of lactose ( $a_w^{(cr)}$ ) was strongly affected by protein content at 25 °C. Crystallization of amorphous sugars in sugar/WPI mixtures was delayed by protein due to reduced nucleation and retarded diffusion during crystal-growth. XRD patterns showed that the crystalline forms of lactose and trehalose could be affected by the presence of water and WPI. The crystallization and crystalline forms of amorphous lactose were affected by trehalose and WPI based on XRD analysis. XRD showed no anhydrous  $\beta$ -lactose and mixed  $\alpha$ -/ $\beta$ -lactose with molar ratios of 4:1 crystals in crystallized lactose/WPI systems (7:3 and 1:1 solids ratios). The enthalpy relaxation ( $H$ -relaxation) of amorphous lactose was affected by the presence of lactose crystals and WPI at 0.33  $a_w$  (25 °C) due to water migration. The  $T_\alpha$  at loss modulus ( $E''$ ) and dielectric loss ( $\epsilon''$ ) peak at each frequency for sugars was affected by the presence of crystals and protein.  $T_\alpha$  shifted to higher temperatures with increasing frequency but it decreased steeply as water content increased. The WLF-derived  $S$  values of sugars decreased with  $a_w$  increasing up to 0.44  $a_w$  but the presence of WPI and  $\alpha$ -type of lactose crystals increased  $S$ . An instant crystallization of amorphous lactose in heating was more rapid in systems with a smaller  $S$ , which also had more extensive water plasticization and lower instant crystallization temperature. We also found that the  $S$  values could be estimated from water contents of glass forming sugar systems.  $S$  gives a quantitative tool to estimate compositional effects on  $\tau$  and for the control of time-dependent solids transformations, such as crystallization.

Amorphous food solids, such as sugars and proteins, are common ingredients in the food and pharmaceutical industries. Thus, understanding the physicochemical

properties of glass forming food solids has a great importance in the development of processing and shelf life control procedures for such ingredients and relevant products. Relaxation times refer to the time factor corresponding to material response to a change in internal or external thermodynamic conditions such as temperature and  $a_w$ , which can provide a new approach for the description of process-structure-function relationships to foods and food constituents. While the “*Fragility*” concept developed by Angell may predict some properties of single glass-forming food components, our WLF-type  $S$  concept, which was set to show a decrease of  $\tau$  from  $10^2$  to  $10^{-2}$  s above glass transition, was superior for the description of relaxation times and solids characterization, and therefore, stability and industrial applicability of relevant foods and pharmaceutical materials. For example, the  $S$  parameter as a new food property can be used to formulate materials in order to improve material performance during drying and powder handling. Also, it can be used to control and predict the physicochemical properties and performance of food solids during storage.

# *TABLE OF CONTENTS*

---

	PAGE
<b>DEDICATION.....</b>	<b><i>ii</i></b>
<b>ACKNOWLEDGEMENTS.....</b>	<b><i>iii</i></b>
<b>ABSTRACT .....</b>	<b><i>v</i></b>
<b>LIST OF FIGURES .....</b>	<b><i>xv</i></b>
<b>LIST OF TABLES .....</b>	<b><i>xvii</i></b>
<b>LIST OF QUATIONS.....</b>	<b><i>xviii</i></b>
<b>ABBREVIATIONS.....</b>	<b><i>xix</i></b>
<b>INTRODUCTION.....</b>	<b><i>1</i></b>

## **CHAPTER I**

### **LITERATURE REVIEW**

<b>1.1. GLASS TRANSITION OF AMORPHOUS FOOD SOLIDS .....</b>	<b><i>7</i></b>
1.1.1. CHARACTERIZATION METHODOLOGIES FOR GLASS TRANSITION .	<i>9</i>
1.1.2. PLASTICIZATION AND FRACTIONAL WATER SORPTION.....	<i>11</i>
1.1.3. GLASS TRANSITION TEMPERATURE IN SOLIDS SYSTEM.....	<i>15</i>
<b>1.2. CRYSTALLIZATION ON AMORPHOUS FOOD SOLIDS .....</b>	<b><i>18</i></b>
1.2.1. CHARACTERIZATION METHODOLOGIES FOR CRYSTALLIZATION	<i>19</i>
1.2.2. PROCESSES OF CRYSTALLIZATION.....	<i>19</i>
1.2.3. LACTOSE – A SUGAR OF INTEREST.....	<i>23</i>
1.2.4. CRYSTALLIZATION OF OTHER FOOD COMPONENTS .....	<i>27</i>

# *TABLE OF CONTENTS*

---

<b>1.3. MECHANICAL/DIELECTRIC PROPERTIES AND STRUCTURAL RELAXATIONS OF FOOD SOLIDS.....</b>	<b>31</b>
1.3.1. MECHANICAL/DIELECTRIC PROPERTIES.....	31
1.3.2. SUB- $T_g$ RELAXATIONS AND ENTHALPY RELAXATION.....	32
1.3.3. ALPHA-RELAXATION AND CORRESPONDING RELAXATION TIMES	36
<b>1.4. MATERIAL CHARACTERISTICS AND FOOD SOLIDS STABILITY ....</b>	<b>40</b>
1.4.1. RELAXATION TIMES AND FOOD SOLIDS STABILIZATION.....	40
1.4.2. FLOW CHARACTERISTICS .....	42
1.4.3. STRENGTH AND FOOD STABILITY.....	48
<b>1.5. CONCLUSIONS.....</b>	<b>48</b>

## **CHAPTER II**

### **X-RAY DIFFRACTION ANALYSIS OF LACTOSE CRYSTALLIZATION IN FREEZE-DRIED LACTOSE/WHEY PROTEIN SYSTEMS**

<b>2.1. INTRODUCTION .....</b>	<b>51</b>
<b>2.2. MATERIALS AND METHODS .....</b>	<b>53</b>
2.2.1. SAMPLE PREPARATION.....	53
2.2.2. WATER SORPTION AND LACTOSE CRYSTALLIZATION .....	54
2.2.3. XRD ANALYSIS .....	55
2.2.4. GLASS TRANSITION TEMPERATURE .....	56
2.2.5. STATISTICAL ANALYSIS .....	56

# *TABLE OF CONTENTS*

---

<b>2.3. RESULTS AND DISCUSSION.....</b>	<b>56</b>
2.3.1. WATER SORPTION .....	56
2.3.2. TIME-DEPENDENT CRYSTALLIZATION AND CRYSTALLIZATION KINETICS .....	59
2.3.3. GLASS TRANSITION AND WATER LOSS.....	62
2.3.4. XRD ANALYSIS .....	68
<b>2.4. CONCLUSIONS.....</b>	<b>73</b>

## **CHAPTER III**

### **STRUCTURAL RELAXATIONS OF AMORPHOUS LACTOSE AND LACTOSE/WHEY PROTEIN MIXTURES**

<b>3.1. INTRODUCTION.....</b>	<b>76</b>
<b>3.2. MATERIALS AND METHODS .....</b>	<b>79</b>
3.2.1. SAMPLE PREPARATION .....	79
3.2.2. THERMAL ANALYSIS .....	80
3.2.3. DYNAMIC-MECHANICAL ANALYSIS .....	81
3.2.4. WLF-MODEL ANALYSIS .....	82
3.2.5. STATISTICAL ANALYSIS .....	83
<b>3.3. RESULTS AND DISCUSSION .....</b>	<b>84</b>
3.3.1. GLASS TRANSITION AND ENTHALPY RELAXATION .....	84
3.3.2. DYNAMIC-MECHANICAL ANALYSIS .....	88
3.3.3. WLF-MODEL ANALYSIS OF ALPHA-RELAXATION TIMES .....	91
3.3.4. STRENGTH PARAMETER AND CRYSTALLIZATION .....	95
<b>3.4. CONCLUSIONS.....</b>	<b>97</b>

# *TABLE OF CONTENTS*

---

## *CHAPTER IV*

### **STRUCTURAL STRENGTH AND CRYSTALLIZATION OF AMORPHOUS LACTOSE IN FOOD MODEL SOLIDS AT VARIOUS WATER ACTIVITIES**

<b>4.1. INTRODUCTION .....</b>	<b>99</b>
<b>4.2. MATERIALS AND METHODS .....</b>	<b>102</b>
4.2.1. SAMPLE PREPARATION .....	102
4.2.1. WATER SORPTION AND TIME-DEPENDENT CRYSTALLIZATION....	103
4.2.3. THERMAL ANALYSIS .....	104
4.2.4. DYNAMIC-MECHANICAL ANALYSIS .....	104
4.2.5. WLF-MODEL ANALYSIS FOR RELAXATION TIMES.....	105
4.2.6. STATISTICAL ANALYSIS.....	105
<b>4.3. RESULTS AND DISCUSSION.....</b>	<b>106</b>
4.3.1. WATER SORPTION .....	106
4.3.2. THERMAL ANALYSIS .....	106
4.3.3. DYNAMIC-MECHANICAL ANALYSIS .....	112
4.3.4. STRENGTH, WATER CONTENTS, AND CRYSTALLIZATION TEMPERATURE .....	113
<b>4.4. CONCLUSIONS.....</b>	<b>117</b>

## *CHAPTER V*

### **CRYSTALLIZATION AND STRUCTURAL RELAXATION TIMES IN STRUCTURAL STRENGTH ANALYSIS OF AMORPHOUS SUGAR/WHEY PROTEIN STYSTEMS**



# *TABLE OF CONTENTS*

---

<b>5.1. INTRODUCTION .....</b>	<b>119</b>
<b>5.2. MATERIALS AND METHODS .....</b>	<b>122</b>
5.2.1. SAMPLE PREPARATION .....	122
5.2.2. WATER SORPTION AND TIME-DEPENDENT CRYSTALLIZATION....	123
5.2.3. XRD ANALYSIS .....	124
5.2.4. THERMAL ANALYSIS .....	124
5.2.5. DYNAMIC-MECHANICAL ANALYSIS .....	125
5.2.6. WLF-MODEL ANALYSIS .....	126
5.2.7. STATISITICAL ANALYSIS .....	126
<b>5.3. RESULTS AND DISSCUSSION .....</b>	<b>127</b>
5.3.1. WATER SORPTION .....	127
5.3.2. TIME-DEPENDENT CRYSTALLIZATION AND CRYSTALLIZATION KINENTIC .....	129
5.3.3. TYPES OF CRYSTALS FORMS.....	133
5.3.4. THERMAL ANALYSIS .....	137
5.3.5. ALAPHA-RELAXATION AND WLF-MODEL ANALYSIS OF $\tau$ .....	141
5.3.6. WATER CONTENT, S, AND CRYSTALLIZATION .....	145
<b>5.4. CONCLUSIONS.....</b>	<b>147</b>

## **CHAPTER VI**

### **WATER SORPTION-INDUCED CRYSTALLIZATION, STRUCTURAL RELAXATIONS AND STRENGTH ANALYSIS OF RELAXATION TIMES IN AMROHOUS LACTOSE/WHEY PROTEIN SYSTEMS**

<b>6.1. INTRODUCTION .....</b>	<b>149</b>
--------------------------------	------------

# *TABLE OF CONTENTS*

---

<b>6.2. MATERIALS AND METHODS .....</b>	<b>152</b>
6.2.1. SAMPPLE PREPARATION.....	152
6.2.2. WATER SORPTION EXPERIMENT .....	153
6.2.3. DIELECTRIC ANALYSIS .....	155
6.2.4. STRENGTH ANALYSIS.....	156
6.2.5. STATISTICAL ANALYSIS.....	156
<b>6.3. RESULTS AND DISSCUSSION .....</b>	<b>156</b>
6.3.1. DYNAMIC WATER SORPTION .....	156
6.3.2. DIELECTRIC PROPERTIES AND $T\alpha$ .....	161
6.3.3. RELAXATION TIMES AND S PARAMETER .....	163
6.3.4. SORPTION-INDUCED CRYSTALLIZATION, RELAXATION TIMES AND S PARAMETER.....	166
<b>6.4. CONCLUSIONS.....</b>	<b>167</b>

## **CHAPTER VII**

### **GENERAL DISCUSSION**

<b>7.1. WATER SORPTION AND TIME-DEPENDENT PHENOMENONA OF FOOD SOLIDS SYSTEMS .....</b>	<b>170</b>
7.1.1. WATER SORPTION ISOTHERMS AND FRACTIONAL SORPTION BEHAVIOUR .....	170
7.1.2. TIME-DEPENDENT CRYSTALLIZATION OF FOOD SOLIDS SYSTEMS .....	172
7.1.3. CRYSTALLIZATION-RELATED STRUCTURAL COLLAPSE IN AMORPHOUS LACTOSE CONTAINING SYSTEMS .....	179

# *TABLE OF CONTENTS*

---

<b>7.2. GLASS TRANSITION-RELATED STRUCTURAL RELAXATIONS OF FOOD SOLIDS SYSTEM .....</b>	<b>181</b>
7.2.1. EFFECTS OF WATER ON GLASS TRANSITION.....	181
7.2.2. ENTHALPY RELAXATION ON LACTOSE CONTAINING SYSTEMS ....	183
7.2.3 ALPHA-RELAXATION AND STRUCTURAL RELAXATION TIMES .....	184
<b>7.3. STRUCTURAL RELAXATION CHARACTERISTICS OF FOOD SOLIDS SYSTEMS .....</b>	<b>187</b>
7.3.1. WLF CONSTANTS .....	187
7.3.2. WLF AND STRENGTH.....	188
7.3.3 STRENGTH AND CRYSTALLIZATION.....	190
<b>7.4 APPLICATIONS OF THE REASERCH OUTCOMES.....</b>	<b>192</b>
7.4.1. FORMULATION AND DESIGN OF HONEY TO POWDER.....	192
7.4.2. POTENTIAL APPLICATIONS IN FOOD INDUSTRY .....	193
<b>7.5. OVERALL CONCLUSIONS.....</b>	<b>195</b>
 <b><u>BIBLIOGRAPHY</u>.....</b>	<b>198</b>
 <b><u>APPENDIX</u></b>	
 <b>APPENDIX I .....</b>	<b>221</b>
<b>APPENDIX II .....</b>	<b>222</b>
<b>APPENDIX III .....</b>	<b>223</b>
<b>APPENDIX IV.....</b>	<b>224</b>

# *LIST OF FIGURES*

---

	PAGE
Fig. (1.1) .....	10
Fig. (1.2) .....	13
Fig. (1.3) .....	22
Fig. (1.4) .....	33
Fig. (1.5) .....	37
Fig. (1.6) .....	39
Fig. (1.7) .....	41
Fig. (1.8) .....	43
Fig. (1.9) .....	45
Fig. (1.10) .....	47
Fig. (2.1) .....	57
Fig. (2.2) .....	62
Fig. (2.3) .....	63
Fig. (2.4) .....	64
Fig. (2.5) .....	65
Fig. (2.6) .....	68
Fig. (2.7) .....	70
Fig. (2.8) .....	72
Fig. (3.1) .....	81
Fig. (3.2) .....	82
Fig. (3.3) .....	85
Fig. (3.4) .....	86
Fig. (3.5) .....	88
Fig. (3.6) .....	91
Fig. (3.7) .....	92

# *LIST OF FIGURES*

---

Fig. (3.8) .....	94
Fig. (4.1) .....	107
Fig. (4.2) .....	109
Fig. (4.3) .....	113
Fig. (4.4) .....	114
Fig. (4.5) .....	116
Fig. (5.1) .....	127
Fig. (5.2) .....	130
Fig. (5.3) .....	133
Fig. (5.4) .....	134
Fig. (5.5) .....	136
Fig. (5.6) .....	137
Fig. (5.7) .....	140
Fig. (5.8) .....	141
Fig. (5.9) .....	143
Fig. (5.10) .....	146
Fig. (6.1) .....	154
Fig. (6.2) .....	158
Fig. (6.3) .....	160
Fig. (6.4) .....	162
Fig. (6.5) .....	164
Fig. (6.6) .....	166
Fig. (7.1) .....	180
Fig. (7.2) .....	187
Fig. (7.3) .....	192
Fig. (7.3) .....	194

# *LIST OF TABLES*

---

	PAGE
Table (1.1) .....	9
Table (1.2) .....	17
Table (2.1) .....	61
Table (2.2) .....	67
Table (3.1) .....	84
Table (3.2) .....	89
Table (4.1) .....	110
Table (5.1) .....	132
Table (5.1) .....	138
Table (6.1) .....	157
Table (6.2) .....	165

# *LIST OF EQUATIONS*

---

	PAGE
Eq. (1.1) .....	14
Eq. (1.2) .....	14
Eq. (1.3) .....	16
Eq. (1.4) .....	16
Eq. (1.5) .....	18
Eq. (1.6) .....	18
Eq. (1.7) .....	38
Eq. (1.8) .....	38
Eq. (1.9) .....	39
Eq. (1.10) .....	39
Eq. (1.11) .....	40
Eq. (1.12) .....	47
Eq. (1.13) .....	47
Eq. (4.1) .....	116
Eq. (5.1) .....	145
Eq. (7.1) .....	172
Eq. (7.2) .....	191

# ABBREVIATIONS

---

$2\theta$ – Diffraction Angels in XRD Measurement	$f$ – Frequency
AP – End Point of Lactose	$F_{1/2}$ – Fragility
Crystallization Based on Water Loss	FP – Point After Storage At 240 h
$a_T$ – Ratio of $\tau$ and $\tau_s$	GAB – Guggenheim-Anderson-de Boer Equation
$a_w$ – Water Activity	GT – Gordon-Taylor Equation
$a_w^{(cr)}$ – Critical $a_w$ for Water	H-relaxation – Enthalpy Relaxation
Sorption-Induced Crystallization	HP – Middle-Point of Lactose Crystallization Based on Water Loss
$a_{wo}^{(cr)}$ – Onset $a_w^{(cr)}$	IR/FTIR – Infrared and Fourier Transforms Infrared
$a_{wp}^{(cr)}$ – Peak $a_w^{(cr)}$	LCR Meter – Inductance, Capacitance, and Resistance Meter
$C$ and $K$ – GAB Constants	LOESS – Local Polynomial Regression Fitting
$C_1$ and $C_2$ – WLF Constants	$m$ – Steepness Index
$C_p$ – Heat Capacity	$m_0$ – Monolayer Value
DDI – Dynamic Dewpoint Isotherms	MD – Maltodextrins
$De$ – Deborah Number	$M_n$ – Average Molecular Weight in Fox-Flory Equation
DE – Dextrose Equivalent, a measure of the amount of reducing sugars present in a sugar product, expressed as a percentage on a dry basis relative to dextrose	$n_1$ to $n_n$ – Multiplier of Each Component in System
DEA – Dielectric Analyzer	NMR – Nuclear Magnetic Resonance
DMA – Dynamic-Mechanical Analyzer	PVL – Polar Light Video Microscope
$d_s$ – $10^4$ Reduction in $\tau$	PVP – Poly vinyl Pyrrolidone
DSC – Differential Scanning Calorimetry	PVP-VA – PVP-co-vinyl-acetate
$Ea$ – Activation Energy	RH – Relative Humidity
ESR – Electron Spin Resonance	



$S$ – Structural Strength Parameter	WPI – Whey Protein Isolates
$SD$ – Standard Deviation	$W_t$ – Total Equilibrium Water Content in System
$S_{dl}$ – Strength of Anhydrous Solids Mixtures	XRD – X-Ray Diffractometry
$S_{d2}$ – Strength of Amorphous Water	$\Delta C_p$ – Changes in $C_p$
SEM – Scanning Electron Microscope	$\Delta C_{p1}$ – Normalized $\Delta C_p$ Derived From DSC First Scan
SSM – Static Sorption Measurement	$\Delta C_{p2}$ – Normalized $\Delta C_p$ Derived From DSC Second Scan
$T_{1/2}$ – Temperature at $\tau = 10^{-6}$ s	$\Delta C_{pn}$ – Normalized $\Delta C_p$ According to The Amorphous Lactose Fraction
$T_{cr}$ – Crystallization Temperature	$\Delta H$ – Recovery of Enthalpy
$T_{cr1}$ and $T_{cr2}$ – Onset and Peak of Calorimetric $T_{cr}$	$\Delta H''$ – Normalized $\Delta H$ According to The Amorphous Lactose Fraction
$T_g$ – Glass Transition Temperature	$\Delta H_{cr}$ – Latent Heat of Crystallization
$T_{g\infty}$ – High Molecular Weight Limiting Value of $T_g$	$E'$ – Storage Modulus
$T_{g1}$ – Onset $T_g$ Derived from First Scan from DSC	$\varepsilon''$ – Dielectric Loss
$T_{g2}$ – Onset $T_g$ Derived from Second Scan from DSC	$E''$ – Loss Modulus
$T_m$ – Melting Temperature	$\eta$ – Viscosity
$T_s$ – Reference Temperature in WLF and VTF Equation	$\eta_s - \eta$ at $T_s$
$T_\alpha$ – $\alpha$ -Relaxation Temperatures	$\theta_{cr}$ – Time for Completing Crystallization
$T_\theta$ – Storage Temperature at which the Crystallization Occurred	$\tau$ – Relaxation Time
$W_1$ to $W_n$ – Water Content in Each Non-crystallized Composition	$\tau_s$ – Relaxation Time at $T_s$
WLF – William-Landel-Ferry Relationship	
VTF – Vogel-Tammann-Fulcher Relationship	

# *INTRODUCTION*

---

Temperature, pressure, and water content are often variables during food processing and storage. These parameters govern rates of both desired and detrimental changes and have enormous effects on the physical state of foods (Slade et al., 1991; Sperling, 2005; Liu et al., 2006). The physicochemical properties of food components, e.g., sugars, polysaccharides, lipids, and proteins, are highly dependent on their physical state because of their importance to both quality and storage stability (Champion et al., 2000; Singh et al., 2007). The solid states of food components include both crystalline and amorphous states (Mullin, 2001; Sperling, 2005). The amorphous state of food solids is metastable and food components may undergo phase and state transitions in various processes and during storage (Le Meste et al., 2002). The reversible transformation of the solid to liquid-like behavior occurs over a temperature range rather than at a constant temperature, which is known as glass transition (Slade et al., 1991). Many properties of glassy food materials are changing dramatically around the glass transition range including modulus and viscosity, volume and thermal expansion, dielectric properties, solidification, and viscous flow (Slade et al., 1991). It should be noted that as the glass transition is approached translational mobility appears and the amorphous food solids exhibit frequency-dependent structural relaxations, time-dependent softening and solid-flow characteristics around glass transition (Champion et al., 2000; Le Meste et al., 2002; Liu et al., 2006). Processes such as baking, air- and freeze-drying, extrusion, flaking, and encapsulation may operate through the glass transition range as the food components may experience the glass transition (Balasubramanian et al., 2016). Recently, numerous authors have reported glass transition data for many food components, e.g., sugars (Wen and Elliott, 2014; Ruiz-Cabrera and Schmidt, 2015), polysaccharides (Potes et al., 2012; Descamps et al., 2013; Chuang et al., 2015; Nurhadi et al., 2016), and proteins (Porter and Vollrath, 2012; George et al., 2014). Moreover, Roos and Drusch (2015) pointed out that the calorimetric  $T_g$  is a useful material descriptor owing to its good correlation with the

structural and thermodynamic properties of individual food systems in various processing and storage conditions.

Sugars can exist in crystalline or amorphous states in food solids. It is important that the microstructure of a food material is maintained in a noncrystalline state; otherwise the flavor, color, taste and texture of the food may be altered during storage (Hartel and Shastry, 1991). In general, amorphous structures of sugars are fairly stable in the glassy state (Slade et al., 1991). Below the  $T_g$ , the mobility of sugar molecules is limited to vibrations and rotations, which kinetically limit crystallization and reduce rapid loss of product stability (Slade et al., 1991; Omar and Roos, 2007). However, as water affects molecular mobility shown by a lowered  $T_g$  due to plasticization, amorphous sugars may exhibit a tendency of crystallization causing physical and chemical deterioration in food ingredients and dairy powders at high storage humidities or temperatures (Hartel and Shastry, 1991; Slade et al., 1991; Aguilar et al., 1994; Miao and Roos, 2005; Ibach and Kind, 2007). Lactose ( $\beta$ -D-galactopyranosyl (1-4)-D-glucopyranose) is often used in the food and pharmaceutical industries and it exhibits a strong tendency to crystallize from its amorphous states, especially at a high storage  $RH$  (Herrington, 1934; Choi et al., 1951; Nickerson, 1979). XRD patterns have shown that amorphous lactose crystallizes into a number of crystalline forms, which differ in melting behavior, solubility, density, crystal morphology, and relative sweetness (Nickerson, 1979; Lai and Schmidt, 1990; Jouppila et al., 1998). Generally, the crystalline forms vary as their formation depends on the presence of other components, which may be related to interactions among sugars, supersaturation in systems, diffusion of molecules or the mutarotation of molecules during either nucleation or crystal-growth stages in crystallization (Jouppila and Roos, 1994ab; Fitzpatrick et al., 2007). The rate of crystallization depends on several factors, such as the rate of nucleation, the time required to remove water, storage temperature and molecular anomerization during crystallization (Aguilar et al., 1994; Drapier-Beche et al., 1997; Jouppila et al., 1998; Haque and Roos, 2005). Roos and Karel (1991a) showed that rates of lactose crystallization were controlled by  $T_g$  values and whey

protein could delay crystallization of lactose and stabilize lactose in skim milk powder at high  $RH$  storage conditions. However, such inhibition of lactose crystallization may not entirely result from the  $T_g$ -dependant state of lactose in binary systems (Mazzobre et al., 2001). The crystallization and glass transition properties of lactose in foods have been well documented and also several technologies are used in investigating the mechanism of protein inhibition of crystallization, i.e., scanning electron microscope (SEM) and protein characterization technology (Jin et al., 2000; Wang, 2005; Shawqi-Barham et al., 2006). Common hypotheses used in attempts to explain the mechanism of inhibition on lactose crystallization by proteins include the bond-hinder theory (Lopez-Diez and Bone, 2000), stereo-hindrance theory (Garti and Leser, 2001; Adhikari et al., 2009) and diffusion-limitation theory (Das et al., 2013). However, little attention has been paid to fractional water sorption, phase separation and water migration effects during food component crystallization.

It is often assumed that the glassy state consists of molecules, which are “frozen” in their positions and motions are limited to vibration and reorientation of small groups of atoms, and those motions do not involve the surrounding atoms and molecules and are mainly local. However, translational mobility within amorphous materials becomes apparent around glass transition (Slade et al., 1991; Roudaut et al., 2004). A dramatic change of molecular mobility results in dramatic variation of kinetics of various changes related to glass transition of amorphous materials, and therefore to structural relaxation phenomena (Debenedetti and Stillinger, 2001; Sperling, 2005; Liu et al., 2006). The structural relaxation phenomena, which reflect the tendency of the material to reach equilibrium, also occur in glassy state and can be characterized by  $\tau$ . Such  $\tau$  refer to the time factor corresponding to material response to a change in internal or external thermodynamic conditions, such as temperature or  $a_w$  (Slade et al. 1991; Champion et al. 2000). It should be noted that the  $\tau$ , which are often related to viscosity ( $\eta$ ), could imply to deformations resulting from variation in molecular motions and describe the viscous flow of the amorphous materials. The glassy state of food components may show an indefinite number of molecular assemblies and glass

structures with varying levels of molecular packing and order. Hence, various time-dependent phenomena and material properties related to glass transition of amorphous food material are kinetic relaxation processes and appear as several structural relaxations (Champion et al., 2000; Donth, 2013). Therefore, modeling of structural relaxations or their relevant  $\tau$  of amorphous food materials is particularly important as small rheological variations in solid properties may result in dramatic changes of materials performance in processing, storage, consumption (sensory properties) and digestion. Since relaxation times related to changes in molecular mobility can be observed from calorimetric, mechanical and dielectric relaxations, glass transition and structural relaxations of amorphous food materials are usually measured using such techniques (Kalichevsky et al., 1992; Syamaladevi et al., 2012; Donth, 2013; Paudel et al., 2015; Sasaki et al., 2016). It should be noted that the assessment of  $\tau$  also requires a careful definition of  $T_g$ , which is preferably set at the calorimetric onset temperature of the heat capacity change over the  $T_g$  range during heating as the  $\tau$  are orders of magnitude larger above the onset  $T_g$ .

Our studies presented in this thesis cover topics described above and were investigated with an emphasis on the amorphous food solid systems, which served as models for studies of physicochemical phenomena including water sorption behavior, crystallization, structural, thermal, and mechanical/dielectric changes, and flow characteristics of dehydrated food and pharmaceutical materials and formulations.

The main hypotheses of the present study were the following:

- (i) The water content, storage temperature, and the state and nature of food components, such as crystals, sugars, and WPI in amorphous food solids systems inhibit and affect crystallization of amorphous sugars.
- (ii) Food components may affect the mechanical/dielectric properties and structural relaxations of amorphous sugar containing systems.
- (iii) Structural relaxation time measured at low  $a_w$  controls the rate of

crystallization and the  $S$  concept provides a measure of relaxation rates in food solid systems.

- (iv) Food components may affect relaxation times and  $S$  value of food solids at low  $a_w$  which can be related to lactose crystallization properties.
- (v) The  $S$  concept could be used in formulation to describe and improve food materials properties and performance in processing and storage and it has a great potential for uses in food industry and product development for applications such as dehydration process and powder handling.

The above hypotheses were tested using a series of objectives:

- (i) Investigate the relationships between the quantity of protein,  $T_g$ , lactose crystallization kinetics and crystalline forms of lactose as derived from water sorption and XRD data at various storage temperatures.
- (ii) Measurement of dynamic-mechanical and dielectric properties of amorphous lactose/WPI mixtures at low water activities ( $\leq 0.44 a_w$ ).
- (iii) Measurement of enthalpy relaxation,  $\alpha$ -relaxation and corresponding  $\tau$  in lactose containing sugar/protein systems.
- (iv) Determination of the influence of water, two different crystalline phases ( $\alpha$ -lactose monohydrate and anhydrous  $\beta$ -lactose crystals) and polymeric food component (WPI), on the calorimetric glass transition, enthalpy relaxations, and  $S$  parameter in systems.
- (v) Investigation of the influence of whey protein on crystallization kinetics and crystalline forms of amorphous trehalose and lactose/trehalose systems at intermediate and high water activities ( $> 0.56 a_w$ ) as well as calorimetric glass transition,  $\alpha$ -relaxation, and structural strength at  $a_w \leq 0.44 a_w$  and isothermal storage conditions (25 °C).
- (vi) Investigation of DDI method as a simple method for measuring and describing the water sorption-induced structural transformation and crystallization in amorphous lactose/WPI systems.

# CHAPTER I

---

Food Eng Rev  
DOI: 10.1007/s12393-017-9166-6



---

REVIEW ARTICLE

*In Press, June 2017*

## LITERATURE REVIEW

## 1.1. GLASS TRANSITION OF AMORPHOUS FOOD SOLIDS

The amorphous solid state of food materials is metastable and food components may undergo a reversible transformation between the solid to liquid-like behaviour. This transformation occurs over a temperature range rather than at a constant temperature in various processes and during storage and is known as glass transition (Slade et al., 1991; Le Meste et al., 2002). Table (1.1) gives some theories developed for understanding glass transition based on its thermodynamic properties and the kinetic nature. It should be noted that the free volume theory, as the most popular theory for the explanations of the occurrence of the glass transition based on the change in thermal expansion coefficient, assumes that molecular motion depends on the presence of holes, vacancies, or voids that allow molecular movement (Sperling, 2005). The holes between molecules provide the free volume that is needed for molecular rearrangement and such free volume increases concomitantly with the temperature increasing due to a high thermal expansion coefficient can be found at high temperature. Knowledge of the glass transition and its associated  $T_g$  is advantageous to food design and formulation as such properties have a tremendous impact on food performance in processing and storage (Slade et al., 1991; Le Meste et al., 2002; Sperling, 2005; Donth, 2013). At high levels of solids, dehydrated foods and glassy solids, e.g., air-dried fruits and freeze-dried materials or spray-dried particles in food powders, may contain components above glass transition and then cause quality changes during storage. For example, the physical state of milk powder is often controlled by the glass transition of lactose, which may affect both dehydration processes and storage stability (Levine and Slade, 1989; Hartel, 2001). Anglea and Others (1993) suggested that, in dehydration, the quality and solid structure of dehydrated foods could be improved by keeping the material temperature close to the  $T_g$  in order to avoid structural and other quality changes. When dehydrated food materials are exposed to atmospheric conditions they often show significant water plasticization, which may result in viscous flow and collapse of



noncrystalline structures as the glass transition is depressed to below ambient temperature (Karathanos, 1993; Telis and Martínez-Navarrete, 2009; Potes et al., 2013). According to Anglea and Others (1993), collapse during dehydration was due to structural mobility, which was a function of viscosity ( $\eta$ ) and governed by the temperature difference,  $T - T_g$ . Sensory crispness of extruded wheat flour and maltodextrin-containing snack was lost at water contents depressing the glass transition to below room temperature (Kaletunc and Breslauer, 1993; Le Meste et al., 2002). The stiffness of an extruded cereal food could increase at low water contents followed by a significant decrease around glass transition (Harris and Peleg, 1996). In baking and cereal processing, glass transition concept has also been used and shown the possibilities of using various sugars to explain and manipulate the quality of cookies (Slade and Levine, 1995; Icoz and Kokini, 2008; Kweon et al., 2009). Moreover, several studies have suggested that reaction rates in food systems are affected by a number of factors, including glass transition (Lievonon et al., 1998; Le Meste et al., 2002; Acevedo et al., 2008). Duckworth (1981) reported that the rates of deteriorative changes at reduced water activities depend on molecular mobility, which governed by the physical state of food solids. It is obvious that rates of chemical reactions can be affected by diffusion and may proceed with an extremely slow rate in a glassy matrix due to diffusion limitation (Karel, 1985; Levine and Slade, 1989; Slade et al., 1991; Le Meste et al., 2006). A significant increase in the rate may occur as the material is transformed into the liquid-like viscous state above  $T_g$  due to increasing molecular mobility. Although the effects of glass transition on reaction kinetics in food processing have not been well established, it seems that food storage below  $T_g$  often extends shelf life as diffusional limitations decrease reaction rates in glassy food materials during storage.

**Table 1.1.** Theories Developed for Explaining the Glass Transition

Theories	References
Free-volume theory	Eyring (1936); Fox and Flory (1950); Cohen and Turnbull (1959)
Kinetic theory	Sperling (2005)
Thermodynamic theory	Sperling (2005); Roos and Drusch (2015)
Mode coupling theory	Perez (1994); Sjögren and Götze (1994); Debenedetti and Stillinger (2001)
Frustration-limited domains	Tarjus and Kivelson (1995)
Entropy-controlled co-operative motions	Adam and Gibbs (1965); Gibbs and DiMarzio (1958)
Hierarchical correlated molecular motions	Perez (1994)

### 1.1.1. CHARACTERIZATION METHODOLOGIES FOR GLASS TRANSITION

Glass transition of amorphous food materials are usually measured using calorimetric techniques, which show as a change in heat capacity ( $C_p$ ) and enthalpy during the measurement (Champion et al., 2000; Le Meste et al., 2002). Generally, the characteristic change in  $C_p$  is often used to observe the thermodynamic changes of materials around their glass transition. Hence, the thermal and thermodynamic properties of amorphous food materials can be measured using thermal analytical techniques such as DSC and dilatometry (Wunderlich, 2005; Sperling, 2005). A DSC measurement, as a most common approach, shows a change in  $C_p$  over the material specific glass transition in food and other systems. In DSC measurement, glass transition appears as an endo-thermal step change in heat flow to a sample resulting from the increase in  $C_p$  when a material is heated to above its glass transition (Fig. 1.1). Roos (2010) pointed that the  $T_g$  should be taken from the calorimetric onset temperature of the  $C_p$  change due to the fact that the onset temperature often agrees with the onset of structural relaxations as well as an end of the change in  $C_p$  during cooling (Fig. 1.1). Besides, amorphous materials often show glass transition-related structural relaxations when exposed to an external, oscillating small stress. Such

relaxations can be followed using dynamical mechanical (thermal) analysis (DMA/DMTA) or mechanical spectroscopy (Kasapis, 2012). Previous studies report that the membranes or stainless steel sheet pockets are often used to avoid loss of water in food solids during DMA/DMTA measurements (Kokini et al., 1994; Potes et al., 2012). The DMA data of food and other systems have shown that the method is more sensitive to changes in material properties around the glass transition than DSC (Kalichevsky and Blanshard, 1992; Sperling, 2006). Corresponding to DMA, DEA can be used in the characterization of liquid and powder samples over a wide range of temperatures. For example, DEA has also been used to observe effects of carbohydrate and protein composition of dairy powders on their thermal and glass

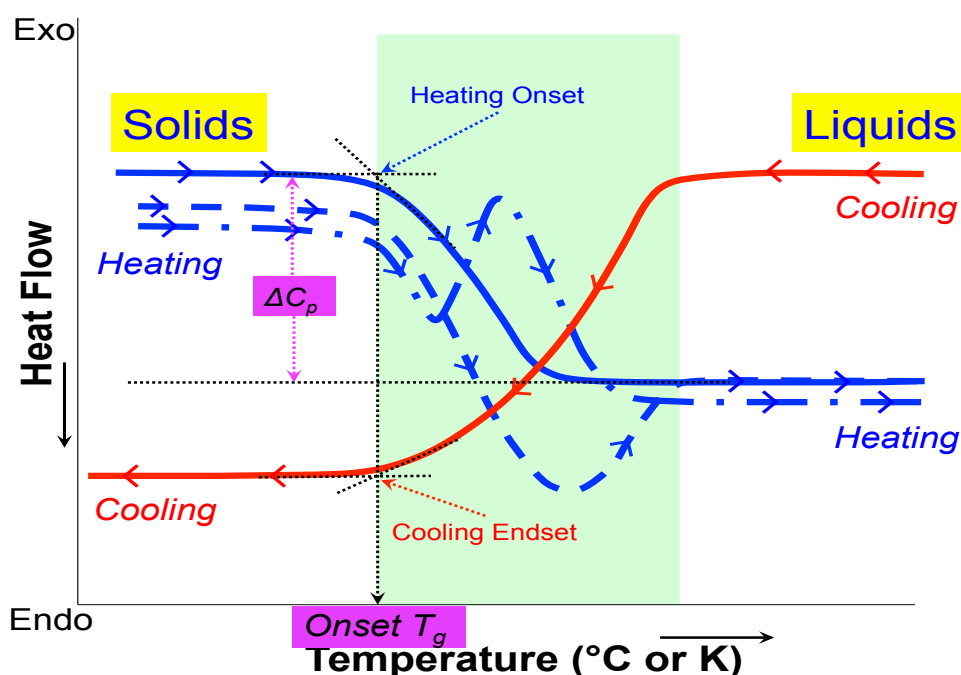


**Fig. 1.1.** Schematic thermograph for reversible glass transition derived from DSC measurement. The glass transition related change of heat capacity ( $\Delta C_p$ ) could be observed in DSC measurements. Calorimetric onset temperature is taken as the glass transition temperature ( $T_g$ ) as heating onset temperature agreed with cooling endset temperature (Angell, 2002).

transition behavior (Silalai et al., 2009). Moreover, several spectroscopic techniques

can be used to observe molecular mobility in amorphous materials. These include infrared and Fourier transform infrared (IR/FTIR), Raman, Electron Spin Resonance (ESR), and various NMR spectroscopies as discussed by Roos and Drusch (2015). These techniques with FTIR and Raman microscopy give detailed information of glass-forming materials in food systems. Söderholm and Other (2000) suggested that the glass transition results in weakening of the hydrogen-bonding network of amorphous glucose by using Raman spectroscopic studies. Microscopies may also be used to locate crystallinity or various amorphous components in food microstructure (Frick and Richter, 1995; Lee and Wand, 2001). You and Ludescher (2010) used fluorescence spectroscopy to derive molecular mobility in various glass-forming materials. One of the key findings of the spectroscopic methods in studies of glass transitions and food material properties has been that the glass transition has only a small effect on the mobility and diffusion of water molecules, and water molecules remain mobile in glassy food systems (Le Meste et al., 2002).

### **1.1.2. PLASTICIZATION AND FRACTIONAL WATER SORPTION**

PLASTICIZATION AND PLASTICIZERS The componential effects, derived from addition of minor food components or so-called “plasticizers”, can significantly alter the glass transition behavior of food solids because of plasticization (antiplasticization) effects during process and storage (Slade et al., 1991; Cao et al., 2009). Plasticization indicates an increase of plasticity, decrease of viscosity, or increased flexibility of a bulk structure by the presence of plasticizers, whereas the small quantities of plasticizer can diversely cause a stiffer, higher tensile strength and more brittle of food solids so called “antiplasticization” (Anderson et al., 1995; Pittia and Sacchetti, 2008; Luk et al., 2013). Plasticizers, which are fully miscible and often have a lower molecular weight than the bulk material, may increase free volume and cause plasticization effects (Sothornvit and Krochta, 2000; Suyatma et al., 2005). Since most amorphous food solids are water-soluble or miscible components, water

(theoretical  $T_g \approx -135\text{ }^{\circ}\text{C}$ ) can be considered as the major component acting as a  $T_g$ -decreasing plasticizer due to its large free volume, according to the free volume theory (Batzer and Kreibich, 1981; Velikov et al., 2001). However, Pittia and Sacchetti (2008) reported an opposite effect, i.e., hardening and toughening, could be observed in some food matrices and in specific moisture or  $a_w$  range and this was referred to an antiplasticization effect. Such phenomenon probably resulted by the physical property measured in food matrix: mechanical testing method, mechanical/dielectric parameter tested, food composition and micro-macrostructure. Therefore, water plays a dual role as a plasticizer and an antiplasticizer in food mixtures (Chang et al., 2000). Both plasticization and antiplasticization effects are possible with concomitant effects on the mechanical/dielectric properties as there is shrinkage and other changes increasing stiffness (antiplasticization), which are not strictly related to  $T_g$  but result from increased mobility (plasticization). Besides water, therefore, other small molecules, e.g., glycerol, xylitol or sorbitol, have also been found to act as plasticizers in food systems, increasing the free volume between the molecules, provided there is no phase separation (Champion et al., 2000; Shaw et al., 2002). Moreover, as the temperature increases to above  $T_g$ , the molecular mobility increases, which is evident from decreasing stiffness and increasing viscous flow of amorphous food solids. In such cases, temperature also has a plasticizing effect on the food materials.

WATER PLASTICIZATION AND FRACTIONAL WATER SORPTION Water is of key importance to food systems affecting processing, microbial safety, sensory perception, storage stability and shelf life (Al-Muhtaseb et al., 2002; Lodi and Vodovotz, 2008). Water sorption isotherms are important to numerous applications, e.g., development of new products (Wang and Brennan, 1991), determination of product stability and shelf life (Jouppila and Roos, 1994a), and process design and control (Peng et al., 2007). Water sorption characteristics as well as other interactions of food solids with water are primarily defined by composition of nonfat components, i.e., carbohydrates and proteins (Al-Muhtaseb et al., 2002). Generally the water sorption characteristic

could be studied by SSM and DDI methods (Labuza et al., 1985; Yuan et al., 2011). In comparison to SSM, DDI method offers another real-time investigation of water sorption properties as it generates a complete dynamic isotherm with 50 to 200 data points quickly and accurately without long equilibration times which are typical of

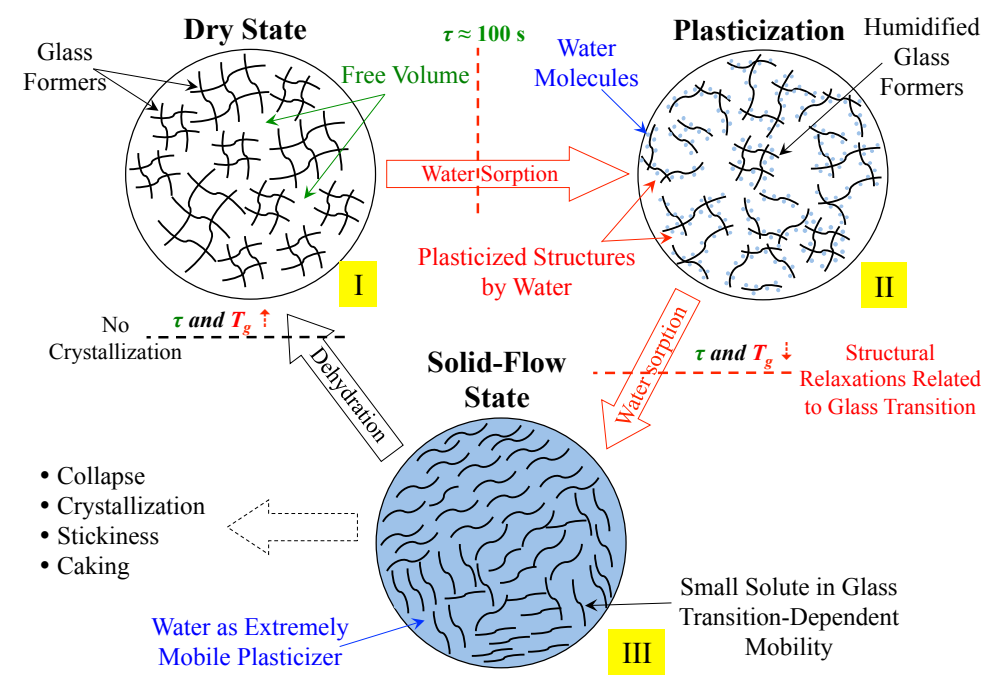


**Fig. 1.2.** Schematic diagram presents the water plasticization effects for a glassy material. The symbols do not represent the real sizes and quantity of components.

SSM methods (Yuan et al., 2011; Schmidt and Lee, 2012). Water sorption can induce many time-dependent phenomena, structural transformations, and phase transitions on food solids due to water plasticization effects. However, the effects of sorbed water on molecular mobility including plasticization are poorly understood mainly because molecular and structural analyses are scarce. Kilbrun and Others (2004) concluded that the water plasticization effect in carbohydrates is via a complex mechanism involving both hydrogen bond formation (or disruption) and changes in the matrix free volume. Fig. (1.2) is the schematic diagram for water sorption-induced plasticization effects of a glassy food material. In the dry state, the

hydrogen bonding between carbohydrate molecules leads to formation of large molecular entities (Fig. 1.2 I). When water is sorbed, it disrupts the hydrogen bonds between carbohydrate chains. Two effects of sorbed water on a glass were proposed. Firstly, water tends to fill the smallest voids in the glassy matrix (Fig. 1.2 I to II). Secondly, the sorbed water increases the degree of freedom of the carbohydrate molecules due to its interference with the intermolecular hydrogen bonding of the carbohydrates and coalescence of the smallest voids under the driving force associated with the reduction of free surface area (Fig. 1.2 II to III). Therefore, the  $T_g$  value of amorphous materials decreases with the increasing water content due to plasticization effects. Potes and Others (2012) found a fractional water sorption behaviour in freeze-dried lactose/maltodextrin (MD) systems up to 0.76  $a_w$  and the Guggenheim-Anderson-de Boer (GAB) isotherm Eq. (1.1), where  $m$  is water content,  $m_0$  is the monolayer value (the amount of water that is sufficient to form a layer of water molecules of the thickness of one molecule on the adsorbing surface),  $C$  and  $K$  are respectively calculated from  $m_0$  could be used for lactose/MD systems to predict their water sorption. According to Potes (2014), the fractional water sorption of lactose/maltodextrin systems can be described according to Eq. (1.2), where  $M$  is water content of amorphous or non-crystalline solid. At equilibrium or at the same temperature, the  $a_w$  across all components of the systems was equal, that is, the steady-state  $a_w$  of each food component is equal to the  $a_w$  measured for the whole system, and the corresponding fractional water contents of each component can be derived from their individual water sorption isotherms. Furthermore, the fractional water sorption has been confirmed in freeze-dried sugar/protein systems (Roos and Potes, 2015).

$$\frac{m}{m_0} = \frac{Cka_w}{(1-ka_w)(1-ka_w+Cka_w)} \quad (1.1)$$

$$M_{TOTAL} = M_{LACTOSE} + M_{MD} \quad (1.2)$$

### 1.1.3. GLASS TRANSITION TEMPERATURE IN SOLIDS SYSTEM

GLASS TRANSITION TEMPERATURE IN MIXTURES The free volume of water in foods is very large compared with that of food solids at the same temperature and pressure. On the other hand, water can also remain mobile in glassy food systems (Slade et al., 1991; Sperling, 2005). Therefore, knowledge of the effects of composition on the  $T_g$  is of significant importance in the evaluation of the technological performance of food solids. Table (1.2) gives calorimetric  $T_g$  data for common food solids. The  $T_g$  value of a given hydrophilic substance is decreased with an increase of water content following a non-linear relationship (Eq. 1.3), such as the Gordon-Taylor (*GT*) equation (Gordon and Taylor, 1952). Truong and Others (2002) derived Eq. (1.3) and applied it not only to binary systems but also to ternary, quaternary, and higher order systems. It should be noted that the fractional water sorption allows quantification of water in specific components within carbohydrates containing solids. Such quantification of water in component fractions is required for the calculation of  $T_g$  data based on *GT* equations. The Couchman-Karatz equation (Eq. 1.4) was identical to the empirical *GT* equation with a constant  $k = \Delta C_{p2}/\Delta C_{p1}$ . The change in heat capacity ( $\Delta C_p$ ) that occurs over the  $T_g$  range is also dependent on composition. The  $\Delta C_p$  of sugars plasticized by water have been found to increase linearly with increasing mass fraction of water (Roos and Karel, 1991; Hatley and Mant, 1993). The assumption of the *GT* equation is ideal volume mixing, which assumes that the two components are miscible and their free volumes are additive (Shamblin et al., 1998). It is also important to note that small amounts of plasticizers or (anti-plasticizers) have no significant effect on  $T_g$ . For example, MD or whey protein isolates (WPI) had no significant effect on  $T_g$  of a co-lyophilized mix with lactose (Potes et al., 2012). The reason is non-ideal mixing due to phase separation and hydrogen bonds might form between the components in the lyophilized mixtures. The calorimetric onset and midpoint  $T_g$  values,  $\Delta C_p$ , and estimated constant  $k$  of *GT* equation for different food solids are given in Table (1.2).



$$T_g = \frac{x_1 T_{g1} + kx_2 T_{g2}}{x_1 + kx_2} \quad (1.3)$$

$$T_g = \frac{x_1 T_{g1} + (\Delta C_{p2} / \Delta C_{p1}) x_2 T_{g2}}{x_1 + (\Delta C_{p2} / \Delta C_{p1}) x_2} \quad (1.4)$$

Where,  $x_1$ ,  $T_{g1}$ , and  $\Delta C_{p1}$  and  $x_2$ ,  $T_{g2}$ , and  $\Delta C_{p2}$  refer to the mole fraction, glass transition temperature, and change in heat capacity at glass transition of the components 1 and 2, respectively. Moreover,  $k$  is the constant for empirical  $GT$  equation.

GLASS TRANSITION AND MOLECULAR WEIGHT The glass transition temperature is strongly dependent on molecular weight as the molecular weight of food materials can be related to free volume (Le Meste et al., 2002). Fox and Flory (1950) reported that components that increase the average molecular weight effectively increase the  $T_g$  of mixtures and tend to level off for materials with higher molecular weights. Common synthetic polymers and a number of natural carbohydrate polymers and polymer mixtures, but not native proteins, have a distribution of molecular weights. Therefore, the molecular weight can be given as the number average molecular weight ( $M_n$ ), which can be used as a measure of the molecular weight distribution (Eq. 1.5). The following Fox-Flory equation (Eq. 1.6), where  $K$  is a constant, and  $T_{g\infty}$  is the high molecular weight limiting value of  $T_g$ , is used to describe the dependence of  $T_g$  on molecular weight in a homogeneous food polymer series, such as saccharides containing glucose monomers. It is obvious that blending miscible low-molecular-weight components with polymers or the decrease of the size of polymer molecules decreases the  $T_g$ . An increase of the size of the polymer molecules

**Table 1.2.** Glass Transition Temperatures ( $T_g$ ), Change of Heat Capacity ( $\Delta C_p$ ) Occurring over Glass Transition, and Estimated  $k$  Values Obtained from Eq. (1.3)

Food solids	Glass transition temperature, $T_g$ (°C) <sup>a</sup>		$\Delta C_p$ (J/g °C)	$k$
	Onset	Midpoint		
Pentoses				
Arabinose	-2	3	0.66	3.55
Ribose	-20	-13	0.67	3.02
Xylose	6	14	0.66	3.78
Hexoses				
Fructose	5	10	0.75	3.76
Fucose	26	31	-	4.37
Galactose	30	38	0.50	4.49
Glucose	31	36	0.63	4.52
Mannose	25	31	0.72	4.34
Rhamnose	-7	0	0.69	3.40
Sorbose	19	27	0.69	4.17
Disaccharides				
Lactose	101, 105 <sup>b</sup> , 109 <sup>b</sup>	-	-	6.56
Lactulose	79	88	0.45	-
Maltose	87	92	0.61	6.15
Melibiose	85	91	0.58	6.10
Sucrose	62	67	0.60	5.42
Trehalose	100, 112 <sup>b</sup>	107	0.55	6.54
Oligosaccharides				
Raffinose	70	77	0.45	-
Sugar alcohols				
Maltitol	39	44	0.56	4.75
Sorbitol	-9	-4	0.96	3.35
Xylitol	-29	-23	1.02	2.76
Maltodextrins <sup>c</sup>				
DE 10	138, 160	-	0.444	-
DE 18	112	-	0.466	-
DE 25	140	-	-	-
Poly vinyl pyrrolidone <sup>d</sup>				
PVP10	92	-	0.25	2.66
PVP24	117	-	0.30	2.66
PVP40	137	-	0.27	2.82
Proteins				
$\alpha$ -Lactalbumin	159	-	-	-
$\beta$ -Lactoglobulin	146	-	-	-

Source: Roos and Drusch (2015). <sup>a</sup> Onset and midpoint of the glass transition temperature range; <sup>b</sup> Maidannyk and Roos (2016); <sup>c</sup> Avaltroni et al. (2004), Potes et al. (2012); <sup>d</sup> Buera et al., (1992).

that occurs in thermosetting results in an increase of  $T_g$ . The Fox-Flory equation has been shown to apply for a number of food polymers and biopolymers, including maltodextrins.

$$M_n = \frac{\sum_i n_i M_i}{\sum_i n_i} \quad (1.5)$$

$$\frac{1}{T_g} = \frac{1}{T_{g\infty}} + \frac{K}{M_n} \quad (1.6)$$

## 1.2. CRYSTALLIZATION ON AMORPHOUS FOOD SOLIDS

Crystallization is a time-dependent phenomenon and first-order phase transition that occurs from a melt or from a solution (Hartel and Shastry, 1991; Mullin, 2001; Wang and Truong, 2017). In amorphous foods with low water contents, crystallization of solids may occur at temperatures above the  $T_g$ , but below  $T_m$  (Hartel and Shastry, 1991). Low molecular weight food solids, such as sugars, organic acids and polyols, can either be in crystalline or amorphous states depending on processing conditions and presence of other components in the system (Slade et al., 1991; Mullin, 2001; Sperling, 2006). Undesired or uncontrolled crystallization event is one of the main issues in the food industry, since crystallization of the solid phase may significantly affect processability and shelf life of food. On the other hand, formation of the solid crystalline phase may also play an important role in many food products, in order to provide certain characteristic size and textural properties (Mazzobre et al., 2001). Therefore, crystallization of amorphous food solids could interfere with food characteristics and structures at various processing and storage conditions, and control of crystallization phenomena is often required to ensure desired sensory and stability characteristics of foods. The crystallization behavior of lactose and some polymeric food components would be introduced in the present section.

### **1.2.1. CHARACTERIZATION METHODOLOGIES FOR CRYSTALLIZATION**

The DSC and XRD were considered as two most widely used approaches to investigate the crystallization behavior of food solids (Levine and Slade, 1991; Hartel and Shastry, 1991). The DSC measurement-derived calorimetric crystallization data of many food solids are well documented (Mazzobre et al., 2001; Buera et al., 2005; Verhoeven et al., 2017). Jouppila and Roos (1994a) used the XRD to analyze crystallization of amorphous lactose and found that pure lactose showed less rapid crystallization with lower  $T-T_g$ . Besides, several other characterization methodologies could be used together with DSC in the study of crystallization process of amorphous food solids. For example, Ottenhof and Others (2003) utilized FTIR together with DSC to monitor the  $T_g$  and crystallization temperature ( $T_{cr}$ ) of amorphous lactose at the  $RH$  range of 0 ~ 33%. They found that the temperature difference between crystallization and glass transition ( $T_{cr}-T_g$ ) decreased from 60 °C to 45 °C in DSC measurement as well as in FTIR measurement, where the  $T_{cr}-T_g$  decreased from approximately 65 °C to 45 °C. The solid-state recrystallization of amorphous sugar containing particles could be visualized using environmentally controlled atomic force microscopy and conventional optical microscopy as reported by Price and Young (2004). Moreover, Mazzobre and Others (2003) applied polarized light video microscopy (PLV) and DSC together to measure crystallization kinetics, induction times, and time for complete sugar crystallization at different storage temperatures. They found that the temperature dependence of crystallization rate and time to complete sugar crystallization measured by PLV were similar to those obtained by DSC.

### **1.2.2. PROCESSES OF CRYSTALLIZATION**

Numerous publications have reported that crystallization is often a three-step process including nucleation (formation of nuclei), propagation (crystal growth), and

maturation (crystal perfection and/or continued growth) (Hartel and Shastri, 1991; Mullin, 2001; Wang and Truong, 2017). The nucleation and crystal growth and corresponding crystallization rates would be respectively introduced as follows:

NUCLEATION Nucleation is the process that precedes crystallization and involves the formation of the crystal nuclei at incipient crystalline phase (Hartel and Shastri, 1991). Generally, nucleation results from the driving force within a metastable state that occurs after supersaturation or supercooling due to solvent removal or a decrease in the temperature of a solution or a melt (Van Hook, 1961; Hartel, 2001). Hartel and Shastri (1991) classified nucleation into primary and secondary mechanisms leading to crystal growth depending on whether the crystalline centers of the crystallizing compounds is absent or present in nucleating system. The primary nucleation may be either homogeneous or heterogeneous. Homogeneous nucleation described by a molecular accretion mechanism occurs spontaneously, which means the molecules of the material arrange together and form the nuclei. Van Hook (1961) reported that the formation of a new phase requires energy due to its higher solubility or vapor pressure, which may cause its disappearance. As defined by the critical size of a nucleus, the requirement for the occurrence of homogeneous nucleation is that molecules form clusters due to molecular collisions. The size of such clusters must become sufficiently large and exceed the energy barrier for nucleation (Hartel and Shastri, 1991). However, homogeneous nucleation requires a fairly large extent of supercooling or supersaturation, and thus, its occurrence even in chemically pure materials are rare. Therefore, most crystallization processes are not homogeneous due to the presence of foreign surfaces and particles that are in contact with the material; that is, heterogeneous nucleation is the most likely mechanism of nucleation in food materials. Heterogeneous nucleation involves the presence of foreign bodies or impurities that provide a surface and may act as the nucleating site. The foreign bodies reduce the energy needed for the formation of the critical nuclei due to it can induce nucleation at degrees of supercooling lower than those required for spontaneous nucleation and therefore facilitate crystallization (Van Hook, 1961;

Mullin, 2001). The extent of supercooling or supersaturation is also lower in the heterogeneous nucleation process than in the homogeneous nucleation process. For example, Hartel and Shastry (1991) reported that sugar syrups that have been filtered might require higher supersaturation for nucleation compared with syrups containing more impurities. Although there is some information on nucleation in supercooled solutions (Van Hook, 1961; Hartel and Shastry, 1991), nucleation phenomena in supercooled amorphous food materials have received little attention. It should be noted that nucleation might become significantly reduced in the presence of other compounds, for example, in foods that are composed of mixtures of several solutes. Secondary nucleation differs from primary nucleation processes in that it occurs in the presence of existing crystal seeds of the nucleating compound. Roos and Drusch (2015) reported that secondary nucleation might result from mechanical reduction of the size of the existing crystals, which may occur due to shear forces. Consequently, secondary nucleation phenomena are common in sugar crystallization processes, and it has many potential applications in food processes, such as freezing of foods.

CRYSTAL GROWTH AND CRYSTALLIZATION RATES The nucleation step in crystallization is followed by crystal growth. Crystal growth requires that molecules are able to diffuse to the surface of the growing nuclei. The rate of the process is very sensitive to the extent of supersaturation or supercooling, temperature, and the presence of impurities. The effects of impurities are particularly important factors to overall crystallization rates in food materials, as impurities may significantly reduce crystallization rates. The diffusion of molecules on the growing nuclei surface is the main requirement of crystal growth. Van Hook (1961) reported increasing rates of crystallization with increasing supersaturation for sucrose when the overall supersaturation level was low. Crystallization became delayed at high levels of supersaturation as well as in the presence of impurities. In addition to diffusion, the growth of existing nuclei requires several other requirements to be accomplished. Hartel and Shastry (1991) reported that such requirements in sugar crystallization might include: (1) diffusion of the compound from bulk to the solid surface; (2)

mutarotation of molecules to the anomeric form for growth; (3) removal of hydration water; (4) diffusion of water away from the crystal surface; (5) proper orientation of the molecules; (6) surface diffusion of the molecules to appropriate sites; (7) incorporation of the growth unit into the crystal lattice; and (8) removal of latent heat. These steps are important in defining the rate-limiting steps for crystallization, and they are used in various crystal growth theories. According to Hartel and Shastri (1991), the diffusion theory assumes that molecular diffusion to the surface is the

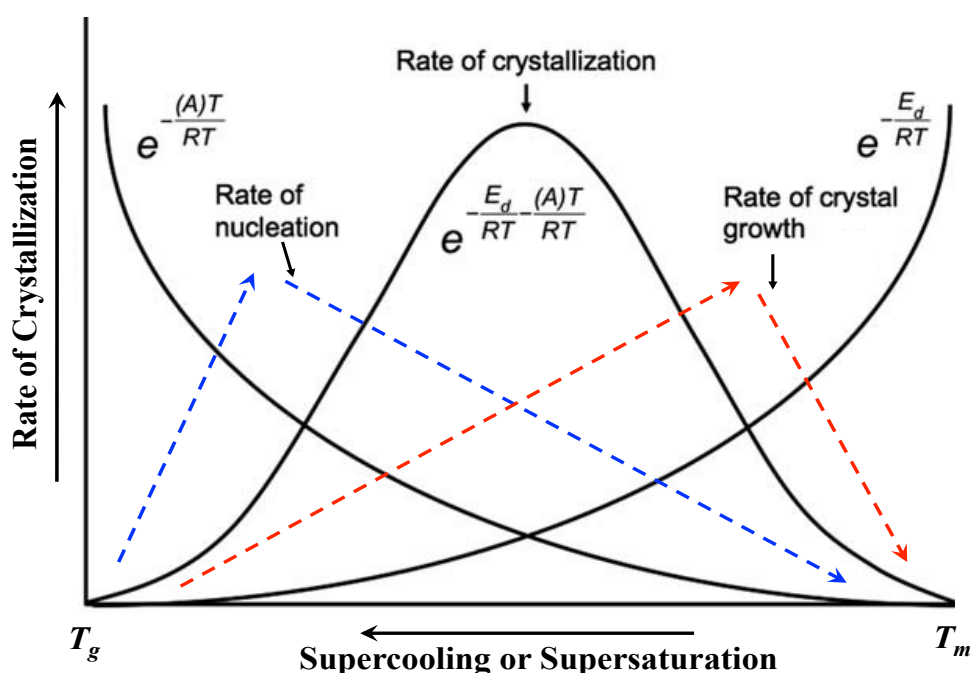


**Fig. 1.3.** Schematic diagram shows a “Bell-Shape” relationship between the changes of supercooling (or temperature from  $T_g$  to  $T_m$ ) and the rates of crystallization (Lauritzen and Hoffman, 1973; Wang and Truong, 2017). The rate of nucleation and crystal growth are represented by blue and red dash line, respectively.

rate-limiting step of crystal growth. Adsorption layer theories assume formation of an adsorption layer of molecules on the crystal surface, in which formation of a growth unit, diffusion of the growth unit to an appropriate site, or incorporation of the growth unit to the lattice may be the rate-limiting factors (Hartel and Shastri, 1991). Along

with the increase of temperature above  $T_g$  but below melting temperature ( $T_m$ ), the rate of crystallization first increased and then decreased showing a “*Bell-Shape*” relationship in Fig. (1.3) introduced by Lauritzen and Hoffman (1973). Their approach describes the combined effects of nucleation and propagation when considering a broader temperature range. On the other hand, the overall crystal growth rate expected to be kinetically hindered by the high viscosity at temperatures close to  $T_g$ , even though there is a large thermodynamic driving force for crystallization (Baird and Taylor, 2012). Similarly, at high levels of supercooling or supersaturation the rate of nucleation is high, but the rate of diffusion is low, which decreases the rate of crystallization. At low levels of supercooling the rate of diffusion is high, but the rate of nucleation is low. Therefore, the maximum rate of crystallization occurs at intermediate levels of supercooling (or supersaturation) or over the half way between  $T_g$  and  $T_m$  (Kedward et al., 2000). Moreover, Jouppila and Roos (1994b) reported that the  $RH$  (or water activity,  $a_w$ ) of food also has bell-shape relationship with the rate of crystallization.

### **1.2.3. LACTOSE – A SUGAR OF INTEREST**

Since carbohydrates, especially sugars, are important ingredients in the food industry and also important components of dehydrated products, an in-depth understanding of sugar crystallization has a great importance in the development of proper processing and shelf-life control procedures for such food ingredients and relevant products under varying temperature, moisture content, and time (Mazzobre et al., 2001). However, a complex mixture of ingredients in a food product causes a complex pattern of crystallization of sugars due to the many inter- or intra-molecular interactions. The presence of some of the ingredients or impurities, e.g., other sugars, proteins, food polymers, etc., may directly disturb the crystallization rate of amorphous sugars by influencing the mechanism of nucleation and crystal growth due to mass transfer limitations or physicochemical interactions with sugar molecules during crystallization. In addition, many ingredients show synergistic effects with



other ingredients. Therefore, detailing the exact effect of an ingredient in food formulation may be quite complex. The end result is that empirical or experimental investigations are generally necessary. However, some general understanding can be developed by looking at the individual effects derived from each ingredient in the crystallization process of amorphous sugars. Lactose is an important ingredient in the dairy industry and also an important component of milk and milk products (Nickerson, 1979; Nasirpour et al., 2007; Gänzle et al., 2008). Hence, understanding the physical transition of lactose has a great importance in the development of proper processing and shelf-life control procedures for dairy ingredients and relevant products. Lactose can be obtained in either crystalline or amorphous molecular structure. The major crystalline forms of lactose are  $\alpha$ -lactose monohydrate and anhydrous  $\beta$ -lactose, while other crystalline forms of lactose could also be found, such as anhydrous  $\alpha$ -lactose or a mixed anhydrous  $\alpha$ -/ $\beta$ -lactose crystal (Haque and Roos, 2005; Nasirpour et al., 2007). In general, lactose crystallization can be affected by many factors during processing and storage, such as water content, temperature, time, pressure, and the presence of impurities, such as salts, other sugar, proteins, and etc.

EFFECT OF WATER ON LACTOSE CRYSTALLIZATION Water plays an important role in the crystallization of amorphous food solids through altering both the crystallization temperature and transition duration. Roos and Karel (1991c) reported that the crystallization and melting temperatures of amorphous lactose were affected by water content and the effect of water was about the same on  $T_{cr}$  and  $T_g$  owing to  $T_{cr}-T_g$  was a fairly constant. This phenomenon consider water being released in amorphous lactose crystallization and then absorbed by the other adjacent lactose molecules still in amorphous state, and thus, causing a concurrently decreasing  $T_g$  of lactose and an increasing crystallization rate with time of incubation as well as lowering  $T_{cr}$ . Jouppila and Others (1997) reported that the maximum rate of crystallization might be expected at around 0.70  $a_w$  based on XRD measurements. Schmitt and Others (1999) investigated the crystallization kinetics of amorphous

lactose in the presence and absence of seed crystals at 57.5% *RH*. The similarity of the isothermal activation energies ( $89.5 \pm 5.6$  kJ/mol) and non-isothermal activation energies ( $71 \pm 7.5$  kJ/mol) for the sample with seeds suggested that crystallization was occurring by growth from a fixed number of preexisting nuclei. Dilworth and Others (2004) found that amorphous lactose crystallizes to a mixture of  $\alpha$ -lactose monohydrate and anhydrous  $\beta$ -lactose and the ratio of the two species formed varies as a function of *RH*. When dry amorphous lactose samples were exposed to a *RH* of higher than 50% at 25°C, the volumetric shrinkage accompanied due to water plasticization and crystallization derived the loss of mechanical strength to hold the structure (Buckton and Darcy, 1995). The critical moisture content to cause the crystallization of lactose has been reported to be around 39% *RH*, although it was affected by some other factors, such as temperature (Jouppila and Roos, 1994b).

EFFECT OF TEMPERATURE ON LACTOSE CRYSTALLIZATION In addition to water content, temperature plays an important role in the relationship between crystallization and glass transition. The time to crystallization of amorphous lactose held isothermally above the glass-transition temperature decreased as the temperature was increased. And the crystallization time of amorphous lactose could be directly related to or even determined by the temperature difference between the storage temperature and glass-transition temperature ( $T - T_g$ ). Clark and Others (2016) reported that amorphous lactose was completely crystalline when a  $T - T_g$  above 31.6 °C after 1.6 hour exposure, while samples at  $T - T_g$  values below 31.6°C were completely amorphous showing no signs of crystallinity after 1.6 h. Hence, they pointed out that the temperature of  $T - T_g$  between 30 °C and 32 °C was found to be a critical range for amorphous lactose to transform into crystal relatively quickly. The types of lactose crystals that form depend on the *RH* and temperature of crystallization, the powder composition, and the time of exposure. Haque and Roos (2005) reported that the main types of crystallized lactose are  $\alpha$ -lactose monohydrate, anhydrous  $\beta$ -lactose, and anhydrous forms of  $\alpha$ -/ $\beta$ -lactose in molar ratios of 5:3 and 4:1. Compared with lactose in the crystalline state, the molecular arrangement of

lactose in the amorphous state is disordered. The collapsed lactose was reported to form some  $\alpha$ -monohydrate, but much more  $\beta$ -lactose than would be formed if the sample were crystallized from non-collapsed lactose (Darcy and Buckton, 1997). It should be noted that the lactose samples at high  $T-T_g$  values could rapidly collapse before crystallization decreasing diffusion and delaying removal of water released by crystallization.

EFFECTS OF IMPURITIES ON LACTOSE CRYSTALLIZATION The presence of impurities e.g., salts, other sugars, carbohydrates and proteins, may reduce the crystallization rate of amorphous lactose. According to previous reports of lactose/salt mixture by Omar and Roos (2007ab), crystallization of amorphous lactose occurs above  $T_g$  but it becomes delayed by addition of salts. Omar and Roos (2007ab) reported that  $NaCl$ ,  $MgCl_2$ , and  $KCl$  were found to affect lactose  $T_{cr}$  less than  $CaCl_2$ . Moreover, the decrease of  $T_{cr}$  for amorphous lactose and lactose/salt mixtures followed the decrease of  $T_g$  and bivalent salts in mixtures with lactose gave a higher  $T_g$  than smaller monovalent ions, which means lactose/ $CaCl_2$  (or  $MgCl_2$ ) mixtures had higher  $T_g$  than pure lactose but lactose/ $NaCl$  and lactose/ $KCl$  mixture resulted in a low  $T_g$ . Sugars are generally mixed to take advantage of the properties of each of the sugars involved, to increase the total level of solids in solution for microbiological concerns or to control the rate of sugar crystallization. Since many sugar products are used in mixture to achieve desirable taste or texture of food, the kinetics of crystallization in sugar mixture has been investigated in a wide range. For example, in lactose/sucrose mixtures, the temperature difference of  $T_{cr}-T_g$  increased from 64 °C to 76 °C when the concentration of lactose increased gradually from 0 to 100 % (Arvanitoyannis and Blanshard, 1994). Mazzobre and Others (2001) found only one  $T_g$  in the thermograms of low water lactose/trehalose mixtures, which indicated the compatibility between the two sugars. Moreover, addition either of lactose, trehalose, or raffinose could increase the  $T_{cr}$  of sucrose for about 30°C, when the additive sugar comprised 10 % of the mixtures (Saleki-Gerhardt and Zografi, 1994). This was probably due to the sugar additives can accumulate at the

solid-particle interface as an adsorbed layer, which might be the reason to inhibit any nucleation that initiated on the surface of the particle. The presence of large macromolecules, such as maltodextrins, proteins, and etc., can cause significant influences on molecular mobility of amorphous sugars, and thus, have a significant effect on the rate of crystallization. In addition, these macromolecules may adsorb to the crystal surface and influence the manner by which sugar molecules attach to the crystal lattice. Potes and Others (2012) reported that the crystallization of lactose in amorphous lactose/MD systems was inhibited with maltodextrin content and the MD with high DE (Dextrose Equivalent) showed a stronger inhibition of crystallization of lactose than lower DE maltodextrin. Li and Others (2016) studied the glass transition and crystallization of amorphous lactose with WPI, and found that with increasing the amount of crystalline lactose in mixture had no significant influence on the  $T_g$  and the initial  $T_{cr}$  at 0.11 to 0.44  $a_w$ . Ibach and Kind (2007) found that amorphous lactose crystallized within 1 min at an air temperature of 100 °C and relative air humidity of 80 %, whereas whey-permeate and whey powders required up to 5 min for lactose crystallization at the same set of conditions. Moreover, the  $T_g$  and  $T_{cr}$  of freeze-dried lactose and lactose/protein mixtures were slightly higher than those of spray-dried lactose and lactose/protein mixtures at corresponding water contents. But  $T_{cr}$  of lactose/*Na*-caseinate and lactose/gelatin mixtures were lower in freeze-dried than in spray-dried materials (Haque and Roos, 2006).

#### 1.2.4. CRYSTALLIZATION OF OTHER FOOD COMPONENTS

CRYSTALLIZATION OF OTHER SUGARS The crystallization behaviour of amorphous sugars has been well documented. For example, Foster and Others (2006) reported a linear relationship between the temperature difference  $T - T_g$  and the cohesiveness of amorphous sugars including sucrose, glucose, fructose, and maltose. They indicated that the cohesiveness could be further related to the crystallization of the amorphous sugar and occur at a rate that is proportional to the rate of crystallization. Ruiz-Cabrera and Schmidt (2015) reported that  $T_g$  and  $T_m$  decreased in

sucrose, fructose, and glucose at higher water content due to the formation of defect sites in the ordered structure of sugar crystals promoted by the water dissolution effect. They pointed out that the  $T_g$  of amorphous sucrose could be lowered from 74 °C to 32 °C, while the  $T_{cr}$  lowered from 130 °C to 92 °C when the water content increased up to 3.13 % (w/w). Saleki-Gerhardt and Zografi (1994) applied a model for nucleation-controlled crystallization from the amorphous state in order to relate the  $T_{cr}$  to  $T_g$  of sucrose at different water content. This confirmed that the effect of water was directly related to the  $T_g$ , and the significant effect of sucrose crystals on isothermal nucleation-controlled induction time was confirmed. According to water sorption testing, the rate of crystallization of amorphous sucrose based on the change of water content followed an exponential law with respect to time after an initial induction period (Makower and Dye, 1956). It was recommended that amorphous sugar is to be stored below  $T_g$  to maintain stability, since the crystallization of amorphous sucrose (at  $a_w$  of 0.33 and above) could occur rapidly at room temperature. That occurred because the  $T_g$  was shifted to well below room temperature. It should be noted that the sugar crystallization also could be considered beneficial for improving the stability of amorphous sugar containing matrix during storage. For example, Schebor and Others (2010) indicated that the formation of hydrate form of sugar crystals could provide additional desiccation by removing water from the amorphous phase and thereby increase the storage stability by increasing  $T_g$  of the remaining amorphous matrix. After correlating the  $T_m$  of amorphous sugars and the water content before crystallization, Kawakami and Others (2006) suggested that water migration occurring between crystalline and amorphous phases could affect the crystallization process. The crystallization rate of amorphous sucrose was found to be slow at first but the rate increased rapidly after a delay due to an autocatalytic effect of the water being excluded from the crystals being available to lower the  $T_g$  of the remaining amorphous sucrose. Trehalose and raffinose were found to have good performance to form hydrated crystals as bioprotectants in dehydrated systems, which is not only related to the kinetic restrictions (temperature above  $T_g$ ), but also a minimum amount of water required to form the hydrated stable crystals (Schebor et

al., 2010). However, it should be noted that the amorphous phase of amorphous sugars would have a short life when  $RH$  is enough for sugar crystallization.

The high-pressure compression could improve the physical stability of the amorphous sugar affecting both glass transition and crystallization. Kagotani and Others (2013) reported that the  $T_g$  and  $T_{cr}$  of amorphous sugars dramatically increased under the compression pressures higher than 443 MPa in comparison with the untreated sugars. The high pressure was reported to disturb water plasticization effects as the amount of sorbed water in sugar decreases. The  $\alpha$ -lactose,  $\alpha$ -maltose, trehalose, and dextran all showed similar trends over the  $RH$  range of 11 ~ 33 % when the compression pressure was higher than 443 MPa. However, Imamura and Others (2010) reported that when freeze-dried amorphous sucrose was subjected to a high pressure of several hundreds of MPa, the formation of a critical nucleus of a sucrose crystal and subsequent crystal growth were found to be accelerated. The changes in crystallization behavior of compressed sucrose appear to be closely related to the increase in the free energy level and the disappearance of pores. Besides glass transition and crystallization, degradation kinetics of the ingredients and mechanical strength of an amorphous sugar matrix are also strongly affected by high pressure (Imamura et al., 2012). The effects of organic compounds, such as urea aconitic acid, mannitol, sobic acid, isobutyric acid, and mixed amino acids, on the rate of sucrose crystal growth at various supersaturations was studied by Smythe (1967). His conclusions were that these compounds inhibit growth on the same order of magnitude as similar concentrations of invert sugar. Organic coloring agents, naturally present in cane and beet juice, have also been shown to inhibit the rate of sucrose crystal growth, although solubility effects were not taken into account. In their study, sucrose crystal growth was seen to increase by about 25 % upon increasing the coloring matter content by 400 % over that normally found in refiner's syrups. Naturally occurring constituents of whey also have an important impact on the crystallization process for refining lactose. Riboflavin has been found to affect both growth rate and product morphology crystal surface and thereby it slows down

specific faces in such a way that thin plate-like crystals are formed. Michaels and van Kreveland (1966) also observed a decrease in the growth rate of specific faces in the presence of riboflavin. At 10 ppm addition of riboflavin, no growth inhibition effect was observed. However, addition of 50 or 100 ppm riboflavin to lactose solution was seen to decrease the growth rate of the individual faces to varying extents. This resulted in the formation of the plate-like crystals observed previously due to the addition of riboflavin.

CRYSTALLIZATION OF POLYMER COMPONENTS Crystallization behavior could be also found in many polymeric materials, such as polysaccharides and proteins. As one of the major energy source and important food ingredient, starch is widely used in many types of food. Starch is usually a mixture of amorphous and crystal phase. The different amylose/amylopectin ratios in starch together with other structural characteristics could significantly affect the glass transition and crystallization (retrogradation) behavior of different types of starches. For example, Jouppila and Roos (1997) reported that the crystallization rate,  $T_m$ , and the extent of crystallization of corn starch could be affected by the  $T-T_g$ . Moreover, corn starch was observed to crystallize into the same crystal form, independent of water content and storage temperature and, therefore of the  $T-T_g$  (Jouppila et al., 1998). Jagannath and Others (2001) found that the  $T_g$  of precooked potato starch was highly relevant factor for the kinetics of starch crystallization as the correlation coefficient of  $T_g$  and half crystallization time of precooked potato starch was 0.9658. Perdomo and Others (2009) reported that the water plasticization effect was attributed to cassava starch retrogradation as sorbed water and expelled water from the crystalline regions decreased the  $T_g$  of the sample. The  $T_g$  of non-waxy and waxy rice starch slightly increased with increasing recrystallization degree, and the highest  $T_g$  was observed in the maximum recrystallization temperature ranges, which was found to be around 30 °C (Baik et al., 1997). Besides starch, other polysaccharides, such as hydrocolloids were also of the research interests considering glass transition and crystallization. Zimeri and Kokini (2002) found that inulin was semicrystalline with both glass

transition and crystallization behavior when stored above  $T_g$  and around 60 °C at 10 % water content. Paes and Others (2010) reported that the recrystallization of ball-milled cellulose at various water contents up to 17 % was always found in the temperature region of 15 ~ 20 °C above  $T_g$ , and the  $T_g$  of ball-milled cellulose was approximately 205 °C at dry state. The  $T_{cr}$  of hydrocolloids-water system (Guar Gum, Locust Bean Gum, and Tara Gum) was found to have similar downtrend with  $T_g$ , along with the increase of moisture content (Naoi et al., 2002). Food proteins are commonly sourced from animal and plant origins, such as dairy proteins (beta-lactoglobulin), egg protein (ovalbumin), and seed proteins (prolamin). Certain proteins are able to form crystalline structures (Hartel, 2013). Magoshi and Others (1992,2002) measured the  $T_g$  and  $T_{cr}$  values of corn, rice, wheat, and soybean proteins. They pointed out that the transition of amorphous random-coil conformation into  $\beta$ -crystal forms was found at the crystallization temperatures. Steam treatment of the corn zein induced partial crystallization of amorphous fraction, resulting in the increase of  $T_g$  and  $T_{cr}$  (Magoshi et al., 1992). Pouplin and Other (1991) suggested an occurrence of partial crystallization in association with changes in structure of wheat gluten protein based on DMTA measurements. However, it should be noted that food polymers are more commonly found in food mixtures than as a pure compound, which would encounter glass transition or crystallization if being subjected to temperature or water changes. But effects of macromolecules on the thermal transitions are often discussed together with low-mass molecules like sugars.

### **1.3. MECHANICAL/DIELECTRIC PROPERTIES AND STRUCTURAL RELAXATIONS OF FOOD SOLIDS**

#### **1.3.1. MECHANICAL/DIELECTRIC PROPERTIES**

Amorphous food materials show varying relaxations with changes in heat content around the calorimetric glass transition. Such relaxations are observed from changes in mechanical and dielectric properties, that is, storage modulus ( $E'$ ), loss modulus



( $E''$ ), dielectric constant ( $\epsilon'$ ), dielectric loss ( $\epsilon''$ ), and  $\tan \delta$  (Angell, 2002). The  $E'$  and  $E''$  in viscoelastic materials measure the stored energy, representing the elastic portion, and the energy dissipated as heat, representing the viscous portion. The  $\epsilon''$  quantifies a dielectric material's inherent dissipation of electromagnetic energy in varying electromagnetic fields. It should be noted that the material (or its polar groups) responds to the stress under bending (or in alternating electric field), and an absorption maximum is obtained at the frequency that equals the molecular motion. The information on the rates of glass transition-related structural relaxations can be used to manipulate and control the rates of changes that occur during food processing, food products developing, and food storage. The DMA and DEA analyzer can be used to detect temperature-dependent dynamic changes and concomitant change in mechanical and dielectric properties and also probe the time scales of molecular motions in the region of the glass transition. Those measurements can be done isothermally to determine the loss factor as a function of frequency or by keeping the frequency constant to determine the response (damping) to the particular frequency as a function of temperature. Above time and frequency dependence of viscoelastic functions reflects the response of the system to the duration of the experiments. The response is dependent on the time required for the slowest rearrangement of molecules, that is, relaxation time. Fig. (1.4) shows the changes in  $E'$  or  $\epsilon'$  and  $E''$  or  $\epsilon''$  in amorphous materials as a function of temperature derived from DMA and DEA measurements. Structural relaxation times of the amorphous food solids are dependent on temperature, pressure, and amount of a plasticizer. The  $\tau$  at the  $E''$  (or  $\epsilon''$ ) peak temperature can be derived from the frequency ( $f$ ) by using  $\tau = 1/2\pi f$  (Maidannyk and Roos, 2016). However, it should be noted that relaxation phenomena reflect the approach of the material toward equilibrium, which occurs also in the glass state, but the relaxation times are orders of magnitude larger than above  $T_g$ .

### 1.3.2. SUB- $T_g$ RELAXATIONS AND ENTHALPY RELAXATION

SUB- $T_g$  RELAXATIONS The large-scale molecular motions become extremely slow

and the molecules are “frozen” at  $T_g$ , and the material cannot respond to further changes in temperature within the experimental time scale thereafter. Thus, the sensitivity of the relaxation processes to temperature is independent of the temperature below  $T_g$  (Le Meste et al., 2002; Donth, 2013). Below the  $T_g$ , even several sub- $T_g$  relaxations, i.e.,  $\beta$ - and  $\gamma$ -relaxation, can be observed in many low molecular weight sugars as temperature decreases, but their origin is still being discussed (Champion et al., 2000). Johari (1976) points that the  $\beta$ -relaxation is caused

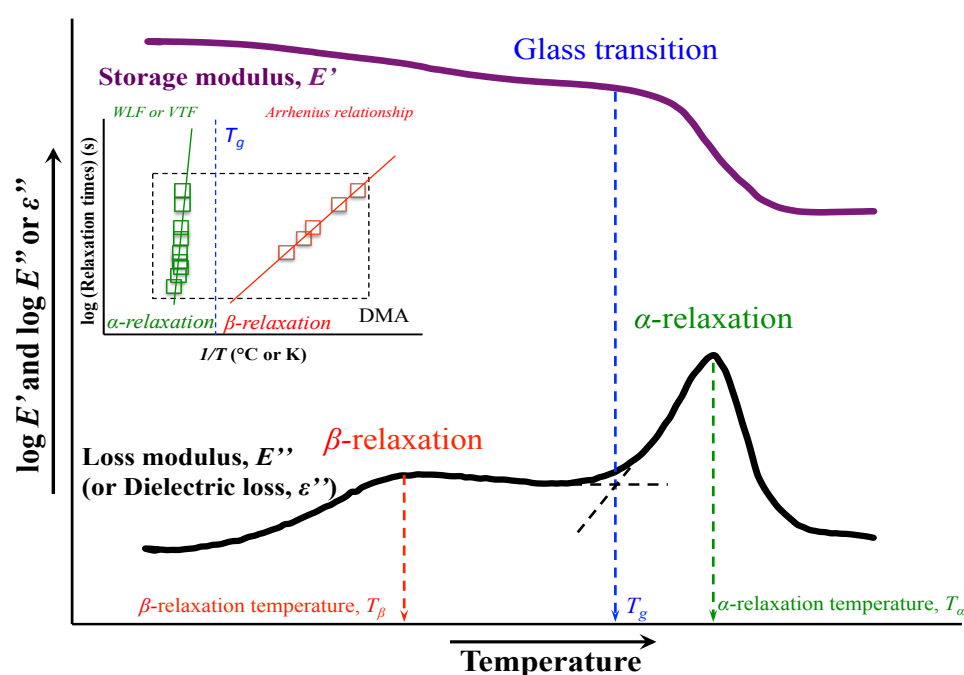


**Fig. 1.4.** The changes of storage modulus ( $E'$ ), loss modulus ( $E''$ ), and dielectric loss ( $\epsilon''$ ) of a glassy material derived from DMA and DEA spectra, respectively. The  $E'$  is high in the glassy state and it decreases dramatically as a result of glass transition temperature,  $T_g$ . The  $E''$  or  $\epsilon''$  show peaks below  $T_g$  due to the occurrence of molecular rotations induced structural relaxations, such as  $\beta$ -Relaxation. A significant peak in  $E''$  or  $\epsilon''$  occurs as  $\alpha$ -relaxation temperature ( $T_\alpha$ ) over the  $T_g$  temperature range.

by the motion of specific chemical groups such as the  $-\text{OH}$  groups branched on sugar molecules. In other words,  $\beta$ -relaxation is the motions of a short sequence of the

molecules in regions where density and intermolecular forces are at minimum. The apparent activation energy ( $E_a$ ), which corresponds to the minimum interaction energy between molecules, can characterize the relaxation processes of amorphous food materials. Champion and Others (2000) reported that the  $E_a$  value range for  $\beta$ -relaxation in sugars is between 40 to 70 kJ/mol. Similarly to  $\beta$ -relaxation,  $\gamma$ -relaxation takes place at lower temperature and is also localized and non-cooperative but is much weaker than  $\beta$ -relaxation (Yoshida, 1995). The loss of crispy texture might result from sub- $T_g$  relaxations or could be associated with motions just preceding the onset of the  $\alpha$ -relaxation (Champion et al., 2000). Moreover, Le Meste and Others (2002) considered the sub- $T_g$  relaxation is a continuation of the  $\alpha$ -relaxation. As the restricted molecular motions existed in glassy state, the relaxation times of  $\beta$ - and  $\gamma$ -relaxations are above 100 s with viscosities above  $10^{12}$  Pa below  $T_g$  and orders of magnitude larger than above  $T_g$  (Angell, 2002).

ENTHALPY RELAXATIONS Amorphous materials are thermodynamically unstable, and during storage their structures tend to relax toward the equilibrium state. Since the enthalpy (or heat capacity) of an amorphous material changes over time, this phenomenon can be defined as enthalpy relaxation ( $H$ -relaxation) or physical aging due to it depends on the thermal history of the materials and the time scale of observation. In glass, the  $H$ -relaxation of amorphous food solids may result from thermal annealing or changes in water content and composition during dehydration and storage (Kim et al., 2003; Liu et al., 2006). It should be noted that the  $H$ -relaxation might appear either as endothermic or exothermic peaks in DSC scans over the  $T_g$  range under different heating and cooling rates. The heating and cooling rate affects the physical state of amorphous food materials in terms of enthalpy, which can be observed from relaxation phenomena as the glass is heated to temperatures above  $T_g$ . For example, cooling followed by heating of an amorphous material at the same rate gives no indication of  $H$ -relaxation phenomena. The exothermic peak often appears in slow heating of the fast-cooled material due to the decreasing enthalpy and a longer time for the molecules to relax is needed above  $T_g$ .

than was allowed during the initial cooling over the same temperature range. An endothermic peak is observed when a slowly cooled material is heated rapidly over glass transition (Fig. 1.1). Because the rapid heating does not allow sufficient time for the molecules to relax at the glass transition corresponding to the initial cooling rate, and extra energy at a higher temperature is needed for the relaxation of molecules to the supercooled liquid-like state. In food storage, the  $H$ -relaxation needs to be taken into consideration when quality is of a concern for foods stored below their  $T_g$  (Yoshida, 1995; Haque et al., 2006). Although currently very few studies have been reported on the relationship between the enthalpy relaxation and food quality, the  $H$ -relaxation is believed to be as important as the glass transition to the quality of food stored below its  $T_g$  (Liu et al., 2006). For example, the  $H$ -relaxation may give information on time-dependent changes (or physical aging) in glass structure of starch, which can be related to free-volume relaxation caused embrittlement in the glassy state (Shogren, 1992; Noel et al., 1993; Enrione et al., 2012). The relationships between  $H$ -relaxation and its relaxation times have been recognized depending on stretched exponential relaxation function and nonlinearity characteristic of  $H$ -relaxation, and their applications in the characterization of physical properties of amorphous sugars and pharmaceutical materials have been documented (Tant and Wilkes, 1981; Champion et al., 2000; Liu et al., 2006). For instance, Wungtanagorn and Schmidt (2001ab) reported that the presence of fructose in glucose/fructose mixtures decreased the relaxation times of  $H$ -relaxation based on DSC measurements. The  $H$ -relaxation of freeze-dried sucrose could be reduced by the presence of some pharmaceutical additives i.e., poly vinylpyrrolidone (PVP), poly vinylpyrrolidone-*co*-vinyl-acetate (PVP/VA), dextran and trehalose, when aged for the same length of time due to the reducing of the mobility of sucrose in mixtures (Shamblin and Zografi, 1998). However, it should be noted that there are still many problems in the application of  $H$ -relaxation in the characterization of physical properties of amorphous food and pharmaceutical materials and the one of the problems is perhaps heterogeneity such as porosity and its effect on physical properties in the macroscopic scale.

### 1.3.3. ALPHA-RELAXATION AND CORRESPONDING RELAXATION TIMES

The  $\alpha$ -relaxation, as a reflection of glass-transition governed molecular motions on amorphous materials, may occur with increasing transition temperature to above  $T_g$ . Compared to sub- $T_g$  relaxations and  $H$ -relaxation, therefore,  $\alpha$ -relaxation is general, cooperative, non-Arrhenius, linked to viscous flow, and synonymous with the glass transition (Yu et al., 2001; Donth, 2013). The  $\alpha$ -relaxation results in a sharp decrease of the  $E'$  and an increase in  $E''$  (or  $\epsilon''$ ) with increasing temperature as a rapid increasing of molecular motion occurred above  $T_g$  during DMA/DEA studies (Fig. 1.3). The  $E'$  has a high value of  $10^{6.5}$  to  $10^{9.5}$  Pa in the glassy state, but suffers a dramatic decrease as  $\alpha$ -relaxation takes place at the glass transition (Roos, 2010). Arrhenius plots showing  $\log f$  against  $1/T$  have suggested that the  $E_a$  of the  $\alpha$ -relaxation is 200 ~ 400 kJ/mol (Kalichevsky and Blanshard, 1993). The  $E''$  and  $\epsilon''$  show a pronounced peak at the  $\alpha$ -relaxation temperature ( $T_\alpha$ ) in Fig. (1.4). Cocero and Kokini (1991) reported that the  $E''$  peak temperature and onset of the  $E''$  peak of glutenin and sugars occurred close to the endset of  $T_g$  measured with DSC, respectively. The  $\alpha$ -relaxation associated  $\tau$  characterizing mechanical properties are related to molecular mobility, which is related to  $T_\alpha$ . DMA and DEA studies of food materials have shown a significant decrease in  $\tau$  around the glass transition when derived from the respective frequency-dependent  $E'/E''$  or  $\epsilon''$ . The  $\tau$  shows that there is a significant increase in mobility of carbohydrate components in food materials within the  $T_g$  range measured by DSC (Champion et al., 2000; Liu et al., 2006). As the temperature is increased to above the  $T_g$ , dramatic decreases in the  $\tau$  of mechanical changes and in viscosity are obvious. Relationships between temperature and  $\tau$  are used in the time-temperature superposition principle, which applies to the mechanical properties of various amorphous materials, including food materials (Ferry, 1980).

VISCOSTIY, RELAXATION TIMES, AND VTF EQUATION Viscosity ( $\eta$ ) is a time-dependent quantity and a measure of the  $\tau$  above glass transition (Sperling, 2005). The temperature dependence of  $\tau$  and  $\eta$  above  $T_g$  is defined by the relationship of Eq. (1.7) and (1.8), where  $a_T$  is a ratio between  $\tau$  and  $\tau_s$  of configurational rearrangements at a temperature  $T$ , to that at a reference temperature,  $T_g$ ;  $\tau$  and  $\eta$ , and  $\tau_s$  and  $\eta_s$ , refer to relaxation time and viscosity at  $T$  and  $T_g$ , respectively. For an amorphous food material, the flow behavior is no longer Arrhenius-like, and its mechanical properties are strongly dependent on temperature where the temperature coefficient (a coefficient indicates the relation between changes in flow behavior and corresponding changes in temperature) increases as temperature decreases.

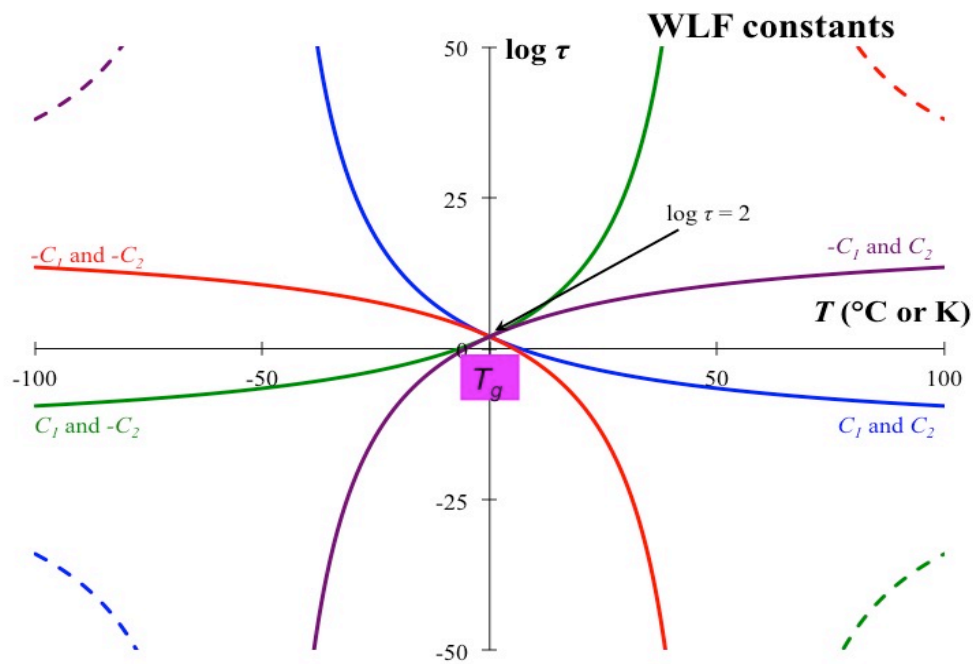


**Fig. 1.5.** WLF plots with the universal constants,  $-C_1 = -17.44$  and  $C_2 = 51.6$  based on Eq. (1.9), and the  $T_g$  as the reference temperature. The structural relaxation times at  $T_g$  are typically found as  $10^2$  s (Angell, 2002).

The most popular expressions are Vogel-Tammann-Fulcher (VTF) equation, power-law, and Williams-Landel-Ferry (WLF) equation, which can be used to

elaborate the  $\eta$  or any other temperature-dependent mechanical/dielectric property at temperatures above  $T_g$ . The VTF equation (Eq. 1.8) is commonly used to predict temperature dependence of  $\eta$  of supercooled liquids and describe changes in  $\tau$  above the glass transition, where  $A$ ,  $D$ , and  $r$  are constants;  $T_s$  refers to a reference temperature,  $T_g$  (Angell et al. 1994).

$$\ln a_T = \ln \left( \frac{\tau}{\tau_s} \right) = \ln \left( \frac{\eta}{\eta_s} \right) \quad (1.7)$$

$$\eta = \eta_s e^{DT_s/(T-T_s)} \quad (1.8)$$

WLF EQUATION Williams and Others (1955) presented a single empirical function (Eq. 1.9), where  $C_1$  and  $C_2$  are constants and  $T_s$  is a reference temperature, to describe the temperature dependence of mechanical properties of amorphous materials above their  $T_g$ . The WLF relationship of the free volume and viscosity may be used to show the applicability of the WLF relationship to fit  $\eta$  and  $\tau$  above the glass transition (Slade et al., 1991). If the suggested “universal” constant values are  $-C_1 = 17.44$  and  $C_2 = 51.6$  for amorphous foods by using of  $T_g$  as the reference temperature (Slade et al., 1991), the WLF relationship is applicable over the temperature range from  $T_g$  to  $T_g + 50$  °C. It should be noted that fitting of the WLF model to experimental  $\tau$  might result in positive or negative values or negative values for the universal constants  $C_1$  and  $C_2$ . The possible combinations result in eight different curves in the WLF plots, as shown in Fig. (1.5), and it also shows the meaning of the constants  $C_1$  and  $C_2$ . It is important to note that the VTF and WLF equations are interconvertible and that the WLF equation can be written in the form of the VTF relationship where slope, however, varies with  $T-T_s$  (Eq. 1.10). Compared to the VTF relationship, the free volume-based WLF theory has probably been the most applicable and simple in predicting the temperature-dependent mechanical properties of amorphous materials.

$$\log a_T = \ln \left( \frac{\tau}{\tau_s} \right) = \ln \left( \frac{\eta}{\eta_s} \right) = \frac{-C_1(T-T_s)}{C_2+(T-T_s)} \quad (1.9)$$

$$\ln \eta = -(C_1 - \ln \eta_s) + \left( \frac{C_1}{\frac{1}{C_2} + \frac{1}{T-T_s}} \right) \frac{1}{T-T_s} \quad (1.10)$$

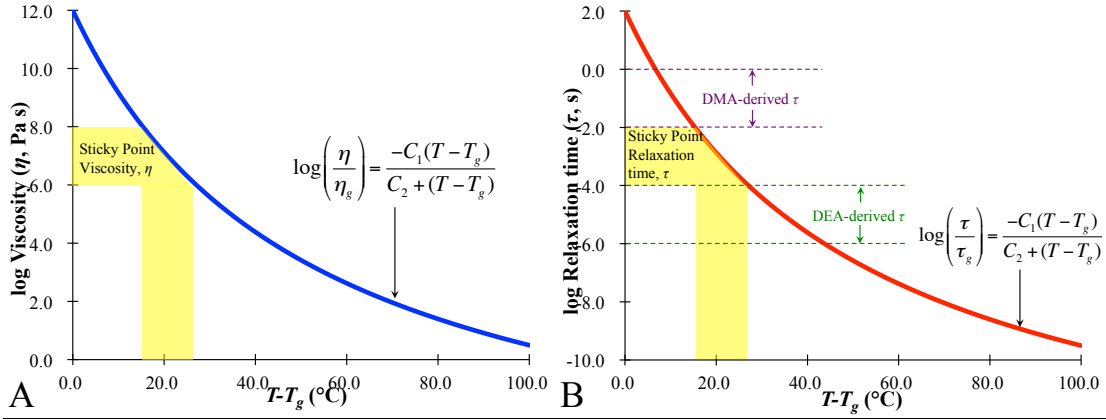


**Fig. 1.6.** Viscosity (A) and mechanical/dielectric relaxation times (B) as measured using DMA and DEA data above  $T_g$  predicted by the WLF-relationship with the universal constants,  $-C_1 = -17.44$  and  $C_2 = 51.6$ . Roos and Others (2016) Reported that the  $\tau$  decreased from  $10^{-2}$  s to  $10^{-4}$  s is known to result in particle stickiness and aggregation at a contact time of 10 s.

The DMA and DEA measurements show that the  $\tau$  data measured around  $T_g$  region for several glass-forming food compounds followed the WLF relationship (Fig. 1.6), while the use of universal constants ( $C_1$  and  $C_2$ ) in WLF equation (Eq. 1.9) in these compounds has been criticized. The universal constants may show a non-Arrhenius trend of changes in  $\tau$  above the  $T_g$  when sufficient data for calculating specific constants for a specific material are unavailable. The  $\tau$  of mechanical and dielectric properties at onset calorimetric  $T_g$  is extremely long, and the experimental determination of  $\tau_g$  is often impossible. Angell (2002) reported a value of 100 s for the use as  $\tau_g$  at onset calorimetric  $T_g$  in Eq. (1.9). If experimental data for  $\tau$  data above the  $T_g$  are available, the material-specific WLF constants may be derived using the linear form of the WLF equation (Eq. 1.11), which demonstrates that a plot of  $1/\ln a_T$



against  $1/(T-T_s)$  give  $1/-C_1$  and  $C_2/C_1$  from the intercept and slope, respectively. Based on DMA and DEA data measured in several food solids by using WLF analysis, the  $C_1$  and  $C_2$  with negative values mathematically determine the gradient of the downward concavity in Fig. (1.5) with red line, which show a rapid decrease of  $\tau$  at temperatures above calorimetric  $T_g$  when derived from the respective frequency-dependent  $E''$  or  $\varepsilon''$  derived  $T_\alpha$  (Roos et al. 2016). Consequently, the WLF analysis for flow behavior uses the material-specific constants to measure and describe the relaxation times above  $T_g$ , and thus, can give a measure for the mixes of glass forming carbohydrates, proteins and other food components.

$$\frac{1}{\ln a_T} = \frac{\log \tau_s}{\log \tau} = \frac{1}{-C_1} - \frac{C_2}{C_1(T-T_s)} \quad (1.11)$$

## **1.4. MATERIAL CHARACTERISTICS AND FOOD SOLIDS STABILITY**

### **1.4.1. RELAXATION TIMES AND FOOD SOLIDS STABILIZATION**

Molecular mobility has been considered as one of the most important properties of food materials, which could be used to control food processability and improve stability of foods during processing and storage. As we mentioned in section (1.3), the use of dynamic-mechanical or dielectric techniques have given mobility maps, which could be used to offer the possibility of estimating mobility over a broad temperature range and present a comprehensive view of the different kinds of motions occurring in amorphous food solids. The molecular mobility of amorphous food solids was affected by many factors, such as temperature and water content. Fig. (1.7) shows a schematic diagram of the relationship between relaxation times and temperature (or water content) of amorphous food solids. In the glassy state, the relaxation times were very high due to the extremely high viscosity limited molecular mobility, and thus, amorphous food solids stay in stability zone. However, Molecular mobility within amorphous food materials becomes apparent around the  $T_g$ . As the

temperature increases to above  $T_g$ , the molecular mobility increases, which is evident from decreasing stiffness and viscosity and increasing solids flow over this critical temperature zone. It should be noted that many time-dependent phenomenon such as crystallization could occur in above critical temperature zone. With the temperature or water content keep increasing, the extent of changes in properties becomes instant

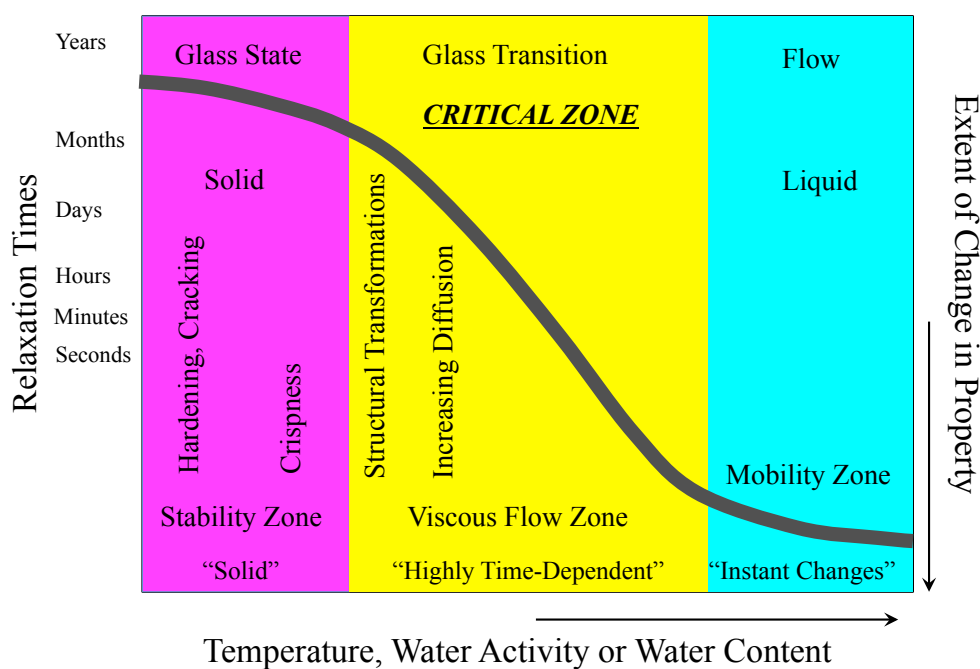


**Fig. 1.7.** A schematic diagram for presenting the relationship of relaxation times and extent of change in properties of food solids, such as textures, structural transformations and etc., concomitantly with temperature, water activity, or water content increases (Roos, 2016).

in food materials as the amorphous materials transfer to liquids (Fig. 1.7). Therefore, the changes of relaxation times in glass transition temperature zone could be considered as a “critical zone” for controlling food stability. Moreover, the Deborah number was applied to provide a useful translation of measured  $\tau$  to real experimental timescales. An important application of the Deborah number ( $De$ , the dimensionless value of relaxation time divided by experiment time) is shown for the time to crystallization of amorphous lactose in Fig. (1.8), which indicated that a comparison

of the structural relaxation times predicted using the WLF equation with the universal constants and time to crystallization showed also excellent agreement (Roos and Karel, 1992). It should be noted that the time to crystallization was measured experimentally and structural relaxation times were derived from dielectric and dynamic-mechanical properties showing a shift factor of  $10^6$  s (Roos and Drusch, 2015). Therefore, the  $De$  number could be expressed as  $De = 1 \text{ s} / 10^6 \text{ s} = 10^{-6}$  based on the data of relaxation times and time to crystallization. The use of the  $De$  with the WLF model gives a significant tool for extrapolation of data from structural relaxation time measurements to real time observations. Such applications are extremely important in the production of food powders as well as in agglomeration processes.

#### 1.4.2. FLOW CHARACTERISTICS

At temperatures below  $T_g$ , the glassy food materials are vitreous, hard, and brittle. The  $T_g$ , therefore, is the critical temperature at which the glassy material softens due to the onset of long-range coordinated molecular motions (Sperling, 2005). An increase in temperature may open a “window”, where  $\tau$  rapidly decreases and allows transformation of glassy materials into the less viscous state and then shows flow characteristics (or viscous flow) due to molecular motions dramatically increasing when  $T_g$  is exceeded. Such flow is time-dependent and the rate of flow may vary significantly around the  $T_g$ . Properties of food solids reflects a rheological phenomenon occurring in the transformation of the solid to liquid-like behavior, which is accompanied with the viscosity and  $\tau$  decreases. It is often achieved as a result of thermal, mechanical and dielectric changes, and water plasticization in the structure formation with a reflection of molecular motions above  $T_g$ . The flow behaviours above glass transition allow the observation of the transition from a rapid change in mechanical and dielectric properties. It is often assumed that product quality can be maintained in the glassy state. Changes in mechanical or dielectric properties may be caused by depression of the  $T_g$  to below storage temperature and

enhancement of viscous flow of amorphous food solids thereafter, which results in dramatic loss of acceptable quality.

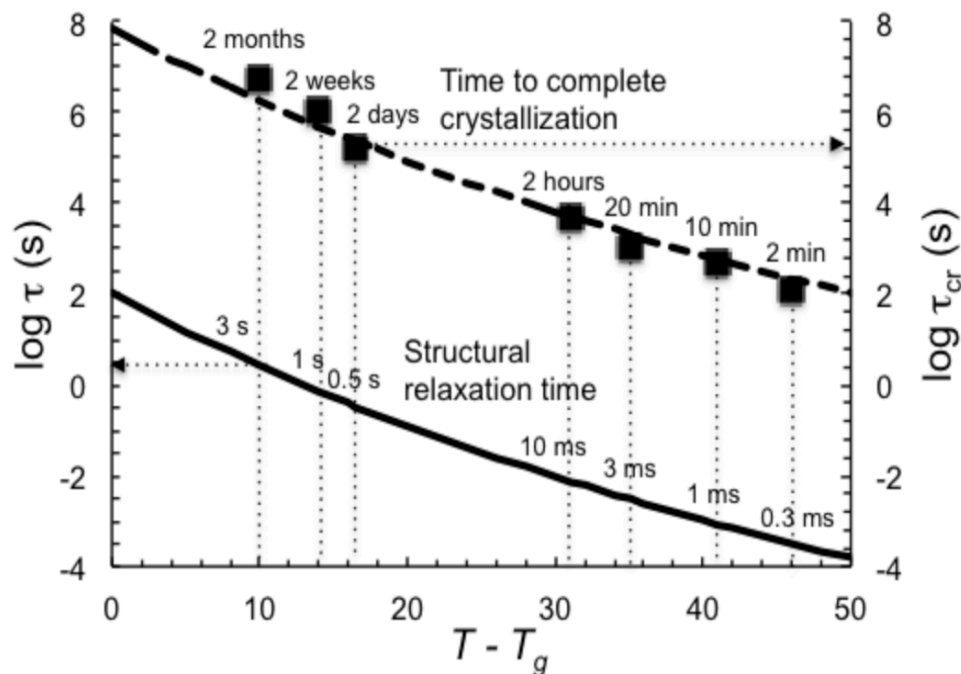


**Fig. 1.8.** WLF-predicted structural relaxation times with WLF fit to experimental time to crystallization for amorphous lactose at temperatures above  $T_g$ . The structural relaxation times show agreement with a shift factor of  $10^6$  s with experimental times to crystallization (Roos and Drusch, 2015).

“FRAGILITY” THEORY Angell (1991, 2002) used Eq. (1.7) derived  $D$  value to classify glass-forming materials to “strong” and “fragile” materials and showed a fragility as the  $F_{1/2}$  fragility ( $F_{1/2} = 2(T_{1/2}/T_g - 1)$ ,  $T_{1/2}$  is a temperature at which  $\tau = 10^{-6}$  s) or “steepness index,  $m$ ” ( $m = [m_{min}(1 + F_{1/2})(1 - F_{1/2})]$ ) according to their deviation from the Arrhenius temperature-dependence above their respective glass transition. The “strong” liquids ( $16 < m < 100$ ) are those following the Arrhenius relationship. However, fragility indicates how quickly the structural relaxation accelerates as a glass approaches and traverses the  $T_g$  region and it increases with increasing deviation from linearity of relaxation times against reciprocal temperature. The “fragile” liquids ( $100 < m < 200$ ) have strong temperature dependence of viscosity and molecular

mobility and exhibit larger changes of relaxation times in the vicinity of the glass transition than strong liquids (Angell, 2002). Moreover, the “strong” and “fragile” behavior of liquids could be interpreted in the terms of differences in configurational space potential energy, which indicates that “fragile” liquids have a high density of configurational states, leading to a rapid thermal excitation whereas “strong liquids” have a lower number in minima of their potential energy surface (Angell, 1988; Crowley and Zografi, 2001). Therefore, the “strong” and “fragile” classification can be used to describe the temperature dependence of the relaxation properties in the equilibrium state. For example, Fig. (1.9) shows the fragility approach with experimental data for  $SiO_2$  that is a strong glass former with Arrhenius behavior above the  $T_g$ . According to the “strong” and “fragile” classification, organic glass formers e.g., Glucose, Glycerol, and Propanol, and water appear as highly fragile glass formers (Fig. 1.9). Hancock and Others (1995) also indicated that the fragility of sugars and pharmaceutical polymers, i.e., sucrose, trehalose, lactose, poly vinylpyrrolidone, etc., can be estimated by calculating an activation enthalpy of structural relaxation at the glass transition from the scanning rate dependency of the  $T_g$  and glass transition width based on a thermal approach using DSC measurements. Similarly, Crowley and Zografi, (2001) proved that the thermal approach had a reasonable predictive ability for the fragility of pharmaceutical materials corresponding to the experimental VTF-derived  $D$  values (Eq. 1.8). The “strong” and “fragile” classification of most glass formers, however, fails in applications because the  $T_g$  values of the materials vary. Our conclusion is in agreement with Hodge (1996), who argued that the  $T_g$  is an inappropriate measure of the thermodynamic contribution to the VTF parameter  $D$  value because of its dependence on a kinetic quantity,  $T_g$ . For example, the  $D$  value increases systematically with increasing  $T_g$  of various carbohydrates and sugars, although their  $\tau$  shows similar temperature dependence above the  $T_g$  but over a different temperature range on the absolute temperature scale. In other words, such materials show similar temperature dependence of  $\tau$  above their individual  $T_g$  and, therefore, should have the same  $D$  and fragility. In this thesis, although the fragility indexes in Fig. (1.9) for glycerol and

glucose are different, they show similar changes in viscosity and  $\tau$  above the  $T_g$  and should be noted as equally fragile. The difference in the apparent fragility of these materials, as an example, is a serious problem and limitation of the fragility approach, which results from the differences in the individual  $T_g$  values and the  $T_g/T$ -scaling. Moreover, water shows the highest fragility and water plasticized food components may be assumed to increase in fragility with increasing water plasticization. Borde and Others (2002) reported that the addition of water in amylopectin could reduce the thermal energy necessary for promoting the cooperative chain motions associated with the glass transition, and thus, it increases the transition steepness and decreases the  $D$  parameter. However, in the present paper, glucose shows higher fragility than water based on literature viscosity data, which is contradictory to the fragility concept (Fig. 1.9). Despite these limitations of the fragility concept, it appears quite obvious that the “fragility” of water plasticized food materials increases with increasing water content.

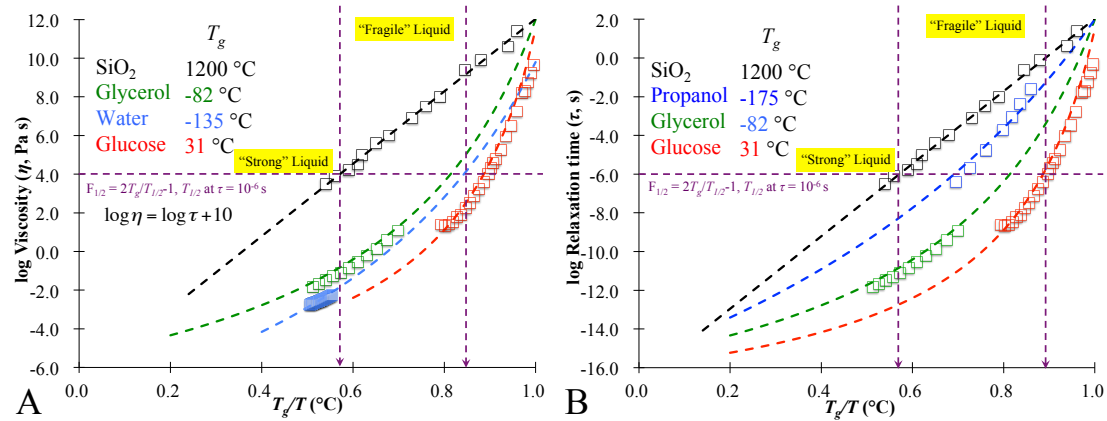


**Fig. 1.9.** Viscosity (A) and relaxation time as predicted by the WLF-relationship (B) above the  $T_g$  shown in “ $T_g$ -scaled” Arrhenius plots according to Angell (2002) with experimental viscosity data for  $\text{SiO}_2$  (Angell, 2002), glucose (Parks and Gilkey, 1951), glycerol (Segur and Oberstar, 1951) and water (Hallett, 1963). According to Angell (2002), fragility is shown as the  $F_{1/2}$  fragility or “steepness index”,  $m = [m_{\min} (1 + F_{1/2})(1 - F_{1/2})]$ , where  $m_{\min}$  is 16 for  $\tau_{\min}$  and 17 for  $\eta_{\min}$ .

STRUCTURAL “STRENGTH” CONCEPT Roos and Others (2016) introduced a simple concept “strength,  $S$ ” with unit of °C, as the temperature difference between the material temperature and its onset  $T_g$  that gives rise to a  $10^4$  reduction in  $\tau$  (or viscosity), to describe the solid-flow characteristics and structural transformations within the mixes of glass forming carbohydrates, proteins and other food components by using WLF model-based analysis of  $\tau$  above the calorimetric  $T_g$ . The  $S$  parameter was developed for the use in studies of noncrystalline food materials and their flow properties in typical processing and storage conditions, where a component or miscible components within food structure may experience the glass transition. Besides the strength of food solids, the Deborah number may be applied to provide a useful translation of measured  $\tau$  to real experimental timescales. Fig. (1.10) is a schematic diagram to show a decrease of  $\tau$  over a number of logarithmic decades for flow, e.g., that critical for stickiness, which can be defined as the critical parameter,  $ds$ , of Eq. (1.12) and a corresponding  $T-T_g$  is given as the strength of the solids,  $S$  (Eq. 1.13). As noted above, the  $\tau$  of glassy food materials, such as mechanical or dielectric  $\tau$  and calorimetric relaxations at the onset calorimetric  $T_g$ , are typically 100 s and assumed to approach  $10^{-14}$  s at high temperatures. Roos (2010) reported that the  $\tau$  of food systems decreased from  $10^2$  to  $10^{-2}$  s corresponding to a decrease in viscosity from  $10^{12}$  to  $10^8$  Pa at  $\sim 30$  °C above the  $T_g$ , which agreed with critical viscosities for collapse in freeze-drying and stickiness in spray drying. Therefore, the strength of carbohydrates-polymeric food systems can be calculated at  $d_s = 4$ . The  $S$  is a simple concept, which describes the time-dependence of solid-flow characteristic and structural transformations of glass formers above the calorimetric  $T_g$ . We expect that the strength of the glass formers and their interaction with other solids contribute to powder characteristics. Moreover, the  $S$  concept is using information of the non-crystalline state of food materials in a systematic manner to guide structure formation in food processing as well as for stability control of resultant products. Such structures can be used to include dispersed phases and their stabilization using various materials.

The derivation of  $S$  is shown as follows. Set the  $\tau$  at  $T_g$  as  $\tau_g$  to replace  $\tau_s$  in WLF equation (Eq. 1.9),  $\log \tau - \log \tau_g$  as  $d_s$  and  $T - T_g$  as  $S$ ,

$$\log \frac{\tau}{\tau_g} = d_s = \frac{-C_1(T-T_g)}{C_2+(T-T_g)} = \frac{-C_1 S}{C_2+S} \quad (1.12)$$

Then,  $S$  can be calculated based on Eq. (1.12) as:

$$S = \frac{d_s C_2}{-C_1 - d_s} \quad (1.13)$$

Where,  $C_1$  and  $C_2$  and  $d_s$  shown in Eq. (1.12) and Eq. (1.13) refer to the material-specific WLF constants and the decrease in the number of logarithmic decades for  $\tau$  ( $d_s = 4$  was used for various food materials).

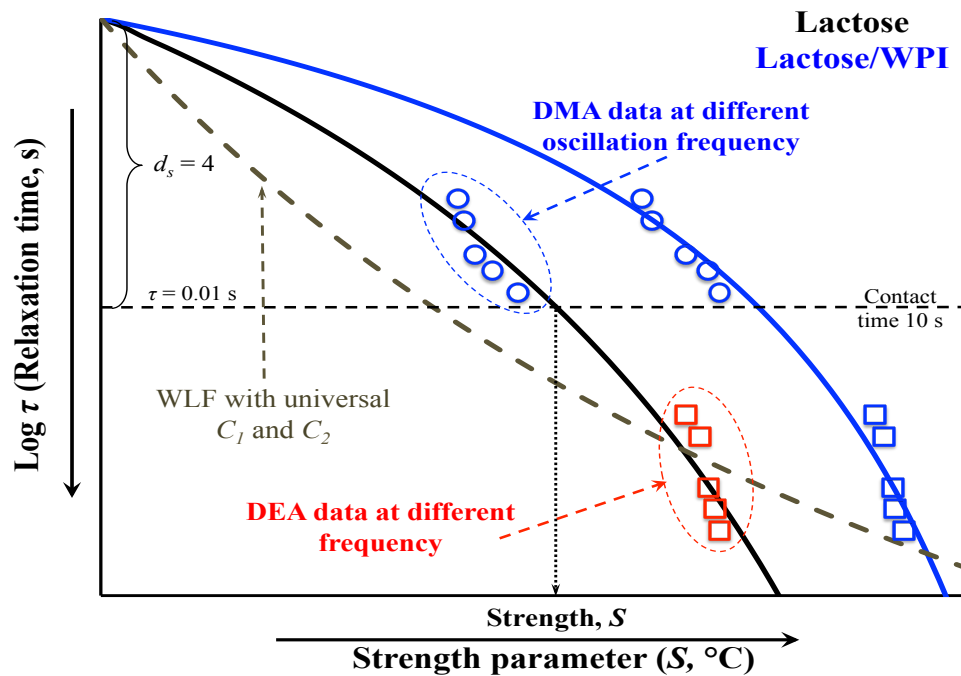


**Fig. 1.10.** The schematic diagram of “strength,  $S$ ” concept, at  $d_s = 4$  decreasing the structural relaxation times ( $\tau \approx 100$  s), as measured using



DMA to  $\tau = 0.01$  s. Such decrease in  $\tau$  is known to result in particle stickiness and aggregation at contact time of 10 s.

### **1.4.3. STRENGTH AND FOOD STABILITY**

As would be expected, the main applications of structural relaxations information of food material properties include optimization of formulation, proper control of processing, and storage conditions to achieve and maintain optimal food quality and desired performance and to provide stability. The processing and storage conditions are often chosen by trial and error without knowledge of the physicochemical changes occurring within food solids. The stability of amorphous food solids during storage is affected by the extent of molecular motions-caused structural relaxations behavior, which can be quantified and described by the  $S$  parameter. Some of the works on effects of structural relaxation times on food processing and storage have been done on stability of low-moisture food solids. In dehydrated foods, changes during storage include deteriorative changes that are strongly dependent on water content as well as loss of structure and volatile components. Collapse and loss of structure of amorphous food materials occur because of viscous flow that results from decreasing viscosity and the materials become unable to support and carry their own mass above glass transition (Levi and Karel, 1995). Collapse can be observed during dehydration processes and subsequent change in the physical state and loss of quality of dehydrated foods (Burin et al., 2004; Meister and Gieseler, 2009). Therefore, the  $S$  parameter could be used as a convenient measure to estimate amorphous food solids tendency of collapse during dehydration process and powder storage.

## **1.5. CONCLUSIONS**

Understanding glass transition, crystallization, and structural relaxations and their coupling with processing and storage performance of amorphous food solids is

essential for the formulation and design of complex food systems. It should be noted that the water properties is also important to be considered as it could interrupt the glass transition, crystallization and structural relaxations of amorphous food solids. The glass transition behavior of food systems may often be misleading in the prediction of characteristics of food components and their storage stability, as  $\tau$  determined for mixtures of carbohydrates and proteins vary and need to be interpreted carefully. The fragility concept, because of its limitations, cannot explain glass forming-properties of food systems, but strength concept gives a simple approach for the description of process-structure-property that can advance innovations in food formulation by mapping engineering properties of food components and their mixes. Moreover, the  $S$  parameter could be used to give a quantitative measure to estimate compositional effects on  $\tau$  and the control of solids properties, such as stickiness, caking, collapse, and etc. Although either glass transition and its-related structural relaxation or crystallization has been extensively investigated in various foods, there is only limited amount of them to build connections between these two transitions and the consequent influence on food properties. Despite the research reviewed in this chapter, it would be valuable to apply this information on other food products, especially those containing larger molecules. The study of solids properties with strength concept for complex food system is another meaningful direction even it usually requires high sensitive characterization methodology to figure out interactions among major components.



Volume 67, 29 October 2015, Pages 1-11

# X-RAY DIFFRACTION ANALYSIS OF LACTOSE CRYSTALLIZATION IN FREEZE-DRIED LACTOSE/WHEY PROTEIN SYSTEMS

Fanghui Fan and Yrjö H. Roos

*School of Food and Nutritional Sciences,  
University College Cork, Cork, Ireland*

## ABSTRACT

Water sorption, time-dependent crystallization and XRD patterns of lactose and lactose/WPI mixtures were studied with glass transition data. The results indicated that the sorbed water of lactose/WPI mixtures was fractional and water contents of individual amorphous components in lactose/WPI mixtures at each  $a_w$  from 25 °C to 45 °C could be calculated. Crystallization occurred in pure lactose whereas partial crystallization was typical of lactose/WPI mixtures (protein content  $\leq 50$  %) at intermediate and high  $a_w$  ( $> 0.44 a_w$ ) from 25 °C to 45 °C. The extents of crystallization were significantly delayed by WPI. The  $T_g$  values of lactose/WPI systems showed the composition-dependent property in systems and might indicate the occurrence of phase separation phenomena during 240 h storage. XRD showed no anhydrous  $\beta$ -lactose and mixed  $\alpha$ -/ $\beta$ -lactose with molar ratios of 4:1 crystals in crystallized lactose/WPI systems (7:3 and 1:1 solids ratios). Reduced crystallization in the presence of WPI was more pronounced possibly because of reduced nucleation and diffusion during crystal-growth. The present study showed that WPI could present an important role in preventing sugar crystallization.

**KEYWORDS,** *Crystallization; Protein inhibition; Crystallization kinetics; Glass transition; XRD patterns*

## 2.1. INTRODUCTION

Crystallization of amorphous sugars has a significant effect on the quality and shelf life of a number of products of biological, pharmaceutical and food industries (Roos, 1996; Das and Langrish, 2012ab; Sormoli et al., 2013). In amorphous systems, crystallization occurs as a result of increased molecular mobility above the glass transition (Slade et al., 1991; Roos and Karel, 1992; Roos and Drusch, 2015; Jouppila et al., 1997). The rates of crystallization of amorphous sugars are governed by water

content,  $RH$ , and the temperature of storage above its  $T_g$ ,  $T - T_g$  (Roos and Karel, 1991a). As water affects molecular mobility shown by a lowered  $T_g$  due to water plasticization, amorphous sugars may exhibit a high tendency for crystallization and a series of consequent problems during food processing and storage (Slade et al., 1991; Ibach and Kind, 2007). Below the  $T_g$ , however, mobility of sugar molecules is limited to vibrations and rotations, which kinetically limits crystallization and reduces rapid loss of product stability (Slade et al., 1991; Omar and Roos, 2007a). Previous studies showed that crystallization of amorphous sugars could be delayed by the presence of other sugars or impurities, i.e. starch (Iglesias and Chirife, 1978), corn syrup solids (Gabarra and Hartel, 1998), trehalose (Mazzobre et al., 2001), proteins (Sillick and Gregson, 2009), and maltodextrins, MD (Potes et al., 2012).

Lactose ( $\beta$ -D-galactopyranosyl (1-4)-D-glucopyranose) is often used in the food and pharmaceutical industries and it exhibits strong tendency to crystallize from its amorphous states, especially at a high storage  $RH$  (Nickerson, 1979). XRD patterns have shown that lactose may crystallize in a complex manner into a number of crystalline forms, mainly  $\alpha$ -lactose monohydrate, anhydrous  $\beta$ -lactose, stable and unstable  $\alpha$ -lactose and anhydrous  $\alpha$ -/ $\beta$ -lactose mixtures in molar ratios of 5:3 and 4:1 (Jouppila et al., 1998; Haque and Roos, 2005). The rate of crystallization depends on several factors, such as the rate of nucleation, the time required to remove water, storage temperature and molecular anomerization during crystallization (Aguilar et al., 1994; Drapier-Beche et al., 1997; Jouppila et al., 1998; Haque and Roos, 2005). Crystalline forms of lactose also differ in melting behaviour, solubility, density, crystal morphology, and relative sweetness (Nickerson, 1979; Lai and Schmidt, 1990). The crystalline forms of lactose in foods vary as their formation depends on the presence of other components, which may be related to interactions between lactose, supersaturation in systems, diffusion of lactose molecules or delayed mutarotation of molecules during nucleation and crystal-growth stages (Berlin et al., 1968; Jouppila and Roos, 1994ab; Jouppila et al., 1997; Fitzpatrick et al., 2007).

Whey protein isolate (WPI) may act as stabilizer in sugar/protein systems during spray drying and freeze-drying (Ratti, 2001; Oetjen and Haseley, 2004; Wang et al., 2010; Carullo and Vallan, 2012). Roos and Karel (1991a) showed that rates of lactose crystallization were controlled by  $T_g$  values and whey protein could delay crystallization of lactose and stabilize lactose in skim milk powder at high  $RH$  storage conditions. However, such inhibition of lactose crystallization may not entirely result from the  $T_g$ -dependant state of lactose in binary systems (Mazzobre et al., 2001; Silalai and Roos, 2010). The crystallization and glass transition properties of lactose in foods have been well documented and also several technologies are used in investigating the mechanism of protein inhibition of crystallization, i.e. SEM and protein characterization technology (Jin et al., 2000; Wang, 2005; Shawqi-Barham et al., 2006). Common hypotheses used in attempts to explain the mechanism of inhibition on lactose crystallization by proteins include the bond-hinder theory (Lopez-Diez and Bone, 2000), stereo-hindrance theory (Garti and Leser, 2001; Adhikari et al., 2009) and diffusion-limitation theory (Das et al., 2013).

The objectives of the present study were to investigate the relationships between the quantity of protein,  $T-T_g$ , lactose crystallization kinetics and crystalline forms of lactose as derived from water sorption and XRD data. This study is useful for understanding lactose/whey protein systems and crystallization of lactose in food and pharmaceutical materials as whey protein may present an important role in preventing sugar crystallization.

## **2.2. MATERIALS AND METHODS**

### **2.2.1. SAMPLE PREPARATION**

$\alpha$ -lactose monohydrate (Sigma-Aldrich, St. Louis, Mo., U.S.) and whey proteins (WPI; Isolac<sup>®</sup>, Carbery Food Ingredients, Co., Ballineen, Ireland; impurities including carbohydrates or lipids < 3 %) were used (O'Loughlin et al., 2013). Lactose was

dissolved in boiled distilled water ( $\sim 100\text{ }^{\circ}\text{C}$ ) to obtain 20 % (w/w) solution and then cooled to room temperature ( $20 \pm 3\text{ }^{\circ}\text{C}$ ). WPI solution with 20 % (w/w) solids was prepared using continuous stirring for 4 h at room temperature. Lactose and WPI solutions at room temperature were used to obtain solids ratios of 1:0, 7:3, 1:1, 3:7, and 0:1 of lactose/WPI, respectively. Samples of mixed solutions (5 mL in total) were prepared in pre-weighted glass vials (10 mL, diameter 24.3 mm  $\times$  height 46 mm; Schott Müllheim, Germany). All samples in the vials (semi-closed with septum) were frozen in a still air freezer at  $-20\text{ }^{\circ}\text{C}$  for 20 h and then subsequently tempered at  $-80\text{ }^{\circ}\text{C}$  for 3 h prior to freeze-drying using a laboratory freeze-dryer (Lyovac GT2 Freeze Dryer, Amsco Finn-Aqua GmbH, Steris<sup>®</sup>, Hürth, Germany). After freeze drying at pressure  $< 0.1\text{ mbar}$ , triplicate samples of each material were stored in evacuated vacuum desiccators over  $P_2O_5$  (Sigma-Aldrich, St. Louis, Mo., U.S.) prior to subsequent analysis.

### 2.2.2. WATER SORPTION AND LACTOSE CRYSTALLIZATION

Water sorption by freeze-dried lactose, WPI, and lactose/WPI at 7:3, 1:1, and 3:7 ratios were monitored by using static sorption method (SSM) for 120 h (non-crystallizing samples) and 240 h (crystallizing samples) over saturated solutions of  $LiCl$ ,  $CH_3COOK$ ,  $MgCl_2$ ,  $K_2CO_3$ ,  $Mg(NO_3)_2$ ,  $NaNO_2$ , and  $NaCl$  (Sigma Chemical Co., St. Louis, Mo., U.S.A.) at respective water activities,  $a_w$ , of 0.11, 0.23, 0.33, 0.44, 0.54, 0.65, and 0.76  $a_w$  depending on storage temperature ( $25\text{ }^{\circ}\text{C}$ ,  $35\text{ }^{\circ}\text{C}$ , and  $45\text{ }^{\circ}\text{C}$ ) (Greenspan, 1977; Labuza et al., 1985), in vacuum desiccators. The  $a_w$  measured (Dew Point Water Activity Meter 4TE, Aqualab, WA, USA) for the systems at each temperature is given in Table 2.1 Evacuated desiccators in incubators (Series 6000, Termaks, Bergea, Norway) were stored at  $25\text{ }^{\circ}\text{C}$ ,  $35\text{ }^{\circ}\text{C}$  and  $45\text{ }^{\circ}\text{C}$ , respectively. Vials with samples were weighted to monitor water sorption at 0, 3, 6, 9, 12, and 24 h followed by 24 h intervals up to 240 h, respectively (Jouppila and Roos, 1994a; Potes et al., 2012). Lactose crystallization was monitored from loss of sorbed water during storage over  $Mg(NO_3)_2$ ,  $NaNO_2$ , and  $NaCl$  at various storage temperatures (Potes et al.,

2012). All vials were closed with septum when transferred out of desiccators and septum was moved when vials were removed for weighing. Water contents of the materials were measured as a function of time, and the average weight of triplicate samples was used in calculations. The GAB equation was fitted to experimental data to model water sorption at 25 °C, 35 °C and 45 °C (Eq. 1.1) (Jouppila and Roos, 1997; Timmermann et al., 2001; Lievonen and Roos, 2002; Torres et al., 2011).

### 2.2.3. XRD ANALYSIS

Vials with pure lactose and lactose/WPI mixtures stored over  $Mg(NO_3)_2$ ,  $NaNO_2$ , and  $NaCl$  at each time point were filled with liquid nitrogen and stored at  $-80\text{ }^{\circ}\text{C}$  for 3 h followed by freeze-drying for 1 day (Haque and Roos, 2005). Such treatment ceased crystallization as a result of the lowering of the temperature and removal of the plasticizing water. The materials were powdered using mortar and pestle and then stored in sealed glass vials packaged in vacuumized plastic bags to prevent exposure to ambient air and water uptake. The XRD patterns were measured by using a STOE Powder XRD (STOE & Cie GmbH, PW 3830 generator, PW 3710 MPD diffractometer, Germany). The XRD was operated with an anode current of 40 mA and an accelerating voltage of 40 kV. Samples were slightly pressed on a steel sample tray covered by plastic slide ( $r = 5\text{ mm}$ ) and exposed to  $CuK\alpha$  radiation at diffraction angles ( $2\theta$ ) from  $5^{\circ}$  to  $30^{\circ}$  (step size,  $0.1^{\circ}$ ; time per step, 5s). The peak search program was the STOE Powder Diffraction Software Package WinX<sup>pow</sup> (STOE & Cie GmbH, Germany) software that was used to locate the peaks in XRD patterns by detecting the minima from the second derivative of the diffractogram. Intensity maxima were given as  $CuK\alpha$  net peak height in counts at  $CuK\alpha$  position in degrees. The types of lactose crystals formed in freeze-dried lactose powder were identified from the location of the characteristic peaks in XRD patterns. Appendix I show the  $2\theta$  for each lactose crystal type as determined from the XRD patterns of  $\alpha$ -lactose monohydrate, anhydrous  $\beta$ -lactose (Sigma Chemical Co. Louis, MO, USA) as well as pure WPI (Isolac<sup>®</sup>, Carbery Food Ingredients, Co., Ballineen, Ireland). The progress



of lactose crystallization was observed from increasing intensities of peaks in XRD patterns at 20.0° ( $\alpha$ -lactose monohydrate), 21.0° and 10.5° (anhydrous  $\beta$ -lactose), 19.2° and 19.7° (anhydrous  $\alpha$ -lactose and  $\beta$ -lactose in molar ratio of 5:3 and 4:1) (Jouppila et al., 1997; Haque and Roos, 2005).

#### **2.2.4. GLASS TRANSITION TEMPERATURE**

The GT equation (Eq. 1.3) has proven to be particularly useful in fitting experimental data on  $T_g$  and water content of amorphous sugars (Roos and Karel, 1991b; Roos, 1995). The  $T_g$  for non-crystalline lactose in mixtures was obtained from Eq. (1.3) at high  $a_w$  storage conditions (Gordon and Taylor, 1952). Potes and Roos (2012) reported that the lactose water contents at high  $RH$  could be estimated by Eq. (1.3), with  $T_{g1}$  of 105 °C for anhydrous lactose and a constant,  $k$ , of 8.1;  $T_{g2}$  for water was -135°C (Potes et al., 2012). The estimated  $T_g$  and corresponding  $T-T_g$  values were calculated for amorphous lactose and lactose/WPI mixtures stored at 25 °C, 35 °C and 45 °C and 0.56, 0.65 and 0.76  $a_w$ , respectively.

#### **2.2.5. STATISITICAL ANALYSIS**

The GAB model and predicted  $T_g$  of amorphous lactose based on GT equation were calculated and fitted by using Microsoft Office Excel 2011 (Microsoft, Inc., U.S.A.). All the measurements were repeated three times as well as the average value of above triplicate measurements was calculated with standard deviation.

### **2.3. RESULTS AND DISCUSSION**

#### **2.3.1. WATER SORPTION**

The GAB sorption isotherms, experimental data for lactose, lactose/WPI 7:3, lactose/WPI 1:1, lactose/WPI 3:7 and WPI over investigated water activity range at

25 °C, 35 °C, and 45 °C, and predicted water contents for non-crystalline lactose

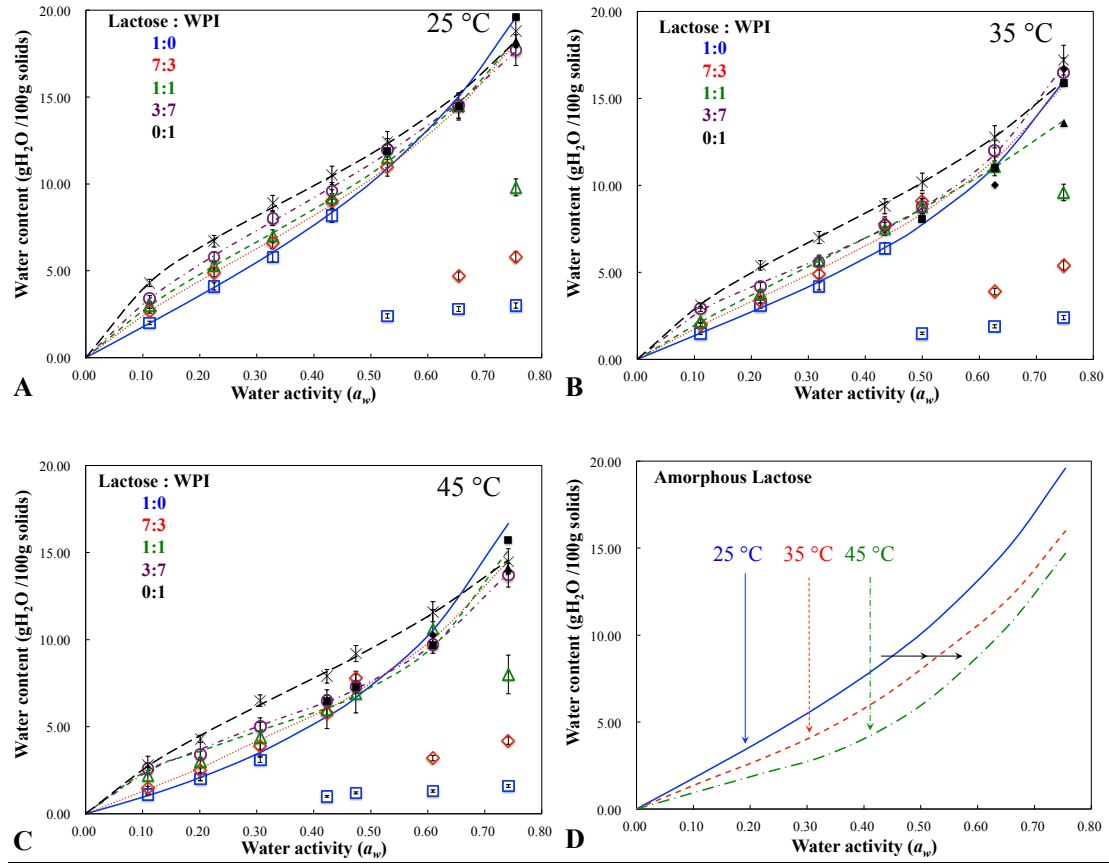


**Fig. 2.1.** The experimental (clear symbols) and calculated water content data (solid symbols) for amorphous lactose, WPI, and lactose/WPI mixtures at solids ratios of 7:3, 1:1, and 3:7 showed from A to C. The blue thick solid (Amorphous Lactose), red dotted (lactose/WPI 7:3), green short dashed (lactose/WPI 1:1), purple dashed-dotted (lactose/WPI 3:7), and black long dashed lines (WPI) correspond to the GAB sorption isotherms. The GAB sorption isotherm of non-crystalline lactose was obtained using experimental data ( $0.11 \sim 0.44 a_w$  at 25 and 35 °C;  $0.11 \sim 0.33 a_w$  at 45 °C) and data derived from lactose/WPI mixture (3:7) ( $0.55 \sim 0.76 a_w$  at 25 and 35 °C;  $0.44 \sim 0.76 a_w$  at 45 °C). The GAB sorption isotherms for non-crystalline lactose/WPI systems at 7:3 and 1:1 mass ratios used experimental data  $0.11 \sim 0.56 a_w$  and fractional water contents for non-crystalline lactose and data measured for lactose/WPI mixture (3:7) to predict sorbed water contents at 0.66 and 0.76  $a_w$ . The potential  $a_w$  shifts phenomena of lactose could be observed in D.

(0.53 ~ 0.76  $a_w$  at 25 and 35 °C; 0.42 ~ 0.74  $a_w$  at 45 °C) and lactose/WPI at 7:3 and 1:1 fraction ratios (0.61~0.76  $a_w$  from 25 °C to 45 °C) were given in Table 2.1 and shown in Fig. (2.1), respectively. Steady-state water contents of each material were used in GAB using data at 96 h although above steady state water contents could be achieved after 72 h storage. Water contents of pure lactose at intermediate and high  $a_w$  ( $> 0.44 a_w$ ) at 25 °C were slightly lower than in previous reports (Jouppila and Roos, 1994ab; Beristain et al., 1996; Omar and Roos, 2007a; Potes et al., 2012). These differences could result from variation in dehydration, sorption time or storage temperature. At each  $a_w$ , the steady state water contents of the materials were depressed by increasing storage temperatures, as there was a decrease in  $RH$  with temperature, which was considered as potential  $a_w$  shifts phenomena by previous studies (Greenspan, 1977; Labuza et al. 1985).

In the present study, the GAB model was fitted to experimental data of pure lactose below 0.56  $a_w$  (25 °C and 35 °C) and 0.44  $a_w$  (45 °C) as lactose crystallization occurred at higher  $a_w$  (Fig. 2.1). Systems with 7:3 ( $< 0.65 a_w$ ) and 1:1 of lactose/WPI ratios ( $< 0.76 a_w$ ) could use water sorption data over a wider  $a_w$  range (Jouppila et al., 1997; Kedward et al., 2000; Timmermann et al., 2001; Potes et al., 2012). As the wider water activity ranges were used in GAB model, the better fitting results would be achieved (Timmermann et al., 2001). Thus, the extrapolated sorption data of non-crystalline components, which predicted by GAB based on water sorption data at over a narrow water activity range ( $\leq 0.44 a_w$ ), could extensively exceed true sorbed water contents and cause significant errors (Potes et al., 2012). In the present study, experimental data at 0.11 ~ 0.44  $a_w$  and water contents at 0.55 ~ 0.76  $a_w$  derived from lactose/WPI mixture at 3:7 ratio (steady state sorbed water contents of non-crystalline components) water sorption data for non-crystalline lactose were used in the GAB model (Fig. 2.1). Sorbed water of lactose/WPI mixtures was fractional and the water contents of individual amorphous components at each  $a_w$  from 25 °C to 45 °C could

be derived according to fractional water sorption behavior (Eq. 1.2). Our study confirmed applicability of fractional water sorption to sugar/protein systems over a wide temperature range (25 ~ 45 °C) and the data provided sorbed water contents for non-crystalline lactose up to 0.76  $a_w$ .

### 2.3.2. TIME-DEPENDENT CRYSTALLIZATION AND CRYSTALLIZATION KINETICS

Sorbed water loss from freeze-dried lactose was most rapid at intermediate and high  $a_w$ . However, no crystallization of amorphous lactose in lactose and lactose/WPI systems occurred at low  $a_w$  ( $< 0.44 a_w$ ) during 10 days of storage at 25 °C to 45 °C. At intermediate and high  $a_w$  (0.55 ~ 0.76  $a_w$ ), lactose crystallization was affected by protein and the loss of sorbed water decreased concomitantly with increasing WPI (Fig. 2.2). WPI showed the strongest inhibition of lactose crystallization reflected by none of mixture losing sorbed water when stored from 25 to 45 °C at 0.54  $a_w$ . No crystallization was observed in lactose/WPI mixtures at 3:7 ratios over the whole water activity and temperature ranges during 240 h of storage (Fig. 2.2). But lactose/WPI at 7:3 and 1:1 showed sorbed water loss at the higher  $a_w$ . The decrease in water was less than in pure lactose which showed formation of a partially crystalline structure in mixtures as reported by Silalai and Roos (2010). Thus, the high RH might weaken protein inhibition of lactose crystallization probably due to rapid molecular mobility and enhanced rates of diffusion as a result of water plasticization (Roos, 1995). Gabarra and Hartel (1998) reported that lower molecular weight carbohydrates exhibited strong molecular motions and high diffusion rates with higher molecular weight carbohydrates at high  $a_w$ . In present study, however, the presence of high-molecular-weight protein could delay the low-molecular-weight lactose crystallization at intermediate water activities probably because of reduced arrangement of lactose molecules at crystal lattices. Lopez-Diez and Bone (2000) assumed that the presence of proteins might exhibit interactions with lactose and reduce lactose crystallization through hydrogen bonding. However, in the present

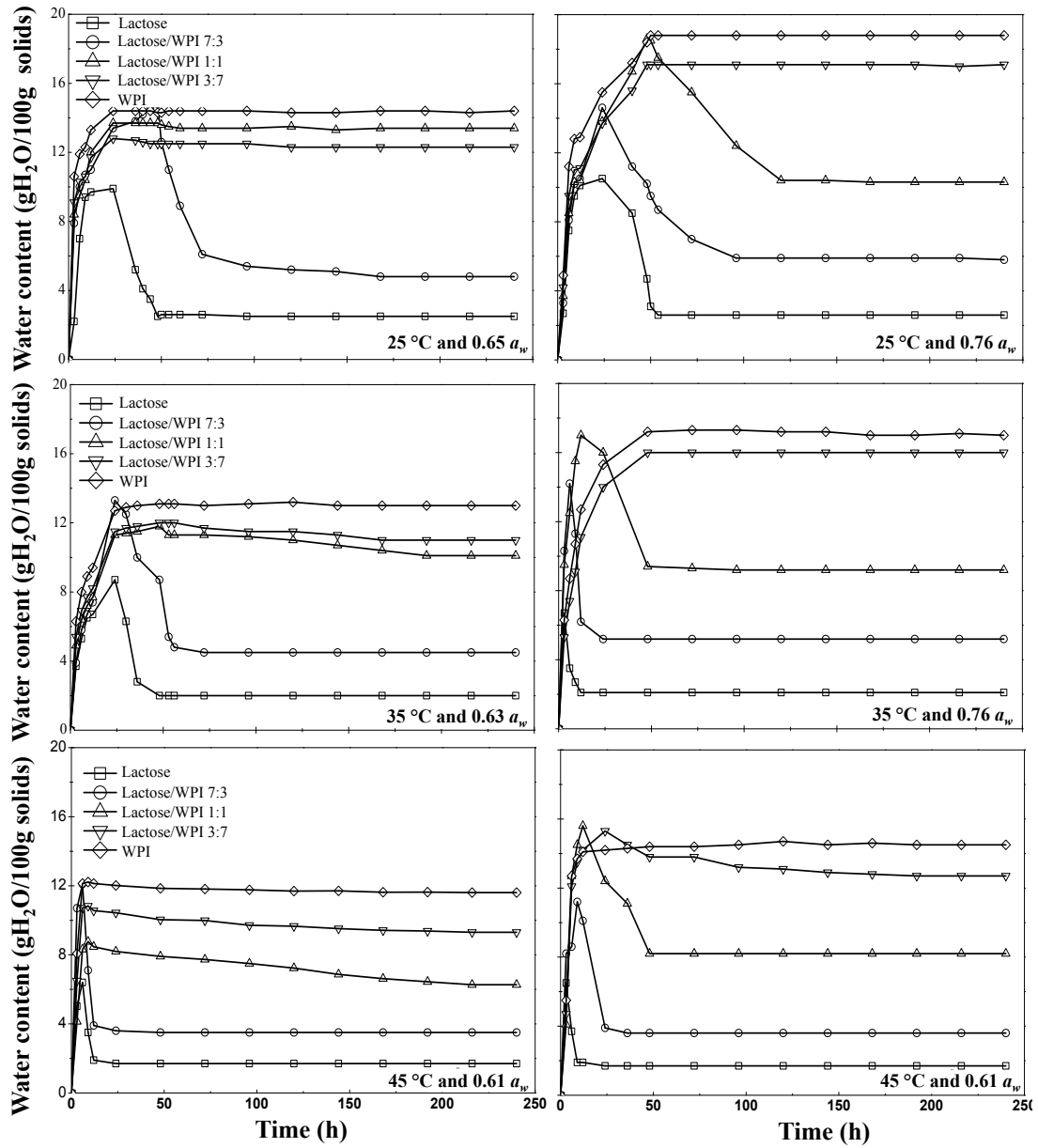
study, we noticed that the water contents in lactose/WPI systems showed composition independent water sorption characteristic, which could be related to the phase separation during water sorption testing (Silalai and Roos, 2010). Such phenomenon indicated that the water was individually hydrogen bonding to protein and lactose, thus, less hydrogen bonds might exist between protein and lactose in mixtures. Therefore, we assumed that the protein-derived crystallization inhibition effects were caused by either physical blocking or steric hindrance and it could reduce molecular diffusion, instead of trapping lactose to protein by hydrogen bonding (Mullin, 2001). We assumed that the lactose molecules might need a long induction time as well as higher activation energy for nucleation to form a stable nuclei center or migrating to the surface of crystal in order to release the water molecules during crystal-growth stage.

Fig. (2.3A) shows the rates of water release during storage in pure lactose and lactose/WPI at high  $a_w$  at 25 to 45 °C. The kinetics of water release was used as a measure of lactose crystallization kinetics (Potes et al. 2012). The inhibition of lactose crystallization by proteins was evident from the rate constant,  $k$ , as  $k$  decreased with the quantity of WPI in lactose/WPI mixtures (7:3 and 1:1 ratios) (Fig. 2.3 A). The relationship between the  $k$  and lactose quantity in lactose/WPI systems at 0.66 and 0.76  $a_w$  is shown in Fig. (2.3B). At 0.66 and 0.76  $a_w$ , the rate of loss of sorbed water of lactose/WPI systems rapidly decreased (close to zero) with increasing WPI content. The  $k$  was significantly depressed by the increasing weight fraction of WPI in systems with  $k$  close to zero below 50% and 70 % of WPI content at 0.65 and 0.76  $a_w$ , respectively (Fig. 2.3 B). Even the storage temperature could significantly affect lactose crystallization; the increasing quantity of WPI could delay the crystallization. Therefore, the kinetics of lactose crystallization in lactose/WPI depends on the lactose/WPI protein content during crystallization, which agreed with previous reports (Jouppila and Roos, 1994a; Gabarra and Hartel, 1998; Silalai and Roos, 2010; Das and Langrish, 2012a; Das et al., 2013).

**Table 2.1.** Water Content and  $a_w$  for Freeze-Dried Non-Crystalline Lactose, Amorphous WPI and Lactose/WPI Mixtures at Mass Ratios of 7:3, 1:1, and 3:7 Stored for 96 h at 25 °C, 35 °C, and 45 °C. The Water Content of Non-Crystalline Lactose at 0.53 to 0.76  $a_w$  (25 °C and 35 °C) and 0.42 to 0.74  $a_w$  (45 °C) Was Derived from Experimental Non-Crystalline Lactose in Lactose/WPI 3:7 ratio. Water Content of Non-Crystalline Lactose/WPI Systems were Obtained from Experimental Data at 0.11 to 0.53  $a_w$  and Fractional Water Content Calculated for Non-Crystalline and Measured for Lactose/WPI 7:3 and 1:1 to Predict Sorbed Water Content for Lactose/WPI Mixtures at 0.61 and 0.76  $a_w$ .

Storage Temperature	$a_w$	Lactose (Non-Crystalline)	Water Content (gH <sub>2</sub> O/ 100 g solids)				
			Lactose	Lactose/WPI 7:3	Lactose/WPI 1:1	Lactose/WPI 3:7	WPI
25 °C	0.11±0.00*	2.0	2.0±0.2	2.7±0.2	3.0±0.1	3.4±0.1	4.3±0.1
	0.23±0.00	4.0	4.0±0.3	4.9±0.1	5.3±0.1	5.8±0.1	6.7±0.1
	0.33±0.00	6.1	6.1±0.3	6.6±0.1	7.0±0.1	8.0±0.3	8.9±0.2
	0.43±0.00	8.4	8.4±0.4	9.0±0.2	9.2±0.0	9.6±0.1	10.5±0.1
	0.53±0.00	10.9	2.4±0.2	11.0±0.2	9.8±0.1	12.0±0.1	12.4±0.1
	0.65±0.01	15.0	2.8±0.4	4.7±0.1	11.5±0.1	14.5±0.3	14.4±0.1
	0.76±0.01	19.6	3.0±0.4	5.8±0.1	12.4±0.6	17.7±0.2	18.8±0.1
	0.11±0.00	1.5	1.5±0.3	2.0±0.1	2.2±0.2	2.9±0.2	3.1±0.1
	0.22±0.01	3.0	3.0±0.1	3.4±0.1	3.8±0.2	4.2±0.1	5.4±0.2
	0.32±0.00	4.5	4.5±0.1	4.9±0.4	5.1±0.1	5.5±0.2	7.0±0.1
35 °C	0.43±0.01	6.4	6.4±0.3	7.6±0.3	6.7±0.2	7.7±0.1	8.8±0.2
	0.50±0.00	7.8	1.5±0.5	9.8±0.3	8.8±0.3	9.1±0.2	10.2±0.2
	0.63±0.00	11.1	1.9±0.6	3.9±0.5	10.1±0.2	12.0±0.2	12.8±0.1
	0.75±0.01	16.0	2.4±0.4	5.5±0.3	9.6±0.2	16.5±0.2	17.2±0.1
	0.11±0.00	1.0	1.0±0.2	1.8±0.3	1.9±0.4	2.6±0.2	2.8±0.1
	0.20±0.00	2.1	2.1±0.1	2.5±0.3	3.0±0.3	3.4±0.1	4.3±0.2
	0.31±0.01	3.5	3.5±0.1	3.9±0.2	4.4±0.1	5.0±0.3	6.5±0.1
	0.42±0.00	5.6	1.2±0.4	5.8±0.2	6.0±0.1	6.5±0.1	7.9±0.1
	0.47±0.01	6.7	0.8±0.5	7.8±0.3	6.9±0.2	7.3±0.2	9.2±0.4
	0.61±0.01	10.5	1.3±0.8	3.3±0.3	9.4±0.3	9.7±0.2	11.7±0.2
45 °C	0.74±0.00	14.7	1.6±0.5	4.2±0.3	8.0±0.4	13.7±0.1	14.5±0.1

\*: Values are mean ± SD (n=3).



**Fig. 2.2.** Isothermal water sorption for freeze-dried lactose, WPI, and lactose/WPI mixture at all mass ratios (7:3, 1:1, and 3:7, w/w) around 0.65 and 0.76  $a_w$  stored at 25 °C to 45 °C for 240 h.

### 2.3.3. GLASS TRANSITION AND WATER LOSS

The  $T_g$  derived from GT equation, water contents and water activities (0.44 ~ 0.76  $a_w$ ) for non-crystalline lactose in freeze-dried pure lactose and lactose/WPI mixtures are shown in Fig. (2.4). Since the GAB gave the water content in each non-crystalline component in binary carbohydrate/protein system according to composition-dependent water sorption, the  $T_g$

values of lactose at a high  $a_w$  could also be obtained using Eq. (1.3) at high water activities at applicable temperatures up to 45 °C. The  $T_g$  values of non-crystalline lactose in mixtures were less than 0 °C at high water activities due to the higher water contents and stronger water plasticization at 25 °C than low and intermediate water activities in systems (Fig. 2.4 B).

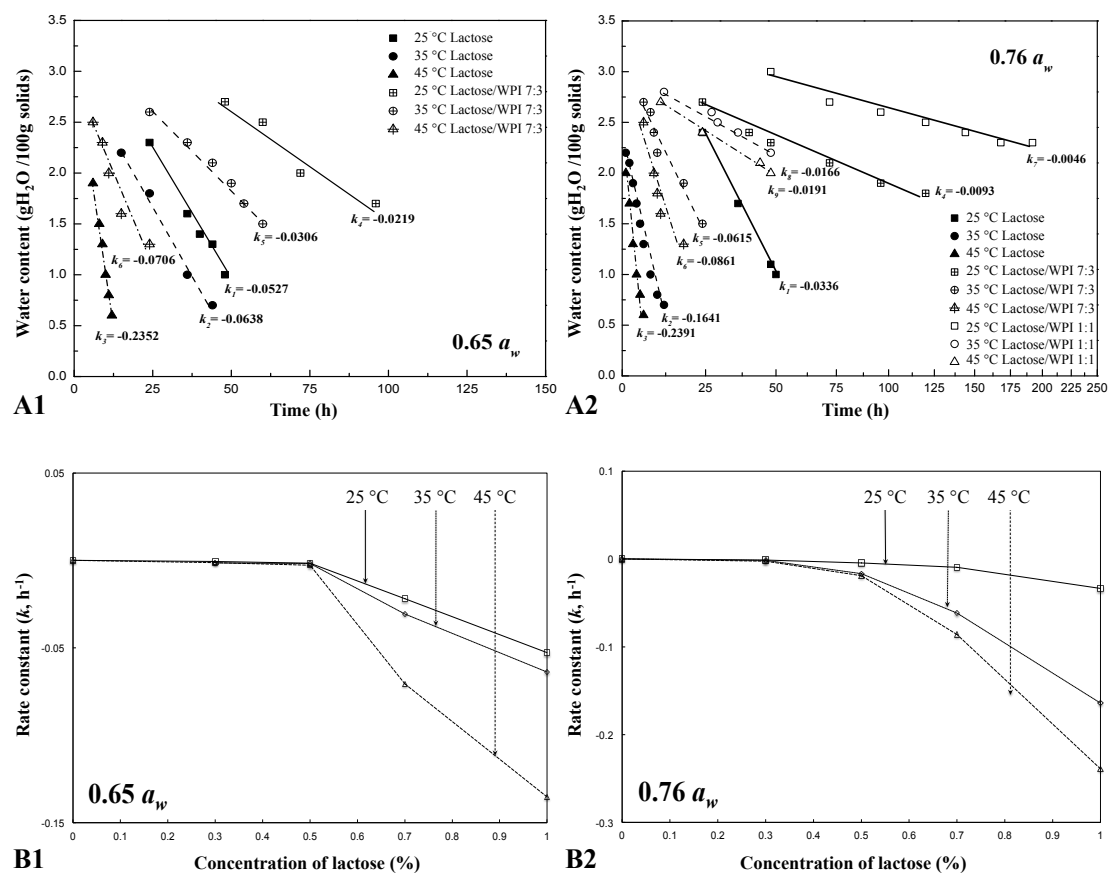


**Fig. 2.3.** Kinetics (A) and rate constant (B) ( $k$ ) for loss of water sorbed by lactose (solid symbols) and lactose/WPI systems at mass ratios of 7:3 (half solid symbols), 1:1 (empty symbols) around 0.66 (A1 and B1) and 0.76  $a_w$  (A2 and B2) under 25 °C, 35 °C and 45 °C, respectively.



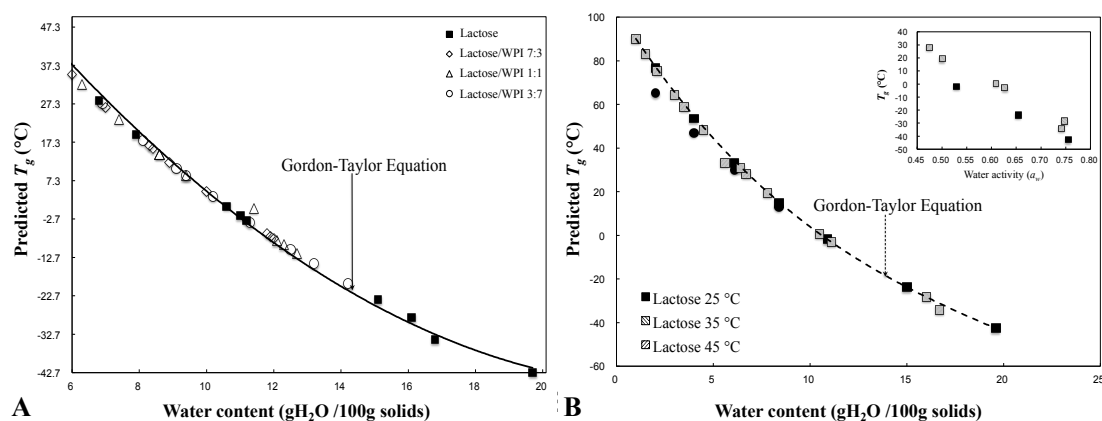


**Fig. 2.4.** Glass Transition Temperature ( $T_g$ ) of Pure Lactose and Lactose/WPI Mixtures Stored from 0.11 to 0.76  $a_w$  (Solid Square) at 25 °C to 45 °C (A) and Reference  $T_g$  Data (Solid Circle) from Silalai and Roos (2011) at Room Temperature (B) Against Water Content and Water Activity (0.54 ~ 0.76  $a_w$ ) Using the GT Equation. Data for  $T_g$  of Anhydrous Lactose and Water were From Potes and others (2012).

The  $T_g$  values of lactose at 0.11 ~ 0.44  $a_w$  agreed with previous studies at  $a_w$  below 0.44 (Silalai and Roos, 2011; Potes et al., 2012). The  $T_g$  in carbohydrates systems depends upon their composition (Gordon and Taylor, 1952). The water content could significantly affect the  $T_g$  values of the mixtures as a result of water plasticization and the  $T_g$  values of lactose could be depressed concomitantly with water content. However, an increase in average molecular weight in a system might cause an increase in  $T_g$  (Slade et al., 1991). According to previous reports (Kedward et al., 2000; Ibach and Kind, 2007; Silalai and Roos, 2010), the phase separation could be found in lactose/protein systems and therefore they had almost composition independent  $T_g$  with  $T_g$  values of systems being mostly dependent on amorphous lactose (Fig. 2.4 A). Therefore, the presence of WPI had a minor effect on the calorimetric  $T_g$  of the mixtures according to previous reports (Potes et al., 2012). The  $T_g$  value of amorphous carbohydrate/WPI systems was primarily dependent on the non-crystalline carbohydrate.

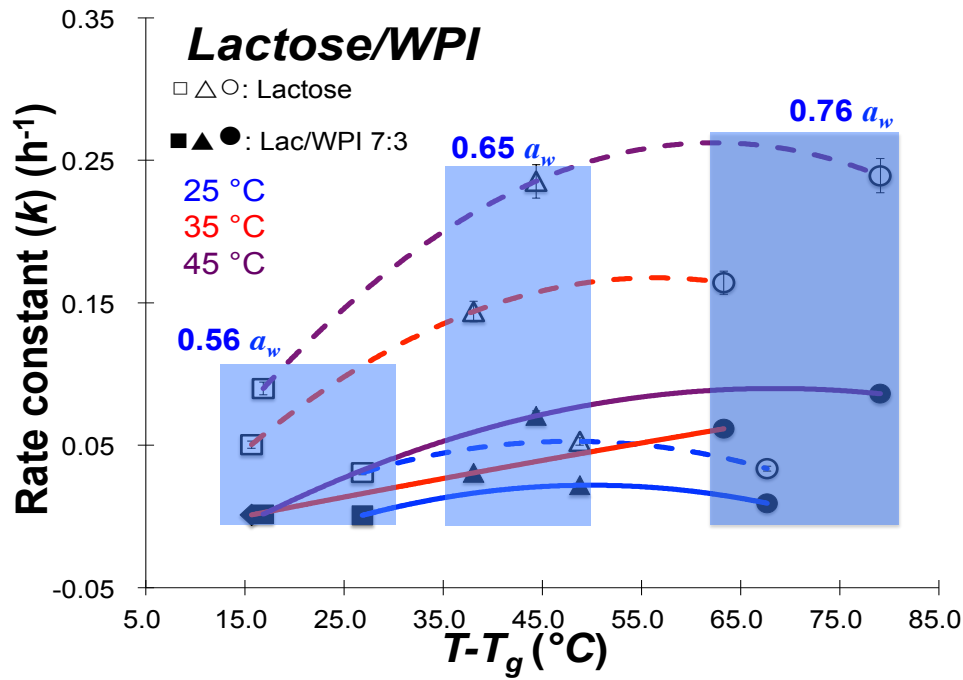


**Fig. 2.5.** Relationship between crystallization rate ( $k$ ) of lactose and  $T-T_g$  in freeze-dried lactose and lactose/WPI mixtures with the mass ratios of 7:3 under 0.56, 0.65, and 0.76  $a_w$  at 25 °C, 35 °C and 45 °C. The  $T_g$  values of amorphous lactose and lactose at high  $a_w$  systems were predicted by  $GT$  equation.

Crystallization rates of amorphous sugars were governed by  $T-T_g$  and the presence of other carbohydrates in lactose crystallization could disturb the crystallization of sugars (Potes et al., 2012). The relationships between  $k$  for pure lactose and lactose/WPI mixture (7:3 mass ratios) and  $T-T_g$  were parabolic (Fig. 2.5). Slade and Levine (1991) reported that the relationship between the rate of crystallization in amorphous materials and  $T-T_g$  was parabolic because, at temperatures close to the  $T_g$ , nucleation was fast, but crystal-growth was slow, and, at temperatures close to  $T_m$ , crystal-growth was fast, but nucleation occurred slowly. The kinetics of lactose crystallization in mixtures could be derived from the rates of reduced sorbed water ( $k$ ) (Potes et al., 2012). The maximum extent of lactose crystallization between 0.65 and 0.76  $a_w$  over a range of temperatures in the present study (Fig. 2.5) agreed with the results of Jouppila and others (1997). Pure lactose and lactose/WPI systems (7:3 and

1:1 mass ratios) showed less rapid lactose crystallization with low  $T-T_g$  at 0.56  $a_w$  from 25 to 45 °C, while the highest crystallization rate occurred between 0.65 to 0.76  $a_w$  around  $T_g + 50$  °C and in the vicinity of the instant crystallization temperature ( $T_{cr}$ ) of lactose at 35 °C and 45 °C (Roos, 2009). However, the highest extent of crystallization in mixtures at 7:3 ratios at 45 °C were not found in our studies (Fig. 2.5). The effect of nucleation rate due to supercooling below melting temperature ( $T_m$ ) was balanced by reduced molecular motion as the temperature was brought closer to  $T_g$  where such motion was assumed to approach very small values, to give a crystallization temperature,  $T_{cr}$ , which was between  $T_g$  and  $T_m$  (Saleki-Gerhardt and Zografi, 1994). In the present study, the extent of crystallization significantly decreased at any  $T-T_g$  and shifted to a higher  $T-T_g$  in mixtures with WPI. The effect of WPI on  $T_{cr}$  was a result of reduced nucleation rate by WPI although the effect on the  $T_g$  was small. The extent of crystallization seems to depend on many factors i.e. the rate of nucleation, solubility of sugars, interaction between protein and water molecules, crystalline forms and anomerization of sugar molecules (Roos and Drusch, 2015). Hence, the effect of WPI on inhibition of crystallization of amorphous lactose was not only linked to an effect on the  $T_g$ , but also involved a specific inhibition such as molecular charge or steric hindrance effects (Saleki-Gerhardt and Zografi, 1994).

During 240 hours of storage, we noted that freeze-dried lactose and lactose/WPI around 0.56  $a_w$ , 0.65  $a_w$  and 0.76  $a_w$  had collapsed structures, except the mixtures at 7:3 ratios. As collapsed samples have a dense microstructure and reduced surface effects that could help the materials retain higher water contents, the collapse phenomenon of dehydrated materials occurred above  $T_g$  and before complete crystallization of amorphous compounds (Roos and Karel, 1991b). The residual water content of the lactose/WPI systems was higher while the structural collapse phenomena was less than in pure lactose. Because protein may have a high  $T_g$  and it could not only hinder the molecular mobility of lactose but also support the

**Table 2.2.** Levelling Off Values for The Different Crystal Types of Freeze-Dried Lactose and Lactose/WPI Mixtures with The Mass Ratios of 7:3 and 1:1 Stored at Various Water Activities and Storage Temperatures.

Storage condition (°C, $a_w$ )	Peak intensity ( $I$ ) indicating the crystal types of lactose <sup>c</sup> ( $\pm 0.01$ ) <sup>e</sup>	Middle-point (HP) of losing sorbed water			End-point (AP) of losing sorbed water			Storage after 10 days (FP)		
		Lactose/WPI 7:3			Lactose/WPI 1:1			Lactose/WPI 7:3		
		Lactose	Lactose/WPI 7:3	Lactose/WPI 1:1	Lactose	Lactose/WPI 7:3	Lactose/WPI 1:1	Lactose	Lactose/WPI 7:3	Lactose/WPI 1:1
25 °C	<b>0.53</b>	10.5°	408	—	—	414	—	—	359	—
		19.2°	625	—	—	743	—	—	684	—
		19.6°	457	—	—	436	—	—	516	—
		20.0°	644	—	—	813	—	—	919	—
		10.5°	412	N/A	—	452	N/A	—	411	N/A
	<b>0.65</b>	19.2°	569	339	—	669	418	—	731	466
		19.6°	469	N/A	—	469	N/A	—	510	N/A
		20.0°	540	770	—	840	941	—	932	1045
		10.5°	443	N/A	N/A	432 (861)	N/A	514 (732)	N/A	N/A
		19.2°	585	225	205	666	345	787	385	293
35 °C	<b>0.76</b>	19.6°	453	N/A	N/A	460	N/A	544	N/A	N/A
		20.0°	705	537	384	762	817	894	944	568
	<b>0.50</b>	10.5°	466	—	—	552 (998)	—	417 (776)	—	—
		19.2°	683	—	—	909	—	690	—	—
		19.6°	414	—	—	591	—	415	—	—
	<b>0.63</b>	20.0°	762	—	—	747	—	1029	—	—
		10.5°	483	N/A	—	513	N/A	425	N/A	—
		19.2°	756	297	—	866	397	796	403	—
		19.6°	615	N/A	—	620	N/A	603	N/A	—
		20.0°	778	820	—	988	919	1036	888	—
45 °C	<b>0.75</b>	10.5°	443	N/A	N/A	536	N/A	481	N/A	N/A
		19.2°	677	654	284	898	744	802	335	284
		19.6°	423	N/A	N/A	567	N/A	549	N/A	N/A
		20.0°	682	685	453	915	773	943	959	526
	<b>0.47</b>	10.5°	359	—	—	379	—	431	—	—
		19.2°	601	—	—	701	—	741	—	—
		19.6°	477	—	—	491	—	497	—	—
		20.0°	998	—	—	1124	—	1044	—	—
		10.5°	501	N/A	—	511(882)	N/A	521 (860)	N/A	—
45 °C	<b>0.61</b>	19.2°	631	356	—	818	434	797	448	—
		19.6°	552	N/A	—	559	N/A	518	N/A	—
		20.0°	900	806	—	1004	902	1021	889	—
	<b>0.74</b>	10.5°	478	N/A	N/A	547(1024)	N/A	541 (910)	N/A	N/A
		19.2°	740	880	221	975	987	926	961	291
		19.6° (22.0°)	512	N/A	N/A	643	N/A	660	N/A	N/A
		20.0°	912	1035	596	1184	1139	1244	1999	666

<sup>a</sup> Peak intensities at diffraction angles of 10.5° or 21.0° (anhydrous  $\beta$ -lactose), 19.1° (anhydrous  $\alpha$ - $\beta$ -lactose mixture with molar ratios of 5:3), 19.6°, 22.0° (anhydrous  $\alpha$ - $\beta$ -lactose mixture with molar ratios of 4:1), 20.0° (g-lactose monohydrate) are indicated with previous reports (Table 1). <sup>b</sup> The highest peak intensity stemmed from different diffraction angle. <sup>c</sup> The diffraction angle showed different changes compared with previous data due to the protein mixed with lactose and increased the spaces between crystal layers.

microstructure under high  $RH$ . Such effects may support surface nucleation but reduce diffusion during crystal growth. Our result showed that lactose crystallization in lactose/WPI systems was more affected by WPI components hindering lactose movement than their glass transition. Exceeding the  $T_g$  by increasing temperature or water content could increase diffusion coefficients, which possibly related to enhance loss of volatiles and increase reaction rates (Roos and Karel, 1991c). This finding emphasized the importance of concentration, molecular size effects, molecular interactions, lattice interference or steric hindrance effects of the mixed components that disturbed nucleation or crystal growth (Iglesias and Chirife, 1978; Mazzobre et al., 2001).

#### 2.3.4. XRD ANALYSIS

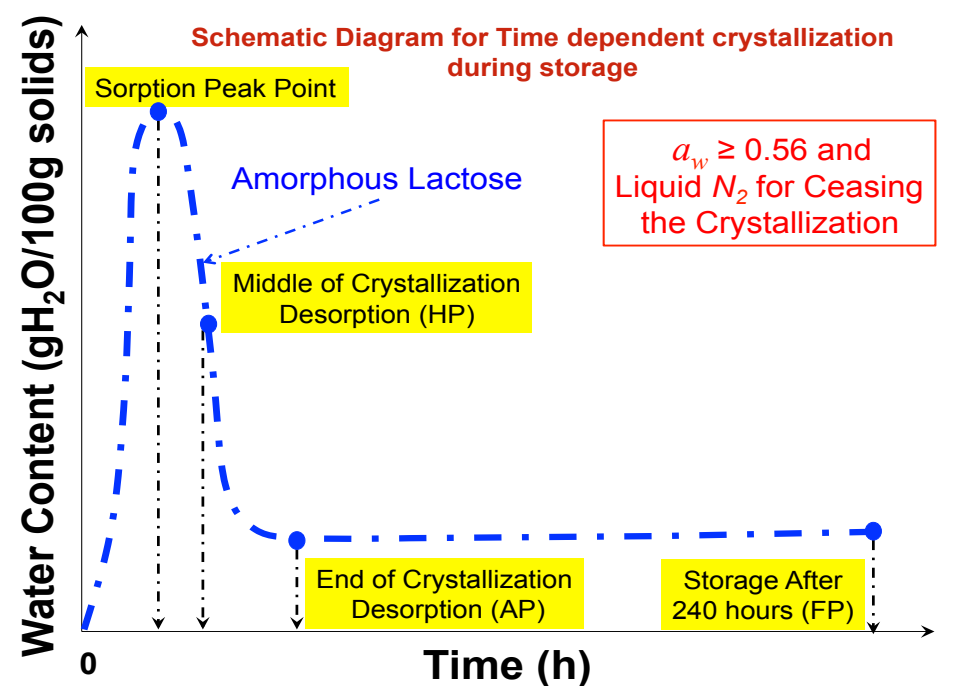
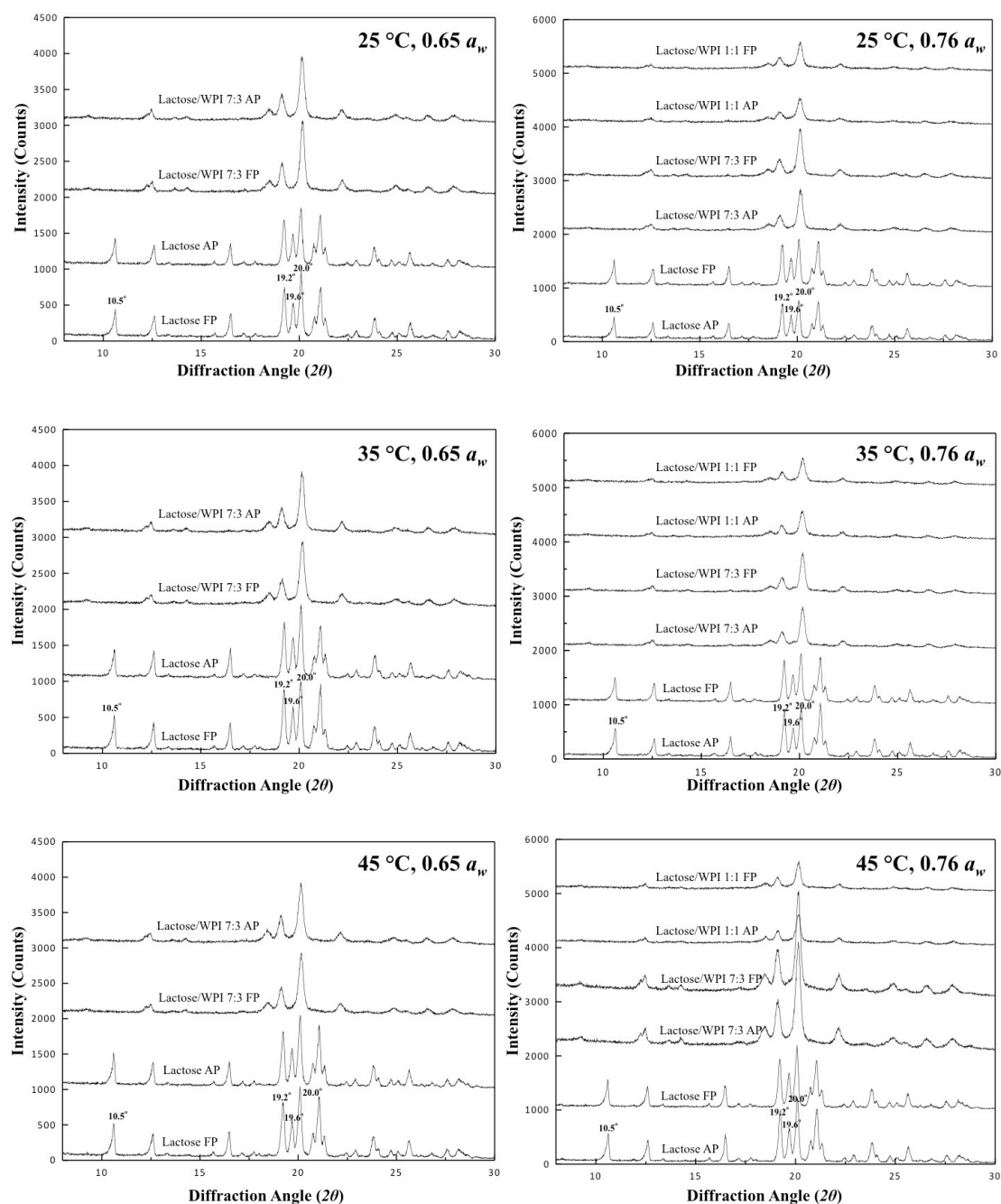


Fig. 2.6. Schematic diagram for time dependent crystallization during storage including the sorption peak point, middle of crystallization desorption (HP), end of crystallization desorption (AP), and the point after 240 h storage (FP).

The XRD analysis was used to identify and confirm the crystalline forms of pure lactose and lactose/WPI systems (7:3 and 1:1, w/w). Fig. (2.6) shows the different time points in time-dependence crystallization, which are corresponding to middle (HP) and end point (AP) of crystallization during sorption as well as the final point (FP) after 240 h storage. The XRD diffraction has shown several types of crystals but an exact quantitative analysis of each crystalline form was not permitted by the XRD analysis (Haque and Roos, 2005). However, Drapier-Beche and Others (1997) assumed that the quantity of each lactose crystalline form ( $\alpha$ -lactose monohydrate, anhydrous  $\beta$ -lactose and  $\alpha$ -/ $\beta$ -lactose mixtures at differential molar ratios) could be indicated by the intensity values at their characteristic diffraction angles ( $2\theta$ ). Each characteristic peak for different crystal types of lactose on  $2\theta$  was determined by XRD using standard reagents in Appendix I, which agreed with previous studies (Jouppila et al., 1997; Haque and Roos, 2005). The freeze-dried pure lactose could mainly crystallize as  $\alpha$ -lactose monohydrate and anhydrous  $\beta$ -lactose at AP and FP around 0.65 and 0.76  $a_w$  over the whole temperature range corresponding with previous studies (Buma and Wiegers, 1967; Jouppila et al., 1998; Haque and Roos, 2005). Drapier-Beche and others (1997) showed that the  $\alpha$ -lactose monohydrate was the dominant crystalline form but anhydrous  $\beta$ -lactose and  $\alpha$ -/ $\beta$ -lactose mixtures at 5:3 and 4:1 were not found in freeze-dried lactose when stored at 0.56  $a_w$ . In the present study, however, the anhydrous  $\beta$ -lactose and  $\alpha$ -/ $\beta$ -lactose mixture with molar ratios 5:3 and 4:1 showed characteristic  $2\theta$  peaks ( $19.2^\circ$  and  $19.6^\circ$ ) by XRD after storage at 0.56  $a_w$ , respectively. The peak intensity for  $\alpha$ -lactose monohydrate, anhydrous  $\beta$ -lactose and  $\alpha$ -/ $\beta$ -lactose mixture at molar ratio of 5:3 in pure lactose and mixtures (7:3 and 1:1) increased from HP to AP except the  $\alpha$ -/ $\beta$ -lactose with 4:1 molar ratios as well as  $\alpha$ -lactose monohydrate around 0.65 and 0.76  $a_w$  from 25 to 45 °C (Table 2.2 and Fig. 2.7). The highest leveling off intensities for all lactose crystalline forms was shown around 0.65  $a_w$  (932 and 1036 counts at 25 °C and 35 °C) and 0.75  $a_w$  (1244 counts at 45 °C) at FP, respectively (Table 2.2). Above results proved that the lactose partly crystallized at HP and the highest extent of crystallization occurred between 0.65 and 0.76  $a_w$  corresponding with Fig. (2.5).



**Fig. 2.7.** X-Ray diffraction patterns for freeze-dried amorphous lactose and lactose/WPI mixtures with the mass ratios of 7:3 and 1:1 at middle (HP) and end point (AP) of losing sorbed water during sorption as well as the final point (FP) after 240 h storage around 0.65 and 0.76  $a_w$ .

Haque and Roos (2005) reported that the recrystallization occurred in crystallized lactose depending on storage water activity and time as found from the peak

intensities of  $\alpha$ -lactose monohydrate and anhydrous  $\beta$ -lactose, which increased and decreased in XRD patterns, respectively. At intermediate and high water activities in our study, the peak intensity of anhydrous  $\beta$ -lactose decreased concomitantly with the increase of the  $\alpha$ -lactose monohydrate peaks for AP to FP (Fig. 2.8). The results showed that recrystallization of lactose progressed above 0.65  $a_w$  at 25 °C and 35 °C. At the higher storage temperature, according to water sorption data, the low residual water was in the crystalline lactose and most likely in  $\alpha$ -lactose monohydrate crystals. Therefore, anhydrous  $\beta$ -lactose could sorb migrating water from crystallizing lactose and recrystallize to  $\alpha$ -lactose monohydrate during storage. The recrystallization of anhydrous  $\beta$ -lactose was rarely observed at high storage temperature using XRD. Simpson and others (1982) reported that  $\alpha$ -lactose monohydrate might have a trend to convert to anhydrous mixtures (5:3 molar ratios) under low water conditions (water contents  $\leq$  6%, w/w) above room temperature. However, a much lower ambient temperature was needed to form crystals with molar ratios 4:1 from  $\alpha$ -lactose monohydrate in storage. In our study, anhydrous  $\alpha$ -/ $\beta$ -lactose crystals at the molar ratio of 5:3 increased from AP to FP probably due to lactose migration from  $\alpha$ -lactose monohydrate, whereas the anhydrous  $\alpha$ -/ $\beta$ -lactose 4:1 remained constant (Fig. 2.8). The intensities of the various crystal forms increased in pure lactose concomitantly with increasing  $a_w$  from 0.65  $a_w$  up 0.75  $a_w$  at 25 °C and 35 °C. Corresponding to the rate of dehydration of sorbed water at the respective temperature and  $a_w$ , the extent of lactose crystallization probably was affected by the presence and quantity of various crystalline forms during recrystallization, which could be governed by the mutarotation of lactose molecules to the anomeric form during crystal-growth stage.

No characteristic peaks of anhydrous  $\beta$ -lactose and  $\alpha$ -/ $\beta$ -lactose mixture at the molar ratio of 4:1 were found for HP, AP, and FP in the presence of WPI in the systems (Fig. 2.8). The recrystallization of lactose was also absent between AP and FP in XRD patterns of lactose/WPI systems (Fig. 2.8). The lactose/WPI mixtures with the ratios of 7:3 and 1:1 contained more  $\alpha$ -lactose monohydrate than anhydrous forms when the



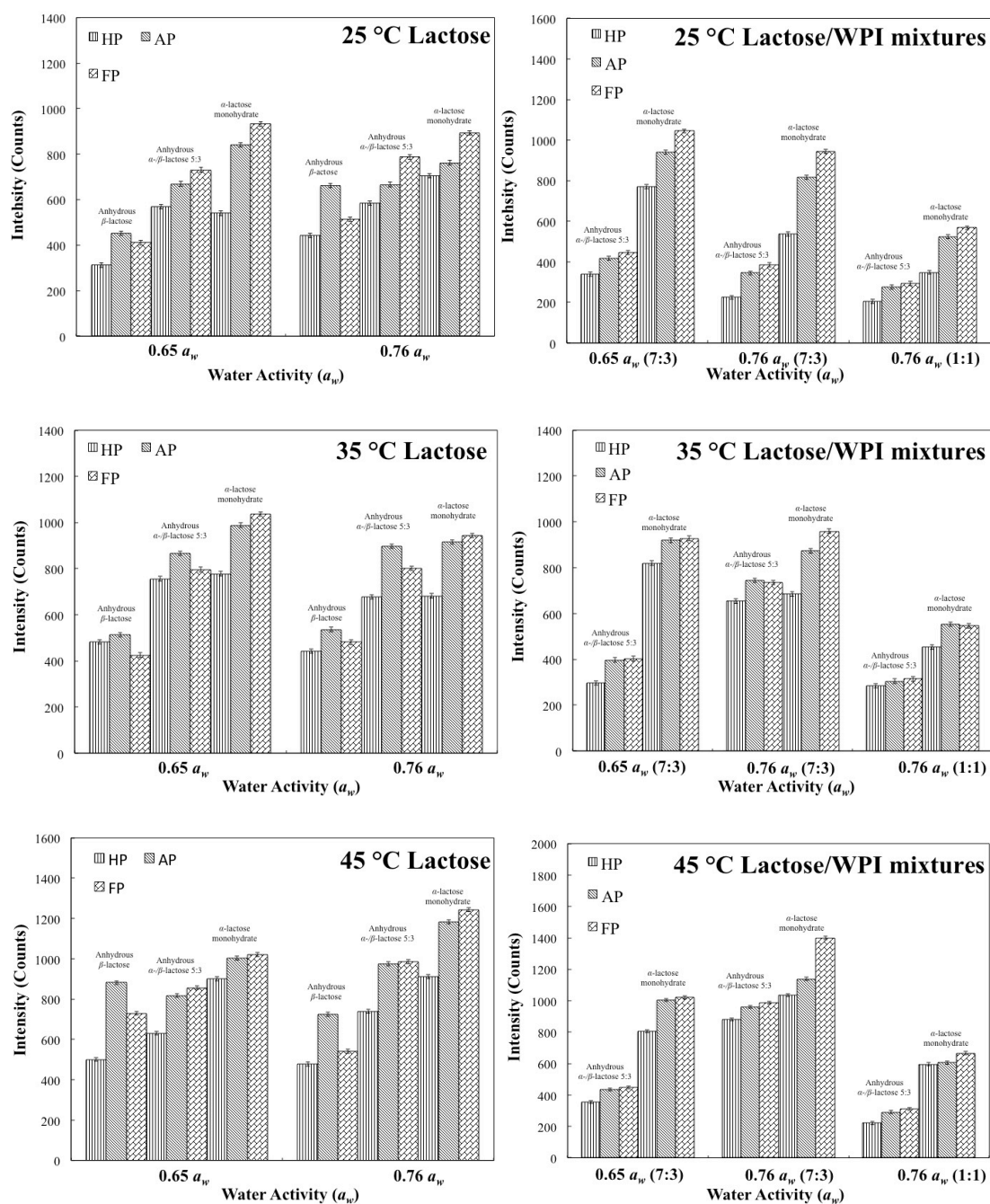


**Fig. 2.8.** Intensity values for  $\alpha$ -lactose monohydrate, anhydrous  $\beta$ -lactose and  $\alpha$ - $\beta$ -lactose mixtures at 5:3 molar ratios based on XRD patterns for freeze-dried amorphous lactose and samples stored around 0.65 and 0.76  $a_w$ .

storage temperature increased from 25 °C to 45 °C at AP (Table 2.2). The intensities of  $\alpha$ -lactose monohydrate and anhydrous  $\alpha$ - $\beta$ -lactose with the molar ratio of 5:3 peaks were lower than were found for pure lactose at 0.67 and 0.76  $a_w$  at 25 °C to 45 °C (Fig. 2.8). The results showed that lactose/WPI system favoured  $\alpha$ -lactose

monohydrate formation from the beginning of storage. Introduction of protein into sugars could probably delay the transport of sugar molecules in systems, increase the energy needed and even the critical size of nucleus (De Yoreo and Vekilov, 2000; Kashchiev, 1999). Hence, the systems could hardly form stable nucleus in the presence of WPI and delay the nucleation of lactose. Das and Langrish (2012a) indicated that the period of losing the sorbed water could be considered as the crystal-growth stage during lactose crystallization. Davis and others (2000) reported that the impurities might distort the crystal structure, change the mutarotation of molecules as well as increase the free energy and solubility of the crystal that could lead to lower effective supersaturation of system during crystal-growth step. According to XRD patterns, in present study, we believed that the WPI could not only increase the solubility of lactose crystals by an effect on the presence of various anomeric forms and hinder the pathways of lactose molecules diffusion but also increase the free energy needed for lactose molecules migration to the surface sites during crystal-growth step. The free energy barrier to desolvation, which is the breaking of bonds to water molecules, is the dominant barrier to attachment of a solute molecule to the crystal-growth step (Chernov, 1984; De Yoreo and Vekilov, 2003). However, the presence of WPI might disturb the breaking of bonds to water molecules that existed on the surface of lactose crystals and affect local water migration. In addition, the unstable anhydrous  $\beta$ -lactose might rapidly convert to  $\alpha$ -lactose monohydrate in system as WPI might offer higher water surrounding at the beginning of crystal-growth step based on XRD patterns. Consequently, we proved that whey protein could be considered as an effective additive that could prevent sugar crystallization, controlling the crystal types and increase the stability of sugars in food and pharmaceutical systems.

## 2.4. CONCLUSIONS

We have shown that amorphous lactose/WPI mixtures have fractional water sorption

properties, and the crystallization of lactose was delayed by the addition and increasing quantity of WPI. The mechanism of protein inhibition of lactose crystallization involved protein that reduced the rate of nucleation, the extent of crystallization, and the number of species of crystalline forms of lactose. The capability of WPI to prevent crystallization of lactose was quantity dependent, i.e., a higher WPI content showed a stronger inhibition. In the following Chapter, DSC can be used to determine the  $T_g$  and the amorphous contents in semi-crystalline lactose/protein mixtures. And also mechanical properties, relaxation times of structure-forming and molecular movements of semi-crystalline sugar/protein systems can be investigated.

## CHAPTER III



Contents lists available at [ScienceDirect](#)

Journal of Food Engineering

journal homepage: [www.elsevier.com/locate/jfoodeng](http://www.elsevier.com/locate/jfoodeng)



Volume 173, 28 October 2016, Pages 106-115

# STRUCTURAL RELAXATIONS OF AMORPHOUS LACTOSE AND LACTOSE/WHEY PROTEIN MIXTURES

Fanghui Fan and Yrjö H. Roos

*School of Food and Nutritional Sciences,  
University College Cork, Cork, Ireland*

## ABSTRACT

Structural relaxations and  $\tau$  of lactose in freeze-dried amorphous lactose and lactose/WPI mixture systems were studied with glass transition data. The results indicated that  $T_g$ , enthalpy relaxation ( $H$ -relaxation) and  $T_\alpha$  of amorphous lactose was affected by the presence of lactose crystals and WPI at 0.33  $a_w$  (25 °C) due to water migration. The  $\tau$  and  $T_\alpha - T_g$  relationship of the materials was successfully modeled by the WLF equation with the material-special constants ( $C_1$  and  $C_2$ ). The  $S$  parameter indicating decrease of  $\tau$  from  $10^2$  to  $10^{-2}$  s could be used to measure the structural stability of lactose systems above their glass transition. The strength of amorphous lactose decreased with  $a_w$  increasing up to 0.44 and enhanced by  $\alpha$ -type of lactose crystals and WPI in storage at 0.33  $a_w$ . Hence, the strength parameter provided a simple and convenient means to measure compositional effects on structure formation in food processing.

**KEYWORDS,** *Lactose; Crystallization; Structural relaxations; WLF model; Strength parameter; Water*

## 3.1. INTRODUCTION

Structural relaxations, as often measured above and somewhat below the glass transition region, reflect the spontaneous approach of an amorphous material towards equilibrium at a rate which often depends on temperature and  $a_w$  of the material (Shamblin and Zograf, 1998; Liu et al., 2006). Structural relaxation times correspond to the kinetically impeded molecular rearrangements and relate to the time-dependent changes of thermodynamic, mechanical or dielectric properties, following a perturbation such as a change in temperature or pressure (Chung et al., 2004; Surana et al., 2004; Haque et al., 2006). A change in enthalpy around the glass transition reflects the non-equilibrium nature of the glassy state and is often referred to as

enthalpy relaxation, which is dependent on the kinetics of molecular freezing around glass transition (Liu et al., 2006). Enthalpy relaxation occurs concomitantly with increasing local translational molecular motions of molecules or parts of polymer molecules when a glassy material is heated to above its glass transition (Shamblin and Zografi, 1998; Wungtanagorn and Schmidt, 2001ab; Liu et al., 2006; Haque et al., 2006). Since the enthalpy relaxation is recognized as an important factor relating to the physical properties of polymers, DSC is routinely used to study enthalpy relaxations associated with the glass transition (Yoshida, 1995; Le Meste et al., 2002; Surana et al., 2004; Roos and Drusch, 2015).

The molecular arrangement in a non-equilibrium glass often tends to lose its “quenched in” excess enthalpy or free volume with time (Hancock et al., 1995). Variations in molecular mobility, including molecular displacement or deformation, molecular migration, molecular diffusion reflecting Brownian movements and rotation of functional groups or polymeric segments around covalent bonds, could be related to processability and stability of food products upon storage (Roudaut et al., 2004). In the glass, long-range cooperative motions are restricted and motions (vibrations of atoms, reorientation of small groups of atoms) are mainly local not involving the surrounding atoms or molecules. A temperature increase to above the  $T_g$  results in a rapid increase of molecular mobility, which is shown by the decreasing viscosity and increasing flowability of the material (Hancock et al., 1995). The relaxation times are the time that is necessary for the recovery from perturbations (Le Meste et al. 2002). Structural relaxations around the glass-liquid transition could show relaxation times of similar timescale of the experimental time scale (Champion et al., 2000). Thus, structural relaxations and  $\tau$  may be related to particle structure, flow characteristics, viscous flow and collapse, and mechanical properties, which control the quality and stability of food materials, particularly in the vicinity and above the onset of the calorimetric glass transition.

Crystallization of amorphous lactose is of practical importance and it may enhance

physical and chemical deterioration in food ingredients and is typical of dairy powders at high storage humidities or temperatures causing a rapid loss of shelf life (Roos and Karel, 1992). It is a dramatic change in material structure that results in complete changes of physicochemical properties. Mechanical properties of amorphous sugars could be affected by their degree of crystallinity (Chung et al., 2002 and 2004) and the presence of other components affecting their glass transition, e.g. water (Downton et al., 1982; Slade et al., 1991), carbohydrates (Cruz et al., 2001; Miao and Roos, 2005) and proteins (Silalai and Roos, 2011a). A characteristic feature of mechanical properties of amorphous sugars, such as the  $T_g$ -dependence, could affect food quality and shelf life during storage (Slade et al., 1991; Silalai and Roos, 2011ab). The glass transition appears as the primary  $\alpha$ -relaxation, which could cover a wide range of time and temperature scales (Urbani et al., 1997; Faivre et al., 1999; Talja and Roos, 2001; Yu, 2001). The frequency-dependent  $\alpha$ -relaxation of amorphous sugars is governed by water content, relative humidity and temperature (Roos and Karel, 1991a). Dynamic-mechanical analysis may be used in studies of structural relaxations below the calorimetric  $T_g$ , the  $\alpha$ -relaxation (primary relaxation) of glass forming carbohydrates, and to derive the  $\alpha$ -relaxation temperature,  $T_\alpha$  (Silalai and Roos, 2011b; Potes et al., 2012). The  $T_\alpha$  may be taken from loss modulus peak temperatures at various frequencies to obtain the corresponding  $\tau$ . In general, WLF model, as an interrelated relationship, is often used to define mobility in terms of the non-Arrhenius temperature dependence of the rate of any diffusion-limited relaxation process occurring at the temperature  $T$ , compared to the rate of the relaxation at the reference temperature, e.g.,  $T_g$ , expressed in terms of  $\tau$  dependence on  $T-T_g$  (Williams et al., 1955; Slade and Levine, 1995; Angell, 1997; Roos and Drusch, 2015).

Previous studies have shown that water and food components in mixed systems vary in their physical and chemical stability (Champion et al., 2000). The importance of glass transition to amorphous solids characteristics has been well recognized but few studies have contributed to the understanding of effects of crystals or glass former on the particle structure and properties in food materials. The objectives of the present

study were to investigate the influence of water, two different crystalline phases ( $\alpha$ -lactose monohydrate and anhydrous  $\beta$ -lactose crystals) and polymeric food component (WPI), on the calorimetric glass transition, enthalpy relaxations,  $\alpha$ -relaxation, and  $\tau$  of freeze-dried amorphous lactose in systems at low water activities ( $\leq 0.44 a_w$ ). We expect that the flow characteristics or strength of the glass former and their interaction with other solids could contribute to powder characteristics. This study is useful for the understanding of the effects of water and food components on the collective relaxation behavior when present with amorphous lactose around the glass transition in food and pharmaceutical materials.

## **3.2. MATERIALS AND METHODS**

### **3.2.1. SAMPLE PREPARATION**

$\alpha$ -lactose monohydrate, anhydrous  $\beta$ -lactose (>99 % lactose) (Sigma-Aldrich, St. Louis, Mo., U.S.) and WPI (Isolac<sup>®</sup>, Carbery Food Ingredients, Co., Ballineen, Ireland; minor components including carbohydrates or lipids < 3%) were used.  $\alpha$ -Lactose monohydrate was dissolved in boiling ( $\sim 100$  °C) deionized water (KB Scientific Ltd. Cork, Ireland) to obtain 20 % (mass) solution and then cooled to room temperature ( $20 \pm 3$  °C). WPI with 20 % (mass) solids in deionized water at room temperature was prepared using continuous stirring for 4 h. Aqueous lactose and WPI with 20 % (mass) solids at room temperature were used to obtain ratios of 7:3, 1:1, and 3:7 of lactose/WPI by mass. Samples (5 mL in total) were prepared in pre-weighted glass vials (10 mL, diameter 24.3 mm  $\times$  height 46 mm; Schott Müllheim, Germany). All samples in the vials (semi-closed with septum) were frozen at  $-20$  °C for 20 h and then subsequently tempered at  $-80$  °C for 3 h prior to freeze-drying using a laboratory freeze-dryer (Lyovac GT2 Freeze-Dryer, Amsco Finn-Aqua GmbH, Steris<sup>®</sup>, Hürth, Germany). After freeze-drying at pressure < 0.1 mbar, triplicate samples of each material were stored in evacuated desiccators over  $P_2O_5$  (Sigma-Aldrich, St. Louis, Mo., U.S.) prior to subsequent analysis.



Freeze-dried lactose was monitored for 120 h over saturated solutions of  $LiCl$ ,  $CH_3COOK$ ,  $MgCl_2$ , and  $K_2CO_3$  (Sigma Chemical Co., St. Louis, Mo., U.S.A.) at respective water activities of 0.11, 0.23, 0.33, and 0.44  $a_w$  depending on storage temperature of 25 °C (Greenspan, 1977; Labuza et al., 1985), in vacuum desiccators. The  $\alpha$ -lactose monohydrate, anhydrous  $\beta$ -lactose, WPI and lactose/WPI at 7:3, 1:1, and 3:7 mass ratios were adjusted to 0.33  $a_w$  (Dew Point Water Activity Meter 4TE, Aqualab, WA, USA) by humidification over saturated solution of  $MgCl_2$  (Sigma Chemical Co., St. Louis, Mo., U.S.A.) in vacuum desiccators in incubators at 25 °C. All vials were closed with septum when removed out of desiccators for weighing and septum was removed when vials were loaded on the balance. All mixtures were made into powder using a mortar and pestle after humidification. After storage at 0.33  $a_w$  and 25 °C, lactose,  $\alpha$ -lactose monohydrates, anhydrous  $\beta$ -lactose and WPI were mixed in order to prepare the crystals containing systems. The solid ratios of  $\alpha$ - and  $\beta$ -type of lactose crystal/lactose systems were 1:4, 2:3, 3:2, and 4:1 (by mass), respectively.

### 3.2.2. THERMAL ANALYSIS

The onset of  $T_g$ ,  $\Delta C_p$  and recovery of enthalpy ( $\Delta H$ ) for each material were determined around glass transition using DSC (Mettler Toledo Schwerzenbach, Switzerland). Samples of all materials were transferred to preweighed standard DSC aluminum pans ( $\sim 40\mu L$ , Mettler Toledo Schwerzenbach, Switzerland), and hermetically sealed before weighing. An empty punctured pan was used as a reference and the instrument was calibrated for temperature and heat flow as reported by Potes and Others (2012). Samples were scanned from  $\sim 30$  °C below to over the  $T_g$  region at 5 °C/min and then cooled at 10 °C/min to initial temperature. A second heating scan was run to well above the  $T_g$  at 5 °C/min. The onset glass transition temperatures derived from two subsequent heating scans,  $T_{g1}$  and  $T_{g2}$ , were recorded using STARe software, version 8.10 (Mettler Toledo Schwerzenbach, Switzerland). The  $\Delta H$  values were calculated from the endothermic peak around the glass transition (Surana et al.,

2005; Haque et al., 2006). Fig. (3.1) gives a schematic diagram for the onset  $T_g$ ,  $\Delta C_p$  and the size of the relaxation peak, which was used to derive  $\Delta H$  values, based on two heating scan using DSC.

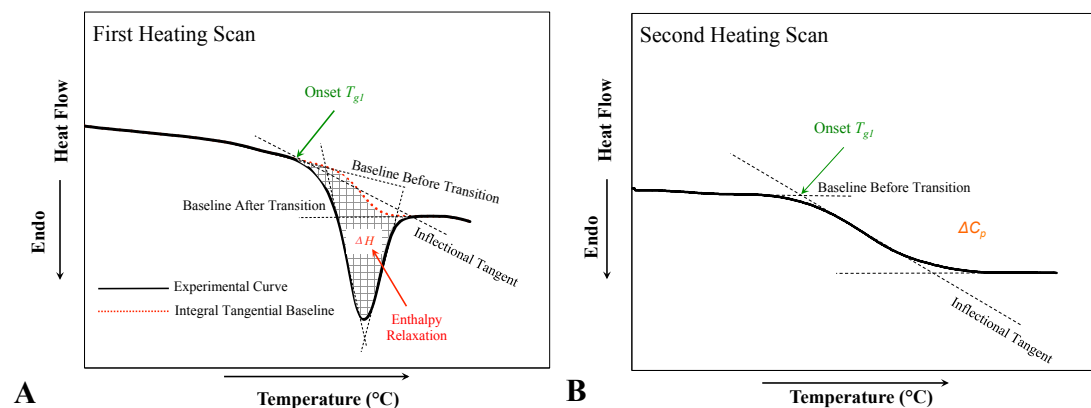


**Fig. 3.1.** The schematic diagram of glass transition associated endotherm as measured using DSC in first (A) and second (B) heating scans. The area under the endotherm associated with glass transition and is defined as enthalpy recovery,  $\Delta H$ , in A.

### 3.2.3. DYNAMIC-MECHANICAL ANALYSIS

Dynamic-mechanical properties of humidified pure lactose and composite materials were studied using DMA (Tritec 2000 DMA, Triton Technology Ltd., UK). The storage modulus ( $E'$ ) and loss modulus ( $E''$ ) as a function of temperature at different frequencies were determined (0.5, 1, 3, 5, and 10 Hz). The DMA instrument was balanced or set at zero to determine the zero displacement position and return the force to the zero position before starting an experiment (Royall et al., 2005). Approximately 100 mg samples of grinded materials were spread on a metal pocket-forming sheet (Triton Technology Ltd., UK). The sheet with sample was crimped along a pre-scored line to form a thin sandwich pocket. This pocket was attached directly between the clamps (the fixed clamp and the driveshaft clamp) inside the measuring head of the DMA. The length, width, and thickness ( $\sim 2$  mm) of the sample pocket between the clamps were measured. Triplicate samples of each

material were analyzed using dynamic measurements and recorded using DMA software version 1.43.00. The measuring head was connected to a liquid nitrogen tank (1 L; Cryogun, Brymill Cryogenic Systems, Labquip Ltd., Dublin, Ireland). Samples were scanned from  $\sim 60$  °C below to over the  $T_g$  region with cooling rate of 5 °C/min and heating rate of 2 °C/min using the single cantilever bending mode (Silalai and Roos, 2011a). During dynamic heating, the samples were analyzed for  $T_\alpha$  determined from the peak temperature of  $E''$  above the glass transition (Potes et al., 2012). Average values for triplicate measurements of peak  $T_\alpha$  of  $E''$  were calculated.

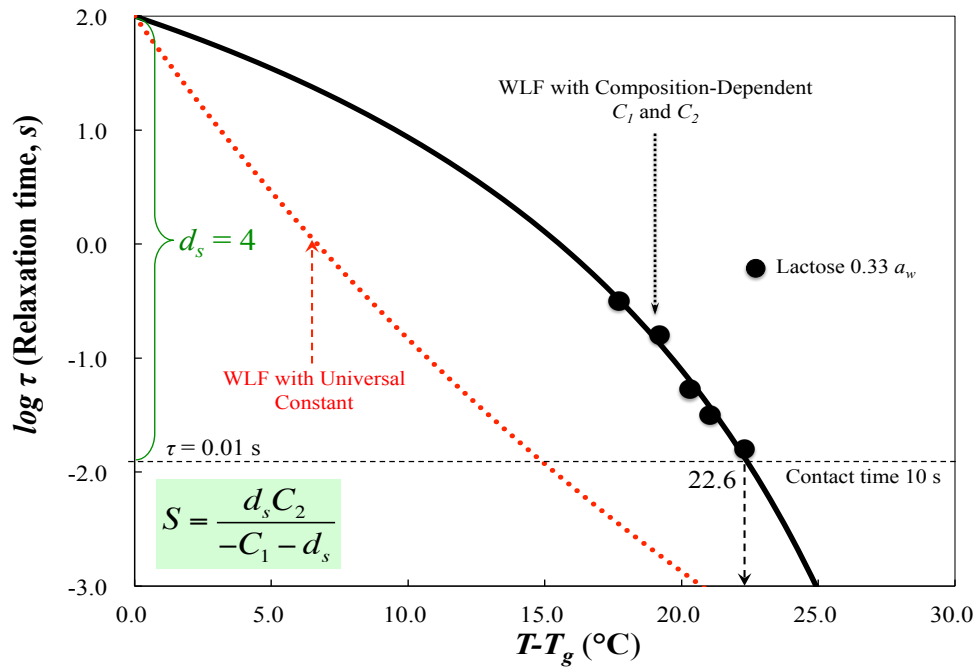


**Fig. 3.2.** The schematic diagram of strength parameters,  $S$ , at  $d_s = 4$  decreasing the structural relaxation time,  $\tau$  (100 s), as measured using dynamic mechanical analysis (DMA) to  $\tau = 0.01$  s. Such decrease in  $\tau$  is known to result in particle stickiness and aggregation at contact time of 10 s (Roos et al., 2016).

### 3.2.4. WLF-MODEL ANALYSIS

The structural relaxation times and the temperature of  $T_a$  above  $T_g$ , were modeled and analyzed using the WLF equation (Eq. 1.9), where  $\tau$  was defined by oscillation frequency set in DMA measurement ( $\tau = 1/2\pi f$ ). The WLF model constants  $-C_1$  and  $C_2$  can be derived from a plot of  $1/\log(\tau/\tau_g)$  against  $1/(T-T_g)$  using experimental relaxation times,  $\tau$ , with the assumption of  $\tau_g = 100$  s at the onset temperature of the calorimetric glass transition,  $T_g$ . Roos and Others (2016) defined a measure for flow characteristics given by strength,  $S$  and introduced a WLF model-based analysis of structural relaxation times within solids affecting flow characteristics in mixes of glass forming carbohydrates, proteins and other food components. Fig. (3.2) is the schematic diagram to show an increase in temperature above calorimetric onset- $T_g$  is quantified for mixes of food solids (amorphous lactose humidified at 0.33  $a_w$ ), which could be considered as the  $S$  parameter. A decrease in the number of logarithmic decades for flow, e.g., that to critical for stickiness, can be defined as the critical parameter,  $d_s$ , of Eq. (1.12) and a corresponding  $T-T_g$  is given as the strength of the solids,  $S$ . The  $d_s$  is the critical decrease of  $\tau$  in the logarithmic scale (can be chosen for each system as an integer depending on the required oscillation frequency). The strength parameter of carbohydrates-polymeric food systems could be calculated at  $d_s = 4$ . The  $S$  parameter is a simple concept, which describes the time-dependence of structural transformations of glass formers above the calorimetric glass transition.

### 3.2.5. STATISITICAL ANALYSIS

The data of enthalpy relaxations and  $\tau$  were calculated and WLF model was fitted to data using Microsoft Office Excel 2011 (Microsoft, Inc., U.S.A.). All measurements were repeated three times as well as the average value with standard deviation of triplicate measurements was calculated.

### 3.3. RESULTS AND DISSCUSSION

#### 3.3.1. GLASSSS TRANSITION AND ENTHALPY RELAXATION

**Table 3.1.** The water content,  $\alpha$ -relaxation temperature,  $T_\alpha$  (0.5 Hz), onset glass transition temperature,  $T_g$ , heat capacity,  $\Delta C_p$ , values of  $C_1$  and  $C_2$  deriving from WLF equation and strength,  $S$  ( $^\circ\text{C}$ , at  $\tau = 0.01$  s), and storage temperature for crystallization in  $\theta_{cr} = 2$  h,  $T_\theta$ , of amorphous lactose stored at different water activities up to 0.44  $a_w$  at 25  $^\circ\text{C}$

$a_w$	Water content (gH <sub>2</sub> O/100 g of solids)	$T_\alpha$ ( $^\circ\text{C}$ )	$T_g$ ( $^\circ\text{C}$ )	$\Delta C_p$ (Jg <sup>-1</sup> K <sup>-1</sup> )	$C_1$	$C_2$	$S$ ( $^\circ\text{C}$ )	$T_\theta$ ( $^\circ\text{C}$ )
Anhydrous	0	128±2	105±3	0.61±0.02	-1.84±0.40	-39.46±0.32	27.2±2.5	132±6
0.11 ± 0.00 <sup>a</sup>	2.0±0.2 <sup>a</sup>	86±3	65±4	0.64±0.02	-2.46±0.32	-41.63±0.41	26.3±1.5	91±6
0.23 ± 0.00	4.0±0.3	59±4	40±2	0.67±0.03	-2.79±0.28	-40.66±0.52	24.8±1.4	65±3
0.33 ± 0.00	6.1±0.3	48±2	30±3	0.72±0.04	-3.37±0.31	-41.72±0.60	22.6±0.7	53±4
0.44 ± 0.00	8.4±0.4	29±3	13±4	0.73±0.02	-4.17±0.47	-40.98±0.58	20.3±2.8	33±7

<sup>a</sup>: Values are mean ± SD ( $n=3$ ).

The onset of  $T_g$  values derived from the second heating scans using DSC for amorphous freeze-dried lactose at low water activities ( $\leq 0.44 a_w$ ) on 25  $^\circ\text{C}$  are shown on Table (3.1). Water as a strong plasticizer could significantly increase the mobility of amorphous lactose, which was shown by the depression of  $T_g$  values (Silalai and Roos, 2011b). In the present study, the glass transition temperature of lactose decreased from 105  $^\circ\text{C}$  (anhydrous state) to 36  $^\circ\text{C}$  (0.44  $a_w$ ) due to water plasticization (Table 3.1). Table (3.2) gives the onset of  $T_{g1}$  and  $T_{g2}$  values of the first and second heat scans of lactose, each crystal/lactose and lactose/WPI mixture studied. As the water activities decreased concomitantly with the quantity of crystal phase increasing, the  $T_{g1}$  and  $T_{g2}$  values of systems with a crystalline phase dispersed within the amorphous matrix were slightly higher than those we found for lactose at 0.33  $a_w$  at 25  $^\circ\text{C}$  (Fig. 3.3). However, no  $T_g$  variation was detected for pure lactose in DSC measurement (Table 3.2). The  $T_{g1}$  values were higher than  $T_{g2}$  in both  $\alpha$ - and  $\beta$ -type of lactose crystal/lactose systems at each mass ratio probably caused by either water

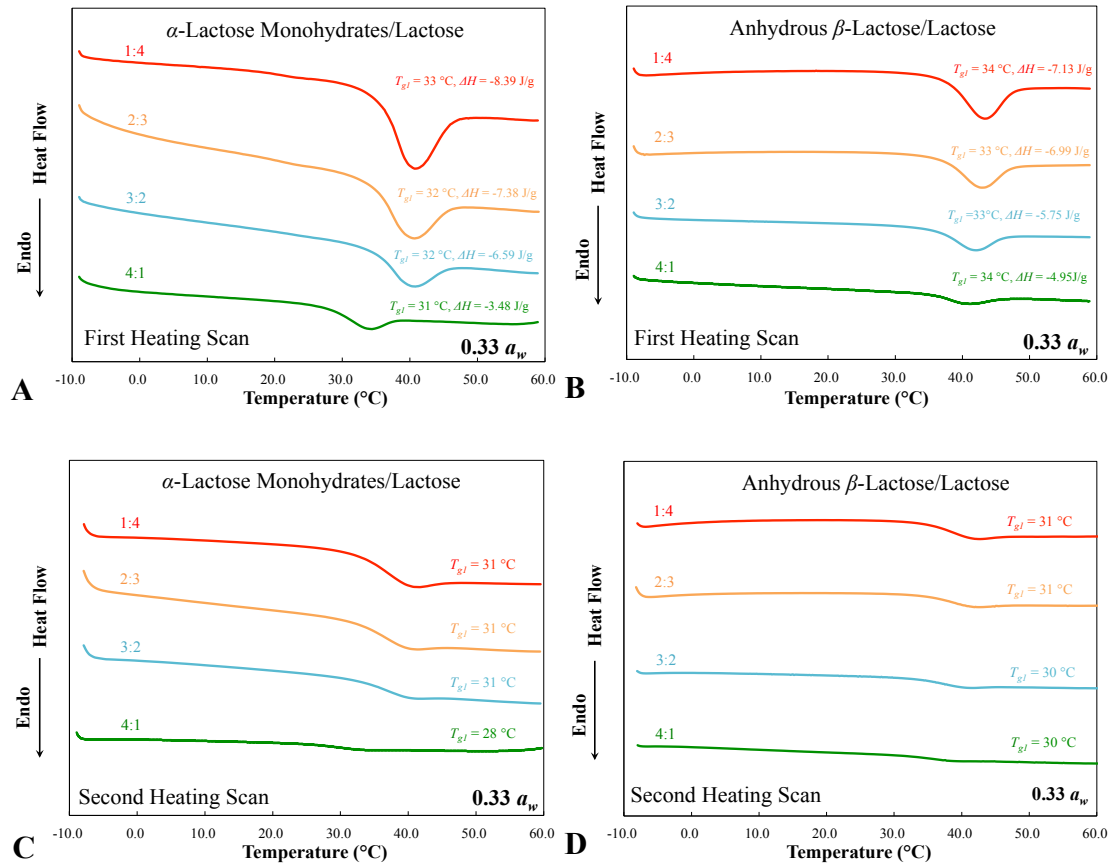


**Fig. 3.3.** DSC scans (A and B for first heating scan,  $T_{g1}$ ; C and D for second heating scan,  $T_{g2}$ ) for both  $\alpha$ - and  $\beta$ -type of lactose crystal containing mixtures with the mass ratios of 1:4, 2:3, 3:2, and 4:1 after storage at  $0.33 a_w$  and  $25^\circ\text{C}$ .

migration or the glass state of lactose had relaxed during DSC heating measurement, while the  $T_{g2}$  showed almost the same values shown in Table (3.2). Compared to  $\alpha$ -lactose monohydrate containing systems, there was a greater variation of  $T_g$  found for  $\beta$  type of lactose crystal/lactose systems at each mass ratio (Table 3.2). This phenomenon implied that the presence of anhydrous  $\beta$ -lactose could enhance the extent of water migration across each component in systems due to its relatively large and rough crystal surface of  $\alpha$ -lactose monohydrate (Raghavan et al., 2000; Gänzle et al., 2008). Water migration could also be found between protein and amorphous phase resulting in variation of  $T_{g1}$  and  $T_{g2}$  in lactose/WPI mixtures after storage at  $0.33 a_w$  and  $25^\circ\text{C}$  (Table 3.2). During storage at  $0.33 a_w$ , sorbed water could migrate across

different phases of mixtures, and thus, cause the variation of onset  $T_g$  as was revealed in DSC measurements. Therefore, a crystalline phase and protein could affect the glass transition of amorphous lactose in lactose containing systems after storage at 0.33  $a_w$  and 25 °C.

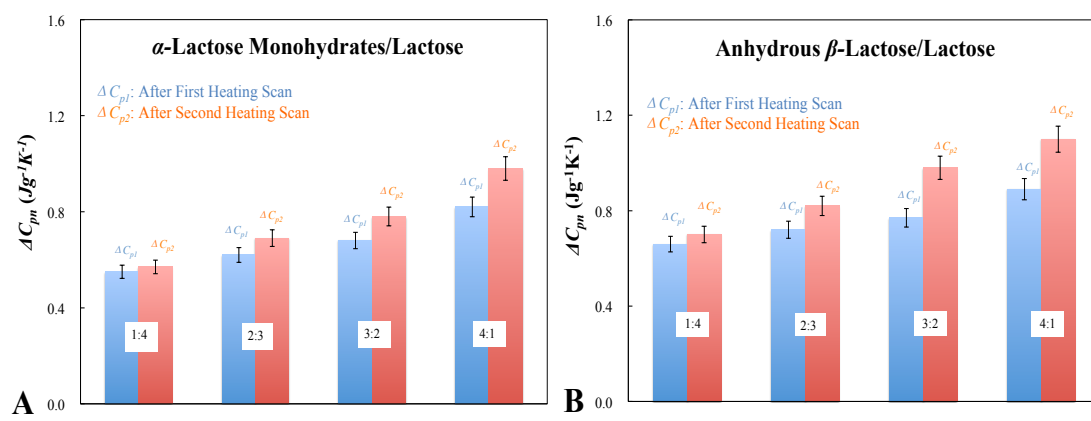


**Fig. 3.4.** Normalized heat capacity values ( $\Delta C_{pn}$ ) after first heating scan ( $\Delta C_{p1}$ ) and second heating scan ( $\Delta C_{p2}$ ) for  $\alpha$ - (A) and  $\beta$ -type (B) of lactose crystal containing amorphous lactose mixtures at 1:4, 2:3, 3:2, and 4:1 mass ratios after storage at 0.33  $a_w$  and 25 °C. The error bars were derived from the standard deviation (SD) value based on triplicated measurements.

The heat capacity of high-water foods is largely due to water. The  $\Delta C_p$  values of pure amorphous lactose increased concomitantly with water content (Table 3.1). Since the  $\Delta H$  and  $\Delta C_p$  were properties of the amorphous fraction, the experimental enthalpy and heat capacity data of each lactose crystal/lactose mixture were normalized according to the amorphous lactose fraction ( $\Delta H''$  and  $\Delta C_{pn}$ ,  $n = 1$  for first heating scan and  $n = 2$  for second heating scan) and then compared with the  $\Delta H$  and  $\Delta C_p$  of pure amorphous lactose (Table 3.2). The  $\Delta H''$  values of both  $\alpha$ - and  $\beta$ - types lactose crystal containing systems decreased concomitantly with crystal content increasing due to the migrating water enhanced vibrations and reorientation of amorphous lactose in mixtures after storage at 0.33  $a_w$  and 25 °C (Fig. 3.3 A and B). Compared with  $\alpha$ -lactose monohydrates, the smaller  $\Delta H''$  values were found in  $\beta$ -type of lactose crystal/lactose

systems caused by a greater extent of water migration (Table 3.2). In co-freeze-dried lactose/WPI systems, however, the movement of amorphous lactose might be disturbed by the presence of protein reflecting on the  $\Delta H''$  values increased corresponding to pure lactose at 0.33  $a_w$  at 25 °C. Fig. (3.4) shows the  $\Delta C_{p1}$  and  $\Delta C_{p2}$  values of crystal/lactose systems based on two DSC heating scans after storage at 0.33  $a_w$  at 25 °C. The  $\Delta C_{pn}$  values of both  $\alpha$ - and  $\beta$ -types lactose crystal/lactose systems increased concomitantly with the content of crystals increasing (Table 3.2). And the difference of  $\Delta C_{pn}$  in  $\beta$ -type of lactose crystal/lactose was bigger than was found for  $\alpha$ -lactose monohydrates containing systems after equilibrium at 0.33  $a_w$  and 25 °C (Fig. 3.4). However, there has no significant variation of  $\Delta C_{pn}$  measured for the first and second heating scans in lactose/WPI mixtures after storage at 0.33  $a_w$  and 25 °C. The variation of  $\Delta C_p$  implied that the quantity of amorphous phase (Raine et al., 1945; Saunders et al., 2004) had changed in crystal/lactose systems and probably induced by either migration of water or lactose between crystal and amorphous phase in DSC heating. After equilibrium at 0.33  $a_w$  and 25 °C, the water in amorphous phase could migrate to crystalline phase and attach on the surface of crystals due to its lower water content. Those migrating water dissolved some lactose on crystalline surface in first heating scan and then increased the  $T_{gl}$  of mixtures corresponding to pure lactose. After second heating scan in DSC, however, the  $T_{g2}$  of mixtures decreased and the  $\Delta C_p$  values of mixtures increased ( $\Delta C_{p2} > \Delta C_{p1}$ ) which could be induced by of the variation in amorphous and crystalline phase contents. To be specific, the amorphous lactose as well as crystals might be produced by lactose dissolving water during cooling scan with cooling rate of 10 °C/min. Fig. (3.5) gives the schematic diagram of the quantities of crystal and amorphous phases in DSC measurement. To overall material composition, we found that the presence of different crystalline phases or protein could affect the enthalpy relaxation of a system through disturbing the local molecular movement of amorphous lactose, as a result of water migrating effects or physical blocking, respectively.



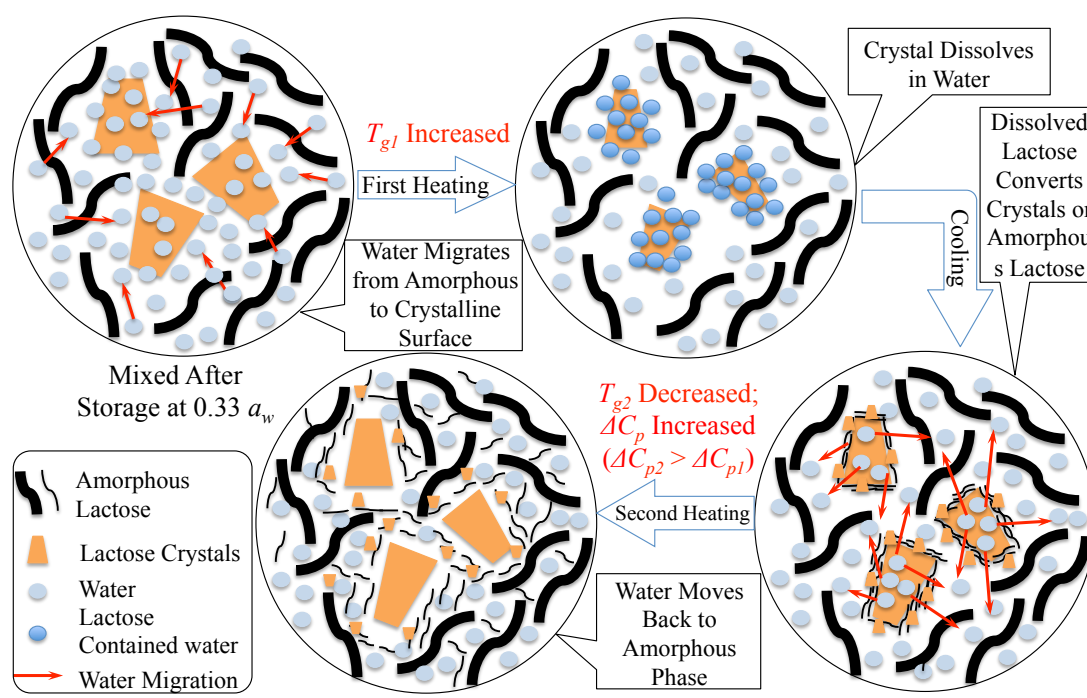


**Fig. 3.5.** The schematic diagrams of the molecular migration and amorphous production between amorphous and crystal phases in lactose crystal/lactose mixtures mixed after equilibrium at 0.33  $a_w$  at 25 °C. The symbols do not represent the real sizes and quantity of components.

### 3.3.2. DYNAMIC-MECHANICAL ANALYSIS

Typically, the rapid changes in mechanical properties of materials in DMA may be induced by many reasons such as water migration (Talja and Roos, 2001; Gonnet et al., 2002). Fig. (3.6) demonstrates the DMA spectra (loss modulus peaks at frequency of 0.5 Hz) for pure amorphous lactose at low water activities ( $\leq 0.44 a_w$ ),  $\alpha$ - and  $\beta$ -types of lactose crystal/lactose mixtures (1:4, 2:3, 3:2, and 4:1 at mass ratios) and lactose/WPI mixtures (7:3, 1:1, and 3:7 at mass ratios) after storage at 0.33  $a_w$  and 25 °C. The  $E''$  is related to the amount of energy converted to heat during relaxations (Roos and Drusch, 2015). The  $E''$  peaks of amorphous lactose decreased and broadened concomitantly with the water activities increasing (Fig. 3.6 A). Therefore, the  $E''$  of glass forming lactose could be altered by the presence of water as the molecular mobility was enhanced by water plasticization as well as the retarded

**Table 3.2.** The onset glass transition temperature and heat capacity of first and second heating stage,  $\Delta C_{p1}$  and  $\Delta C_{p2}$ ,  $T_{g1}$  and  $T_{g2}$ , normalized recovery of enthalpy,  $\Delta H''$ ,  $T_a$  (0.5 Hz), values of  $C_1$  and  $C_2$  values and strength parameter ( $S$ ) based on WLF equation and storage temperature for crystallization in  $\theta_{cr} = 2$  h,  $T_\theta$  of humidified lactose,  $\alpha$ - and  $\beta$ -type of lactose crystal/lactose mixtures (1:4, 2:3, 3:2, and 4:1 mass ratios), and lactose/WPI mixtures (7:3, 1:1, and 3:7 mass ratios) at 0.33  $a_w$  and 25 °C, respectively.

Materials	Water content (gH <sub>2</sub> O/100 solids)	$a_w$	$T_{g1}$ (°C)	$T_{g2}$ (°C)	$T_a$ (°C)	$\Delta H''$ (J/g) <sup>b</sup>	$\Delta C_{p1}$ (Jg <sup>-1</sup> K <sup>-1</sup> ) <sup>c</sup>	$\Delta C_{p2}$ (Jg <sup>-1</sup> K <sup>-1</sup> ) <sup>c</sup>	$C_1$	$C_2$ (K)	$S$ (°C)	$T_\theta$ (°C)
Lactose	6.1 ± 0.3	0.33 ± 0.00 <sup>a</sup>	30 ± 1	30 ± 2	48 ± 2	-8.47 ± 1.22	0.72 ± 0.04	0.72 ± 0.04	-3.37 ± 0.31	-41.72 ± 0.60	22.6 ± 0.7	53 ± 3
$\alpha$ -Crystals/Lactose 1:4	5.1 ± 0.1	0.32 ± 0.01	33 ± 1	31 ± 1	50 ± 3	-8.37 ± 0.76 <sup>*</sup>	0.55 ± 0.06	0.57 ± 0.06	-2.15 ± 0.23	-35.63 ± 0.42	23.2 ± 1.0	54 ± 2
$\alpha$ -Crystals/Lactose 2:3	3.9 ± 0.3	0.32 ± 0.00	32 ± 2	31 ± 0	52 ± 1	-7.38 ± 0.42	0.62 ± 0.09	0.69 ± 0.15	-2.30 ± 0.19	-38.89 ± 0.50	24.7 ± 0.9	56 ± 1
$\alpha$ -Crystals/Lactose 3:2	2.6 ± 0.2	0.33 ± 0.01	32 ± 1	31 ± 0	53 ± 1	-6.59 ± 0.97	0.68 ± 0.05	0.78 ± 0.04	-2.24 ± 0.32	-40.94 ± 0.62	26.2 ± 1.7	57 ± 2
$\alpha$ -Crystals/Lactose 4:1	1.5 ± 0.5	0.33 ± 0.00	31 ± 3	28 ± 2	53 ± 1	-3.48 ± 0.88	0.82 ± 0.15	0.98 ± 0.22	-2.08 ± 0.45	-42.70 ± 0.53	28.1 ± 2.6	58 ± 5
$\beta$ -Crystals/Lactose 1:4	5.2 ± 0.2	0.32 ± 0.01	34 ± 1	31 ± 1	49 ± 1	-7.13 ± 0.58	0.66 ± 0.00	0.70 ± 0.03	-4.93 ± 0.26	-49.35 ± 0.64	22.1 ± 0.9	55 ± 2
$\beta$ -Crystals/Lactose 2:3	4.0 ± 0.1	0.32 ± 0.00	33 ± 2	31 ± 0	47 ± 1	-6.99 ± 0.79	0.72 ± 0.05	0.82 ± 0.08	-7.04 ± 0.34	-57.18 ± 0.50	20.7 ± 0.8	51 ± 1
$\beta$ -Crystals/Lactose 3:2	2.8 ± 0.4	0.32 ± 0.00	33 ± 2	30 ± 0	45 ± 1	-5.75 ± 0.28	0.77 ± 0.07	0.98 ± 0.02	-4.64 ± 0.23	-38.93 ± 0.52	18.0 ± 0.7	48 ± 1
$\beta$ -Crystals/Lactose 4:1	1.4 ± 0.3	0.32 ± 0.01	34 ± 5	30 ± 0	42 ± 1	-4.95 ± 0.07	0.89 ± 0.12	1.10 ± 0.01	-7.24 ± 0.18	-44.46 ± 0.41	15.8 ± 0.4	46 ± 0
Lactose/WPI 7:3	6.6 ± 0.1	0.33 ± 0.01	34 ± 3	33 ± 1	58 ± 4	-11.87 ± 0.55	0.70 ± 0.02	0.68 ± 0.12	-4.40 ± 0.34	-74.75 ± 0.76	35.6 ± 1.8	69 ± 3
Lactose/WPI 1:1	7.0 ± 0.1	0.33 ± 0.00	35 ± 1	31 ± 1	66 ± 4	-12.74 ± 0.48	0.76 ± 0.01	0.77 ± 0.02	-2.98 ± 0.32	-74.81 ± 0.71	42.9 ± 2.4	75 ± 3
Lactose/WPI 3:7	8.0 ± 0.3	0.33 ± 0.00	39 ± 1	30 ± 1	73 ± 6	-14.68 ± 0.81	0.95 ± 0.04	0.97 ± 0.08	-2.17 ± 0.42	-74.30 ± 0.54	48.2 ± 3.6	78 ± 5

<sup>a</sup>; Values are mean ± SD ( $n=3$ ).

<sup>b</sup>, <sup>c</sup>; Experimental data of  $\Delta H''$  and  $\Delta C_{pm}$  were normalized from the  $\Delta H'$  and  $\Delta C_p$  of pure amorphous lactose based on fractional ratios in each mixture.

viscous flow characteristics of amorphous lactose. However, the peak height of  $E''$  values significantly decreased concomitantly with the  $\alpha$ -lactose monohydrate and anhydrous  $\beta$ -lactose content increasing in crystal/lactose mixtures after storage at 0.33  $a_w$  and 25 °C (Fig. 3.6 B and C). The water migration, in this study, could enhance viscous flow of lactose by the presence of crystals due to enhanced molecular movement of amorphous lactose. However, the peaks and broadness of  $E''$  for lactose/WPI mixtures were significantly changed concomitantly with the content of WPI increasing, compared with pure lactose after storage at 0.33  $a_w$  and 25 °C (Fig. 3.6 D). As expected, the  $E''$  results reflected the amorphous lactose content of the mixtures as the crystalline phase and WPI existed in separate phases apart from the amorphous lactose (Silalai and Roos, 2011b).

The  $T_\alpha$  was determined from the peak temperature of  $E''$  in the DMA spectra (Talja and Roos, 2001; Silalai and Roos, 2011ab; Potes et al., 2012). The  $T_\alpha$  values of pure amorphous lactose were given on Table (3.1). Since the physical state of amorphous carbohydrate systems is strongly influenced by the concentration of water, the  $T_\alpha$  of pure lactose at lower activities was varying from 29 °C (0.44  $a_w$ ) to 128 °C (anhydrous state) at a frequency of 0.5 Hz, which agreed with previous studies (Cruz et al., 2001; Renzetti et al., 2012). As the molecules within the amorphous phase have insufficient mobility under the perturbation,  $T_\alpha$  of glassy materials under oscillation could indicate the extent of molecular mobility of the amorphous components (Royall et al., 2005). Recently, the free volume theory and its effects on molecular mobility were successfully applied to describe the increase in diffusivity observed in food materials (Meinders and Van Vliet, 2009). As the  $T_\alpha$  values of amorphous lactose decreased by water, the water could increase the free volume as well as the extent of molecular mobility of amorphous lactose at 25 °C (Table 3.1). In Table (3.2), the  $T_\alpha$  values of anhydrous  $\beta$ -lactose containing crystal/lactose systems at each ratio were lower than those of  $\alpha$ -type of lactose crystal/lactose systems after storage at 0.33  $a_w$  due to a greater water migration as noted above. However, the presence of WPI increased the  $T_\alpha$  values of lactose/WPI mixtures, which was caused by the

physicochemical interactions derived from protein and then reduced the movement of amorphous lactose by proteins. Therefore, our study indicated that the presence of separate phases of components could alter the movement of amorphous lactose molecules, and thus, affect the structural relaxations and viscous flow characteristics of amorphous sugars.

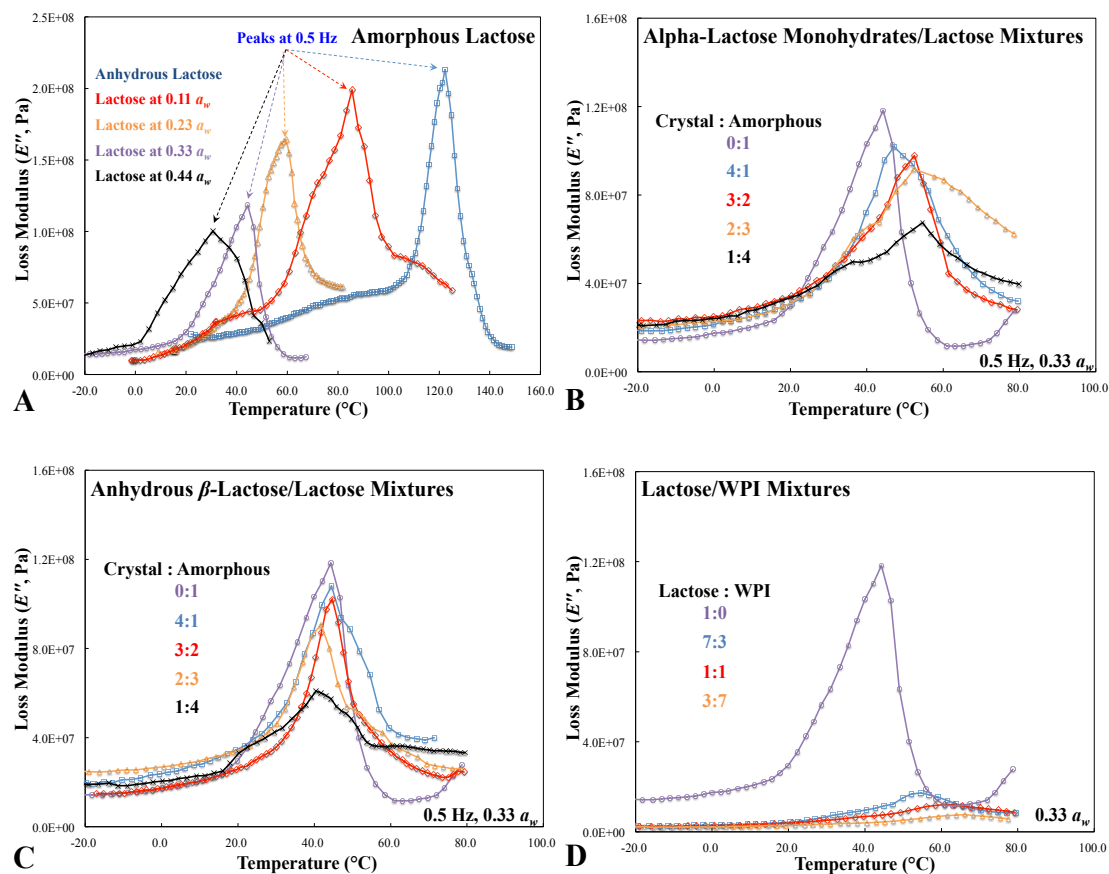


**Fig. 3.6.** The DMA spectra of  $E''$  for pure amorphous lactose at water activities below 0.44  $a_w$  (A),  $\alpha$ - and  $\beta$ -type of lactose crystal/lactose mixtures with mass ratio of 1:4, 2:3, 3:2, and 4:1 (B and C) and lactose/WPI mixtures with 7:3, 1:1, and 3:7 mass ratios (D) at frequency of 0.5 Hz after storage at 0.33  $a_w$  at 25  $^{\circ}\text{C}$ . The  $\alpha$ -relaxation temperature was characterized based on the peak of each loss modulus (Potes et al., 2012).

### 3.3.3. WLF-MODEL ANALYSIS OF ALPHA-RELAXATION TIMES

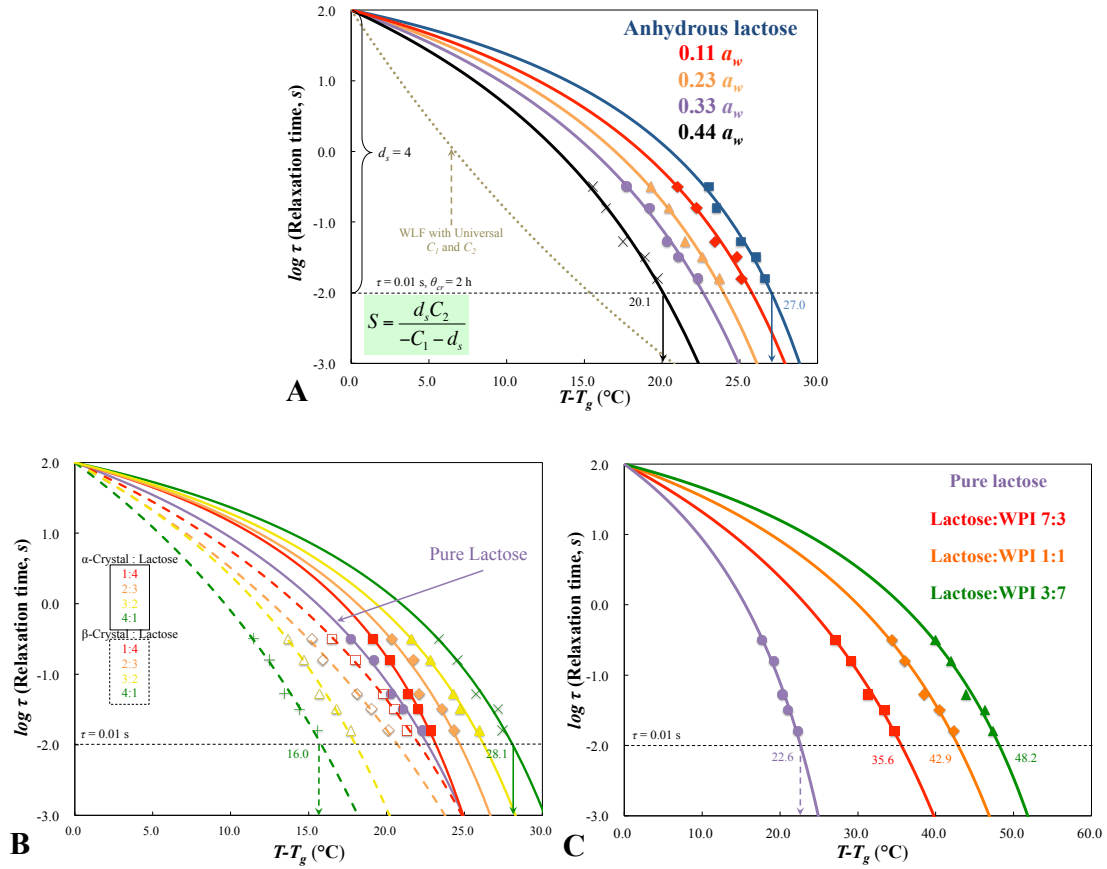


**Fig. 3.7.** Strength parameters ( $S$ ) of pure lactose at various water activities ( $0 a_w \sim 0.44 a_w$ ) (A),  $\alpha$ - and  $\beta$ -type of lactose crystal/lactose (1:4, 2:3, 3:2, and 4:1 mass ratios) (B), and lactose/WPI mixtures (7:3, 1:1, and 3:7 mass ratios) (C) after storage at  $0.33 a_w$  and  $25$  °C at  $d_s = 4$  decreasing the structural relaxation time,  $\tau$ , As measured using dynamic mechanical analysis (DMA) to  $\tau = 0.01$  s. The WLF equation with universal  $-C_1$  and  $C_2$  ( $-17.44$  and  $51.6$ ) were plotted (black dotted line) as a reference.

Angell (1991) established classification of glass formers to “fragile” or “strong” materials. A fragile material deviates considerably from the Arrhenius temperature dependence above the glass transition, which means that there is a significant change in the molecular mobility in the vicinity of the glass transition. A strong glass former shows less dramatic changes in relaxation times above the glass transition and follows the Arrhenius temperature dependence. The key principle of the “fragility” or “fragile” vs. “strong” classification of glass-forming liquids is the steepness of the plot showing

viscosity,  $\log \eta$  or structural relaxation time  $\log \tau$  as viscosity and dielectric or mechanical relaxation times approach  $10^{12}$  Pas and  $10^2$  s, respectively, at the onset of the calorimetric glass transition (Angell, 2002). However, Roos (2012) pointed out that the main shortcoming of above fragility concept was an anomaly in that materials may have different fragilities, although their viscosities and relaxation times at any  $T-T_g$  values are the same, therefore they should have the same fragility. On the other hand, for many materials, the same  $T-T_g$  corresponds to the same relaxation time (or viscosity), but the  $T_g/T$  values differ because the  $T_g$  values differ (Roos et al., 2015). Hence, the  $T_g/T$  plotting shows that the fragilities of each substance differ according to their individual  $T_g$  values. Thus, the fragility concept as discussed by Angell (2002) may not be very useful for biological and food systems. Roos (2012) also recommended that that WLF equation was valid over the temperature range within the rubbery or supercooled liquid state and was also used to describe time and temperature dependent behavior of amorphous materials. However, the WLF equation with universal constants,  $-C_1$  and  $C_2$ , could not be used to model experimental  $\log \tau$  against  $\Delta T$  data of amorphous lactose at low water activities (brown dotting line in Fig. 3.7 A). As the material-specific constants  $-C_1$  and  $C_2$  gave a very good fit to experimental data of lactose and its mixtures, the  $-C_1$  and  $C_2$  constants were material-specific constants with numerical values varying with composition based on WLF equation in food systems.

When the storage temperature increases to above  $T_g$ , however, amorphous materials loose solid characteristics concomitantly with decreasing  $\tau$ , which is reflected on the decreasing viscosity and increasing flowability of the materials (Lillie and Gosline, 1990; Slade et al., 1991). Such loss of solid characteristics results in collapse of cell walls in porous structures typical of dehydrated foods. Fig. (3.7A) shows the  $S$  values of pure lactose after storage at low water activities ( $\leq 0.44 a_w$ ) as derived from the modified WLF model analysis (downwards concavity around glass transition). And the material-specific constants  $-C_1$  and  $C_2$ , and  $S$  of humidified lactose stored at low water activities ( $\leq 0.44 a_w$ ) are given in Table (3.1). We found that water could

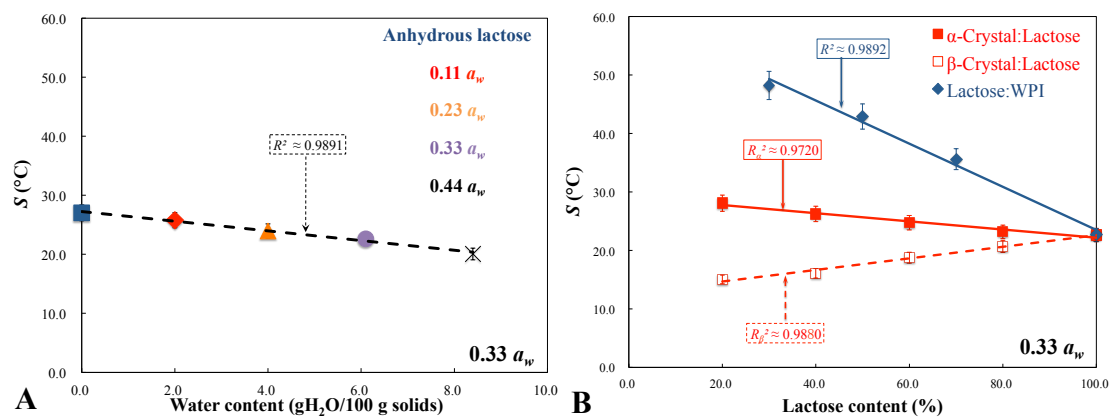


**Fig. 3.8.** The linear relationship established based on  $S$  and water content of amorphous pure lactose (A) at low water activities on 25 °C. B showed that the relationship and correlation coefficient,  $R^2$ , between  $S$  values and the quantity of amorphous lactose in  $\alpha$ - and  $\beta$ - type of lactose crystal/lactose mixtures ( $R_{\alpha}^2$  and  $R_{\beta}^2$ ), lactose/WPI mixtures ( $R_w^2$ ) after storage at 0.33  $a_w$  and 25 °C, respectively.

govern the structural strength or viscous flow characteristics of glass forming lactose as the  $S$  value showed a linear relationship with water content ( $R^2 \approx 0.9891$ ) (Fig. 3.8 A). Fig. (3.7B and C) demonstrated that the presence of crystalline phase and WPI could affect the strength of amorphous lactose containing mixture after storage at 0.33  $a_w$  and 25 °C. Table (3.2) gives the values of  $C_1$  and  $C_2$ , and  $S$  parameters for lactose,  $\alpha$ - and  $\beta$ -type of lactose crystal/lactose and lactose/WPI mixtures after storage at 0.33  $a_w$  and 25 °C, respectively. The  $S$  of  $\alpha$ -lactose monohydrate and WPI containing amorphous lactose mixtures showed a greater value ( $23 \text{ °C} \leq S \leq 28 \text{ °C}$  for  $\alpha$ -type of lactose crystal/lactose systems and  $36 \text{ °C} \leq S \leq 48 \text{ °C}$  for lactose/WPI mixtures), whereas  $\beta$ -type of lactose crystal/lactose system had a smaller  $S$  value ( $16 \text{ °C} \leq S \leq 22 \text{ °C}$ ) compared to pure amorphous lactose ( $S \approx 21 \text{ °C}$ ) (Table 3.2). The anhydrous  $\beta$ -lactose might reduce the strength of mixtures and enhance the flow characteristic of solids due to migrating water effects, whereas the  $\alpha$ -lactose monohydrate could keep the whole system strong due to less dramatic structural changes above the glass transition. The WPI could improve the strength of co-freeze-dried lactose/WPI

systems probably because of the existence of physicochemical interactions, which could disturb the molecular mobility of glass forming components in mixtures above glass transition at 0.33  $a_w$  and 25 °C (Fig. 3.7 C). Therefore, the strength of amorphous systems, derived from WLF analysis, could be affected by the presence of water, other phases or polymeric components due to both water migration and physicochemical interactions between lactose and WPI, which could reduce molecular mobility of amorphous sugars.

The strength was governed by the fraction of amorphous lactose in both of  $\alpha$ - and  $\beta$ -type of lactose crystal/lactose and lactose/WPI mixtures after storage at 0.33  $a_w$  and 25 °C (Fig. 3.8 B), respectively. In the present study, the strength of  $\beta$ -type of lactose crystal containing mixtures increased concomitantly with the increasing of amorphous lactose content. And the protein could increase stiffness of lactose/WPI mixtures, which was reflected on the  $S$  values increased with the WPI content increasing, significantly. Therefore, the strength of amorphous lactose containing mixtures could be altered by the presence of different crystalline phases and components. The  $S$  parameter could be considered as an effective approach to quantify the strength of amorphous materials. And it may be related to flow properties, viscous flow and collapse, and mechanical properties, which could control processing as well as the quality and stability of food and pharmaceutical materials.

#### **3.3.4. STRENGTH PARAMETER AND CRYSTALLIZATION**

Crystallization during food storage often results from an exposure of noncrystalline food components to temperatures above their glass transition. And it may also be observed from changes in water content or water activities as found in water sorption studies. As we noted in Chapter 2, lactose crystallization was time-dependent and could be affected by the presence of protein. We defined a  $T-T_g$  as the strength of the solids at  $\tau = 0.01$  s (Eq. 1.12). The relationship between  $\tau$  and real time for completing crystallization,  $\theta_{cr}$ , of amorphous lactose could be determined by water sorption (Roos



and Karel, 1992). When the glass forming lactose was stored above its  $T_g$ , the temperature above glass transition could be considered as a critical storage temperature of amorphous lactose for completing crystallization ( $T_\theta$ ) within  $\tau = 0.01$  s, which approximately equals 2 h for  $\theta_{cr}$  (Roos and Drusch, 2015). Specifically, when the storage temperature of materials exceeded  $T_\theta$ , the  $\theta_{cr}$  dramatically decreased and thus caused a rapid loss of shelf life, whereas the  $\theta_{cr}$  could be increased as the storage temperature was below  $T_\theta$ . Table (3.1) gives the  $T_\theta$  of lactose under varying  $a_w$ . The  $T_\theta$  of anhydrous lactose (132 °C) within  $\theta_{cr} = 2$  h could be calculated from  $S \approx 27$  °C and onset of  $T_g \approx 105$  °C in the present study. These results agreed with those of Roos and Karel (1991), who reported that the crystallization of anhydrous amorphous lactose occurred within 2 h when storage temperature was 135 °C in a DSC study. As water content increased, the  $T_\theta$  values of pure lactose decreased to 33 °C at 0.44  $a_w$  (Table 3.1). Hence, the  $\theta_{cr}$  of lactose could be depressed by the presence of water caused by water plasticization. The  $T_\theta$  of  $\alpha$ -type of crystal containing mixtures increased concomitantly with the content of  $\alpha$ -lactose monohydrate, whereas the anhydrous  $\beta$ -lactose depressed the  $T_\theta$  of systems after storage at 0.33  $a_w$  and 25 °C (Table 3.2). This phenomenon was due to the greater extent of water migration effects in  $\beta$ -type lactose crystal containing systems, which enhanced the molecular mobility, and thus reduced the  $\theta_{cr}$  of amorphous lactose. On the other hand, we found that  $\alpha$ -lactose monohydrate could enhance the shelf life and stability of amorphous lactose due to the  $T_\theta$  increasing after storage at 0.33  $a_w$  and 25 °C. As reduced crystallization in the presence of WPI was more pronounced, the strength of lactose/WPI systems increased and thus delayed the crystallization behavior due to the  $T_\theta$  varying from 69 °C up to 78 °C with the increasing of protein content after storage at 0.33  $a_w$  and 25 °C (Table 3.2). Therefore, water could play an important role governing the structural strength and  $\theta_{cr}$  of amorphous sugars, whereas crystals and WPI could be used to control the structural strength and crystallization rate. The strength characteristic could be used to control the shelf life and quality of amorphous sugars as  $S$  value could be used to predict the critical storage temperature of crystallization.

### 3.4. CONCLUSIONS

We have shown that structural relaxations and relaxation time of amorphous lactose and lactose/WPI mixture could be affected by the mixture composition, i.e., different crystalline phases and protein, using WLF model analysis. A structural strength concept based on WLF model analysis was validated and the  $S$  parameter provided a simple and convenient means to measure structural strength of amorphous sugar containing mixtures. The structural strength concept, using the information of the non-crystalline state of food materials in systematic manner, could be used to quantify structure formation in food processing as well as for stability control of resultant products. For further researching, the crystallization properties as well as strength of sugars and sugar/protein systems will be continually investigated in food and pharmaceutical materials.



## STRUCTURAL STRENGTH AND CRYSTALLIZATION OF AMORPHOUS LACTOSE IN FOOD MODEL SOLIDS AT VARIOUS WATER ACTIVITIES

Fanghui Fan and Yrjö H. Roos

*School of Food and Nutritional Sciences,  
University College Cork, Cork, Ireland*

## ABSTRACT

Freeze-dried lactose and lactose/WPI mixtures were used as amorphous food models at various  $a_w$ , and the effects of temperature and water and WPI contents on physical state were analysed. Thermal behaviour and mechanical properties were studied and WLF model was fitted to structural relaxation times. The WLF-analysis gave a  $S$  parameter that was used to describe structural strength of the food solids. Our results showed that lactose and WPI in mixtures exhibited fractional water sorption. Thermal properties and structural strength of the solids were affected by water and WPI while  $T_g$  measured for the lactose/WPI systems followed that of the lactose component and showed phase separation of lactose and proteins. A relationship between  $S$  and water content was established, whereas the crystallization of amorphous lactose was more rapid in systems with a smaller  $S$ . Therefore,  $S$  provided a simple and convenient measure of  $\tau$  controlling structure formation in food processing as well as to control lactose crystallization.

**KEYWORDS,** *Structural strength; Crystallization; Relaxation time; WLF-analysis; Lactose; Water*

## 4.1. INTRODUCTION

The physical state of food solids, e.g., sugars, polysaccharides and proteins, has received an increasing attention in food and pharmaceutical industries because of its importance to both processing and shelf life control (LeBail et al., 2003; Sperling, 2006). Industrial dehydration technologies, e.g., freeze-drying and spray-drying, remove water and provide many reconstituted products with sensorial properties resembling those of the original foods, e. g., powdered milk (Silalai and Roos, 2011a), potato flakes (Turner et al., 2006) and dry pasta (Aguilera et al., 2003; Gowen et al., 2008). Dehydrated foods show stability achieved by converting at least some of the

solids to an amorphous solid state, i.e., temperature and water content are controlled to reduce structural relaxations within the noncrystalline solid state (Slade et al., 1991; Lloyd et al., 1996). In various dehydrated food and biological materials, therefore, the physical state of solid food components may determine the success of structure formation (Biliaderis, 1991; Roos et al., 2016). Lactose is a common and typical noncrystalline food component (Gänzle et al., 2008). Lactose in dehydrated products may exist either as a very viscous glass or as a more liquid-like “rubbery” amorphous structure and in any ratio of the crystalline and amorphous states. The solid-like glass exhibits a high viscosity ( $\approx 10^{12}$  Pa s) with solid appearance and strong hygroscopic properties (Gänzle et al., 2008). Moreover, amorphous lactose may undergo time-dependent changes, i.e., crystallization, with increasing rates at increasing temperatures and water contents (Slade et al., 1991; Sperling, 2006). Therefore, the physical state and physicochemical characteristics of amorphous lactose were important parameters in processing and storage of dehydrated lactose-based products such as powdered milk (Jouppila et al., 1997).

Recent studies have shown that dried foods exhibit glass transitions when exposed to a humid atmosphere, which may greatly affect chemical and physical changes during food processing and storage. The change of amorphous materials from the glassy state to the rubbery state occurs above glass transition temperature, which is specific for each food component (Champion et al., 2000). When temperature increases to above  $T_g$ , a rapid increase of molecular mobility occurs, which is detected from decreasing viscosity and increasing flowability of glass-forming materials. The effects of the glass transition on component crystallization have shown that glass transition affects and often explains the occurrence of such behavior in foods (Slade et al., 1991; Chung et al., 2004; Roos and Drusch, 2015). Structural relaxations, as often measured above or somewhat below the glass transition region, reflect the spontaneous approach of amorphous materials towards equilibrium at a rate, which depends on temperature and water activity of the material. The corresponding structural relaxation times are the time that is necessary for the recovery from perturbations (Le Meste et al., 2002; Liu

et al., 2006). Structural relaxations measured around the glass-liquid transition are of similar timescale to the experimental time scale. Therefore, structural relaxations and  $\tau$  may be related to particle structure, flow characteristics, viscous flow and collapse, and mechanical properties, which control the quality and stability of food materials, particularly in the vicinity and above the onset of the calorimetric glass transition. The Williams-Landel-Ferry model is often fitted to structural relaxation times above  $T_g$  to show the non-Arrhenius temperature dependence of molecular mobility and the rate of diffusion-limited relaxation processes as related to  $T_g$  and expressed in terms of  $\tau$  dependence on  $T-T_g$  (Angell, 2002; Sperling, 2006).

Crystallization of an amorphous food component results in a dramatic change in structure of dried food materials due to the occurrence of a rapid molecular motion above  $T_g$ ; particularly mechanical properties and time-dependent solid flow characteristics are affected (Sperling, 2006; Roos and Drusch, 2015). The rate of amorphous lactose crystallization depends on several factors, such as the rate of nucleation, the time required to remove water, molecular anomerization and storage temperature above  $T_g$ ,  $T-T_g$  (Ibach and Kind, 2007). Crystallization of amorphous lactose is of practical importance and it may enhance physical and chemical deterioration in food ingredients and is typical of dairy powders at high storage humidities or temperatures causing a rapid loss of shelf life (Ibach and Kind, 2007; Gänzle et al., 2008). Mechanical properties of amorphous sugars could be affected by their degree of crystallinity and the presence of other components affecting glass transition e.g., water (Slade et al., 1991), carbohydrates (Cruz et al., 2001) and proteins (Regand and Goff, 2006). The frequency-dependent  $\alpha$ -relaxation of amorphous sugars is governed by water content, relative humidity and temperature (Faivre et al., 1999). As the measurements of solid flow characteristics over the glass transition region are extremely difficult, Roos and Others (2016) defined a measure for solids flow characteristics given by “structural strength,  $S$ ” and introduced a WLF model-based analysis of structural relaxation times within solids affecting flow characteristics in food materials. The strength concept gave a measure of resistance to

structural changes for glass-forming solids and could be used to describe the solids properties, such as crystallization, in mixes of sugars and polymeric food components.

Whey protein isolates may act as stabilizers, which are widely used in sugar-protein systems during spray drying and freeze-drying in the food and pharmaceutical industries (Zhou and Labuza, 2007; Wang et al., 2010). Our previous studies showed that WPI could affect crystallization of amorphous sugars in powders at high relative humidity storage in Chapter II. However, the effects of the structural strength of the amorphous compounds on properties of dried milk and other food materials in processing and shelf life need to be established. Therefore, the objectives of the present study were to investigate the influence of water and WPI on the calorimetric glass transition and lactose crystallization, structural relaxation times and structural strength of freeze-dried amorphous food models (lactose/WPI systems) after storage at various  $a_w$ . We expected that the relationship between structural strength and crystallization of the glass former and their interaction with other solids could contribute to powder characteristics, which could be widely used in practical applications.

## **4.2. MATERIALS AND METHODS**

### **4.2.1. SAMPLE PREPARATION**

The food models in our study were prepared using  $\alpha$ -lactose monohydrate (Sigma-Aldrich, St. Louis, Mo., U.S.A.) and whey protein isolate (WPI; Isolac<sup>®</sup>, Carbery Food Ingredients, Co., Ballineen, Ireland; impurities including carbohydrates and lipids < 3 %). De-ionized water (KB Scientific, Cork, Ireland) was used for all experimental work. Lactose was dissolved in de-ionized water to obtain 20 % (mass) solution. WPI solution with 20 % (mass) solids was prepared using continuous stirring for 4 h at room temperature ( $\sim 23$  °C). Lactose and WPI solutions at room temperature were used to obtain mass ratios of 7:3, 1:1, and 3:7 of lactose/WPI by

mass, respectively. Samples (5 mL in total) were prepared in pre-weighted glass vials (10 mL, diameter 24.3 mm × height 46 mm; Schott Müllheim, Germany). All samples in the vials (semi-closed with septum) were frozen in a still air freezer at −20 °C for 20 h and then subsequently tempered at −80 °C for 3 h prior to freeze-drying using a laboratory freeze-dryer (Lyovac GT2 Freeze Dryer, Amsco Finn-Aqua GmbH, Steris®, Hürth, Germany). It should be noted that the temperature of condenser is −40 °C for secondary drying (desorption) during freeze-drying process. After freeze-drying at pressure < 0.1 mbar, triplicate samples of each material were stored in evacuated vacuum desiccators over  $P_2O_5$  (Sigma-Aldrich, St. Louis, Mo., U.S.) prior to subsequent analysis.

#### 4.2.2. WATER SORPTION AND TIME-DEPENDENT CRYSTALLIZATION

Water sorption by freeze-dried lactose, lactose/WPI mixtures and WPI at each ratio was monitored for 120 h (non-crystallizing samples) and 240 h (crystallizing samples) over saturated solutions of  $LiCl$ ,  $CH_3COOK$ ,  $MgCl_2$ ,  $K_2CO_3$ ,  $Mg(NO_3)_2$ ,  $NaNO_2$ , and  $NaCl$  (Sigma Chemical Co., St. Louis, Mo., U.S.A.) at respective water activities of 0.11, 0.23, 0.33, 0.44, 0.54, 0.65, and 0.76  $a_w$  at 25 °C, in vacuum desiccators. The  $a_w$  measured (Dew Point Water Activity Meter 4TE, Aqualab, WA, USA) for each sample at 25 °C is given in Table (4.1). Evacuated desiccators in incubators (Series 6000, Termaks, Bergea, Norway) were stored at 25 °C. Vials with samples were weighted to monitor water sorption at 0, 3, 6, 9, 12, and 24 h followed by 24 h intervals up to 240 h, respectively. Lactose crystallization was monitored from release of sorbed water during storage over saturated solutions of  $NaNO_2$  and  $NaCl$  at 25 °C. Water contents of the materials were measured as a function of time, and the average weights of triplicate samples were used in calculations. The GAB equation (Eq. 1.1) was used to fit the experimental data of water sorption at 25 °C (Timmermann et al., 2001).



### 4.2.3. THERMAL ANALYSIS

The onset glass transition temperature, onset and peak crystallization temperature ( $T_{cr1}$  and  $T_{cr2}$ ) for each material was determined using DSC (Mettler Toledo Schwerzenbach, Switzerland). Samples of all materials were transferred to preweighed standard DSC aluminum pans ( $\sim 40\mu\text{L}$ , Mettler Toledo Schwerzenbach, Switzerland), and hermetically sealed before weighing. An empty punctured pan was used as a reference. Samples were scanned from  $\sim 60\text{ }^{\circ}\text{C}$  below to over the  $T_g$  region at  $5\text{ }^{\circ}\text{C}/\text{min}$  and then cooled at  $10\text{ }^{\circ}\text{C}/\text{min}$  to initial temperature. A second heating scan was run to well above the  $T_g$  at  $5\text{ }^{\circ}\text{C}/\text{min}$ . The onset  $T_g$  for glass transition, onset  $T_{cr1}$  and peak  $T_{cr2}$  for crystallization were derived from second heating scans and recorded using STARe software, version 8.10 (Mettler Toledo Schwerzenbach, Switzerland), respectively. Appendix II gives a schematic diagram for the onset  $T_g$ , onset  $T_{cr1}$  and peak  $T_{cr2}$ , latent heat of crystallization ( $\Delta H_{cr}$ ) based on second heating scan using DSC. The GT equation (Eq. 1.3) has proven to fit to experimental data on  $T_g$  at various water contents of amorphous sugars.

### 4.2.4. DYNAMIC-MECHANICAL ANALYSIS

Dynamic-mechanical properties of humidified lactose and lactose/WPI systems were studied using dynamic-mechanical analyzer (DMA, Triton 2000, Triton Technology Ltd., UK). The storage modulus ( $E'$ ) and loss modulus ( $E''$ ) as a function of temperature at different frequencies were determined (0.5, 1.0, 3.0, 5.0, and 10.0 Hz). The DMA instrument was balanced or set at zero to determine the zero displacement position before starting an experiment. Approximately 100 mg samples of grinded materials were spread on a metal pocket-forming sheet (Triton Technology Ltd., UK). The sheet with sample was crimped along a pre-scored line to form a thin sandwich pocket. This pocket was attached directly between the clamps (the fixed clamp and the driveshaft clamp) inside the measuring head of the DMA. The length, width, and thickness ( $\sim 2\text{ mm}$ ) of the sample pocket between the clamps were measured.

Triplicate samples of each material were analyzed using dynamic measurements and recorded using DMA software version 1.43.00. The measuring head was connected to a liquid nitrogen tank for cooling (1 L; Cryogun, Brymill Cryogenic Systems, Labquip Ltd., Dublin, Ireland). Samples were scanned from  $\sim 60$  °C below to over the  $\alpha$ -relaxation region with cooling rate of 5 °C/min and heating rate of 2 °C/min using the single cantilever bending mode. During dynamic heating, the samples were analyzed for  $T_\alpha$  determined from the peak temperature of  $E''$  above the glass transition. Average values for triplicate measurements of peak  $T_\alpha$  were calculated.

#### 4.2.5. WLF-MODEL ANALYSIS FOR RELAXATION TIMES

The  $\tau$  and the temperature of  $T_\alpha$  above  $T_g$ , were modeled and analyzed using the WLF equation (Eq. 1.9), where  $\tau$  was defined by oscillation frequency set in DMA measurement ( $\tau = 1/2\pi f$ ). The WLF model constants  $C_1$  and  $C_2$  were derived from a plot of  $1/\log(\tau/\tau_g)$  against  $1/(T-T_g)$  using experimental relaxation times,  $\tau$ , with the assumption of  $\tau_g = 100$  s at the onset temperature of the calorimetric glass transition,  $T_g$  (Angell, 2002). The  $S$  parameter corresponds to a critical increase in temperature above  $T_g$ , and describes structural strength of glass formers above calorimetric onset glass transition temperature (Roos et al., 2016). A decrease in the number of logarithmic decades for flow, e.g., that to stickiness of a sugar, can be defined as the critical parameter,  $d_s$ , of Eq. (1.12) and a corresponding  $T-T_g$  is given as the structural strength of the solids,  $S$  (Supplementary Information). As the  $S$  is given as temperature corresponding to a critical  $\tau$  for a key amorphous component within a material, it also provides a measure of resistance to structural changes, i.e., the higher value of  $S$  refers to a more flow resisting system at similar  $T-T_g$  conditions.

#### 4.2.6. STATISTICAL ANALYSIS

The GAB model, predicted  $T_g$  of systems based on GT equation and the data of  $\tau$  were calculated and fitted using Microsoft Office Excel 2011 (Microsoft, Inc., U.S.A.). All

measurements were repeated three times as well as the average values with standard deviation of triplicate measurements were calculated.

## 4.3. RESULTS AND DISCUSSION

### 4.3.1. WATER SORPTION

The experimental data for lactose, lactose/WPI mixtures, and WPI over whole experimental  $a_w$  range at 25 °C is shown in Table (4.1) and Fig. (4.1A). Steady-state water contents of each material were used in GAB using data at 120 h. The GAB model was fitted to experimental data of pure lactose below 0.56  $a_w$  as lactose crystallization as shown by release of sorbed water occurred at higher  $a_w$  (Fig. 4.1 A). The wider the water activity ranges used in GAB model, the better fitting results would be achieved (Timmermann et al., 2001). However, extrapolated sorption data of non-crystalline components using the GAB model derived from water sorption data over a narrow water activity ( $\leq 0.44 a_w$ ) range overestimate sorbed water contents and result in significant errors (Potes et al., 2012). Systems with 7:3 ( $\leq 0.65 a_w$ ) and 1:1 of lactose/WPI ratios ( $\leq 0.76 a_w$ ) provided fractional water sorption data over a wider  $a_w$  range. In the present study, experimental data at 0.11 ~ 0.44  $a_w$  and fractional water contents at 0.55 ~ 0.76  $a_w$  derived from lactose/WPI mixture at 3:7 ratio (steady state sorbed water content of non-crystalline components) for non-crystalline lactose were used in the GAB model (Fig. 4.1 A). Fractional water contents of lactose in WPI mixtures at each  $a_w$  at 25 °C could be derived using Eq. (1.2), which agreed the reports derived from Potes and Others (2012).

Sorbed water release from freeze-dried lactose was most rapid at high  $a_w$ . However, no crystallization of amorphous lactose in lactose and lactose/WPI systems was likely at low  $a_w \leq 0.44$  during 10 days of storage at 25 °C. At 0.65 and 0.76  $a_w$ , lactose crystallization was affected by protein and the release of sorbed water decreased concomitantly with increasing WPI content. No lactose crystallization was observed

in lactose/WPI mixtures at 3:7 ratios over the whole  $a_w$  during 240 h of storage (Fig. 4.1 A). But lactose/WPI at 7:3 and 1:1 showed less sorbed water at the higher  $a_w$ . The decrease in water was less than in pure lactose which showed formation of partially

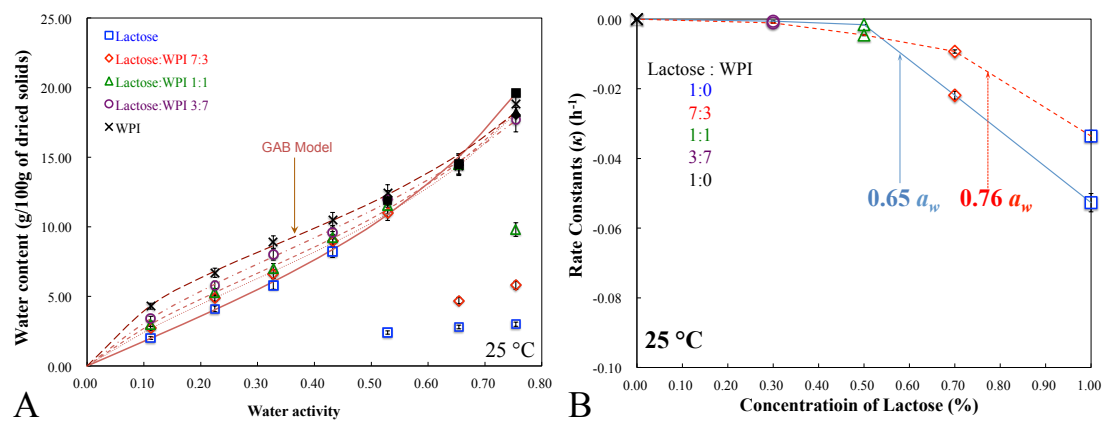


**Fig. 4.1.** Water fitted by GAB model (A) at  $0.11 \leq a_w \leq 0.76$  and crystallization kinetics (B) for freeze-dried lactose and lactose/WPI mixtures at all ratios (7:3, 1:1, and 3:7, w/w) at 0.65 and 0.76  $a_w$  and 25 °C. The experimental (clear symbols) and calculated water content data (solid symbols) for amorphous lactose, WPI, and lactose/WPI mixtures at solids ratios of 7:3, 1:1, and 3:7 showed in A. The thick solid (Amorphous Lactose), dotted (lactose/WPI 7:3), short dashed (lactose/WPI 1:1), dashed-dotted (lactose/WPI 3:7), and long dashed lines (WPI) correspond to the GAB sorption isotherms. The GAB sorption isotherm of non-crystalline lactose was obtained using experimental data ( $0.11 \sim 0.44 a_w$  at 25 °C) and data derived from lactose/WPI mixture (3:7) ( $0.55 \sim 0.76 a_w$  at 25 °C). The GAB sorption isotherms for non-crystalline lactose/WPI systems at 7:3 and 1:1 mass ratios used experimental data  $0.11 \sim 0.56 a_w$  and fractional water contents for non-crystalline lactose and data measured for lactose/WPI mixture (3:7) to predict sorbed water contents at 0.65 and 0.76  $a_w$ .

crystalline structures in mixtures. The high  $RH$  might weaken protein inhibition of lactose crystallization probably due to rapid molecular mobility of lactose and enhanced rates of diffusion as a result of water plasticization. In the present study,

however, the presence of high-molecular-weight protein could delay the low-molecular-weight lactose crystallization at intermediate  $a_w$  because of retarded diffusion of lactose molecules onto crystal lattices. In addition, we noticed that the fractional water contents in lactose/WPI systems showed composition independent water sorption characteristic, which suggested phase separation of lactose and whey proteins. Therefore, we assume that the lactose molecules may need a long diffusion time for nucleation to form stable nuclei or migration to the surface of crystals in order to release the water molecules during crystal-growth stage. The kinetics of water release was used as a measure of lactose crystallization rate (Potes et al., 2012). The inhibition of lactose crystallization by proteins was evident from the rate constant,  $k$ , as the  $k$  decreased (or the absolute value of  $k$  increased) with the quantity of WPI in lactose/WPI mixtures (7:3 and 1:1, w/w). The relationship between the  $k$  and lactose quantity in lactose/WPI systems at 0.66 and 0.76  $a_w$  is shown in Fig. (4.1B). At 0.65 and 0.76  $a_w$ , the rate of release of sorbed water of lactose/WPI systems rapidly decreased (close to zero) with increasing WPI content. The  $k$  was significantly depressed by the increasing weight fraction of WPI in systems with  $k$  close to zero below 50 % and 70 % of WPI content at 0.65 and 0.76  $a_w$  (Fig. 4.1 B). Even the storage  $RH$  could significantly affect lactose crystallization; the increasing quantity of WPI could delay the crystallization. Therefore, the kinetics of lactose crystallization in lactose/WPI was dependent on the protein content during crystallization.

#### 4.3.2. THERMAL ANALYSIS

The thermal transitions of lactose in dried food models could be detected by using DSC measurements. The thermograms were typical of crystallizable amorphous materials showing glass transition, and subsequent exothermal crystallization. In the present study, the lactose and lactose/WPI systems showed typical thermal behavior in DSC thermograms and the onset of lactose glass transition temperature ( $T_g$ ) and crystallization temperature at onset and peak values ( $T_{cr1}$  and  $T_{cr2}$ ) after storage at  $a_w \leq$

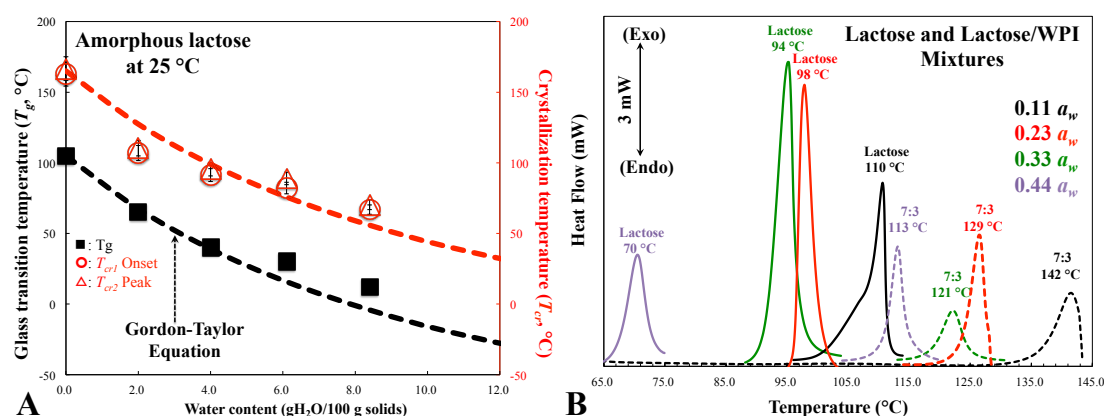


**Fig. 4.2.** The onset glass transition temperatures ( $T_g$ ) and crystallization temperatures (onset  $T_{cr1}$  and Peak  $T_{cr2}$ ) against water content (or  $a_w$ ) (A) and DSC thermograms of crystallization (B) of amorphous lactose after storage at low  $a_w$  and 25 °C. The onset  $T_g$  was fitted by GT equation (Eq. 1.3). It should be noted that the solid line in B represent pure amorphous lactose and dash line represent the lactose/WPI mixtures.

0.44 are given on Table (4.1). Theories of water activity as a mobility-controlling factor were complemented by information on the glass transition of amorphous food components at various levels of water plasticization (Slade and Levine, 1991; Roos and Drusch, 2015). Above the  $T_g$ , the increasing of free volume and molecular mobility leads to decreased viscosity, therefore, leading a change in physical structure of amorphous substances (Slade et al., 1991). In the present study, the onset  $T_g$  values of lactose decreased from 105 °C (anhydrous state) to 14 °C (0.44  $a_w$ ) due to water plasticization which could significantly increase the mobility of amorphous lactose. And the depressed  $T_g$  of lactose in the presence of water could lead to rapid collapse of structure, stickiness and probably increased rates of deteriorative reaction in the plasticized rubbery state. For WPI, however, the  $T_g$  was not observed (Table 4.1). The  $T_g$  values of non-crystalline lactose against water content and water activity (0.11 ~ 0.44  $a_w$ ) are given in Table (4.1) and the GT equation (Eq. 1.3) with  $k \approx 9.1 \pm 0.5$  (Fig. 4.2 A) was fitted to experimental data of amorphous lactose successfully. Since the GAB gave the water content in each non-crystalline component in sugar/protein systems according to fractional water sorption, the  $T_g$  values of pure lactose could be

**Table 4.1.** Water Content, Water Activity ( $a_w$ ), Onset of Glass Transition Temperature ( $T_g$ ),  $\alpha$ -Relaxation Temperature ( $T_{\alpha}$ ), Onset and Peak of Crystallization Temperature ( $T_{cr1}$  and  $T_{cr2}$ ), Latent Heat of Crystallization ( $\Delta H_{cr}$ ), and WLF Material-Specific Constants ( $C_1$  and  $C_2$ ) and Strength Parameter ( $S$ ) of Amorphous Lactose and Lactose/WPI Mixtures After Storage at Low  $a_w$  ( $\leq 0.44$   $a_w$ ) and 25 °C.

Materials	Ratios (w/w)	$a_w$	Water content (gH <sub>2</sub> O/100 g solids) <sup>a</sup>	$T_g$ (°C)	$T_{\alpha}$ (°C)	$T_{cr1}$ (°C)	$T_{cr2}$ (°C)	$\Delta H_{cr}$ (J/g)	$C_1$	$C_2$ (°C)	$S$ (°C)
Lactose	--	0	0	105±3 <sup>b</sup>	128±2	163±2	167±1	107±3	-1.84±0.40	-39.46±0.32	27.2±2.5
		0.11	2.0 ± 0.2	65±4	86±3	107±1	110±0	80±3	-2.46±0.32	-41.63±0.41	26.3±1.5
		0.23	4.0 ± 0.3	40±2	59±4	91±0	96±1	69±6	-2.79±0.28	-40.66±0.52	24.8±1.4
		0.33	6.1 ± 0.3	30±3	48±2	82±3	89±2	56±1	-3.37±0.31	-41.72±0.60	22.6±0.7 <sup>d</sup>
		0.44	8.4 ± 0.4	14±4	29±3	67±0	70±0	38±2	-4.17±0.47	-40.98±0.58	20.3±2.8
Lactose/WPI	7:3	0	0	107±1	134±2	-	-	-	-2.88±0.33	-57.19±0.53	33.3±2.0
		0.11	2.7 ± 0.2	61±2	89±3	126±0	142±0	57±4 <sup>c</sup>	-2.26±0.42	-52.24±0.63	33.4±2.5
		0.23	4.9 ± 0.1	41±1	60±3	123±0	136±0	61±3	-2.67±0.32	-56.55±0.65	33.9±1.9
		0.33	6.6 ± 0.4	33±1	58±4	121±1	125±1	43±4	-4.40±0.34	-74.75±0.76	35.6±1.8
		0.44	9.0 ± 0.2	16±2	34±0	110±1	113±1	50±2	-1.98±0.44	-36.06±0.75	24.1±2.1
Lactose/WPI	1:1	0	0	110±3	145±4	-	-	-	-1.61±0.24	-56.3±0.65	40.0±1.7
		0.11	3.0 ±0.1	60±2	96±4	138±1	149±0	18±3	-2.33±0.34	-69.46±0.55	43.9±2.6
		0.23	5.3 ± 0.1	40±1	77±2	123±4	133±1	50±3	-2.24±0.32	-66.62±0.44	42.7±1.0
		0.33	7.0± 0.4	31±1	66±4	128±3	134±5	35±2	-2.98±0.32	-74.81±0.71	42.9±2.4
		0.44	9.2 ± 0.0	16±2	44±2	N/A	N/A	N/A	-1.55±0.43	-45.20±0.77	32.6±2.0
Lactose/WPI	3:7	0	0	115±5	162±5	-	-	-	-0.53±0.38	-57.7±0.66	50.9±2.2
		0.11	3.4 ± 0.1	58±4	96±6	124±1	144±2	15±4	-1.49±0.44	-68.58±0.70	50.0±2.0
		0.23	5.8 ± 0.1	38±2	78±1	127±1	145±1	48±6	-1.37±0.46	-62.13±0.77	46.0±2.3
		0.33	8.0 ± 0.4	30±3	73±2	N/A	N/A	N/A	-2.17±0.42	-74.30±0.54	48.2±3.6
		0.44	9.6 ± 0.1	17±2	55±2	N/A	N/A	N/A	-1.06±0.48	-53.10±0.65	42.0±2.1

<sup>a</sup>: The water contents of lactose and lactose/WPI mixtures are derived from Fan and Roos (2015).<sup>b</sup>: Values are mean ± SD (n=3); <sup>c</sup>: The  $\Delta H_{cr}$  value for each lactose/WPI mixture was normalized to pure amorphous lactose based on fractional ratios based on the experimental data; <sup>d</sup>: The strength parameters of lactose and lactose/WPI mixtures at 0.33  $a_w$  are derived from Fan and Roos (2016a) .

obtained at intermediate and high water activities ( $\geq 0.56 a_w$ ) based on Eq. (1.3). The predicted  $T_g$  values of non-crystalline lactose were less than 0 °C at high water activities as the higher water contents exhibited a strong plasticization effect on lactose. However, protein only showed slight effects on the glass transition of amorphous lactose in WPI containing systems reflecting on the slight variation of  $T_g$  values on each  $a_w$  studied at 25 °C (Table 4.1). According to previous studies (Ibach and Kind 2007), phase separation occurred in lactose/protein systems and therefore they had a composition-independent  $T_g$  with  $T_g$  values of systems being mostly dependent on amorphous sugars. Therefore, as noted above, the presence of protein had a minor effect on the calorimetric  $T_g$  of the sugar and sugar containing mixtures after storage at low  $a_w$  and 25 °C.

The DSC crystallization thermograms for amorphous lactose and lactose/WPI mixtures are shown in Fig. (4.2B). In the present study, both onset and peak  $T_{cr}$  value of amorphous lactose were a function of water content, and decreased with increasing water contents, showing similar behavior to  $T_g$  as noted above. According to Chapter II, the protein could delay crystallization behavior of amorphous sugars. Similarly, in the present study, the presence of WPI significantly increased the  $T_{cr1}$  and  $T_{cr2}$  of amorphous lactose due to protein causing physical barrier effects (Table 4.1). The effects of water content were about the same for  $T_{cr}$  and  $T_g$  as indicated by a fairly constant values for  $T_{cr}-T_g$  of amorphous lactose, which agreed with Roos and Karel (1991a). For pure lactose, in this study, the increase in water content caused about an equal decrease in  $T_g$  and  $T_{cr}$  and the average  $T_{cr}-T_g$  values of lactose were approximately 55 °C (Fig. 4.2 A). The heat released by pure lactose during crystallization ( $\Delta H_{cr}$ ) various with water content (Fig. 4.2 B). A lower  $T_{cr}$  with higher water activities confirmed an increased mobility of lactose molecules caused by water plasticization. At the same storage condition, the normalized  $\Delta H_{cr}$  value of lactose in lactose/WPI (7:3, w/w) was lower than for pure lactose owing to the lactose partly crystallized in protein-containing systems caused by physical barrier effects deriving from protein disturbing the crystallization of lactose (Table 4.1). However, as the



crystallization of high protein-containing lactose mixtures (1:1 and 3:7, w/w) were immediately followed by the melting endotherm, the variation in the  $\Delta H_{cr}$  values obtained by peak integration because of the difficulty of setting the integration baseline.

#### 4.3.3. DYNAMIC-MECHANICAL ANALYSIS

Fig. (4.3) demonstrates the DMA spectra ( $E''$  peaks at frequency of 0.5 Hz) for lactose/WPI mixture solids (7:3, 1:1, and 3:7, w/w) at  $a_w \leq 0.44$ . Typically, mechanical properties of materials in DMA may be induced by many reasons such as molecular interactions and water plasticization (Lopez-Diez and Bone, 2004). Therefore, the  $E''$  of glass forming lactose could be dependent on the presence of water as water plasticization increased the free volume as well as the molecular mobility of amorphous lactose. Fig. (4.3) shows WLF plots of peak of  $E''$  with the variation of WPI content at  $a_w \leq 0.44$  and 25 °C. Structural relaxation times increased and the peak of  $E''$  flattened concomitantly with increasing protein contents in lactose/protein systems at low  $a_w$  and 25 °C (Fig. 4.3). Such effects of protein on lactose retarded diffusion and the  $E''$  results reflected the amorphous lactose content of the mixtures, as the protein existed in separate phases apart from the amorphous lactose.

The  $T_\alpha$  values of pure amorphous lactose and lactose in WPI mixtures are given on Table (4.1). Since the physical state of amorphous carbohydrate systems is strongly influenced by water, the  $T_\alpha$  of pure lactose at lower water activities was varying from 29 °C (0.44  $a_w$ ) to 128 °C (anhydrous state) at a frequency of 0.5 Hz, which agreed with previous studies (Silalai and Roos, 2011; Renzetti et al., 2012). Recently, the free volume theory and its effects on molecular mobility were successfully applied to describe the increase in diffusivity observed in food materials (Meinders and Van Vliet, 2009). As the  $T_\alpha$  values of amorphous lactose and lactose/WPI mixtures were decreased by water, the water could increase the free volume as well as the extent of

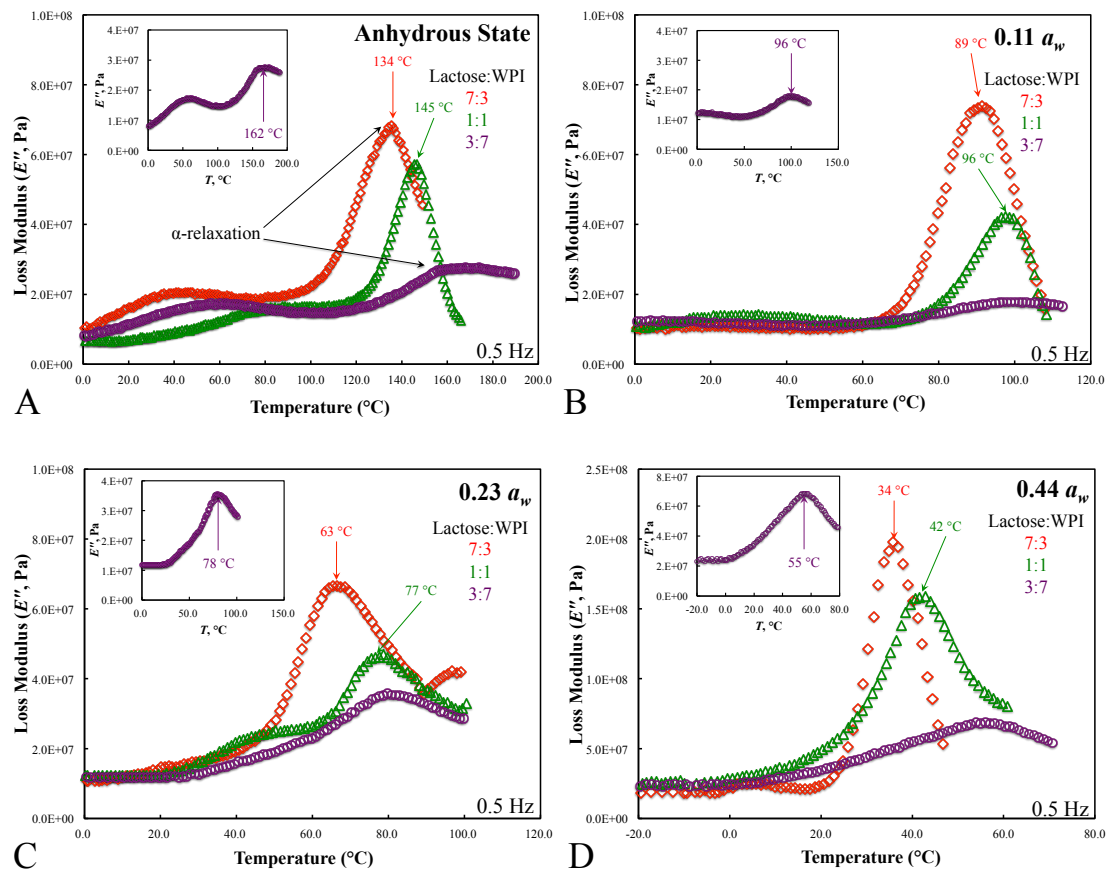


**Fig. 4.3.** The DMA spectra of loss modulus ( $E''$ ) for lactose/WPI mixtures with 7:3, 1:1, and 3:7 (w/w) at 0.5 Hz after storage at  $a_w \leq 0.44$  and 25 °C. The  $\alpha$ -relaxation temperature was characterized based on the peak of each loss modulus.

molecular mobility of amorphous lactose at 25 °C (Table 4.1). However, the presence of WPI increased the  $T_\alpha$  values of lactose/WPI mixtures after storage at the same storage  $a_w$ , which was caused by physical blocking (Table 4.1). Therefore, our study indicated that the presence of separate phases of components could alter the movement of amorphous lactose molecules, and thus, affect the structural relaxations and viscous flow characteristics of amorphous sugars.

#### 4.3.4. STRENGTH, WATER CONTENTS, AND CRYSTALLIZATION TEMPERATURE

When the storage temperature increases to above  $T_g$ , amorphous materials loose solid

characteristics concomitantly with decreasing  $\tau$ , which is reflected on the decreasing viscosity and increasing flowability of the solids. Such loss of solid characteristics results in collapse of cell walls in porous structures typical of dehydrated foods. Fig. (4.4) shows the  $S$  values of pure lactose and lactose/WPI mixtures after storage at  $a_w \leq 0.44$  as derived from the modified WLF model analysis. We found that water could

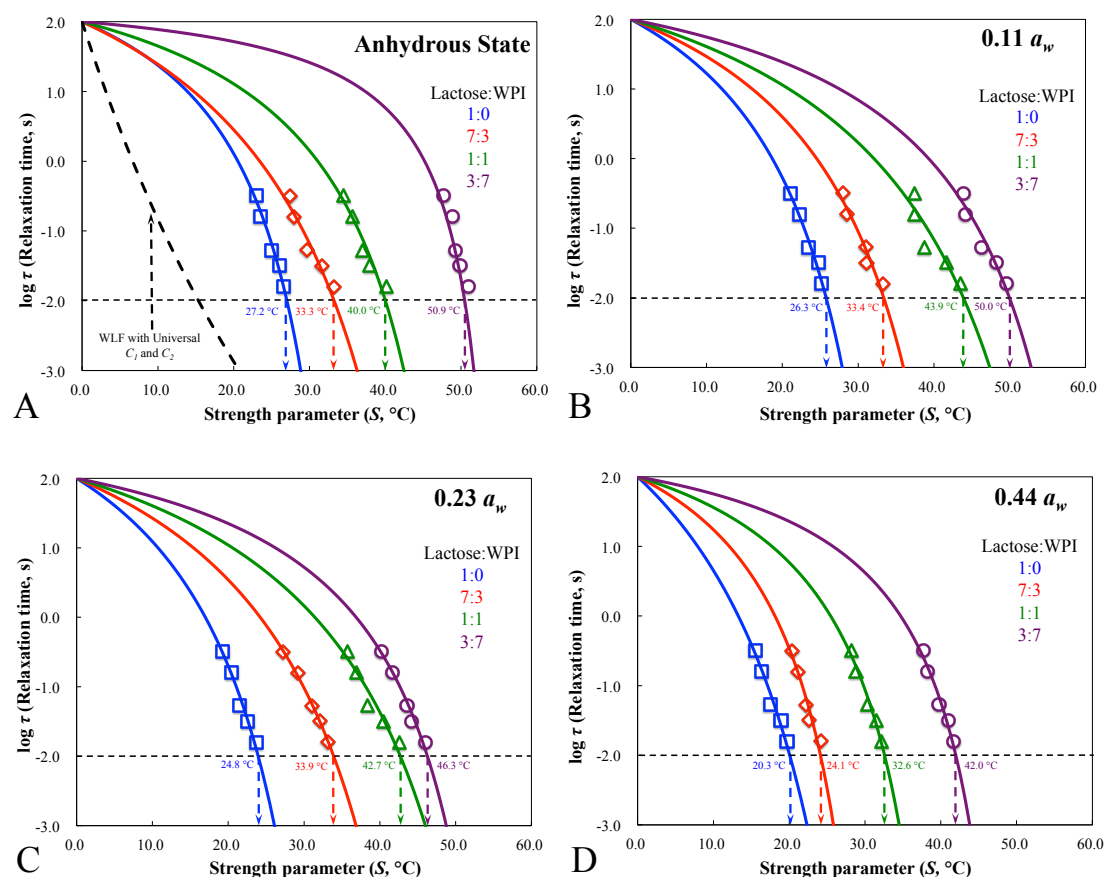


**Fig. 4.4.** Plots indicating the WLF-based  $S$  parameters of amorphous lactose and lactose/WPI mixtures (7:3, 1:1, and 3:7, w/w) at  $a_w \leq 0.44$  after storage at 0.33  $a_w$  and 25 °C

govern the structural strength or viscous flow characteristics of glass forming lactose as the  $S$  value decreased concomitantly with increasing water content (Table 4.1). Fig. (4.4) demonstrated that the presence of protein could affect the strength of amorphous lactose containing mixture after storage at low  $a_w$  and 25 °C. The  $S$  of WPI containing amorphous lactose mixtures showed a greater value corresponding to pure amorphous

lactose (Fig. 4.4). Therefore, the structural strength of amorphous systems, derived from WLF analysis, could be affected by the presence of water or polymeric components, i.e., protein. The  $S$  parameter may be related to flow properties, viscous flow and collapse, and mechanical properties of food and pharmaceutical materials.

The structural strength of glass forming sugars, which was studied around glass transition, could be quantified by the  $S$  value, which was determined by amorphous components at low  $a_w$  in this study. The presence of other components, especially water, could affect the structural strength of amorphous lactose containing system due to increased molecular mobility of the glass former, which was reflected on decreasing  $S$  values. Fig. (4.5A) shows the relationship of  $S$  against water content of amorphous lactose at low  $a_w$  ( $\leq 0.44 a_w$ ). The structural strength decreased and viscous flow increased with increasing water content. In the present study, we found that the experimental data on  $S$  and water content of amorphous lactose and lactose/WPI mixtures could be successfully fitted by Eq. (4.1) that is a Gordon-Taylor type equation at low  $a_w$ . As the water contents of non-crystalline lactose at whole  $a_w$  could be estimated by GAB model based on Eq. (1.1), the estimated  $S$  and corresponding water content could be calculated for amorphous lactose at 25 °C and high  $a_w$  (Fig. 4.5 A). Therefore, the predicted  $S$  of non-crystalline lactose, where crystallization occurred, could be calculated based on Eq. (4.1) using predicted water content data at high  $a_w$ . The relationship between crystallization temperatures ( $T_{cr1}$  and  $T_{cr2}$ ) and strength parameter of amorphous lactose was also shown on Fig. (4.5B) with a high correlation coefficient ( $R_1^2 \approx 0.9638$  and  $R_2^2 \approx 0.9750$ ). The crystallization temperature was decreased with the decreasing of  $S$  values due to the low structural strength represented a rapid molecular mobility occurred in amorphous lactose (Fig. 4.5 B).

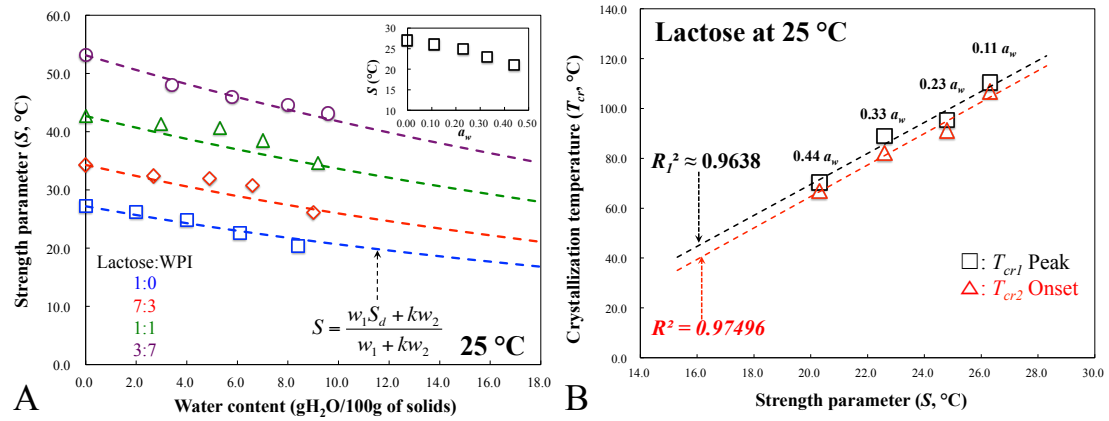


**Fig. 4.5.** The relationship between strength ( $S$ ) against water content (or  $a_w$ ) of amorphous lactose and lactose/WPI mixtures at  $a_w \leq 0.44$  and 25 °C (A). The dash lines represent the calculated  $S$  values for lactose and lactose/WPI mixtures using Eq. (4.1) from 0 to 0.76  $a_w$ , respectively. The crystallization temperature (onset  $T_{cr1}$  and peak  $T_{cr2}$ ) of pure lactose at low  $a_w \leq 0.44$  also shown in B.

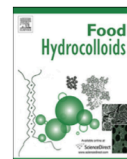
However, as the presence of other components, i.e., WPI, increased the  $S$  value of lactose/WPI systems, the lactose crystallization temperature was enhanced even high water content existed in systems. Therefore, the present study showed that WPI could present an important role in enhancing structural strength and preventing sugar crystallization. And the structural strength or viscous flow of amorphous lactose could be estimated by their water content and the crystallization behavior of amorphous lactose could be controlled by structural strength in processing as well as the quality and stability of food and pharmaceutical materials.

$$S_p = \frac{w_1 S_{d1} + k w_2 S_{d2}}{w_1 + k w_2} \quad (4.1)$$

Where,  $S_p$  refers to the predicted  $S$  value of lactose,  $S_{d1}$ ,  $S_{d2}$ ,  $k$ ,  $w_1$ , and  $w_2$  refer to the  $S$  value of anhydrous lactose (27.0 °C) and amorphous water (6.0 °C, Maidannyk et al., 2017), a constant ( $2.5 \pm 0.5$ ) and the weight fraction of the 1 (lactose) and 2 (water) in humidified amorphous lactose, respectively.

#### 4.4. CONCLUSIONS

We have shown that amorphous lactose and lactose/WPI have fractional water sorption properties, and the crystallization of lactose was delayed by the addition and increasing the quantity of WPI. The structural relaxations and structural strength of amorphous lactose could be controlled by the mixture composition, i.e., water and WPI. A structural strength concept based on WLF model analysis was validated and the  $S$  parameter was connected to crystallization behavior of amorphous sugars in food storage such dairy powders.



Volume 60, 9 March 2016, Pages 85-97

## CRYSTALLIZATION AND STRUCTURAL RELAXATION TIMES IN STRUCTURAL STRENGTH ANALYSIS OF AMORPHOUS SUGAR/WHEY PROTEIN SYSTEMS

Fanghui Fan and Yrjö H. Roos

*School of Food and Nutritional Sciences,  
University College Cork, Cork, Ireland*

## ABSTRACT

Water sorption, crystallization, calorimetric glass transition temperature, structural relaxations and relaxation times of freeze-dried sugars (lactose and trehalose) and whey protein isolates in mixed systems were measured at various water activities ( $a_w \leq 0.76$ , and 25 °C). The results indicated that sugar/WPI mixtures showed fractional water sorption behavior. The crystallization and crystalline forms of lactose were affected by trehalose and WPI based on XRD analysis. DMA analysis showed that the  $\alpha$ -relaxation temperatures at loss modulus peak at frequency of 0.5 Hz for sugar/protein systems were affected by the presence of water and WPI. The  $\tau$  and  $T_\alpha - T_g$  relationships in sugar/WPI systems were successfully modeled by using the WLF model. The WLF-type structural strength ( $S$ ), indicating decrease of  $\tau$  from  $10^2$  to  $10^{-2}$  s, of trehalose decreased with  $a_w$  up to 0.44 (from 15.8 to 12.1 °C) but WPI increased  $S$ . Moreover, a relationship for  $S$  and water content for glass forming sugar systems at  $a_w \geq 0.56$  was established. The  $S$  concept gave a quantitative measure to estimate compositional effects on  $\tau$  and could be used to estimate crystallization of food solids components.

**KEYWORDS,** *Crystallization; X-ray Diffraction; Structural Relaxations; Strength Parameter; WLF model; Water*

## 5.1. INTRODUCTION

Sugars can exist in crystalline or amorphous states in food solids. It is important that the microstructure of a food material is maintained in a noncrystalline state; otherwise the flavor, color and taste of the food may be altered during storage (Hartel and Shastry, 1991; Roos and Drusch, 2015). In the glassy state, for example, volatiles are encapsulated in the amorphous glass. Exceeding the  $T_g$  by increasing temperature or moisture content increases diffusion coefficients, structural collapse and sometimes



crystallization takes place releasing encapsulated volatiles and possibly increases reaction rates such as browning (Omatete and King, 1978; Simatos and Karel, 1988). In general, amorphous structures of sugars are fairly stable in the glassy state (Slade et al., 1991). However, at temperatures close to or above glass transition temperature molecular mobility increases and solids are converted to viscous liquids showing time-dependent flow (White and Cakebread, 1966; Roudaut et al., 2004; Roos and Drusch, 2015). As water affects molecular mobility shown by a lowered  $T_g$  due to plasticization, amorphous sugars may exhibit a tendency of crystallization causing physical and chemical deterioration in food ingredients and dairy powders at high storage humidities or temperatures (Hartel and Shastry, 1991; Roos and Karel, 1991; Slade et al., 1991; Aguilar et al., 1994; Miao and Roos, 2005; Ibach and Kind, 2007). The rates of crystallization of amorphous sugars are governed by water content, relative humidity and the temperature of storage above  $T_g$ ,  $T - T_g$ . Previous studies showed that crystallization of amorphous sugars could be delayed by the presence of other components, i.e. starch (Iglesias and Chirife, 1978), corn syrup solids (Gabarra and Hartel, 1998), proteins (Silalai and Roos, 2010) and carbohydrates (Mazzobre et al., 2001; Sillick and Gregson, 2010; Potes et al., 2012).

$\alpha$ ,  $\alpha$ -Trehalose ( $\alpha$ -D-glucopyrano-syl- $\alpha$ -D-glucopyranoside) is a non-reducing and naturally occurring disaccharide of glucose monomers with high  $T_g$  (Lammert et al., 1998; De Gusseme et al., 2003). Indeed, trehalose can be added to biologically active solutions to overcome the limited stability range of proteins (pH, temperature, salt concentration, etc.) or effectively prevent the partial or even total degradation of biomolecules due to the lethal thermal or dehydration stresses encountered during industrial conservation methods (lyophilization) (Iglesias and Chirife, 1978; Crowe et al., 1983; Roser, 1991; Uritani et al., 1995; Miller et al., 1997; Schiraldi et al., 2002). Trehalose also has preservation capabilities of bio-systems such as cells, vaccines or therapeutic proteins employed in the food, pharmaceutical or cosmetics industry, whereas amorphous trehalose may undergo crystallization when exposed to a high humidity (Green and Angell, 1989; Miller and De Pablo, 2000; Elbein et al., 2003).

Lactose ( $\beta$ -D-galactopyranosyl (1–4)-D-glucopyranose) is often used in the food and pharmaceutical industries and it exhibits strong tendency to crystallize from its amorphous states, especially at high storage humidities (Nickerson, 1979). X-ray diffraction patterns have shown that amorphous lactose crystallizes into a number of crystalline forms, which differ in melting behavior, solubility, density, crystal morphology, and relative sweetness (Nickerson, 1979; Lai and Schmidt, 1990; Jouppila et al., 1998). Generally, the crystalline forms vary as their formation depends on the presence of other components, which may be related to interactions among sugars, supersaturation in systems, diffusion of molecules or the mutarotation of molecules during either nucleation or crystal-growth stages in crystallization (Jouppila and Roos, 1994ab; Fitzpatrick et al., 2007).

Crystallization results in a dramatic change in structure of glass forming sugars with complete changes of mechanical properties and time-dependent flow characteristics (Chung et al., 2002; Chung et al., 2004; Chung et al., 2004). Mechanical properties around the glass transition show a  $\alpha$ -relaxation, which could be investigated by dynamic mechanical analysis and detected from changes in loss modulus ( $E''$ , mechanical energy dissipation), storage modulus ( $E'$ , mechanical energy storage) and  $\tan \delta$  ( $\tan \delta = E'' / E'$ ) (Angell et al., 2000). A characteristic feature of mechanical properties of amorphous sugars, such as the  $T_g$ -dependence, could affect food quality and shelf life during storage (Slade et al., 1991; Silalai and Roos, 2010 and 2011). Mechanical properties of amorphous sugars could be affected by the presence of other components affecting their glass transition, e.g. water (Downton et al., 1982; Slade et al., 1991), carbohydrates (Cruz et al., 2001; Miao and Roos, 2005) and proteins (Silalai and Roos, 2010). As the measurements of solid flow characteristics or viscosity in the  $T_g$  region are extremely difficult, Roos and others (2016) defined a measure for flow characteristics given by “*strength, S*” and introduced a WLF model-based analysis of structural relaxation times within solids affecting flow characteristics in mixes of sugars and polymeric food components.

Whey protein may act as stabilizer in sugars/protein systems during spray drying and freeze-drying (Ratti, 2001; Oetjen and Haseley, 2004; Wang et al., 2010; Carullo and Vallan, 2012). Previous studies showed that whey protein could delay crystallization of amorphous sugars in powder systems at high *RH* storage conditions due to reduced nucleation and diffusion during crystal-growth stage. However, characterization of the glass-forming properties is important for amorphous sugars and polymeric materials made to powders. The objectives of the present study were to investigate the influence of whey protein on crystallization kinetics and crystalline forms of amorphous trehalose and lactose/trehalose systems at high water activities ( $> 0.56 a_w$ ) as well as calorimetric glass transition,  $\alpha$ -relaxation, and structural strength at low water activities ( $\leq 0.44 a_w$ ) at isothermal storage conditions (25 °C). We expect that strength parameter provides a measure of relaxation rates and describes solids properties, i.e., crystallization, in sugars/protein systems, which could contribute to time-dependent powder characteristics in food and pharmaceutical materials.

## 5.2. MATERIALS AND METHODS

### 5.2.1. SAMPLE PREPARATION

$\alpha$ ,  $\alpha$ -Trehalose dihydrate (Hayashibara Co. Ltd, Okayama, Japan),  $\alpha$ -lactose monohydrates (Sigma-Aldrich, St. Louis, Mo., U.S.) and whey protein isolates (Isolac<sup>®</sup>, Carbery Food Ingredients, Co., Ballineen, Ireland; impurities including carbohydrates and lipids  $< 3$  %) were used. De-ionized water (KB Scientific, Cork, Ireland) was used for all experimental work. Lactose and trehalose was dissolved in boiled de-ionized water ( $\sim 100$  °C) to obtain 20 % (mass) solution. WPI solution with 20 % (mass) solution was prepared using continuous stirring for 4 h at room temperature ( $\sim 23$  °C). Lactose and trehalose solutions at room temperature were used to obtain solids ratios of 2:3, 1:1, and 3:2 of lactose/trehalose mixtures by mass. Trehalose and WPI solutions at room temperature were used to obtain solids ratios of 7:3, 1:1, and 3:7 of trehalose/WPI by mass, respectively. Similarly, lactose, trehalose

and WPI solutions were used to obtain solid ratios of 2:3:5, 1:1:5, and 3:2:5 of lactose/trehalose/WPI by mass, respectively. Samples (5 mL in total) were prepared in pre-weighted glass vials (10 mL, diameter 24.3 mm × height 46 mm; Schott Müllheim, Germany). All samples in the vials (semi-closed with septum) were frozen in a still air freezer at  $-20\text{ }^{\circ}\text{C}$  for 20 h and then subsequently tempered at  $-80\text{ }^{\circ}\text{C}$  for 3 h prior to freeze-drying using a laboratory freeze-dryer (Lyovac GT2 Freeze Dryer, Amsco Finn-Aqua GmbH, Steris®, Hürth, Germany). After freeze-drying at pressure  $< 0.1\text{ mbar}$ , triplicate samples of each material were stored in evacuated vacuum desiccators over  $P_2O_5$  (Sigma-Aldrich, St. Louis, Mo., U.S.) prior to subsequent analysis.

### 5.2.2. WATER SORPTION AND TIME-DEPENDENT CRYSTALLIZATION

Water sorption by freeze-dried lactose, trehalose, lactose/trehalose, trehalose/WPI, lactose/trehalose/WPI, and WPI at each ratios was monitored for 120 h (non-crystallizing samples) and 240 h (crystallizing samples) over saturated solutions of  $LiCl$ ,  $CH_3COOK$ ,  $MgCl_2$ ,  $K_2CO_3$ ,  $Mg(NO_3)_2$ ,  $NaNO_2$ , and  $NaCl$  (Sigma Chemical Co., St. Louis, Mo., U.S.A.) at respective water activities ( $a_w$ ) of 0.11, 0.23, 0.33, 0.44, 0.54, 0.65 and 0.76  $a_w$  at  $25\text{ }^{\circ}\text{C}$  (Greenspan, 1977; Labuza et al., 1985), in vacuum desiccators. The  $a_w$  measured (Dew Point Water Activity Meter 4TE, Aqualab, WA, USA) for the systems at  $25\text{ }^{\circ}\text{C}$  is given in Table (5.1). Evacuated desiccators in incubators (Series 6000, Termaks, Bergea, Norway) were stored at  $25\text{ }^{\circ}\text{C}$ . Vials with samples were weighted to monitor water sorption at 0, 3, 6, 9, 12, and 24 h followed by 24 h intervals up to 240 h (Jouppila and Roos, 1994b). Lactose and trehalose crystallization was monitored from loss of sorbed water during storage over  $Mg(NO_3)_2$ ,  $NaNO_2$ , and  $NaCl$  at  $25\text{ }^{\circ}\text{C}$ . All vials were closed with septums when removed desiccators and septums were opened for weighing. Water contents of the materials were measured as a function of time, and the average weights of triplicate samples were used in calculation. The GAB equation (Eq. 1.1) was used to fit the experimental data to model water sorption at  $25\text{ }^{\circ}\text{C}$  (Timmermann et al., 2001; Lievonen and Roos,

2002; Torres et al., 2011).

### 5.2.3. XRD ANALYSIS

Vials with trehalose, lactose/trehalose, trehalose/WPI, and lactose/trehalose/WPI mixtures stored over  $\text{NaNO}_2$  and  $\text{NaCl}$  were filled with liquid nitrogen and stored at  $-80^\circ\text{C}$  for 3 h followed by freeze-drying for 1 day. Such treatment ceased crystallization as a result of the lowering of the temperature (Haque and Roos, 2005). The materials were powdered using mortar and pestle and then stored in sealed glass vials to prevent exposure to ambient air and water uptake. The XRD patterns were measured by using a STOE Powder X-ray diffractometer (STOE & Cie GmbH, PW 3830 generator, PW 3710 MPD diffractometer, Germany). The X-ray diffractometer was operated with an anode current of 40 mA and an accelerating voltage of 40 kV. Samples were slightly pressed on a steel sample tray covered by plastic slide ( $r = 5$  mm) and exposed to  $\text{CuK}\alpha$  radiation at diffraction angles ( $2\theta$ ) from  $5^\circ$  to  $30^\circ$  (step size,  $0.1^\circ$ ; time per step, 5 s). The peak search program was the STOE Powder Diffraction Software Package WinXpow (STOE & Cie GmbH, Germany) software that was used to locate the peaks in XRD patterns by detecting the minima from the second derivative of the diffractograms. Intensity maxima were given as  $\text{CuK}\alpha$  net peak height in counts at  $\text{CuK}\alpha$  position in degrees. The types of lactose and trehalose crystals formed in freeze-dried trehalose and lactose/trehalose and protein containing sugars powder were identified from the location of the characteristic peaks in XRD patterns. The progress of lactose and trehalose crystallization was observed from increasing intensities of peaks in XRD patterns at  $12.5^\circ$ ,  $16.5^\circ$ , and  $20.1^\circ$  for  $\alpha$ -lactose monohydrate,  $21.0^\circ$  and  $10.6^\circ$  for anhydrous  $\beta$ -lactose,  $19.2^\circ$  and  $19.7^\circ$  for anhydrous  $\alpha$ -lactose and  $\beta$ -lactose in molar ratio of 5:3,  $17.8^\circ$  for anhydrous trehalose,  $15.2^\circ$  and  $23.8^\circ$  for trehalose dihydrate (Jouppila et al., 1998; Miao and Roos, 2005).

### 5.2.4. THERMAL ANALYSIS

The onset  $T_g$  for each material was determined using differential scanning calorimeter (DSC) measurements (Mettler Toledo Schwerzenbach, Switzerland). Samples of all materials were transferred to preweighed standard DSC aluminum pans ( $\sim 40\mu\text{L}$ , Mettler Toledo Schwerzenbach, Switzerland), and hermetically sealed before weighing. An empty punctured pan was used as a reference. Samples were scanned from  $\sim 30\text{ }^\circ\text{C}$  below to over the  $T_g$  region at  $5\text{ }^\circ\text{C}/\text{min}$  and then cooled at  $10\text{ }^\circ\text{C}/\text{min}$  to initial temperature. A second heating scan was run to well above the  $T_g$  at  $5\text{ }^\circ\text{C}/\text{min}$ . The onset  $T_g$  was derived from second heating scans and recorded using STARE software, version 8.10 (Mettler Toledo Schwerzenbach, Switzerland). The GT equation (Eq. 1.3) has proven to fit to experimental data on  $T_g$  at various water contents of amorphous sugars.

#### **5.2.5. DYNAMIC-MECHANICAL ANALYSIS**

Dynamic-mechanical properties of humidified sugars and sugar/WPI systems were studied using DMA (Tritec 2000 DMA, Triton Technology Ltd., UK). The storage modulus ( $E'$ ) and loss modulus ( $E''$ ) as a function of temperature at different frequencies were determined (0.5, 1, 3, 5, and 10 Hz). The DMA instrument was balanced or set at zero to determine the zero displacement position before starting an experiment. Approximately 100 mg samples of grinded materials were spread on a metal pocket-forming sheet (Triton Technology Ltd., UK). The sheet with sample was crimped along a pre-scored line to form a thin sandwich pocket. This pocket was attached directly between the clamps (the fixed clamp and the driveshaft clamp) inside the measuring head of the DMA. The length, width, and thickness ( $\sim 2\text{ mm}$ ) of the sample pocket between the clamps were measured. Triplicate samples of each material were analyzed using dynamic measurements and recorded using DMA software version 1.43.00. The measuring head was connected to a liquid nitrogen tank for cooling (1 L; Cryogun, Brymill Cryogenic Systems, Labquip Ltd., Dublin, Ireland). Samples were scanned from  $\sim 60\text{ }^\circ\text{C}$  below to over the  $T_g$  region with cooling rate of  $5\text{ }^\circ\text{C}/\text{min}$  and heating rate of  $2\text{ }^\circ\text{C}/\text{min}$  using the single cantilever

bending mode (Silalai and Roos, 2011a). During dynamic heating, the samples were analyzed for  $T_\alpha$  determined from the peak temperature of  $E''$  above the glass transition. Average values for triplicate measurements of peak  $T_\alpha$  were calculated.

#### 5.2.6. WLF-MODEL ANALYSIS

Williams-Landel-Ferry model is often used to define mobility in terms of the non-Arrhenius temperature dependence of the rate of diffusion-limited relaxation processes occurring at temperature  $T$ , compared to the rate of the relaxation at a reference temperature, e.g.,  $T_g$ , expressed in terms of  $\tau$  dependence on  $T-T_g$  (Williams et al., 1955; Slade and Levine, 1995; Angell, 1997). The  $\tau$  and the temperature of  $T_\alpha$  above  $T_g$ , were modeled and analyzed using the WLF equation (Eq. 1.9), where  $\tau$  was defined by oscillation frequency set in DMA measurement ( $\tau = 1/2\pi f$ ). The WLF model constants  $C_1$  and  $C_2$  were derived from a plot of  $1/\log(\tau/\tau_g)$  against  $1/(T-T_g)$  using experimental relaxation times,  $\tau$ , with the assumption of  $\tau_g = 100$  s at the onset temperature of the calorimetric glass transition,  $T_g$  (Angell, 2002). The strength parameter corresponds to an allowable increase in temperature above  $T_g$ , and describes softening of glass formers above the calorimetric glass transition (Roos et al., 2016). A decrease in the number of logarithmic decades for flow, e.g., that to critical for stickiness, can be defined as the critical parameter,  $d_s$ , of Eq. (1.12) and a corresponding  $T-T_g$  is given as the strength of the solids,  $S$ . As the  $S$  is given as temperature corresponding to a critical  $\tau$  for a key amorphous component within a material, it also provides a measure of resistance to structural changes, i.e., the higher value of  $S$  refers to a stiffer system.

#### 5.2.7. STATISITICAL ANALYSIS

The GAB model, predicted  $T_g$  of systems based on GT equation and the data of  $\tau$  were calculated and fitted by using Microsoft Office Excel 2011 (Microsoft, Inc., U.S.A.).

All measurements were repeated three times as well as the average values with standard deviation of triplicate measurements were calculated.

## 5.3. RESULTS AND DISSCUSSION

### 5.3.1. WATER SORPTION

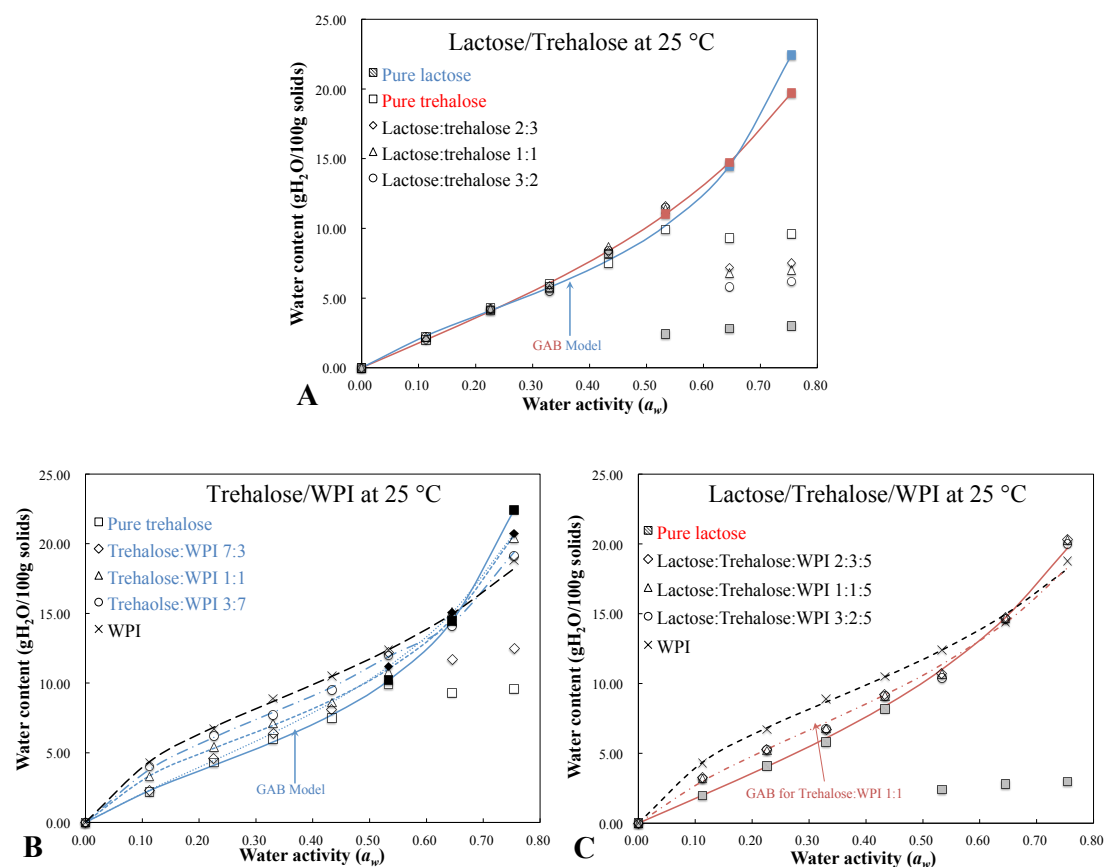


**Fig. 5.1.** The experimental and calculated water content data (solids symbols) for amorphous trehalose and trehalose/WPI at solids ratios of 7:3, 1:1, and 3:7 (w/w), and lactose/trehalose with 2:3, 1:1, and 3:2 (w/w), and lactose/trehalose/WPI mixtures with ratios of 2:3:5, 1:1:5, and 3:2:5 (w/w) showed from A to C.

The GAB sorption isotherms, experimental data for lactose, trehalose, trehalose/WPI, lactose/trehalose, lactose/trehalose/WPI mixtures and WPI over all studied water activities (0.11 ~ 0.76  $a_w$ ) at 25 °C, and water contents derived for non-crystalline lactose, trehalose (0.56 ~ 0.75  $a_w$ ) and trehalose/WPI (7:3 and 1:1, w/w) mixtures



(0.65 ~ 0.76  $a_w$ ) are given in Table (5.1). Steady-state water contents of each material were used in GAB (Eq. 1.1) using data at 120 h although steady-state water contents could be achieved after 72 h storage. Water sorbed by trehalose, lactose/trehalose (2:3, 1:1, and 3:2, w/w) and trehalose/WPI mixtures (7:3, w/w) increased with the increasing of  $a_w$  up to 0.44  $a_w$ , and then leveled off at higher  $a_w$ , corresponding to the formation of a stable crystalline structure (Table 5.1). The residual water contents of trehalose after storage at 240 h under high  $a_w$  agreed with previous reports and the slightly different results were due to experimental error, variation in dehydration, sorption time, storage temperature or crystallinity (Roe and Labuza, 2005; Miao and Roos, 2005). The steady-state water contents of trehalose were slightly higher than those of lactose as amorphous trehalose could crystallize with two hydrate water molecules (~ 10 gH<sub>2</sub>O/ 100 g solids) at  $a_w \geq 0.56$   $a_w$  under 25 °C (Table 5.1). Corresponding to the water sorption testing, no crystallization was found in high WPI containing sugar mixtures ( $\geq 50$  %). As we expected, lactose/trehalose/WPI mixtures (2:3:5, 1:1:5, and 3:2:5, w/w) sorbed almost the same quantity of water as trehalose/WPI mixtures (1:1, w/w) at all  $a_w$  due to fractional water sorption behavior, which agreed with previous reports (Potes et al., 2012).

The GAB model was fitted to experimental data of trehalose, and lactose/trehalose mixtures below 0.44  $a_w$  as crystallization occurred at higher water activities (Fig. 5.1). The binary sugar system at all ratios sorbed similar quantity of water at  $a_w \leq 0.44$ , in accordance with individual sugars in agreement with fractional water sorption of binary lactose/trehalose systems (Fig. 5.1 A). Since the sorbed water of amorphous sugars/WPI systems was found as the sum of fractional quantities, the water content of individual amorphous component at each  $a_w$  could be derived from their fractional water sorption data. Previous reports also confirmed that the wider  $a_w$  ranges were applied, the better fitting performance were achieved in GAB model (Timmermann et al., 2001). Therefore, in the present study, experimental data at 0.11 ~ 0.44  $a_w$  and water content at 0.56 ~ 0.76  $a_w$  derived for trehalose/WPI mixture at 3:7 ratio (steady-state sorbed water content of non-crystalline components) from water sorption

data for non-crystalline trehalose were used in the GAB model (Fig. 5.1 B). Similarly, the water contents of binary sugar systems with any component ratios at high  $a_w$  could be calculated using the GAB water contents of non-crystalline components. According to fractional water sorption, in the present study, the predicted water content of trehalose showed a more sigmoid water sorption isotherm at  $a_w \geq 0.65$  than lactose due to its strong hydroscopic, flexible structural properties and high solubility in water reported by previous studies (Lammert et al., 1997; Gänzle et al., 2008). In addition, the GAB model was also used to fit the water contents of lactose/trehalose/WPI mixtures (2:3:5, 1:1:5, and 3:2:5, w/w) and showed a very similar sigmoid behavior as trehalose/WPI mixtures (1:1, w/w) (Fig. 5.1 C). Consequently, the fractional water sorption behavior was confirmed and validated for amorphous binary sugar systems and sugars/protein systems at 25 °C.

### **5.3.2. TIME-DEPENDENT CRYSTALLIZATION AND CRYSTALLIZATION KINENTIC**

Sorbed water release from freeze-dried lactose was most rapid as crystallization occurred during 10 days of storage at 25 °C at high  $a_w$  ( $\geq 0.65 a_w$ ), compared with pure trehalose and lactose/trehalose systems (Fig. 5.2). However, no crystallization of amorphous lactose, trehalose and their mixtures at all ratios studied occurred at low  $a_w$  ( $\leq 0.44 a_w$ ). The loss of sorbed water in lactose/trehalose systems at each ratio occurred more slowly than in pure lactose, which showed that crystallization of lactose was delayed (Fig. 5.2 A and B). Since trehalose possessed a similar molecular size as lactose, the movement of both sugar molecules was disturbed which delayed nucleation and crystal-growth (Lammert et al., 1997; Lopez-Diez and Bone, 2000; De Gusseme et al., 2003; Miao and Roos, 2005). Previous studies reported that the presence of protein caused physical blocking effects and delayed lactose crystallization in protein containing sugars/protein systems at a high  $a_w$  (Silalai and Roos, 2011). Similarly, in this study, we observed that the presence of high-molecular-weight WPI delayed trehalose crystallization at  $a_w \geq 0.65$  at 25 °C

(Fig. 5.2 C and D). As noted above, the inhibition of trehalose crystallization in trehalose/WPI mixtures was due to protein molecules causing physical barriers for trehalose diffusion at high  $a_w$ . Hence, in the present study, the presence of other components in amorphous sugar containing systems, i.e., protein or sugars, could alter the movement of amorphous sugar molecules, and thus, affect the sugar crystallization behavior.

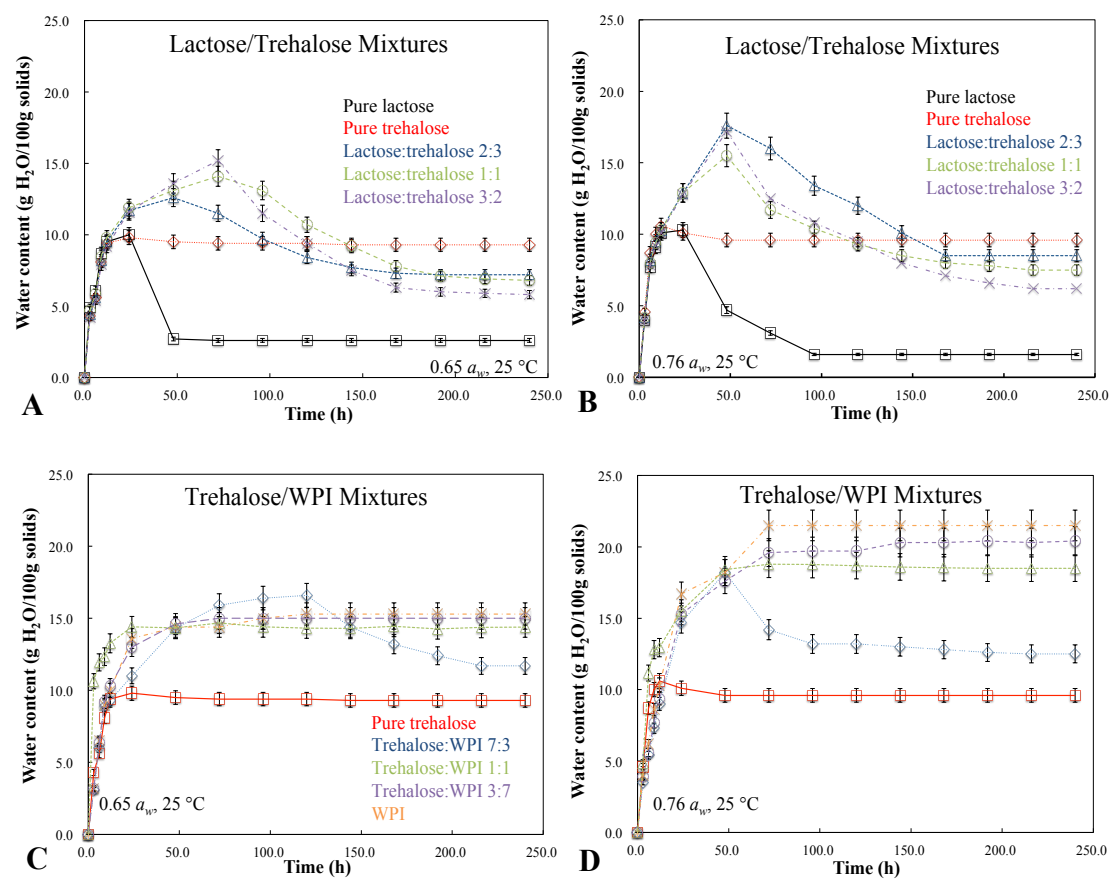


**Fig. 5.2.** Isothermal water sorption for freeze-dried lactose, trehalose, lactose/trehalose mixture, trehalose/WPI, and WPI at all studied ratios (w/w) at 0.65 and 0.76  $a_w$  stored under 25 °C.

At high water activities ( $\geq 0.65 a_w$ ), the difference in time to loss of sorbed water indicated that different crystallization rates of sugars applied in lactose/trehalose, trehalose/WPI mixtures with each ratio studied at 25 °C (Fig. 5.3). The inhibition of lactose crystallization by trehalose and proteins was evident from the rate constant ( $k$ ),

as  $k$  decreased with the increasing of quantity of trehalose or WPI, significantly (Fig. 5.3 A and B). The relationship between the  $k$  against sugar quantity in lactose/trehalose and WPI containing sugar systems at 0.65 and 0.76  $a_w$  is also shown in Fig. (5.3C and D). Previous studies reported that amorphous trehalose could mainly crystallize as trehalose dihydrate due to its high solubility at 25 °C, which means a relatively low driving force for trehalose crystallization at high  $a_w$  (Lammert et al. 1997). As a low solubility was reported for lactose at 25 °C (Gänzle et al. 2008), a relative large driving force was present for lactose crystallization and lactose could crystallize into various anomeric crystalline forms at high  $a_w$ , i.e., anhydrate or monohydrate crystalline forms. At 0.65 and 0.76  $a_w$ , the  $k$  of lactose/trehalose systems rapidly decreased (close to zero) with increasing trehalose content based on water sorption testing (Fig. 5.3 C). The inhibition of lactose crystallization in lactose/trehalose mixtures was explained by either the crystallization driving force of system lowered by high-soluble trehalose or the molecular movements of lactose or trehalose were disturbed by each other during crystallization in systems. The  $k$  was significantly depressed by the increasing weight fraction of protein in lactose/trehalose/WPI systems with  $k$  close to zero above 50 % and 70 % of WPI content at 0.65 and 0.76  $a_w$  (Fig. 5.3 D). In the present study, the crystallization kinetics in sugars/WPI was dependent on the amorphous sugar content during crystallization and the presence of proteins could affect the sugar crystallization via physical-blocking effects by proteins, which agreed with previous reports (Jouppila and Roos, 1994a; Gabarra and Hartel, 1998; Silalai and Roos, 2010; Das and Langrish, 2012; Das et al., 2013). Therefore, although the high water activities could induce rapid molecular mobility and enhanced diffusion rates of molecules, the increasing quantity of trehalose or WPI could delay the crystallization of sugars through disturbing the molecular movement of amorphous lactose. It should be noted that the crystallization behavior of the single component in a sugars mixture could not be fully described by the results of sorption study only. Thus, in the present study, the changes of crystalline forms of each sugar in above mixtures were confirmed by an XRD study.

**Table 5.1.** Water contents and  $a_w$  for freeze-dried lactose ( $L$ ), trehalose ( $T$ ), lactose/trehalose ( $L-T$ ), WPI, trehalose/WPI ( $T-W$ ) and lactose/trehalose/WPI ( $L-T-W$ ) mixtures with all ratios studied after storage from 0.11 to 0.76  $a_w$  at 25 °C. The calculated water content for non-crystalline trehalose and lactose is shown in second and third columns based on fractional water sorption

$a_w$	Non-crystalline			Water Content (gH <sub>2</sub> O/ 100 g solids)											
	Trehalose ( $T$ )	Lactose ( $L$ ) <sup>b</sup>	$T$	$L^b$	$L-T$	$L-T$	$L-T$	$L-T$	$T-W$	$T-W$	$T-W$	$L-T-W$	$L-T-W$	$L-T-W$	WPI ( $W$ ) <sup>b</sup>
0.11±0.00 <sup>a</sup>	2.3	2.0	2.2±0.3	2.0±0.2	2.2±0.3	2.2±0.2	2.2±0.2	2.3±0.3	3.3±0.3	3.4±0.3	3.3±0.1	3.2±0.2	3.2±0.2	3.2±0.1	4.3±0.1
0.23±0.00	4.1	4.0	4.3±0.2	4.0±0.3	4.5±0.2	4.3±0.1	4.2±0.1	4.6±0.5	5.4±0.3	5.8±0.2	5.3±0.1	5.2±0.3	5.2±0.3	5.3±0.2	6.7±0.1
0.33±0.00	5.8	6.1	6.0±0.1	6.1±0.3	5.9±0.1	5.7±0.2	5.5±0.1	6.4±0.4	7.1±0.2	8.0±0.2	6.7±0.2	6.8±0.2	6.8±0.2	6.8±0.1	8.9±0.2
0.43±0.00	7.7	8.4	7.5±0.4	8.4±0.4	8.7±0.1	8.3±0.3	8.4±0.1	8.1±0.3	8.6±0.1	9.6±0.2	9.2±0.0	9.1±0.2	9.1±0.2	9.1±0.3	10.5±0.1
0.53±0.00	10.2	10.9	9.4±0.3	2.4±0.2	11.6±0.1	11.4±0.4	11.5±0.3	12.2±0.2	10.8±0.1	12.0±0.2	10.7±0.3	10.7±0.4	10.7±0.4	10.4±0.3	12.4±0.1
0.64±0.01	14.5	15.0	9.3±0.2	2.8±0.4	7.2±0.4	6.8±0.5	5.8±0.4	11.7±0.4	15.1±0.3	14.5±0.4	14.7±0.2	14.7±0.6	14.7±0.6	14.6±0.2	14.4±0.1
0.76±0.01	22.4	19.6	9.6±0.2	3.0±0.4	7.5±0.3	8.9±0.4	6.2±0.5	12.5±0.5	20.4±0.2	17.7±0.2	20.3±0.4	20.3±0.3	20.3±0.3	20.0±0.3	18.8±0.1

<sup>a</sup> Values are mean ± SD (n=3). <sup>b</sup> The water sorption data of lactose and WPI were published by Fan & Roos (2015).

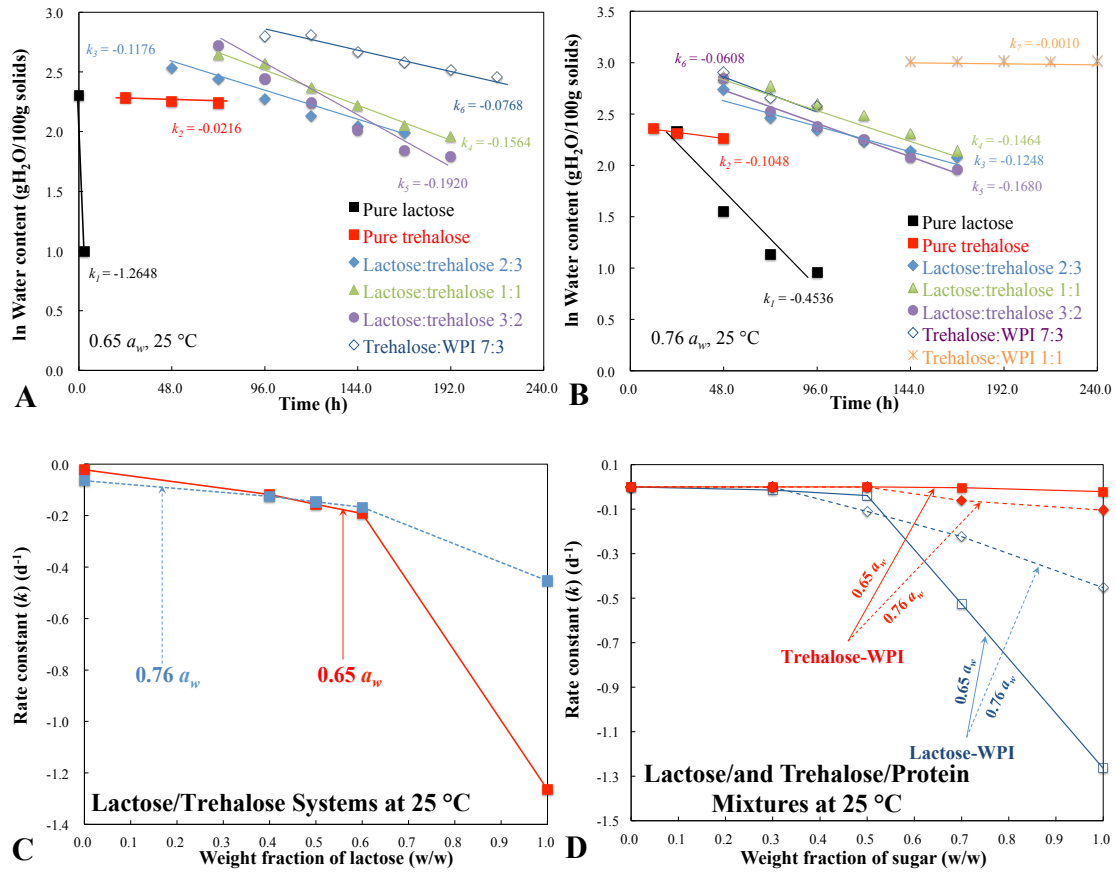


**Fig. 5.3.** Kinetics (A and B) and rate constant, *k* (C and D), for water sorbed by lactose, trehalose, lactose/trehalose, lactose/WPI, and trehalose/WPI systems at each ratio studied around 0.65 and 0.76 *a<sub>w</sub>* at 25 °C, respectively.

### 5.3.3. TYPES OF CRYSTALS FORMS

Fig. (5.4) demonstrates the XRD patterns of lactose, trehalose, lactose/trehalose (2:3, 1:1 and 3:2, w/w), and trehalose/WPI (7:3, 1:1 and 3:7, w/w) mixtures studied after storage at 0.65 and 0.76 *a<sub>w</sub>* at 25 °C. Previous reports have commented on the complexity of XRD patterns of crystallized lactose and lactose-containing materials (Simpson et al., 1982; Jouppila et al., 1998; Biliaderis et al., 2002). Therefore, the most important step was to observe the most characteristic peaks of given crystal forms in the XRD patterns. An approximate quantity of each sugar crystalline form could be derived from the intensity values at specific diffraction angles ( $2\theta$ ). An exact

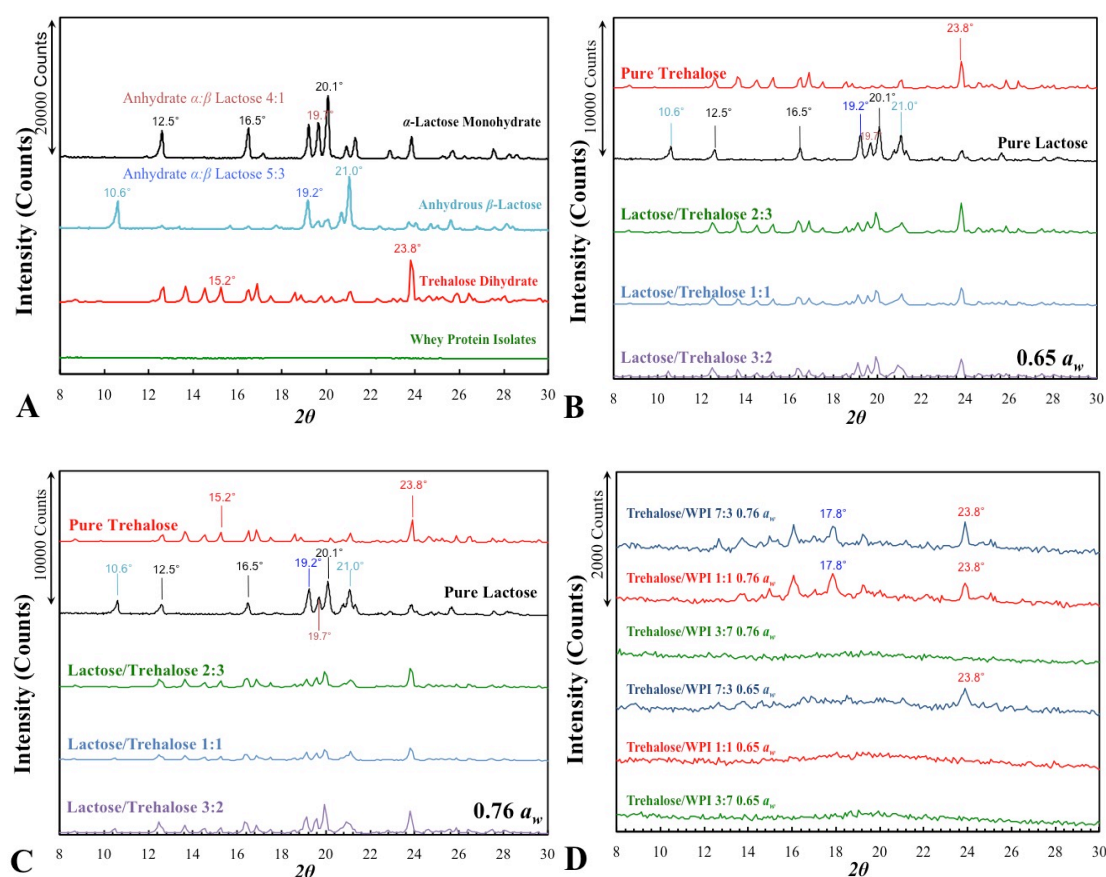


**Fig. 5.4.** X-ray diffraction patterns for  $\alpha$ -Lactose monohydrates (12.5°, 16.6°, and 20.1°), anhydrous  $\beta$ -lactose (10.6° and 21.0°), anhydrous  $\alpha/\beta$ -lactose at 4:1 (19.7°) and 5:3 (19.2°), and trehalose dihydrate (23.8°) are shown on A. The XRD patterns of freeze-dried lactose, trehalose, lactose/trehalose with 2:3, 1:1, and 3:2 solid ratios shown on B and C, and trehalose/WPI mixtures (3:7, 1:1, and 3:7, w/w) shown on D after 240 h storage at 0.65 and 0.76  $a_w$ .

quantitative analysis of each crystalline form was not possible as the diffraction peaks represented more than one type of crystals (Drapier-Beche et al., 1997; McGarvey et al., 2003). Each characteristic  $2\theta$  peak for different crystal types of lactose and trehalose was determined by XRD using standard reagents in Fig. (5.4 A), which agreed with previous studies (Jouppila and Roos, 1998; McGarvey et al., 2003; Miao and Roos, 2005). Characteristic peaks for crystal hydrates ( $\alpha$ -lactose monohydrate and trehalose dihydrate), in the present study, were respectively observed at 12.5°, 16.5°, 20.1°, and 23.8°, whereas the characteristic peak was also observed for anhydrous

$\beta$ -lactose ( $10.6^\circ$  and  $21.0^\circ$ ) in amorphous sugar systems at 0.65 and 0.76  $a_w$ . As reported by Simpson and others (1982), the anhydrous forms of lactose crystal with  $\alpha$ - and  $\beta$ -lactose in molar ratios of 5:3 and 4:1 could be identified by the XRD patterns at diffraction angles of  $19.2^\circ$  and  $19.7^\circ$ , which were also observed in our study for all samples of lactose and lactose/trehalose mixtures (Fig. 5.4 B and C). Trehalose dihydrate was also identified by the XRD patterns in lactose/trehalose mixtures at 0.65 and 0.76  $a_w$  (Fig. 5.4 B and C), which agreed with previous reports (Cardona et al., 1997; McGarvey et al., 2003). Hence, the lactose and trehalose crystallized independently into their characteristic crystals in binary sugar mixtures at high  $a_w$  based on XRD patterns, which agreed with previous report (Miao and Roos, 2005). In the present study, the high leveled-off water contents in lactose/trehalose mixtures based on water sorption testing resulted from trehalose dihydrate formation and incomplete crystallization retaining sorbed water in amorphous phase. Trehalose dihydrate crystals were detected in trehalose/WPI mixtures with 7:3 (0.65 and 0.76  $a_w$ ) and 1:1 solid ratios (0.76  $a_w$ ) at 25 °C by XRD analysis (Fig. 5.4 D). Moreover, an obvious characteristic peak ( $17.8^\circ$ ) was identified by XRD patterns in trehalose/WPI mixture with 7:3 (0.65 and 0.76  $a_w$ ) and 1:1 solid ratios (0.76  $a_w$ ) after storage at 25 °C (Fig. 5.4 D). Owing to the diffraction peaks in XRD patterns were often contributed from more than one type of crystal, the characteristic peak ( $17.8^\circ$ ) could be possibly induced by trehalose dihydrate. Corresponding to water sorption testing, the water content in trehalose should be reach approximately 10 % (gH<sub>2</sub>O/100g solids) if all amorphous phase crystallized as dihydrate crystals. However, the fractional water sorption indicated the fractional water sorbed by trehalose in WPI containing systems (7:3 and 1:1, w/w) was lower than the 10 % (gH<sub>2</sub>O/100g solids), which indicated that trehalose partly crystallized in trehalose/WPI systems after storage at 25 °C. Corresponding to above XRD patterns, therefore, the anhydrous trehalose was possibly formed during crystallization in the presence of WPI after storage at high  $a_w$ .



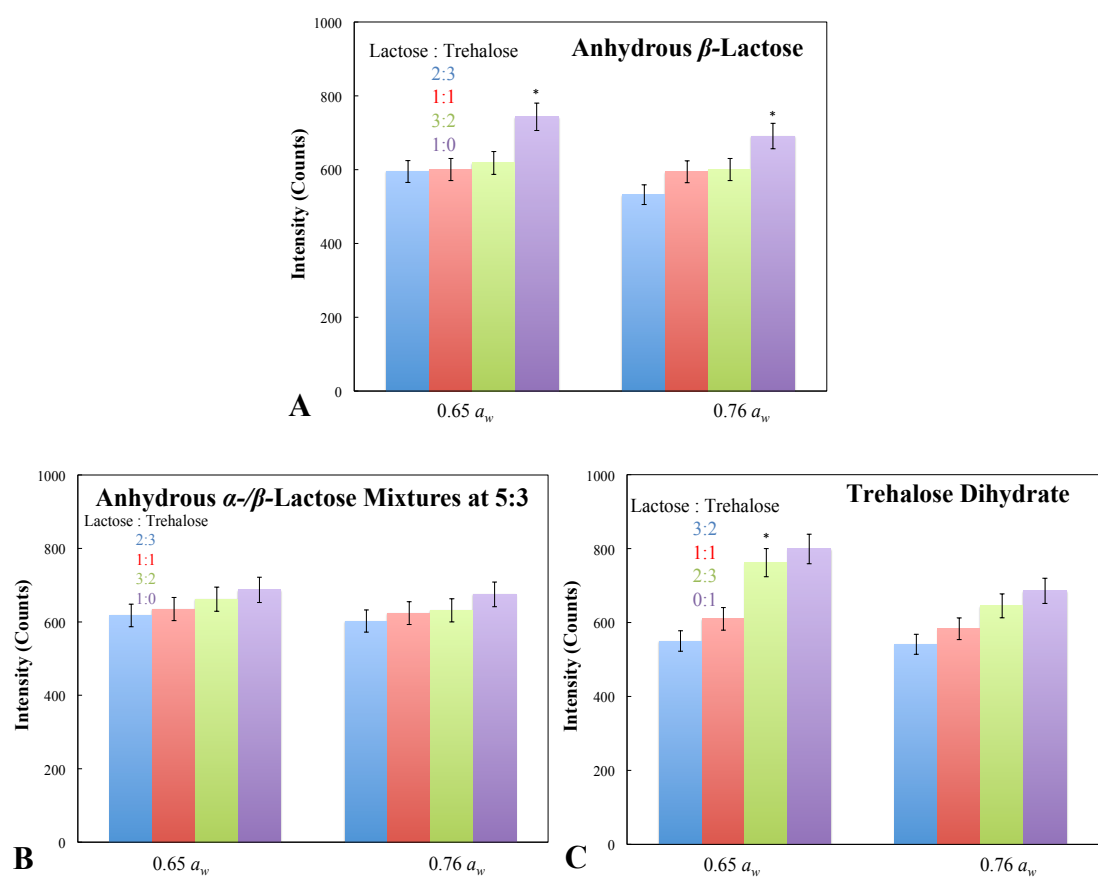


**Fig. 5.5.** Intensity values for anhydrous  $\beta$ -lactose (A),  $\alpha$ -/ $\beta$ -lactose mixtures at 5:3 molar ratios (B), and trehalose dihydrate (C) based on XRD patterns for freeze-dried amorphous lactose/trehalose system stored at 0.65 and 0.76  $a_w$ .

The characteristic peak intensity values of anhydrous  $\beta$ -lactose, anhydrous  $\alpha$ -/ $\beta$ -lactose with molar ratio 5:3 and trehalose dihydrate in lactose/trehalose and trehalose/WPI systems after storage at 0.65 and 0.76  $a_w$  are shown on Fig. (5.5). The peak intensity values of anhydrous  $\beta$ -lactose and  $\alpha$ -/ $\beta$ -lactose with molar ratio 5:3 increased concomitantly with the quantity of trehalose increasing in lactose/trehalose mixtures after storage at 0.65 and 0.76  $a_w$  (Fig. 5.5 A and B). And the peak intensity values of trehalose dihydrate increased with the increasing of trehalose contents in binary sugar systems (Fig. 5.5 C). Previous crystallization studies reported that lactose crystallized as anhydrate forms and then recrystallized to monohydrates, which was governed by the mutarotation of lactose molecules to the different anomeric form during crystal-growth stage (Iglesias and Chirife, 1978). As trehalose

could disturb the movement of lactose molecules in lactose/trehalose mixtures, the recrystallization from anhydrous lactose to monohydrates could also be depressed by the presence of trehalose. Lower intensity peak values of trehalose dihydrate were identified in the presence of WPI in high  $a_w$ , compared with pure trehalose (Fig. 5.4 D). The decreasing of quantity of trehalose dihydrate by the presence of WPI could be explained by the protein causing physic blocking effects in trehalose/WPI systems, which delayed the time demanded for crystallization of trehalose after storage at high  $a_w$  at 25 °C.

### 5.3.4. THERMAL ANALYSIS

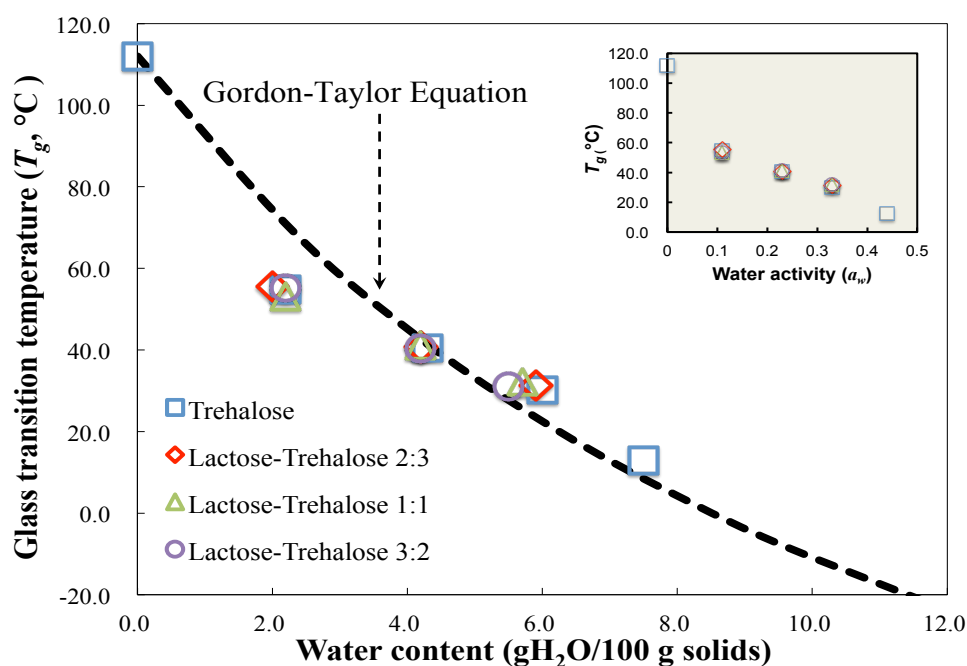


**Fig. 5.6.** The onset  $T_g$  of pure trehalose and trehalose/lactose mixtures (2:3, 1:1, and 3:2, w/w) stored from 0.11 to 0.44  $a_w$  at 25 °C against water content and water activities fitted by  $GT$  equation.

**Table 5.2.** The onset  $T_g$ ,  $T_a$ , composition-dependence  $C_1$  and  $C_2$ , and  $S$  for freeze-dried, trehalose, lactose/trehalose mixtures at solid ratios of 2:3, 1:1, and 3:2, trehalose/WPI mixtures at solid ratios of 7:3, 1:1, and 3:7 and lactose/trehalose/WPI mixture at 2:3:5, 1:1:5, and 3:2:5 solid ratios after storage at low  $a_w$  ( $\leq 0.44$ ) at 25 °C.

Materials	Ratios (w/w)	$a_w$	$T_g$ (°C)	$T_a$ (°C)	$-C_1$	$C_2$ (°C)	$S$ (°C)
Trehalose	-	0.11±0.00 <sup>a</sup>	55±3	69±2	1.25±0.30	-20.70±0.62	15.8±1.3
Trehalose	-	0.23±0.01	41±2	53±3	1.91±0.25	-21.51±0.43	14.6±0.9
Trehalose	-	0.33±0.00	30±1	41±4	2.68±0.31	-22.34±0.60	13.4±1.0
Trehalose	-	0.44±0.02	13±2	23±2	3.10±0.41	-21.48±0.50	12.1±0.9
Lactose/Trehalose	2:3	0.11±0.00	54±3	71±3	3.15±0.42	-34.06±0.46	19.1±1.5
		0.23±0.02	41±1	55±3	2.77±0.31	-29.08±0.54	17.2±1.1
		0.33±0.00	31±2	45±2	2.16±0.37	-23.70±0.52	15.4±1.3
Lactose/Trehalose	1:1	0.11±0.00	55±2	70±3	3.57±0.29	-40.14±0.38	21.2±1.0
		0.23±0.01	41±2	56±2	3.56±0.32	-35.93±0.45	19.0±1.0
		0.33±0.01	32±1	46±3	2.06±0.38	-25.52±0.50	16.8±1.7
Lactose/Trehalose	3:2	0.11±0.01	55±3	75±2	2.09±0.22	-36.18±0.43	23.8±1.1
		0.23±0.02	40±2	58±3	1.24±0.32	-26.09±0.52	19.9±1.0
		0.33±0.00	31±2	47±3	1.62±0.41	-25.91±0.61	18.4±2.0
Trehalose/WPI	7:3	0.11±0.00	55±1	81±1	2.16±0.33	-49.94±0.54	32.4±2.1
		0.23±0.02	42±2	63±1	3.46±0.35	-47.64±0.60	25.5±1.5
		0.33±0.01	33±1	52±2	3.01±0.32	-39.20±0.61	22.4±1.3
		0.44±0.03	22±3	38±2	3.85±0.40	-40.52±0.69	20.6±0.7
Trehalose/WPI	1:1	0.11±0.02	50±2	82±2	2.40±0.30	-60.80±0.53	38.0±2.0
		0.23±0.01	39±1	67±2	1.92±0.38	-48.93±0.62	33.1±2.4
		0.33±0.00	31±3	56±1	3.07±0.41	-55.49±0.60	31.4±1.1
		0.44±0.01	16±2	38±2	2.14±0.45	-41.54±0.63	27.1±2.3
Trehalose/WPI	3:7	0.11±0.02	51±1	92±3	1.59±0.31	-67.04±0.51	48.0±3.0
		0.23±0.01	39±2	73±2	1.64±0.42	-55.71±0.52	39.5±2.4
		0.33±0.01	30±1	62±2	1.22±0.43	-45.34±0.61	34.7±1.0
		0.44±0.00	16±1	42±1	1.68±0.41	-44.08±0.66	31.0±2.5
Lactose/Trehalose/WPI	2:3:5	0.11±0.02	55±1	70±1	1.34±0.33	-22.66±0.51	17.0±1.4
		0.23±0.03	43±1	61±4	1.19±0.43	-26.73±0.61	20.6±2.0
		0.33±0.01	34±2	55±3	1.46±0.42	-32.60±0.63	23.9±2.2
		0.44±0.00	25±1	49±1	2.31±0.40	-46.26±0.68	29.3±2.1
Lactose/Trehalose/WPI	1:1:5	0.11±0.00	57±1	73±2	3.47±0.30	-37.28±0.50	20.0±1.1
		0.23±0.01	44±1	62±2	2.90±0.34	-38.72±0.56	22.4±1.3
		0.33±0.01	32±1	53±3	2.89±0.21	-45.06±0.43	26.2±1.4
		0.44±0.01	25±1	47±3	2.90±0.33	-48.37±0.48	28.0±1.5
Lactose/Trehalose/WPI	3:2:5	0.11±0.01	56±2	71±3	3.92±0.32	-39.32±0.51	19.9±1.1
		0.23±0.00	45±1	64±2	4.24±0.21	-51.33±0.54	24.9±1.0
		0.33±0.02	30±1	53±3	2.70±0.27	-46.23±0.47	27.6±1.3
		0.44±0.01	21±1	47±4	1.97±0.35	-45.53±0.52	30.5±1.4

<sup>a</sup> Values are mean ± SD (n = 3).

The onset  $T_g$  derived from the second heating scans using DSC for humidified amorphous trehalose, trehalose/lactose, trehalose/WPI and lactose/trehalose/WPI systems studied at low water activities ( $\leq 0.44 a_w$ ) at 25 °C are shown on Table (5.2). The  $T_g$  values of trehalose, in the present study agreed with previous studies at  $a_w$  below 0.44 (Green and Angell, 1989; Silalai and Roos, 2011). For the pure WPI, however, the  $T_g$  was not observed in the present study as glass transitions of proteins are less obvious than those of small sugars (Zhou and Labuza, 2007; Roos and Potes, 2015). The  $T_g$  values of non-crystalline trehalose and lactose/trehalose mixtures (2:3, 1:1 and 3:2, w/w) against water contents and water activities ( $0.11 \sim 0.44 a_w$ ) are shown in Fig. (5.6). Since the GAB gave the water content in each non-crystalline component in trehalose/protein systems according to fractional water sorption, the  $T_g$  values of pure trehalose could be obtained at intermediate and high water activities ( $\geq 0.56 a_w$ ) and the experimental data of amorphous trehalose and lactose-trehalose mixtures were fitted using GT equation (Eq. 1.3) with  $k \approx 9.1 \pm 0.5$ , successfully. The  $T_g$  values of non-crystalline trehalose and lactose/trehalose in mixtures were less than 0 °C at high water activities due to the higher water contents and stronger plasticization effects. As trehalose and lactose/trehalose mixtures sorbed the same quantity of water after storage at low water activities ( $\leq 0.44 a_w$ ), the  $T_g$  was close to the  $T_g$  of individual sugar (Table 3.1 and 5.2). The  $T_g$  values of WPI containing sugar systems, in the present study, were slightly higher than those of pure trehalose due to anti-plasticization at low water contents (Slade and Levine, 1991; Haque and Roos, 2004). According to previous reports (Kedward et al., 2000; Ibach and Kind, 2007; Silalai and Roos, 2010), phase separation could occur in sugar/protein systems and therefore they had almost composition-independent  $T_g$  with  $T_g$  values of systems being mostly dependent on amorphous sugars. Therefore, the presence of protein had a minor effect on the calorimetric  $T_g$  of the sugar and sugar mixtures after storage at 25 °C.

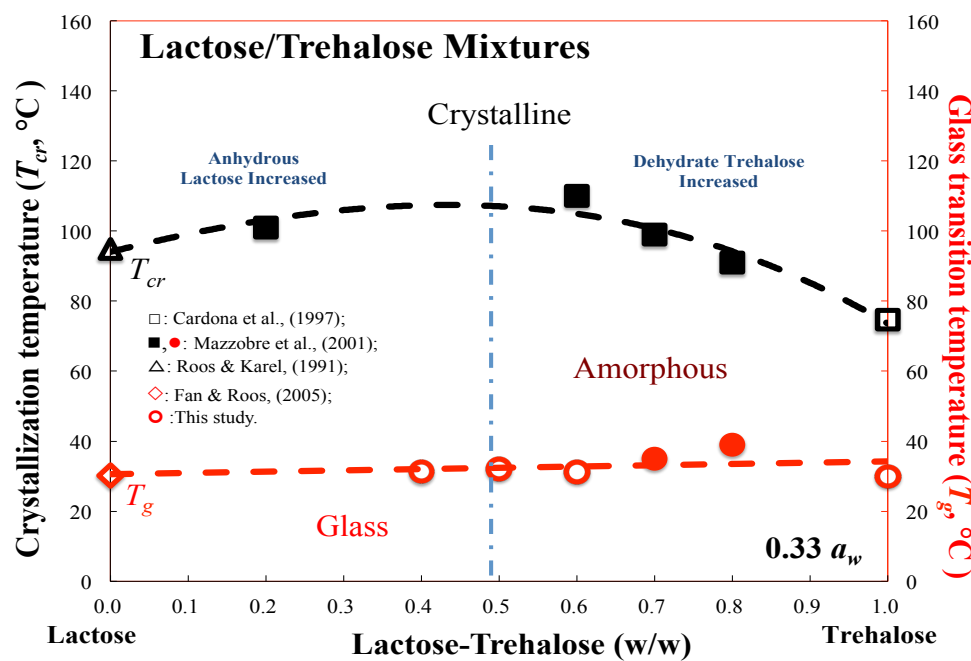


**Fig. 5.7.** Literature values for the state diagram of the lactose/trehalose mixtures after storage at 0.33  $a_w$  at 25 °C, including onset  $T_{cr}$  and  $T_g$  measured by DSC.

Fig. (5.7) shows a composite state diagram of the lactose, trehalose and lactose/trehalose mixtures at 0.33  $a_w$  based on  $T_g$  derived from our study and literature crystallization temperature ( $T_{cr}$ ) data using DSC measurement reported in available sources (Roos and Karel, 1991a; Mazzobre et al., 2001). The two lines shown in Fig. (5.7) were  $T_g$  line and instant crystalline line derived from calorimetric  $T_{cr}$  of lactose/trehalose system, respectively. As seen in Fig. (5.7), the  $T_g$  value of each lactose/trehalose mixture was very close to individual sugars due to the similar water contents of individual sugar and sugars mixtures after storage at 0.33  $a_w$  at 25 °C. The literature  $T_{cr}$  values in lactose/trehalose system increased concomitantly with the increasing of trehalose content in lactose-dominating system (lactose > 50 %, w/w) and leveled off at lactose content around approximately 50 % (w/w). However, the literature  $T_{cr}$  values of mixtures rapidly decreased when trehalose became to dominating components in binary sugar systems (Fig. 5.7). The molecules of lactose and trehalose in binary sugar systems need more energy to form stable nucleus and

move onto lattice due to above two sugar molecules disturbed each other during crystallization as noted above, and thus, the literature  $T_{cr}$  values increased in lactose/trehalose systems. Consequently, we found that the literature  $T_{cr}$  values in binary sugar systems could be affected by the quantity of each component as the presence of similar-molecular-size individual sugar could disturb the molecular movement of each other during crystallization.

### 5.3.5. ALPHA-RELAXATION AND WLF-MODEL ANALYSIS OF $\tau$

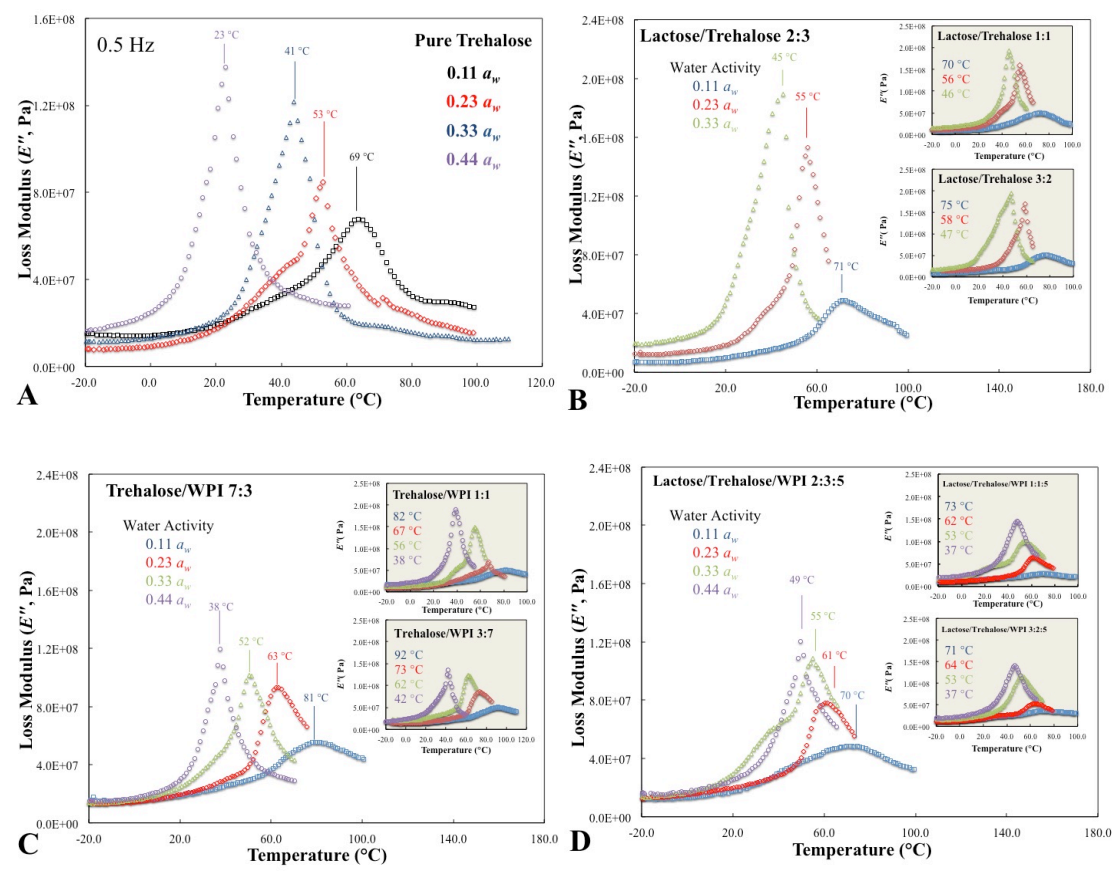


**Fig. 5.8.** The DMA spectra of  $E''$  for pure amorphous trehalose at water activities below  $0.44 a_w$  (A), lactose/trehalose mixtures at ratio of 2:3, 1:1, and 3:2 (w/w) (B), trehalose/WPI mixtures at 7:3, 1:1, and 3:7 (w/w) (C) and lactose/trehalose/WPI mixtures at 2:3:5, 1:1:5, and 3:2:5 (w/w) at frequency of 0.5 Hz after storage at 25 °C. The  $T_\alpha$  was characterized based on the peak of each loss modulus.

Fig. (5.8) demonstrates the DMA spectra ( $E''$  peaks at frequency of 0.5 Hz) for pure trehalose ( $\leq 0.44 a_w$ ), lactose/trehalose ( $\leq 0.33 a_w$ ), trehalose/WPI and lactose/trehalose/WPI mixtures. The  $E''$  peaks of amorphous trehalose and lactose/trehalose mixtures decreased and broadened concomitantly with water activity decreasing at low  $a_w$  (Fig. 5.8 A and B). Typically, the changes in mechanical properties of materials in DMA may be induced by many reasons such as molecular interactions (Lopez-Diez and Bone, 2004) and water plasticization (Silalai and Roos, 2011). Therefore, the  $E''$  of glass forming trehalose and lactose/trehalose mixtures could be dependent on the presence of water. The  $E''$  of lactose/trehalose systems showed a peak at each ratio, whereas a weaker peak was found for pure trehalose at each  $a_w \leq 0.33$ , compared with each lactose containing sugar system (Fig. 5.8 B). However, the peak of  $E''$  significantly flattened concomitantly with the increasing of protein quantity in trehalose/WPI and lactose/trehalose/WPI mixtures after storage at  $a_w \leq 0.44 a_w$  and 25 °C (Fig. 5.8 C and D). Above resulted by the molecular mobility of amorphous sugars was disturbed by the presence of protein due to protein causing physical blocking effects.

The  $T_\alpha$  was determined from the peak temperature of  $E''$  in the DMA spectra (Talja and Roos, 2001; Silalai and Roos, 2011ab). The  $T_\alpha$  values of pure amorphous trehalose are given in Table (5.2). Since the physical states of amorphous carbohydrate systems are strongly influenced by the concentration of water, the  $T_\alpha$  of pure trehalose at lower water activities was increased from 23 °C (0.44  $a_w$ ) to 69 °C (0.11  $a_w$ ) at a frequency of 0.5 Hz in this study, which agreed with previous studies (Cruz et al., 2001; Renzetti et al., 2012). These changes in systems could be explained by the free volume theory (Royall et al., 2005; Meinders and van Vliet, 2009). As water increased the free volume in the system and molecular mobility of the amorphous components, the  $T_\alpha$  values of lactose/trehalose mixtures slightly changed compared to pure trehalose due to the mixtures sorbed similar quantity of water as each individual sugar after storage at each low  $a_w$  at 25 °C (Table 5.2). However, the presence of WPI could increase the  $T_\alpha$  values of trehalose/WPI and

lactose/trehalose/WPI mixtures, which were caused by the protein causing physical blocking effects and reduced the movement of amorphous sugars (Table 5.2). Therefore, our study indicated that the presence of large-molecular-size protein could affect the  $\alpha$ -relaxations of amorphous sugars, significantly.

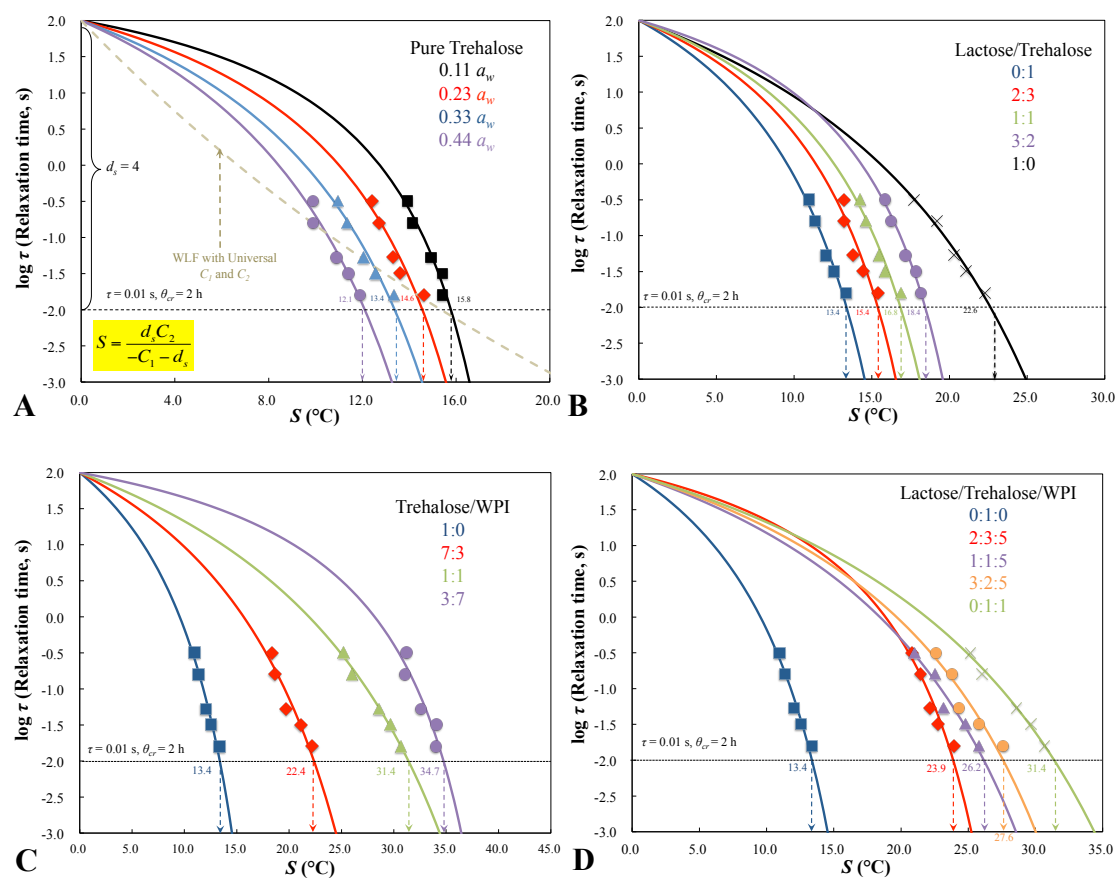


**Fig. 5.9.** Strength parameters ( $S$ ) of pure trehalose at various water activities (0 ~ 0.44  $a_w$ ) (A), lactose/trehalose mixtures at ratio of 2:3, 1:1, and 3:2 (B), trehalose/WPI mixtures at 7:3, 1:1, and 3:7 mass ratios (C), and lactose/trehalose/WPI mixtures at 2:3:5, 1:1:5, and 3:2:5 (D) at frequency of 0.5 Hz after storage at 0.33  $a_w$  at  $d_s = 4$  decreasing the structural relaxation time,  $\tau$ , as measured using DMA to  $\tau = 0.01$  s. Such decrease in  $\tau$  is known to result in particle stickiness and aggregation at a contact time of 10 s. The WLF equation with universal  $-C_1$  and  $C_2$  (-17.44 and 51.6 °C) were plotted (black dotted line) as a reference.

While the “fragility” concept developed by Angell (2002) may predict some



properties of single glass-forming food components, the  $S$  concept based on modified WLF modeling with the material-specific constants. Numerical values varying with composition ( $C_1$  and  $C_2$ ) were used to describe solid flow characteristics of amorphous materials based on time and temperature dependent behavior in food solids. The  $S$  parameter combines the characterization of material state of the system and relaxation times factor and shows the critical temperature difference, at which a sharp change in properties of the system occurs. This parameter is simple in use and it describes viscous flow characteristics of glass forming materials. Table (5.2) gives the material-specific  $C_1$  and  $C_2$ , and  $S$  values for pure trehalose, lactose/trehalose, trehalose/WPI and lactose/trehalose/WPI mixtures at all ratios studied at low  $a_w$  ( $\leq 0.44 a_w$ ) (downwards concavity around glass transition), respectively. When the storage temperature increased to above  $T_g$ , amorphous materials lost solid characteristics concomitantly with decreasing  $\tau$ , which is reflected on the decreasing viscosity and increasing flowability of the materials (Lillie and Gosline, 1990; Slade et al., 1991). Such loss of solid characteristics results in collapse of cell walls in porous structures typical of dehydrated foods. Fig. (5.9A) shows the  $S$  values of pure trehalose after storage at low water activities ( $0.44 a_w$ ) as derived from the modified WLF model analysis. We found that water could govern the structural strength or viscous flow characteristics of glass forming trehalose (Fig 5.9 A). And the trehalose could affect the structural strength of glass forming sugar as the  $S$  value of lactose/trehalose mixtures slightly decreased concomitantly with the quantity of trehalose increasing at  $0.33 a_w$  due to trehalose could disturb the molecular mobility of amorphous lactose (Fig. 5.9 B). The results of Fig. (5.9C and D) and Table (5.2) also demonstrated that the presence of WPI could affect the strength of amorphous trehalose and lactose/trehalose mixtures as the  $S$  value were greater than for pure trehalose and trehalose/WPI at 1:1 solid ratio at each  $a_w$ , respectively. As the components diffuse independently in sugar/protein system, the  $S$  parameter only provides a measure of relaxation rates of key component, which is amorphous sugar in this study. The presence of polymeric components, i.e., WPI, could improve the strength of amorphous sugar due to protein could become a physical barrier for the

movement of sugar molecules in system. As we expected, the strength parameter could measure the compositional effects and related to control the quality and stability of amorphous sugars/protein systems.

### 5.3.6. WATER CONTENT, $S$ , AND CRYSTALLIZATION

The structural strength of glass forming sugars in this study, which was studied around glass transition, could be expressed as the  $S$  value. As the  $S$  concept is a measure of resistance to structural relaxations and flow, the  $S$  values could be determined by the extent of molecular mobility of amorphous sugars. The presence of other components, such as water and protein, could affect the structural strength of amorphous sugar containing systems by disturbing the molecular movements of sugars. Hence, we plotted Fig. (5.10) to show the relationship of the  $S$  value against water contents of trehalose, lactose/trehalose and trehalose/WPI mixtures with all ratios studied above. As we expected, the  $S$  values of systems decreased with the water content increasing in trehalose, lactose/trehalose and trehalose/WPI mixtures due to water plasticization effects (Fig. 5.10). Moreover, we built an available non-linear model (Eq. 5.1) to interpret the relationship between  $S$  values and water contents in glass forming trehalose and lactose/trehalose mixtures (2:3, 1:1, and 3:2, w/w) at  $a_w \leq 0.44$  and achieved a very good fitting performance (Fig. 5.10). As the predicted water contents of non-crystalline sugars at  $a_w \geq 0.56$  could be estimated by GAB model (Eq. 1.1) based on fractional water sorption behavior, the estimated  $S$  values could be calculated for amorphous trehalose and lactose/trehalose mixtures by using Eq (5.1), respectively. Since the predicted  $S$  of glass forming trehalose and lactose/trehalose mixtures decreased following the increases of water content as we noted above, above model (Eq. 5.1) could be considered and used to predict the structural strength of glass-forming sugars using when exposed to high  $a_w$ .

$$S_p = \frac{w_1 S_{d1} + w_2 S_{d2} + k w_3 S_{d3}}{w_1 + w_2 + k w_3} \quad (5.1)$$

Where,  $S_{d1}$ ,  $S_{d2}$ ,  $S_{d3}$ ,  $k$ ,  $w_1$ ,  $w_2$  and  $w_3$  refer to the  $S$  value of anhydrous trehalose (17.6 °C reported by Roos & et al., 2016), anhydrous lactose (27.2 °C reported by Chapter III), amorphous water (6.0 °C reported by Maidannyk et al., 2017) a constant ( $\approx 5.5 \pm 0.5$ ) and the weight fraction of the 1 (trehalose), 2 (lactose) and 3 (water) in mixtures, respectively.

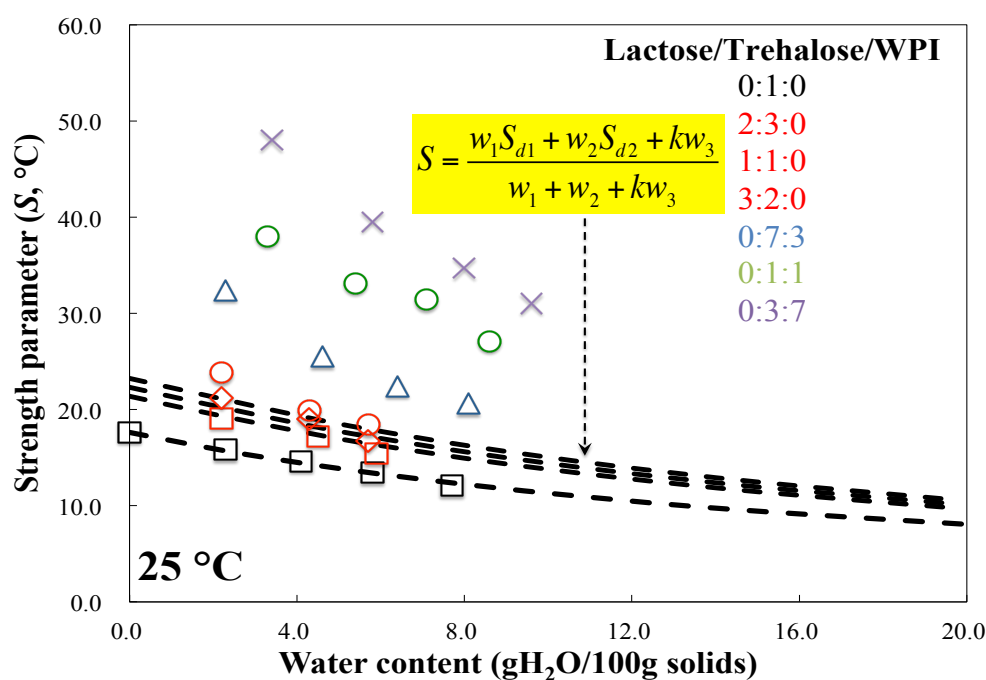


**Fig. 5.10.** The relationship between water content and  $S$  of pure trehalose, lactose/trehalose (2:3, 1:1, and 3:2, w/w), and trehalose/WPI mixtures (7:3, 1:1, and 3:7, w/w) after storage at low  $a_w \leq 0.44$  and 25 °C. The black dash lines represent the calculated  $S$  for trehalose and lactose/trehalose mixtures using Eq (5.1) from 0 to 0.76  $a_w$ .

Crystallization during food storage often results from an exposure of amorphous sugars to high  $a_w$  condition due to the water plasticization depressed the  $T_g$  and increased the molecular mobility of noncrystalline sugars in systems (Roos and Karel, 1991a; Biliaderis et al. 2002). As noted above, the predicted  $S$  value for amorphous trehalose and lactose/trehalose mixtures significantly decreased after storage at 0.65

and 0.76  $a_w$  and the occurring of crystallization was observed in water sorption testing. Furthermore, the  $S$  values of trehalose/WPI system increased with the increasing of protein quantity and a reduced crystallization derived by protein was observed in our study. Therefore, we believed that the  $S$  concept could be used to control the crystallization of glass forming sugars as well as the quality and stability of food solids.

## 5.4. CONCLUSIONS

We have shown that amorphous trehalose/WPI and lactose/trehalose mixtures have fractional water sorption properties, and the crystallization of lactose/trehalose mixtures was delayed by the addition and increasing quantity of trehalose and WPI. The capability of trehalose and WPI to prevent crystallization of lactose in binary sugar mixtures was quantity dependent, i.e., a higher trehalose or WPI content showed a stronger inhibition. The  $\alpha$ -relaxations,  $\tau$  and  $T_\alpha$  of amorphous trehalose, lactose/trehalose and lactose/trehalose/WPI mixture could be affected by the mixture composition, i.e., water, trehalose and WPI, using WLF model analysis. A  $S$  concept based on WLF model analysis was validated and the  $S$  parameter could measure the compositional effects and control solids properties, i.e., crystallization, in food processing as well as for stability control of resultant products in practical applicability. For further researching, the relationship between crystallization temperatures and structural strength of glass-forming sugar containing systems will be continually studied in more complex food systems.



# WATER SORPTION-INDUCED CRYSTALLIZATION, STRUCTURAL RELAXATIONS AND STRENGTH ANALYSIS OF RELAXATION TIMES IN AMORPHOUS LACTOSE/WHEY PROTEIN SYSTEMS

Fanghui Fan<sup>a</sup>, Tian Mou<sup>b</sup>, Bambang  
Nurhadi<sup>a</sup>, and Yrjö H. Roos<sup>a</sup>

<sup>a</sup> *School of Food and Nutritional Sciences;* <sup>b</sup> *School  
of Mathematical Sciences, University College Cork,  
Cork, Ireland*

## ABSTRACT

Water sorption-induced crystallization,  $\alpha$ -relaxations and relaxation times of freeze-dried lactose/whey protein isolate systems were studied using dynamic dewpoint isotherms method and dielectric analysis, respectively. The fractional water sorption behavior of lactose/WPI mixtures shown at  $a_w \leq 0.44$  and the critical  $a_w$  for water sorption-related crystallization ( $a_w^{(cr)}$ ) of lactose were strongly affected by protein content based on DDI data. DEA results showed that the  $\alpha$ -relaxation temperatures of amorphous lactose at various relaxation times were affected by the presence of water and WPI. The  $\alpha$ -relaxation-derived strength parameter ( $S$ ) of amorphous lactose decreased with  $a_w$  up to 0.44  $a_w$  but the presence of WPI increased  $S$ . The linear relationship for  $a_w^{(cr)}$  and  $S$  for lactose/WPI mixtures was also established with  $R^2 > 0.98$ . Therefore, DDI offers another structural investigation of water sorption-related crystallization as governed by  $a_w^{(cr)}$ , and  $S$  may be used to describe real time effects of structural relaxations in noncrystalline multicomponent solids.

**KEYWORDS,** *Dynamic Dewpoint Isotherms; Crystallization;  $\alpha$ -Relaxation; Relaxation Times; Strength; Water Activity*

## 6.1. INTRODUCTION

Water is of key importance to food systems affecting processing, microbial safety, sensory perception, and a storage stability and shelf life (Al-Muhtaseb et al., 2002; Lodi and Vodovotz, 2008). Water sorption may be affected by time-dependent phenomena, structural transformations, and phase transitions of food solids. Such transitions may affect rates of deteriorative changes and decrease the storage stability of dehydrated foods, e.g., powdered milk (Silalai and Roos, 2011a), potato flakes (Turner et al., 2006), and dry pasta (Aguilera et al., 2003; Gowen et al., 2008). Water

sorption isotherms are important to numerous applications, e.g., development of new products (Wang and Brennan, 1991), determination of product stability and shelf life (Jouppila and Roos, 1994ab), and process design and control (Peng et al., 2007). The dynamic dewpoint isotherm (DDI) method was developed to generate water sorption isotherms using single samples in a dynamically changing water vapor pressure (Yuan et al., 2011). The DDI method developed along with dynamic vapor sorption provides a continuous measurement of water content ( $c_w$ ) and water activity ( $a_w$ ). DDI differs from static sorption measurement, which measure  $c_w$  for equilibrated materials at known  $a_w$  (Schmidt and Lee, 2012). Also, DDI makes it possible to generate complete dynamic isotherms with 50 to 200 data points quickly and accurately without long equilibration times which are typical of SSM methods (Yuan et al., 2011; Schmidt and Lee, 2012). Therefore, DDI method offers another real-time investigation of water sorption-related material properties, i.e., crystallization and deliquescence (Yao et al., 2011), in food processing as well as for the control of storage stability and shelf life of resultant products.

Water sorption characteristics, as well as other interactions of food solids with water, are defined by composition of nonfat components, i.e., carbohydrates and proteins (Roos and Drusch, 2015). Characterization of glass formation of complex food solids systems has been of particular interest in recent years (Ibach and Kind, 2007; Babu and Nangia, 2011). Amorphous food materials exist in a supercooled and non-equilibrium state below their respective equilibrium melting temperature with no well-defined structure. The nonequilibrium state may exhibit an indefinite number of glass structures with varying levels of molecular packing and order. When temperature increases to above glass transition temperature, a rapid increase of molecular mobility occurs and the glass-forming material transforms to a viscous liquid, which dramatically affects various physicochemical properties of food solids (Slade et al., 1991; Bhandari and Howes, 1999). Structural relaxations in amorphous food materials around or above the glass transition occur as a result of molecular mobility changes due to variations in external thermodynamic conditions e.g.,

pressure and temperature. Glass transition may also result internally in materials because of changes in plasticizer or solvent contents, e.g., water, which can induce dramatic changes in solids properties and directly affect processing, storage, bioavailability, and delivery properties of food materials (Yu et al., 2001; Roos and Drusch, 2015). Relaxation times correspond to the kinetically impeded and time-dependent molecular rearrangements that are responsible for solids structure and properties, e.g., flow characteristics, viscous flow and collapse, mechanical or dielectric properties, and crystallization (Sperling, 2005). Such properties may be used to control the quality and stability of food materials during processing and storage (Champion et al., 2000).

The  $\alpha$ -relaxation and relaxation times of glass forming food materials around calorimetric  $T_g$  could be studied and determined by dielectric analysis (DEA) (Moates et al., 2001; Clerjon et al., 2003). The  $\alpha$ -relaxation temperature ( $T_\alpha$ ) may also be taken from the dielectric loss ( $\epsilon''$ ) peak temperature at various frequencies to obtain corresponding relaxation times (Silalai and Roos, 2011). The Williams-Landel-Ferry (WLF) model is often used to model relaxation times of the non-Arrhenius temperature dependence of relaxation processes occurring above  $T_g$ , and the  $\tau$  is shown against  $T-T_g$  (Slade et al., 1991). The WLF-relationship applies over the temperature range covering the rubbery or supercooled liquid state and it was also used to describe time and temperature dependent behavior of food solids systems. The “strength” concept and strength parameter developed by Roos and Others (2016) combined the characterization of material state and relaxation times to describe the critical temperature difference at which a sharp change in properties of the material occurs. On the other hand, the  $S$  parameter based on WLF modeling was used to describe amorphous food solids and their properties for typical processing and storage conditions where a component or miscible components within food structure may experience the glass transition. Besides the strength of food solids, the Deborah number was applied to provide a useful translation of measured relaxation times to real timescales. Therefore, the strength concept gives a quantitative measure to



estimate compositional effects on relaxation times to describe properties of food solids above measured  $T_g$ .

Lactose ( $\beta$ -D-galactopyranosyl (1–4)-D-glucopyranose) is one of the most common and important ingredients in many formulated foods and pharmaceutical materials, and it exhibits strong water-dependent properties, i.e., glass transition and crystallization from its amorphous states during storage (Nickerson, 1979; Gänzle et al., 2008). Understanding glass transition-related structural relaxations and their coupling with water sorption properties is essential for modeling the physical state of dairy-based food systems at various conditions and the design of complex formulations. The importance of glass transition to amorphous solids characteristics has been well recognized but few studies have contributed to understanding effects of glass former or polymer, i.e., protein, on the water sorption characteristics and structural relaxations in food formulations. Therefore, the major objective of the present study was to investigate the influence of food polymeric components (whey protein isolates, WPI) on the water sorption properties of freeze-dried amorphous lactose/WPI mixtures using the DDI measurement data at 25 °C. The strength analysis was carried out to determine the  $S$  parameter for lactose/WPI systems by analyzing their relaxation times measured by DEA after storage at  $a_w \leq 0.44$   $a_w$  and 25 °C. These data are useful for the understanding of the effects of proteins on water sorption properties of amorphous lactose and collective structural relaxation behavior when present with amorphous lactose around the glass transition in well-mixed food and pharmaceutical materials.

## **6.2. MATERIALS AND METHODS**

### **6.2.1. SAMPLE PREPARATION**

$\alpha$ -Lactose monohydrate (>99 % lactose) (Sigma-Aldrich, St. Louis, Mo., U.S.) and whey protein isolate (WPI; Isolac<sup>®</sup>, Carbery Food Ingredients, Co., Ballineen, Ireland;

minor components including carbohydrates or lipids < 3%) were used. Aqueous lactose and WPI with 20 % (mass) solids at room temperature were used to obtain ratios of 7:3, 1:1, and 3:7 of lactose/WPI by mass. Mixed solutions (5 mL in total) were prepared in pre-weighted glass vials (10 mL; Schott Müllheim, Germany). All solutions in the vials (semi-closed with septum) were frozen at  $-20\text{ }^{\circ}\text{C}$  for 20 h and then subsequently tempered at  $-80\text{ }^{\circ}\text{C}$  for 3 h prior to freeze-drying using a laboratory freeze-dryer (Lyovac GT2 Freeze-Dryer, Amsco Finn-Aqua GmbH, Steris<sup>®</sup>, Hürth, Germany). After freeze-drying at pressure < 0.1 mbar, triplicate samples of each material were stored in evacuated desiccators over  $P_2O_5$  at  $25\text{ }^{\circ}\text{C}$  (Sigma-Aldrich, St. Louis, Mo., U.S.) prior to subsequent analysis.

#### **6.2.2. WATER SORPTION EXPERIMENT**

The water sorption of freeze-dried samples was studied using an AquaSorp isotherm generator (AIG; Decagon Devices, Inc. Pullman WA, USA). The airflow continuously passes over the sample in AIG until certain interval time or when there was a mass or  $a_w$  change of sample, then the flow stopped and the snapshot of the sorption process was taken by directly measuring mass and  $a_w$  based on a high precision magnetic force balance and chilled-mirror dewpoint sensor (Decagon Devices, Inc. Pullman WA, USA). Based on above principle the dynamic water sorption of DDI can be comparable to real-time sorption process for a material with fast vapor diffusion or by reducing the sample size. In the present study, approximately 600 mg of each sample (dried powder), which could cover the bottom of stainless steel sample cup, was used in measurements. Measurement parameters were 0.05 to 0.90  $a_w$  at a temperature of  $25\text{ }^{\circ}\text{C}$ , airflow of 300 ml/min (Schmidt and Lee, 2012). At certain interval time, the airflow stopped automatically then the weight change and the  $a_w$  of the sample were recorded. After initial  $c_w$  was determined, the mass was converted to the  $c_w$  of the sample at the corresponding  $a_w$  and a plot of the dynamic sorption isotherm using the SorpTrac software, version 1.03.3 (Decagon Devices, Pullman, WA, USA) was generated. Since each DDI run is unique, the

sorption section of the working isotherm was obtained in duplicate, each on a different sample.

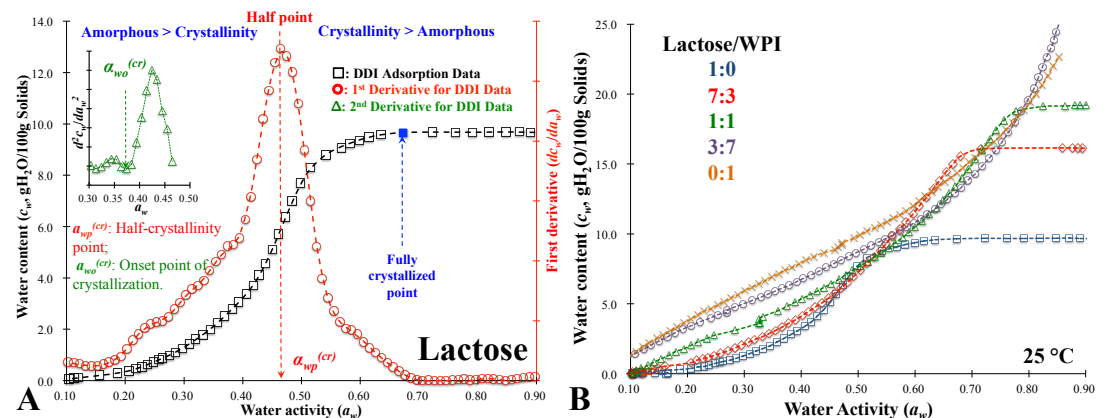


**Fig. 6.1.** The  $a_w^{(cr)}$  for freeze-dried lactose respectively taking the peak  $a_w$  of first derivative ( $a_{wp}^{(cr)}$ ) and onset  $a_w$  of the second derivative ( $a_{wo}^{(cr)}$ ) on DDI sorption data at 25 °C (A). B shows the DDI curves for lactose and lactose/WPI mixtures with 7:3, 1:1, and 3:7 mass ratios by running at 25 °C, respectively.

The critical  $a_w$  value for water sorption-induced crystallization ( $a_w^{(cr)}$ ) of lactose and lactose/WPI mixtures were analyzed and determined by calculating the changes of  $c_w$  in DDI of each sample using derivative analysis (Yuan et al., 2011). The procedures used to obtain the first and the second derivative was as follows. Attempts to leave out noise and find the peak location, the  $a_w$  and  $c_w$  data derived from DDI were smoothed using LOESS (local polynomial regression fitting) smoothing (second-degree polynomial) with a span of 11 points using the R programme, version 3.2.3 (The R Foundation<sup>©</sup>, Murray Hill, NJ, USA). The smoothed data set was fit using a smoothing cubic spline after which the first derivative of the fit was taken. The peak  $a_w$  of the 1<sup>st</sup> derivative function ( $a_{wp}^{(cr)}$ ) based on smoothed DDI data was taken as acceleration point for lactose crystallization. The smoothing and fitting procedures were repeated for the 1<sup>st</sup> derivative after which the 2<sup>nd</sup> derivative was obtained from the 1<sup>st</sup> derivative. Water sorption data showed that a substantial peak on the 2<sup>nd</sup> derivative developed with onset around the calorimetric  $T_g$  corresponding  $a_w$ ,

$a_{wo}^{(cr)}$  (Fig. 6.1 A). The water plasticization to above the glass transition induced translational mobility of lactose. Such mobility with further water plasticization could increase free volume to provide water sorption sites and hydrogen bonding structuring of the lactose/water system to accommodate water with less direct lactose-lactose interactions. The programmed codes for achieving first and second derivative analysis in R programme were shown on Appendix III.

### 6.2.3. DIELECTRIC ANALYSIS

DEA was used to measure dielectric properties from the dielectric constant or permittivity ( $\epsilon'$ ), dielectric loss ( $\epsilon''$ ), and their ratio  $\tan \delta = (\epsilon''/\epsilon')$  as a function of temperature. The  $\epsilon'$  describes an alignment of dipoles and the  $\epsilon''$  describes an energy that is required to align dipoles (Talja and Roos, 2001). In the present study, the freeze-dried lactose and lactose/WPI at 7:3, 1:1, and 3:7 mass ratios were humidified for 120 h over saturated solutions of  $CH_3COOK$ ,  $MgCl_2$ , and  $K_2CO_3$  (Sigma Chemical Co., St. Louis, Mo., USA) to obtain respective water activities of 0.23, 0.33, and 0.44  $a_w$  at equilibrium in vacuum desiccators in incubators at storage temperature of 25 °C. Dielectric properties of both dry and humidified samples were analyzed using dielectric analyzer (DS6000, Triton Technology Ltd., UK), with titanium sample holders as the electrodes. The LCR meter (inductance, capacitance, and resistance; LCR-819) and DEA instrument were calibrated and zeroed with the open-short circuit of the electrodes before starting experiments. Samples were ground and approximately 600 mg samples were placed between parallel plate titanium capacitors (diameter = 33 mm) with the thickness less than 2 mm. Triplicate samples of each material were analyzed using dynamic measurements and recorded using Triton Laboratory software (version 1.0.330). Samples were analyzed in triplicate using dynamic measurements and scanned from ~ 60 °C below to over the  $T_g$  region with cooling rate of 5 °C/min and heating rate of 2 °C/min at frequencies of 0.5, 1.0, 5.0, 10.0, and 20.0 kHz. The measuring head was connected to a liquid nitrogen tank (1L; Cryogun, Brymill cryogenic systems, Labquip (Ireland) Ltd., Dublin, Ireland). As

noted above,  $T_\alpha$  determined from the temperature of  $\varepsilon''$  at the peak were used to determine the relaxation times.

#### **6.2.4. STRENGTH ANALYSIS**

The relaxation times and  $T_\alpha$  corresponding to  $\varepsilon''$  peak above  $T_g$  were modeled using the WLF equation (Eq. 1.9). The relaxation times were defined by frequency set in DEA measurements ( $\tau = 1/2\pi f$ ). The WLF model constants  $C_1$  and  $C_2$  were derived from a plot of  $1/\log(\tau/\tau_g)$  against  $1/(T-T_g)$  using experimental  $\tau$  with the assumption of  $\tau_g = 100$  s at the calorimetric onset temperature of the  $T_g$  (Angell, 2002). A decrease in the number of logarithmic decades for flow, e.g., that being critical for stickiness, could be used as the critical parameter,  $d_s$ , of Eq. (1.12) and the corresponding  $T-T_g$  was defined as the strength of the solids,  $S$ . As the  $S$  values are given as temperature corresponding to a critical  $\tau$  for a key amorphous component within a material, it also provides a measure of resistance to structural changes, i.e., the higher value of  $S$  refers to a stiffer system at a corresponding  $T-T_g$ .

#### **6.2.5. STATISTICAL ANALYSIS**

The second derivative analysis of DDIs sorption data was carried out in *R* Programme and the strength analysis of dielectric  $\alpha$ -relaxation associated relaxation times were calculated and fitted by using Microsoft Office Excel 2011 (Microsoft, Inc., USA). All measurements were repeated three times, as well as the average values with the standard deviation of triplicate measurements were calculated.

### **6.3. RESULTS AND DISCUSSION**

#### **6.3.1. DYNAMIC WATER SORPTION**

**Table 6.1.** The Onset and Peak  $a_w^{(cr)}$  for Water-Induced Crystallization ( $a_{wo}^{(cr)}$  and  $a_{wp}^{(cr)}$ ) in Freeze-Dried Lactose, Lactose/WPI Mixtures at 7:3, 1:1, and 3:7 Mass Ratios During DDI Sorption Process at 25 °C.

Sample	Ratios	$a_{wo}^{(cr)}$	$a_{wp}^{(cr)}$
Lactose	-	0.381±0.010 <sup>a</sup>	0.467±0.003
Lactose/WPI	7:3	0.547±0.018	0.643±0.001
Lactose/WPI	1:1	0.623±0.028	0.708±0.006
Lactose/WPI	3:7	0.773±0.013	0.857±0.001

<sup>a</sup>: Values are mean ± SD (n=3)

The DDI for pure lactose ( $a_w \leq 0.50$ ), WPI, and lactose/WPI mixtures with the mass ratios of 7:3 ( $a_w \leq 0.70$ ), 1:1 ( $a_w \leq 0.80$ ), and 3:7 followed the typical sigmoid shape of water sorption isotherms (type II) in Fig. (6.1B). The fractional water sorption of components, exhibited by amorphous sugar/protein mixtures, has been reported by previous studies (Roos and Potes, 2015). Similarly, the fractional water sorption properties were proved in DDIs as the sorbed water in amorphous lactose/WPI mixtures could be calculated as the sum of fractional quantities at  $a_w \leq 0.44$  (Fig. 6.1 B). However, if water sorption rates of components vary DDI data may reflect such differences. Fig. (6.2) gives the DDI water sorption and literature SSM data for freeze-dried lactose and lactose/WPI mixtures at 7:3, 1:1, and 3:7 mass ratios at 25 °C. The water contents in DDIs of lactose were lower than those of corresponding SSM isotherms (Fig. 6.2 A). Such differences in the DDI sorption data reflected the non-equilibrium state of amorphous solids and the relatively short equilibration time in comparison to SSM giving a systematic error for the water content as full dehydration may not take place at low  $a_w$ . The SSM-isotherms comparable  $c_w$  data are shown on the DDIs of lactose/WPI mixtures at various protein contents (Fig. 6.2 B-D). The DDI sorption data of pure amorphous WPI, however, showed shape-comparable sorption isotherms to corresponding SSM isotherms (Fig. 6.2 E). Such similarity in water sorption by the two methods indicated that the amorphous WPI showed a slow equilibration reducing time to water vapor diffusion and water penetration during DDI sorption. The DDI sorption data for amorphous lactose leveled off at high water activities ( $\geq 0.50$   $a_w$ ) as a result of lactose crystallization (Fig. 6.2 A). In lactose/WPI

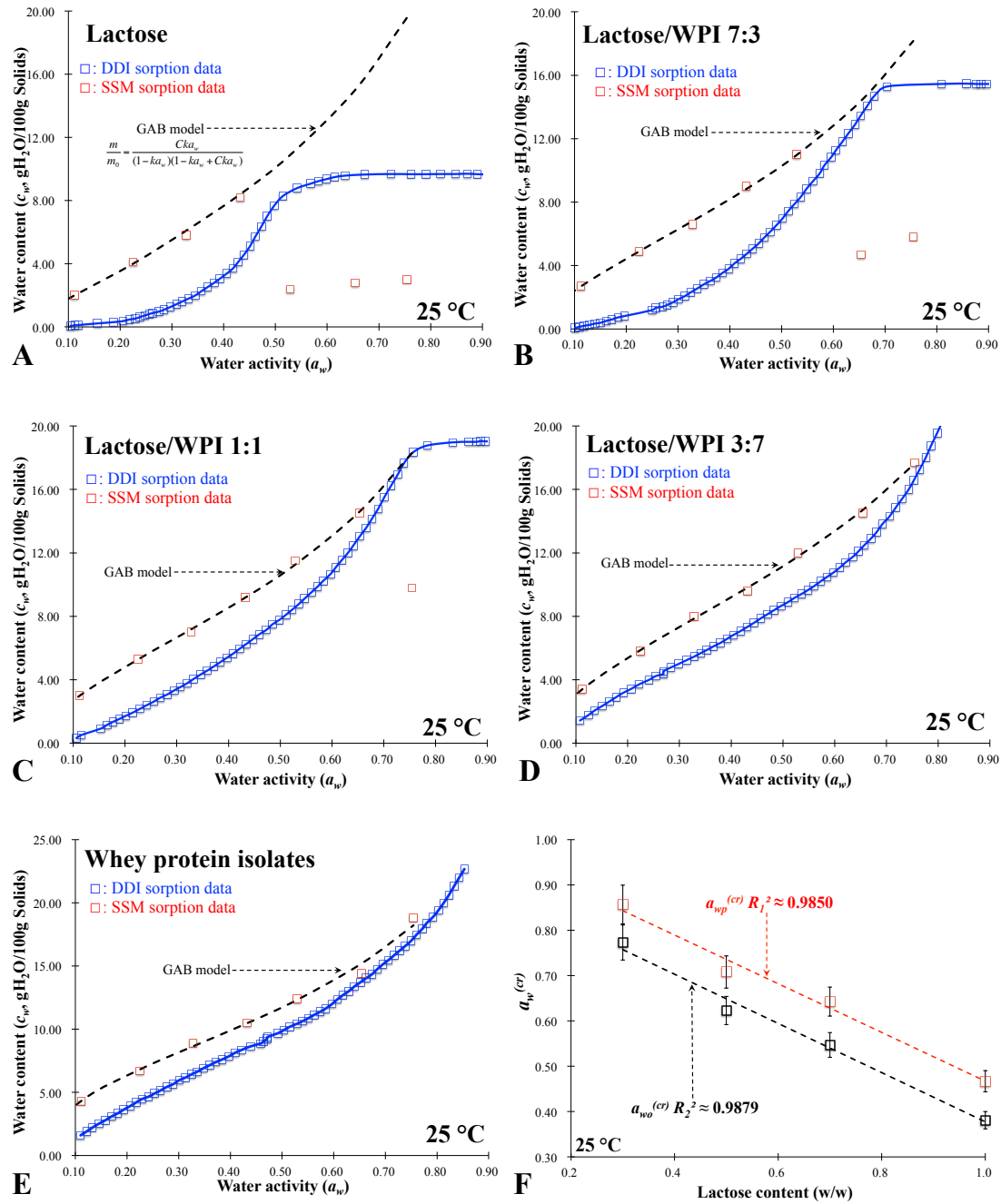


**Fig. 6.2.** The comparison diagram between DDI and literature SSM data of freeze-dried lactose and lactose/WPI mixtures (7:3, 1:1, and 3:7, w/w) at flow rates of 300 ml/min at 25 °C (A-E). The  $a_w^{(cr)}$  shows a highly linear relationship with lactose content ( $R^2 > 0.98$ ) in lactose/WPI mixtures (F). The literature SSM sorption data were derived from chapter II.

systems lactose molecules form a continuous phase around WPI molecules, but WPI components may hinder diffusion of the noncrystalline lactose. In comparison to pure lactose, therefore, the presence of WPI in lactose/WPI mixtures delayed crystallization and extended the sigmoid sorption behaviors to a higher  $a_w$  range (Fig. 6.2 B-C). This phenomenon agreed with previous studies, which indicated that the crystallization of lactose could be delayed by the presence of polymeric components (Silalai and Roos, 2011). As noted above, the presence of other components, e.g., protein, with amorphous sugars, affected water sorption as well as the crystallization as a result of water plasticization.

The  $a_w^{(cr)}$  values of amorphous lactose and lactose/WPI mixtures at each ratio are shown in Table (6.1). Fig. (6.2F) showed a linear relationship with high correlation coefficient ( $R^2 > 0.98$ ) for  $a_w^{(cr)}$  values against lactose content of amorphous lactose/WPI systems at 25 °C, which indicated that the  $a_w^{(cr)}$  was that of the lactose component rather than for the entire system although protein affected structural relaxation times (Roos and Potes, 2015). In the present study, the  $a_{wo}^{(cr)}$  was considered as a critical  $a_w$  point for glass-forming lactose plasticized by water to flow and accommodate increasing free volume and water uptake during DDI sorption process. The  $a_{wp}^{(cr)}$  was a turning point where the rate of water uptake became less than the rate of lactose crystallization. Corresponding to previous X-ray study (Jouppila et al., 1997), therefore, we assumed that the  $a_{wo}^{(cr)}$  and  $a_{wp}^{(cr)}$  were the onset and half-crystallinity point of lactose crystallization, respectively. In the present study, the  $a_{wo}^{(cr)}$  of pure amorphous lactose occurred at 0.381  $a_w$  at 25 °C (Table 6.1). This result agreed with previous calorimetric studies that the glass transition of freeze-dried lactose after humidification at 0.44  $a_w$  at room temperature was around 15 °C as well as the critical  $a_w$  of 0.37 of amorphous lactose (Jouppila and Roos, 1994). Both onset and peak  $a_w^{(cr)}$  values of lactose/WPI mixtures increased concomitantly with increasing protein content (Table 6.1). Fig. (6.3) gives a schematic diagram for the dynamic water sorption process of amorphous lactose and



lactose/WPI mixtures. From I to II (Fig. 6.3 A), the water sorbed by amorphous lactose could plasticize the structure of glass formers resulting in breaking the

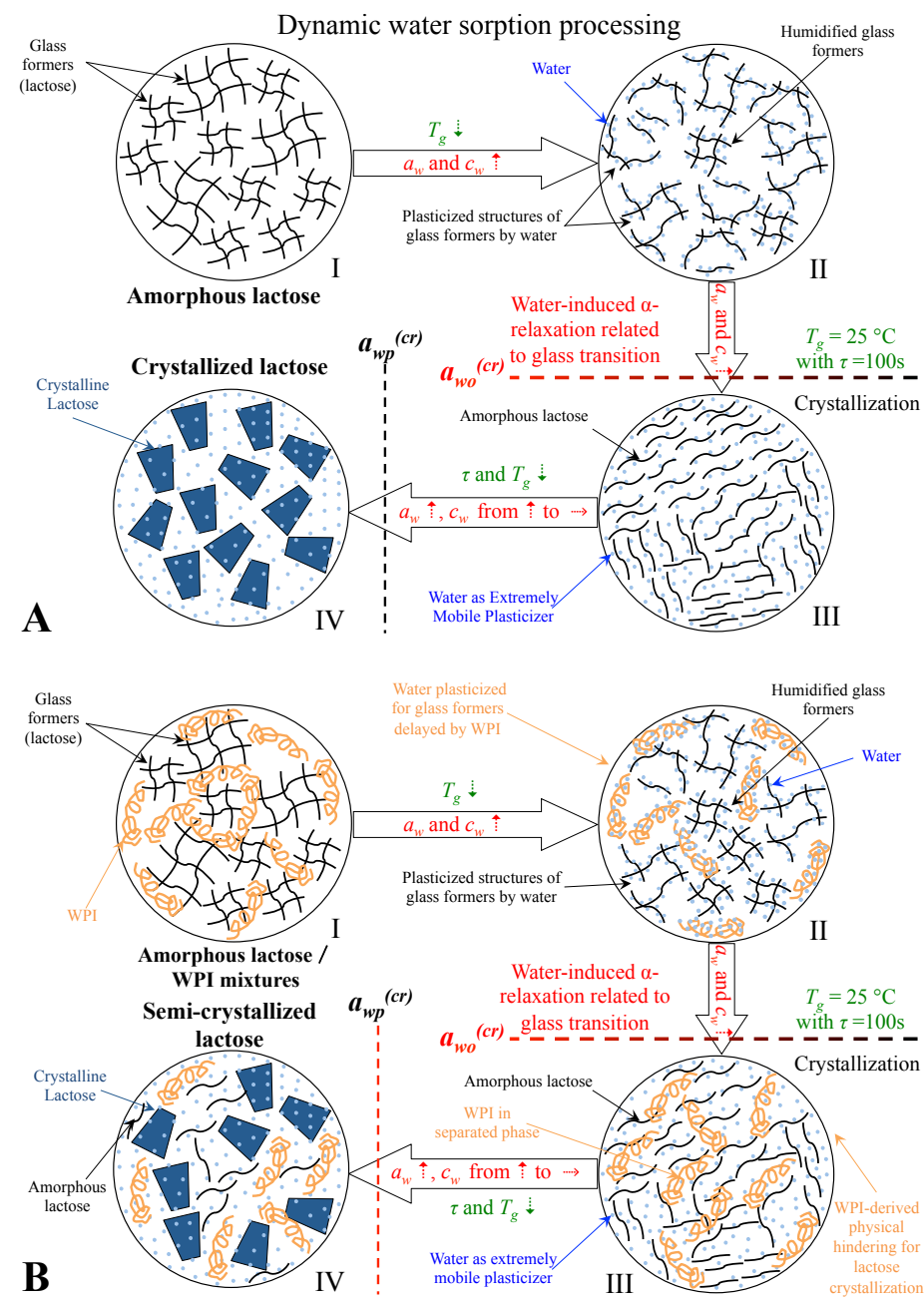


**Fig. 6.3.** Schematic diagrams for water-Induced  $\alpha$ -relaxation and crystallization on amorphous lactose (A) and lactose/WPI mixtures (B) in dynamic water sorption processes, respectively. The symbols do not represent the real size and quantity of components.

hydrogen bonds between lactose molecules and the relaxation times of amorphous lactose decreased (Slade et al., 1991). As  $a_w$  increased to above  $a_{wo}^{(cr)}$ , the mobilization of glass formers was strongly enhanced by water plasticization (Fig. 6.3 A II-III). When the  $a_w$  exceeded  $a_{wp}^{(cr)}$ , the lactose crystallinity rapidly increased until most of lactose crystallized during the DDI sorption process (Fig. 6.3 A III-IV). However, the presence of WPI hindered water plasticization effects as the  $a_{wo}^{(cr)}$  increased in lactose/WPI mixtures (Fig. 6.3 B II-III). Moreover, the  $a_{wp}^{(cr)}$  of lactose/WPI mixtures increased concomitantly with the WPI content and delayed the lactose crystallization in mixtures (Fig. 6.3 B III-IV). Therefore, the  $a_w^{(cr)}$  values of the DDI data indicate the glass transition resulting in mobilization and crystallization of amorphous lactose in food and pharmaceutical materials.

### 6.3.2. DIELECTRIC PROPERTIES AND $T_\alpha$

Fig. (6.4) shows the dielectric loss ( $\epsilon''$  peaks at a frequency of 1.0 kHz) for lactose and lactose/WPI mixtures with mass ratios of 7:3, 1:1, and 3:7 after storage below 0.44  $a_w$  at 25 °C. Dielectric properties of the materials were affected by molecular interactions and water plasticization. The magnitude of the  $\epsilon''$  peak correlated directly to  $a_w$  of amorphous lactose at low water activities ( $0.23 \leq a_w \leq 0.44$ ) as water content increased and plasticization enhanced the mobility of lactose molecules. This agreed with Silalai and Roos (2011) who reported that  $\epsilon''$  peaks found for skim milk powder increased in magnitude with increasing  $a_w$  (Fig. 6.4 A). The  $\epsilon''$  describes an energy loss that is used by polar groups in materials under the alternating electric field. The lower levels of WPI containing lactose/WPI mixtures ( $\leq 30$  %) showed higher magnitudes of  $\epsilon''$  peaks than pure lactose after humidification at the same  $a_w$  and 25 °C (Fig. 6.4 B-D). Therefore, the  $\epsilon''$  data followed the amorphous lactose content of the mixtures as WPI and lactose exist in separate phases. Table (6.2) gives the  $T_\alpha$  value of each material in dielectric analysis at 1.0 kHz, which occurred above the corresponding calorimetric onset  $T_g$  measured by differential scanning calorimeter

(DSC) in agreement with Silalai and Roos (2011). The presence of water, in the present study, decreased the  $T_\alpha$  values of amorphous lactose and lactose/WPI mixtures

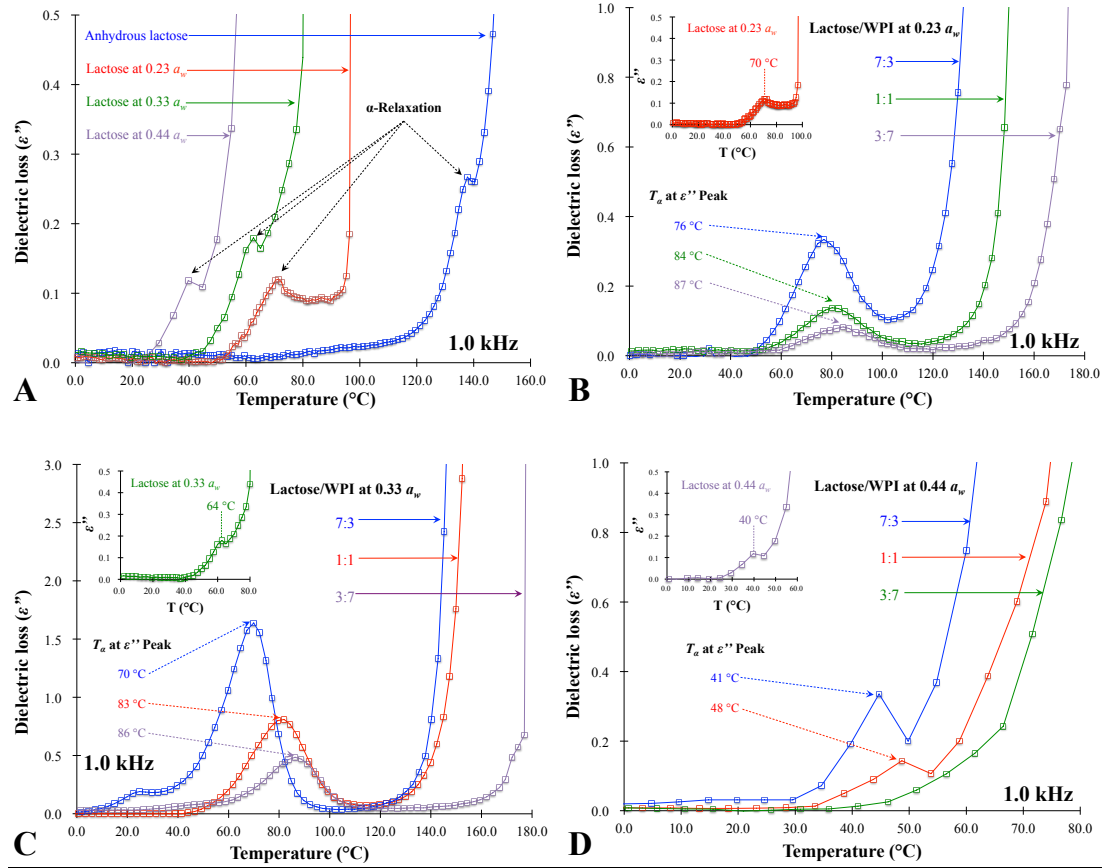


**Fig. 6.4.** The DEA spectra and peak temperature of  $\epsilon''$  as  $T_\alpha$  of amorphous lactose (A) and lactose/WPI mixtures with 7:3, 1:1, and 3:7 mass ratios after storage at 0.23  $a_w$  (B), 0.33  $a_w$  (C), and 0.44  $a_w$  (D) under 25 °C.

as the peak temperature of  $\epsilon''$  concomitantly decreased with increasing  $a_w$  (Table 6.2). The  $T_\alpha$  values of amorphous lactose could be significantly increased by WPI in lactose/WPI mixtures (Table 6.2). Lactose can be assumed to exist separated from protein. The frequency-dependent  $T_\alpha$  indicated an apparent relaxation time of lactose in WPI mixtures. Water plasticization enhanced the molecular mobility of lactose molecules which consequently decreased the peak temperature of  $\epsilon''$ . However, the WPI contained in mixtures hindered the molecular mobility of lactose and increased the apparent relaxation times and  $T_\alpha$ . In our previous studies, similarly, the presence

of other components, i.e., water and protein, affected the structural relaxations, relaxation times and  $T_\alpha$  of glass-forming sugars in freeze-dried sugars/protein systems based on dynamic-mechanical analysis (DMA).

### 6.3.3. RELAXATION TIMES AND S PARAMETER

Both DEA and DMA measurements allowed determination of structural relaxation times from the  $\alpha$ -relaxation data at various frequencies. The structural relaxation times can be related to stickiness characteristics of food powders as well as other mechanical properties of food solids, such as the collapse of structure or viscosity and diffusion (Clerjon et al., 2003). Fig. (6.5) shows structural relaxation times from our experiments and literature. The WLF-relationship of Williams and Others (1955) was developed on the basis that most inorganic and organic glass formers showed similar decreases in  $\tau$  and viscosity over the temperature range of  $T_g$  to  $T_g+100K$ . The use of WLF-relationships often assumes that the structural relaxation time obtained using dielectric measurements reach 100 s at the calorimetric onset  $T_g$  (Angell, 2002; Roos et al., 2015). In the present study, the WLF-relationship with “universal” constants ( $-C_1 = -17.44$  and  $C_2 = 51.6$ ) did not fit the experimental data but material-specific constants gave a good fitting performance for lactose and lactose/WPI mixtures at  $a_w$  below 0.44 and 25 °C (Fig. 6.5). Table (6.2) gives material-specific WLF constants for amorphous lactose and lactose/WPI mixtures obtained from structural relaxation times of the DEA and published DMA measurements. The material-specific  $C_1$  for amorphous lactose increased concomitantly with  $a_w$  increasing, whereas both  $C_1$  and  $C_2$  decreased by the presence of WPI content at  $a_w$  below 0.44 (Table 6.2). It is important to note that fitting of the WLF model to experimental relaxation times may result in positive or negative values for the constants  $C_1$  and  $C_2$  (Roos and Drusch, 2015). In the present study, the  $C_1$  and  $C_2$  with negative values determined the downward concavity for WLF relationship, which showed the profiles for the decreases of relaxation times of amorphous lactose at temperatures above calorimetric  $T_g$ . Therefore, the material-specific WLF constants could be used to

describe material properties and structural relaxation processes of amorphous lactose at various water activities. The presence of other components, e.g., water and protein, affected the structural overall relaxation processes as well as apparent relaxation times of lactose/WPI mixtures.

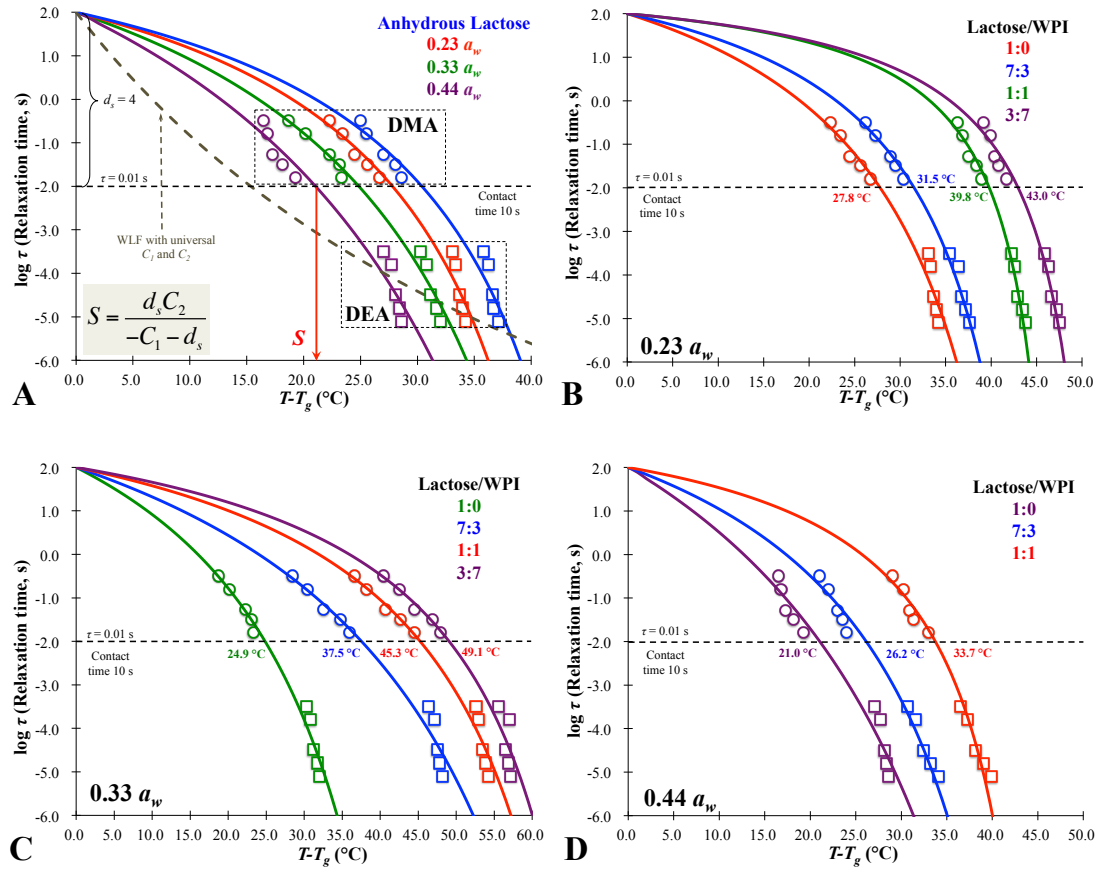


**Fig. 6.5.** Strength parameters ( $S$ ) of freeze-dried amorphous lactose at various water activities (0 ~ 0.44  $a_w$ ) (A), lactose/WPI mixtures at mass ratio of at 7:3, 1:1, and 3:7 at frequency of 1.0 kHz after storage at 0.23  $a_w$  (B), 0.33  $a_w$  (C) and 0.44  $a_w$  (D) at  $d_s = 4$  decreasing  $\tau$  as measured using DEA and literature DMA (Fan and Roos, 2016a) down to 0.01 s. Such decrease in  $\tau$  is known to result in particle stickiness and aggregation at a contact time of 10 s.

The decrease of relaxation times to  $10^{-2}$  s corresponded to a decrease in viscosity from  $10^{12}$  Pa s to  $10^5$  Pa s reaching critical viscosities for collapse and stickiness of amorphous food solids (Bellows and King, 1973; Downton et al., 1982). Roos and Others (2016) recommended a WLF model-based strength analysis for amorphous

sugars/protein systems. The  $S$  parameter for glass-forming components calculated by using material-specific WLF constants defined an allowable increase in temperature above the onset of the calorimetric  $T_g$  until  $\tau = 0.01$  s. As the lactose and protein diffusion was uncoupled the  $S$  parameter followed relaxation times of amorphous lactose. Table (6.2) gives the  $S$  values of amorphous lactose and lactose/WPI mixture at low  $a_w$  based on the strength analysis using experimental structural relaxation times derived from DEA and published DMA data. In the present study, the  $S$  values of

**Table 6.2.** The Literature Onset  $T_g$ ,  $T_\alpha$  at 1.0 kHz, Material-Specific  $C_1$  and  $C_2$ , and  $S$  for Freeze-Dried Lactose, Lactose/WPI Mixtures at Solid Ratios of 7:3, 1:1, and 3:7 After Storage at Low  $a_w$  ( $\leq 0.44$ ) at 25 °C.

Sample	$a_w$	$T_g$	$T_\alpha$	$-C_1$	$C_2$	$S$
Lactose	0.00	105±3 <sup>a</sup>	138±2	3.19±0.31	-54.63±0.63	30.4±0.7
	0.23	40±2	72±1 <sup>b</sup>	3.47±0.23	-51.93±0.42	27.8±1.0
	0.33	30±3	64±3	4.93±0.19	-55.48±0.56	24.9±0.8
	0.44	14±1	40±1	7.66±0.45	-61.36±0.66	21.0±1.6
Lactose/WPI 7:3	0.23	40±1	76±1	2.38±0.33	-50.31±0.64	31.5±0.9
	0.33	30±1	70±1	5.15±0.21	-85.88±0.50	37.5±1.0
	0.44	13±1	41±3	4.13±0.35	-53.15±0.52	26.2±1.3
Lactose/WPI 1:1	0.23	41±1	84±1	0.98±0.43	-49.55±0.41	39.8±0.5
	0.33	30±2	83±1	2.87±0.44	-77.72±0.76	45.3±0.5
	0.44	14±2	48±5	1.83±0.25	-49.18±0.63	33.7±0.4
Lactose/WPI 3:7	0.23	41±2	87±0	1.07±0.38	-54.47±0.66	43.0±0.7
	0.33	30±3	86±4	2.30±0.29	-77.28±0.73	49.1±0.5
	0.44	13±2	N/A	-	-	-

<sup>a</sup>: The onset  $T_g$  of lactose and lactose/WPI mixtures are derived from Chapter III; <sup>b</sup>: Values are mean ± SD (n=3);

freeze-dried lactose with different water activities agreed with our earlier data. The presence of water decreased the structural strength of amorphous lactose at  $a_w$  below 0.44, whereas the  $S$  values of lactose/WPI mixtures were significantly higher than was found for pure lactose (Table 6.2). As the  $S$  parameter provides a measure of structural transformation, a low  $S$  value referred to a more rapid structural change. Such rapid changes occurred in the presence of water as the structural relaxations of amorphous lactose were enhanced by water plasticization. However, the relatively higher  $S$  exhibited by lactose/WPI mixtures indicated that the mixes were

strengthened against structural deformation as protein offered a structural supporting effect. Therefore, the  $S$  parameters based on dielectric/mechanical relaxations can be used to describe compositional effects of amorphous food solids systems. Such data can be used to control shrinkage in dehydration and possibly rates of physicochemical changes in food storage.

#### 6.3.4. SORPTION-INDUCED CRYSTALLIZATION, RELAXATION TIMES AND $S$ PARAMETER

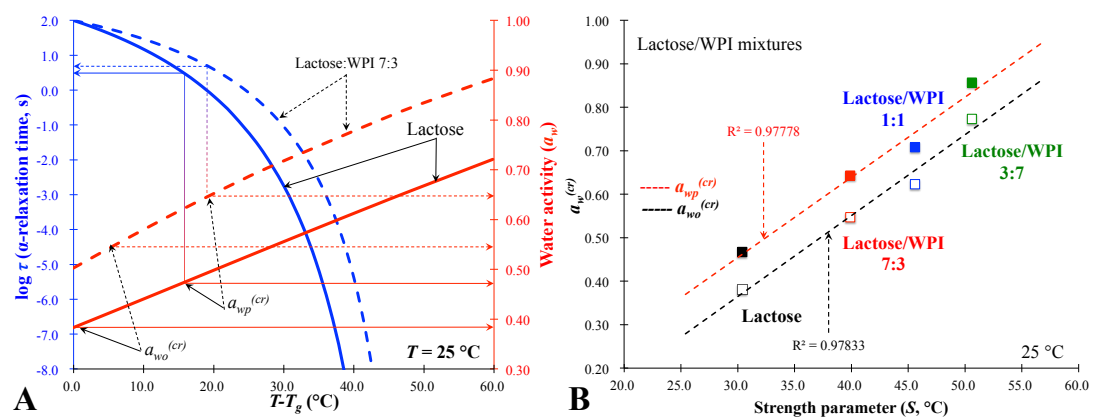


**Fig. 6.6.** The relationship between  $a_w$  and  $T - T_g$  of amorphous lactose and lactose/WPI mixture at 7:3 (w/w) with their corresponding relaxation times (A). B shows the relationship between strength parameter ( $S$ ) and  $a_w^{(cr)}$  for amorphous lactose and its WPI containing mixtures at 25 °C.

The relationships between  $a_w$  and  $T - T_g$  of amorphous lactose and lactose/WPI mixtures against their corresponding relaxation times are shown in Fig. (6.6 A). The water-induced structural relaxations of food solids systems, observed in isothermal water sorption, are likely to correlate with crystallization above glass transition. The relaxation times of lactose dramatically decreased with increasing  $T - T_g$  as the  $T_g$  was depressed by water (Fig. 6.6 A). The crystallization of lactose was initialized above  $a_{wo}^{(cr)}$  and rapidly occurred along decreasing structural relaxation times during water sorption process. The water sorption-induced lactose crystallization could stop at 0.7

$a_w$  based on the DDI sorption data, where the  $\tau$  decreased approximately 4 logarithmic decades (Fig. 6.6 A). As we expected, the  $a_{wo}^{(cr)}$  for water-induced crystallization was delayed to occur at higher  $a_w$  in the presence of WPI (Fig. 6.6 A). The decrease of structural relaxation times,  $a_{wp}^{(cr)}$  and crystallization of amorphous lactose can be controlled by WPI during exposures to high humidities (Fig. 6.6 A). Fig. (6.6B) shows a plot of onset and peak  $a_w^{(cr)}$  against  $S$  for anhydrous lactose and lactose/WPI mixtures. There was a linear relationship between  $a_w^{(cr)}$  and  $S$  with high correlation ( $R^2 > 0.97$ ). The pure lactose had a lower  $a_w^{(cr)}$  and  $S$  value than WPI containing systems (Fig. 6.6 B). This result indicated that the structural strength could be related to water-induced crystallization of amorphous sugars during isothermal water sorption. Therefore, we believe that the DDI provided parameters describe the structural changes and crystallization behavior of amorphous sugars during water plasticization. The  $S$  parameter could be used to estimate time-dependent water sorption-induced solid properties of amorphous food mixtures during storage at various water activities, i.e., structural transformations and deformation. Moreover, proteins as commonly used components could be used in food and pharmaceutical systems to control water sorption properties as well as structural relaxation rates and crystallization.

## 6.4. CONCLUSIONS

We have shown that the freeze-dried lactose and lactose/WPI mixtures have fractional water sorption properties. Water sorption-induced relaxations and crystallization were delayed in the presence of WPI in amorphous lactose/WPI mixtures. The  $T_\alpha$  values of amorphous lactose in lactose/WPI mixtures at  $a_w \leq 0.44$  were affected by the mixture composition, i.e., water, and WPI. The WLF analysis based  $S$  parameter with relaxation times data from DEA and DMA was dependent on mixture composition. It was used to interpret water sorption-induced crystallization of amorphous lactose in mixtures with WPI. The combination of dielectric and mechanical properties offers a new approach in understanding glass transition-related structural relaxations



occurring in food processing and storage. Such information also advances innovations in food formulation through mapping of structural relaxation times of food components and their mixes.

## *CHAPTER VII*

---

### GENERAL DISCUSSION

## 7.1. WATER SORPTION AND TIME-DEPENDENT PHENOMENONA OF FOOD SOLIDS SYSTEMS

### 7.1.1. WATER SORPTION ISOTHERMS AND FRACTIONAL SORPTION BEHAVIOUR

WATER SORPTION ISOTHERMS Water activity (or equilibrium  $RH$ ), storage temperature, and the contents of nonfat components in mixtures showed a significant impact on water sorption behaviour and sorption isotherms of amorphous food solids system based on SSM data. At each  $a_w$ , in Chapter II, the steady-state water contents of the materials were depressed by increasing storage temperature, as there was a decrease in  $RH$  with temperature, which was considered as potential  $a_w$  shift phenomena by previous studies (Greenspan, 1977; Labuza et al., 1985). The GAB sorption isotherm model was fitted to experimental data of pure lactose below 0.56  $a_w$  (25 °C and 35 °C) and 0.44  $a_w$  (45 °C) as lactose crystallization occurred at higher  $a_w$ . Systems with 7:3 ( $< 0.65 a_w$ ) and 1:1 of lactose/WPI ratios ( $< 0.76 a_w$ ) could use water sorption data over a wider  $a_w$  range in GAB sorption isotherms (Fig. 2.1). It should be noted that, however, the extrapolated sorption data of non-crystalline components, which were predicted by GAB based on water sorption data over a narrow water activity range ( $\leq 0.44 a_w$ ), could extensively exceed true sorbed water contents and cause significant errors. The GAB sorption isotherms also showed that the water sorbed by amorphous pure trehalose, lactose/trehalose, and trehalose/WPI mixtures (7:3, w/w) increased with increasing  $a_w$  up to 0.44  $a_w$ , and then leveled off at higher  $a_w$ , corresponding to the formation of a stable crystalline structure (Chapter V). In comparison to lactose, our studies found that the steady-state water contents of amorphous trehalose were slightly higher owing to amorphous trehalose which could crystallize with two hydrate water molecules ( $\sim 10 \text{ gH}_2\text{O}/100 \text{ g solids}$ ) at  $a_w \geq 0.56 a_w$  at 25 °C.

Our results showed that the presence of other components, e.g., protein, with

amorphous sugars, could affect water sorption behaviour in the present study. That was found in sorption isotherms based on DDI measurement. For example, the DDI data for pure lactose ( $a_w \leq 0.50$ ), WPI, and lactose/WPI mixtures with the mass ratios of 7:3 ( $a_w \leq 0.70$ ), 1:1 ( $a_w \leq 0.80$ ), and 3:7 respectively followed the typical sigmoid shape (type II) of water sorption isotherms according to Fig. (6.2) in Chapter VI. In comparison to pure lactose, the presence of WPI in lactose/WPI mixtures extended the sigmoid sorption behaviours to a higher  $a_w$  range, which agreed with SSM sorption data. It should be noted that the water contents in DDIs of lactose were lower than those of corresponding SSM isotherms due to the DDI sorption data. Those data reflected the non-equilibrium state of amorphous solids and the relatively short equilibration time in comparison to SSM giving a systematic error for the water content as full dehydration may not take place at low  $a_w$ . Moreover, the DDI sorption data of pure amorphous WPI showed shape-comparable sorption isotherms to corresponding SSM isotherms (Fig. 6.2). Such similarity in water sorption by the two methods indicated that the amorphous WPI showed a slow equilibration reducing time to water vapor diffusion during DDI sorption.

FRACTIONAL WATER SORPTION Our water sorption data derived from Chapter II showed that the sorbed water contents of binary sugar/protein systems were proportional to quantities sorbed by the system components over a wide temperature range (25 ~ 45 °C). That indicated that the sorbed water of amorphous lactose/WPI systems was the sum of fractional quantities. According to fractional water sorption, the data provided sorbed water content for non-crystalline lactose up to 0.76  $a_w$  (Fig. 2.1). This result agreed with previous studies, which showed the additivity of water sorption data of sucrose with PVP and PVP-VA systems (Shamblin and Zografi, 1999) and lactose/maltodextrin systems (Potes et al., 2012). We also found such fractional water sorption properties in DDI sorption data for amorphous lactose/WPI mixtures, which were not reported in the literature before. Similarly, the binary sugar system at all ratios sorbed similar quantity of water at  $a_w \leq 0.44$ , in accordance with individual sugars in agreement with fractional water sorption of binary lactose/trehalose systems

(Fig. 5.1 in Chapter V). In comparison between lactose and trehalose GAB isotherms, the predicted water sorption data of trehalose showed a more sigmoid sorption isotherm at  $a_w \geq 0.65$  than lactose due to its strong hydroscopic, flexible structural properties and high solubility in water reported by previous studies (Lammert et al., 1998; Gänzle et al., 2008). In addition, the fractional water sorption behavior was confirmed in ternary lactose/trehalose/WPI systems and its corresponding GAB isotherms showed a very similar sigmoid behavior as trehalose/WPI mixtures (Fig. 5.1). Compared to the previous reports of fractional water sorption behaviour in a binary solids system (Potes et al., 2012), the present study successfully applied such sorption behaviour in describing the carbohydrates containing multi-compositional systems according to Eq (7.1). However, it should be noted that fractional water sorption behavior could not be applied in non-homogeneous solid systems due to heterogeneity such as porosity affects the water sorption for the whole system.

$$W_t = n_1 W_1 + \dots + n_n W_n \quad (7.1)$$

Where,  $W_t$  is the total equilibrium water content in the system;  $n_1$  to  $n_n$  are the multiplier of each component in the system;  $W_1$  to  $W_n$  are the water content in each non-crystallized composition.

### 7.1.2. TIME-DEPENDENT CRYSTALLIZATION OF FOOD SOLIDS SYSTEMS

WATER SORPTION-INDUCED CRYSTALLIZATION Our study found that the presence of other components in amorphous sugar containing systems, i.e., water, sugars, and protein, could alter the crystallization behaviour of sugar molecules, and thus, affect the water sorption-induced time-dependent crystallization behavior of such systems. For example, sorbed water loss from freeze-dried lactose was most rapid at intermediate and high water activities ( $0.55 \sim 0.76 a_w$ ) based on Fig. (2.2) in Chapter II. The crystallization of lactose was delayed by the presence of trehalose as

the variation of sorbed water in lactose/trehalose systems at each ratio occurred more slowly than in pure lactose (Fig. 5.2). Since trehalose possessed a similar molecular size as lactose, the movement of both sugar molecules was disturbed in addition to steric factors, which delayed nucleation and crystal-growth (Lammert et al., 1997; Lopez-Diez and Bone, 2000; De Gusseme et al., 2003; Miao and Roos, 2005). Moreover, lactose crystallization was affected by protein and the loss of sorbed water decreased concomitantly with increasing WPI (Fig. 2.2). The decrease in water was less than in pure lactose which showed formation of a partially crystalline structure in lactose/WPI mixtures as reported by Silalai and Roos (2010). This result indicated that the presence of high-molecular-weight protein could delay the water-induced crystallization of low-molecular-weight lactose probably because of reduced arrangement of lactose molecules at crystal lattices. Lopez-Diez and Bone (2000) assumed that the presence of proteins might exhibit interactions with lactose and reduce lactose crystallization through hydrogen bonding. However, Chapter II and IV pointed out that the water contents in lactose/WPI systems showed composition independent water sorption characteristic, which could be related to the phase separation during water sorption testing (Silalai and Roos, 2010). Such phenomenon indicated that the water was individually hydrogen bonding to protein and lactose, thus, less hydrogen bonds might exist between protein and lactose in mixtures. Therefore, we assumed that the protein-derived crystallization inhibition effects caused by either physical blocking or steric hindrance, which could reduce molecular diffusion, instead of trapping lactose to protein by hydrogen bonding. The lactose molecules in lactose/WPI mixtures might need a long induction time as well as higher activation energy for nucleation to form a stable nuclei center or migrating to the surface of crystal in order to release the water molecules during crystal growth stage.

According to DDI data in Chapter VI, we introduced a critical water activity ( $a_w^{(cr)}$ ) for time-dependent crystallization of amorphous sugars, which were not reported in any previous literature. And, we found that the presence of other components, e.g., protein, with amorphous sugars, affected water sorption as well as  $a_w^{(cr)}$  of amorphous

lactose as a result of water plasticization. Corresponding to previous X-ray study (Jouppila et al., 1997), we assumed that the DDI sorption data-derived  $a_{wo}^{(cr)}$  and  $a_{wp}^{(cr)}$  were the onset and half-crystallinity point of lactose crystallization, respectively. Table (6.1) given that the  $a_{wo}^{(cr)}$  of pure amorphous lactose occurred at 0.381  $a_w$  at 25 °C, which agreed with previous calorimetric studies that the glass transition of freeze-dried lactose after humidification at 0.44  $a_w$  at room temperature was around 15 °C as well as the critical  $a_w$  of 0.37 of amorphous lactose. Fig. (6.3) showed that the water sorbed by amorphous lactose could plasticize the structure of glass formers resulting in breaking the hydrogen bonds between lactose molecules and the relaxation times of amorphous lactose decreased. Therefore, as  $a_w$  increased to above  $a_{wo}^{(cr)}$ , the mobilization of glass formers was strongly enhanced by water plasticization. When the  $a_w$  exceeded  $a_{wp}^{(cr)}$ , the lactose crystallinity rapidly increased until most of lactose crystallized during the DDI sorption process. Both onset and peak  $a_w^{(cr)}$  values of lactose/WPI mixtures increased concomitantly with increasing protein content due to the presence of WPI physicochemically hindered water plasticization effects and crystal growth stage and delayed the lactose crystallization in mixtures.

CRYSTALLIZATION KINETICS Although the high water activity could induce rapid molecular mobility and enhance diffusion rates of molecules, in the present study, we found that the increasing quantity of trehalose and WPI could disturb the water-induced crystallization kinetics of amorphous lactose. As we mentioned in Chapter II, the kinetics of lactose crystallization in mixtures could be derived from the rates of reduced sorbed water,  $k$ . The maximum extent of lactose crystallization between 0.65 and 0.76  $a_w$  over a range of temperatures agreed with the results of Jouppila and Others (1997). The inhibition of lactose crystallization by trehalose and proteins was evident from the  $k$  decrease with increasing quantity of trehalose or WPI (Fig. 5.3). Previous studies reported that amorphous trehalose could mainly crystallize as trehalose dihydrate due to its high solubility at 25 °C, which means a relatively low driving force for trehalose crystallization at high  $a_w$  (Lammert et al., 1997). As a low

solubility was reported for lactose at 25 °C (Gänzle et al., 2008), a relatively large driving force was present for lactose crystallization and lactose could crystallize into various anomeric crystalline forms at high  $a_w$ , i.e., anhydrate or monohydrate crystalline forms. Therefore, the inhibition of lactose crystallization in lactose/trehalose mixtures was explained by either the crystallization driving force of system lowered by highly soluble trehalose or the molecular movements of lactose or trehalose were disturbed by each other during crystallization in amorphous mixtures. According to Fig. (2.3), the  $k$  was significantly depressed by the increasing weight fraction of WPI in systems with  $k$  close to zero below 50 % and 70 % of WPI content at 0.65 and 0.76  $a_w$ , respectively. Even the storage temperature could significantly affect lactose crystallization; an increasing quantity of WPI could delay the rate of lactose crystallization. As we noted in Chapter I, the relationship between the rate of crystallization in amorphous materials and  $T-T_g$  was parabolic (or “bell-shape”) because, at temperatures close to the  $T_g$ , nucleation was fast, but crystal-growth was slow, and, at temperatures close to  $T_m$ , crystal growth was fast, but nucleation occurred slowly (Fig. 1.2). Therefore, the crystallization kinetics in sugars/WPI was dependent on the amorphous sugar content during crystallization and the presence of proteins could affect both nucleation and crystal growth stages in sugar crystallization via physical-blocking effects.

**THERMAL PROPERTIES** According to DSC measurements in Chapter IV, both calorimetric onset and peak  $T_{cr}$  values of amorphous lactose were a function of water content, and decreased with increasing water contents, showing similar behavior to  $T_g$  as noted above. The effects of water content were about the same for  $T_{cr}$  and  $T_g$  as indicated by a fairly constant values for  $T_{cr}-T_g$  of amorphous lactose, which agreed with Roos and Karel (1991a). For pure lactose, for example, the increase in water content caused about an equal decrease in  $T_g$  and  $T_{cr}$  and the average  $T_{cr}-T_g$  values of lactose were approximately 55 °C (Fig. 4.2 A). A lower  $T_{cr}$  at higher water activities confirmed an increased mobility of lactose molecules caused by water plasticization. The  $T_{cr}$  values in amorphous lactose/trehalose systems could be affected by the



quantity of each component as the presence of similar-molecular-size individual sugar could disturb the molecular movement of each other during crystallization. In Chapter V, we firstly plotted a state diagram of lactose/trehalose mixtures in Fig. (5.7). According to such state diagram, the  $T_g$  value of each lactose/trehalose mixture was very close to those of the individual sugars due to the similar water contents of individual sugars and sugars mixtures after storage at 0.33  $a_w$  at 25 °C. The molecules of lactose and trehalose in binary sugar systems need more energy to form stable nucleus and move onto lattice. That showed that the two sugar molecules disturbed each other during crystallization as noted above, and thus, the  $T_{cr}$  values increased in lactose/trehalose systems. To be specific, the  $T_{cr}$  values in lactose/trehalose system increased concomitantly with increasing trehalose content in lactose-dominating system (lactose < 50 %, w/w) and leveled off at lactose content around approximately 50 % (w/w). However, the  $T_{cr}$  values of mixtures rapidly decreased when trehalose became to dominating components in binary sugar systems. The heat released by pure lactose during crystallization ( $\Delta H_{cr}$ ) varied with water content, which could be found in Table (4.1) and Fig. (4.2B). The presence of WPI significantly increased the  $T_{cr}$  of amorphous lactose due to protein causing physical barrier effects (Fig. 4.2 B). The  $\Delta H_{cr}$  value of lactose in lactose/WPI (7:3, w/w) was lower than for pure lactose as lactose partly crystallized in protein-containing systems (Table 4.1). That was caused by physical barrier effects of protein might disturbing the crystallization of lactose. However, as crystallization in high protein containing lactose mixtures (1:1 and 3:7, w/w) was immediately followed by the melting endotherm, there was variation in the  $\Delta H_{cr}$  values obtained by peak integration because of the broad dynamic crystallization range and difficulty of setting the integration baseline.

CRYSTAL TYPES AND RECRYSTALLIZATION According to XRD patterns, our studies found that amorphous lactose could crystallize as  $\alpha$ -lactose monohydrate, anhydrous  $\beta$ -lactose and  $\alpha$ -/ $\beta$ -lactose mixture with molar ratios 5:3 and 4:1 after storage at 0.56  $a_w$  (Fig. 2.6). This result disagreed with previous studies (Drapier-Beche et al., 1997), which indicated that  $\alpha$ -lactose monohydrate was the

dominant crystalline form but anhydrous  $\beta$ -lactose and  $\alpha$ -/ $\beta$ -lactose mixtures at 5:3 and 4:1 were not present in freeze-dried lactose when stored at 0.56  $a_w$ . The X-ray diffraction peak intensities at specific  $2\theta$  for  $\alpha$ -lactose monohydrate, anhydrous  $\beta$ -lactose and  $\alpha$ -/ $\beta$ -lactose mixture at molar ratio of 5:3 in pure lactose and mixtures (7:3 and 1:1) increased from middle to end point of crystallization during sorption except the  $\alpha$ -/ $\beta$ -lactose with 4:1 molar ratio as well as  $\alpha$ -lactose monohydrate at 0.65 and 0.76  $a_w$  from 25 to 45 °C storage (Table 2.2). The highest leveling off intensities for all lactose crystalline forms was shown around 0.65  $a_w$  (25 °C and 35 °C) and 0.75  $a_w$  (45 °C) at final point of crystallization, respectively. Above results proved that the lactose partly crystallized after crystallization and the highest extent of crystallization occurred between 0.65 and 0.76  $a_w$  corresponding with previous statements (Jouppila et al., 1998). At intermediate and high water activities in our study, the peak intensity of anhydrous  $\beta$ -lactose decreased concomitantly with the increase of the  $\alpha$ -lactose monohydrate peaks for end point of crystallization at 240 h (Fig. 2.7). The results showed that recrystallization of lactose progressed above 0.65  $a_w$  at 25 °C and 35 °C. At the higher storage temperature, according to water sorption data, the low residual water was in the crystalline lactose and most likely in  $\alpha$ -lactose monohydrate crystals. Therefore, anhydrous  $\beta$ -lactose could sorb migrating water from crystallizing lactose and recrystallize to  $\alpha$ -lactose monohydrate during storage. The recrystallization of anhydrous  $\beta$ -lactose was rarely observed at high storage temperature using XRD. Simpson and Others (1982) reported that  $\alpha$ -lactose monohydrate might have a trend to convert to anhydrous mixtures (5:3 molar ratios) under low water conditions (water contents  $\leq$  6%, w/w) above room temperature. However, a much lower ambient temperature was needed to form crystals with molar ratios 4:1 from  $\alpha$ -lactose monohydrate in storage. In our study, anhydrous  $\alpha$ -/ $\beta$ -lactose crystals at the molar ratio of 5:3 increased from endpoint of crystallization to 240 h probably due to lactose migration from  $\alpha$ -lactose monohydrate, whereas the anhydrous  $\alpha$ -/ $\beta$ -lactose 4:1 remained constant after storage at 0.33  $a_w$  and 25 °C. The intensities of the various crystal forms increased in pure lactose concomitantly with increasing  $a_w$  from 0.65  $a_w$  up to 0.75  $a_w$  at 25 °C and 35 °C. Corresponding to the rate of dehydration of sorbed

water at the respective temperature and  $a_w$ , the extent of lactose crystallization probably was affected by the presence and quantity of various crystalline forms during recrystallization, which could be governed by the mutarotation of lactose molecules to the anomeric form during crystal growth stage.

Chapter V indicated that the lactose and trehalose crystallized independently into their characteristic crystals in binary sugar mixtures at high  $a_w$  based on XRD patterns, which agreed with previous findings (Miao and Roos, 2005). Characteristic peaks for crystal hydrates ( $\alpha$ -lactose monohydrate and trehalose dihydrate) were respectively observed at 12.5°, 16.5°, 20.1° and 23.8°, whereas the characteristic peak was also observed for anhydrous  $\beta$ -lactose (10.6° and 21.0°) in amorphous sugar systems at 0.65 and 0.76  $a_w$ . The anhydrous forms of lactose crystals with  $\alpha$ - and  $\beta$ -lactose in molar ratios of 5:3 and 4:1 could be identified from the XRD patterns at diffraction angles of 19.2° and 19.7°, which occurred in our study in all samples of lactose and lactose/trehalose mixtures (Fig. 5.4). Trehalose dihydrate was also identified from the XRD patterns in lactose/trehalose mixtures at 0.65 and 0.76  $a_w$  (Fig. 5.4), which agreed with previous reports (Cardona et al., 1997; McGarvey et al., 2003). In Table 5.1, the high leveled-off water contents in lactose/trehalose mixtures based on water sorption testing resulted from trehalose dihydrate formation and incomplete crystallization retaining sorbed water in the amorphous phase. As we noted above, lactose crystallized as anhydrites and then recrystallized to monohydrate, which was governed by the mutarotation of lactose molecules to the different anomeric form during crystal growth stage (Iglesias and Chirife, 1978). As trehalose could disturb the movement of lactose molecules in lactose/trehalose mixtures, the recrystallization from anhydrous lactose to monohydrates could also be depressed by the presence of trehalose. For example, the peak intensity values of anhydrous  $\beta$ -lactose and  $\alpha$ -/ $\beta$ -lactose with molar ratio 5:3 increased concomitantly with the quantity of trehalose increasing in lactose/trehalose mixtures after storage at 0.65 and 0.76  $a_w$  (Fig. 5.5). And the peak intensity values of trehalose dihydrate increased with increasing trehalose contents in binary sugar systems (Fig. 5.5). Trehalose dihydrate

crystals were detected in trehalose/WPI mixtures with 7:3 (0.65 and 0.76  $a_w$ ) and 1:1 solid ratios (0.76  $a_w$ ) at 25 °C by XRD analysis. Moreover, an obvious characteristic peak (17.8°) was identified from XRD patterns of the trehalose/WPI mixture with 7:3 (0.65 and 0.76  $a_w$ ) and 1:1 solid ratios (0.76  $a_w$ ) after storage at 25 °C (Fig. 5.4). Diffraction peaks in XRD patterns indicated more than one type of crystal; the characteristic peak (17.8°) could be possibly induced by trehalose dihydrate. Corresponding to water sorption testing, the water content in trehalose should reach approximately 10 % (gH<sub>2</sub>O/100g solids) if all amorphous phase crystallized as dihydrate crystals. However, the fractional water sorption indicated the fractional water sorbed by trehalose in WPI containing systems (7:3 and 1:1, w/w) was lower than the 10 % (gH<sub>2</sub>O/100g solids), which implied that trehalose partly crystallized in trehalose/WPI systems after storage at 25 °C. Corresponding to XRD studies, therefore, the anhydrous trehalose was possibly formed during crystallization in the presence of WPI after storage at high  $a_w$ . Lower intensity peak values of trehalose dihydrate were identified in the presence of WPI in high  $a_w$ , compared with pure trehalose (Fig. 5.4). The decreasing quantity of trehalose dihydrate in the presence of WPI could be explained by the protein causing physical blocking effects in trehalose/WPI systems, which delayed the time to crystallization of trehalose during storage at high  $a_w$  at 25 °C.

### **7.1.3. CRYSTALLIZATION-RELATED STRUCTURAL COLLAPSE IN AMORPHOUS LACTOSE CONTAINING SYSTEMS**

After 240 hours of storage, we noted that freeze-dried lactose and lactose/WPI at high water activities ( $a_w > 0.56$ ) had collapsed structures including mixtures at 7:3 ratios. For example, Fig. (7.1) showed the structural changes of lactose/WPI mixtures with different mass ratios after storage at 0.65  $a_w$  and 25 °C up to 240 h. As collapsed samples have a dense microstructure and reduced surface effects that could help the materials retain higher water contents, the collapse phenomenon of dehydrated materials occurred above  $T_g$  and before complete crystallization of amorphous

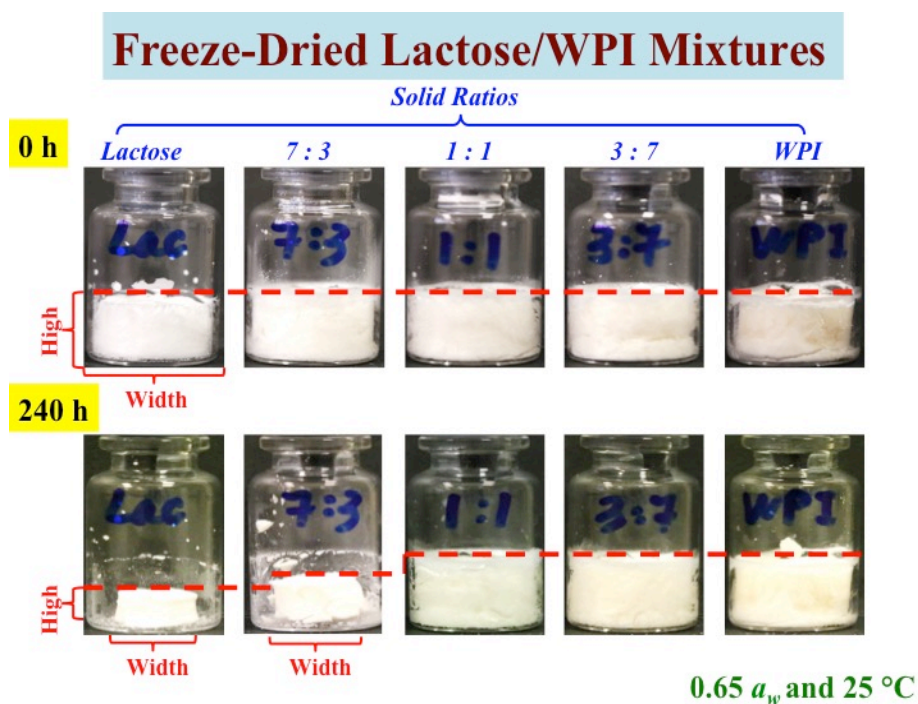


**Fig. 7.1.** Structural collapse of freeze-dried lactose, lactose/WPI mixtures with 7:3, 1:1, and 3:7 mass ratios, and pure WPI after storage at 0.65  $a_w$  and 25 °C up to 240 h.

compounds (Roos and Karel, 1991b). Theories of water activity as a mobility-controlling factor were complemented by information on the glass transition of amorphous food components at various levels of water plasticization (Slade et al., 1991; Roos and Drusch, 2015). Above the  $T_g$ , an increased free volume and molecular mobility leads to decreased viscosity, therefore, leading a change in physical structure of amorphous substances (Slade et al., 1991). And the depressed  $T_g$  of lactose in the presence of water could lead to rapid collapse of structure, stickiness and probably increased rates of deteriorative reaction in the plasticized rubbery state. For example, Roos and Karel (1991c) pointed out that the aroma retention during drying and storage of dried foods, i.e., infant formula, is closely related to collapse during drying and crystallization. Volatile losses are high above  $T_g$  corresponding critical water content. Hence, the control of temperature and water plasticization can be used to control release of volatiles. In the glassy state volatiles are encapsulated in the amorphous glass. Above  $T_g$ , collapse and sometimes crystallization takes place

releasing encapsulated volatiles. It should be noted that some volatiles might also decrease crystallization temperature of the amorphous matrix (To and Flink, 1978). The residual water content of the lactose/WPI systems was higher while the structural collapse phenomena were less than in pure lactose. That is because protein may have a high  $T_g$  and it could not only hinder the molecular mobility of lactose but also support the microstructure under high  $RH$ . Such effects may support surface nucleation but reduce diffusion during crystal growth. Our results showed that lactose crystallization in lactose/WPI systems was more affected by WPI components hindering lactose movement than their glass transition. Moreover, exceeding the  $T_g$  by increasing temperature or water content could increase diffusion coefficients, which possibly related to enhance loss of volatiles and increased reaction rates (Omatete and King, 1978; Simatos and Karel, 1988). This finding emphasized the importance of concentration, molecular size effects, molecular interactions, lattice interference or steric hindrance effects of the mixed components that disturbed solid properties, i.e., crystallization and structural collapse, and control the stability of food solids in processing and storage.

## **7.2. GLASS TRANSITION-RELATED STRUCTURAL RELAXATIONS OF FOOD SOLIDS SYSTEM**

### **7.2.1. EFFECTS OF WATER ON GLASS TRANSITION**

WATER PLASTICIZATION AND  $T_g$  Chapter III showed that the calorimetric  $T_g$  values of lactose and lactose containing systems showed typical endo-thermal step change in heat flow based on DSC thermograms after storage at  $a_w \leq 0.44$ . According to DSC thermograms, we found that the onset  $T_g$  values of lactose decreased from 105 °C (anhydrous state) to 14 °C (0.44  $a_w$ ) due to water plasticization which could significantly increase the mobility in amorphous lactose (Table 4.1). For the pure WPI, however, the  $T_g$  was not observed in DSC thermograms as the glass transitions of proteins are less obvious than those of amorphous small sugars (Zhou and Labuza,

2007; Roos and Potes, 2015). Since the GAB gave the water content in each non-crystalline component in sugar/protein systems according to fractional water sorption, the  $T_g$  values of pure amorphous lactose and trehalose could be obtained at intermediate and high water activities ( $\geq 0.56 a_w$ ) and the GT equation and sugar mixtures could be fitted to experimental data of amorphous sugar, successfully. It should be noted that the estimated  $T_g$  values of non-crystalline sugars were less than 0 °C at high water activities as the higher water contents exhibited a strong plasticization effect on amorphous sugars. As trehalose and lactose/trehalose mixtures sorbed the same quantity of water after storage at low water activities ( $\leq 0.44 a_w$ ), the  $T_g$  was close to the  $T_g$  of individual sugars (Table 5.1). However, protein only showed slight effects on the glass transition of amorphous sugars in WPI containing systems reflecting the slight variation of  $T_g$  values at each  $a_w$  studied at 25 °C. According to previous studies (Ibach and Kind, 2007), phase separation occurred in sugars/protein systems and therefore they had a composition-independent  $T_g$  with  $T_g$  values of systems being mostly dependent on amorphous sugars. Therefore, as noted above, the presence of protein had a minor effect on the calorimetric  $T_g$  of the sugar and sugar containing mixtures after storage at low  $a_w$  and 25 °C.

WATER MIGRATION After studying the onset of  $T_{g1}$  and  $T_{g2}$  values of the first and second heat scans of each crystal/lactose and lactose/WPI mixture, we firstly reported that the water molecules could migrate between crystalline and amorphous phase of lactose during storage at 0.33  $a_w$  and 25 °C (Table 3.2). As the water activities decreased concomitantly with the quantity of crystal phase increasing, for instance, the  $T_{g1}$  and  $T_{g2}$  values of semi-crystalline systems with a crystalline phase dispersed within the amorphous matrix were slightly higher than those we found for lactose at 0.33  $a_w$  at 25 °C (Fig. 3.3). However, no  $T_g$  variation was detected for pure lactose in DSC measurement (Table 3.2). The  $T_{g1}$  values were higher than  $T_{g2}$  in both  $\alpha$ - and  $\beta$ -type of lactose crystal/lactose systems at each mass ratio probably caused by either water migration or the glass state of lactose had relaxed during DSC heating measurement, while the  $T_{g2}$  showed almost the same values shown in Table (3.2).

Compared to  $\alpha$ -lactose monohydrate containing systems, there was a greater variation of  $T_g$  found for  $\beta$ -type of lactose crystal/lactose systems at each mass ratio. This phenomenon implied that the presence of anhydrous  $\beta$ -lactose could enhance the extent of water migration across each component in systems probably due to its relatively large and rough crystal surface than  $\alpha$ -lactose monohydrate (Raghavan et al. 2000; Gänzle et al. 2008).

### 7.2.2. ENTHALPY RELAXATION ON LACTOSE CONTAINING SYSTEMS

The presence of different types of lactose crystals and protein could affect the enthalpy relaxation of amorphous lactose containing system through disturbing the local molecular movement of amorphous lactose, as a result of water migrating and physical blocking effects, respectively. As the  $\Delta C_p$  of high-water foods is largely due to water (Roos and Drusch, 2015), the  $\Delta C_p$  values of pure amorphous lactose increased concomitantly with water content according to Fig (3.3) in Chapter III. Since the  $\Delta H$  and  $\Delta C_p$  were properties of the amorphous fraction, the  $\Delta H$  values of both  $\alpha$ - and  $\beta$ -types lactose crystal containing systems decreased concomitantly with crystal content increasing due to the migrating water enhanced vibrations and reorientation of amorphous lactose in mixtures after storage at 0.33  $a_w$  and 25 °C (Table 3.2). Compared with  $\alpha$ -lactose monohydrate, the smaller  $\Delta H$  values were found in  $\beta$ -type of lactose crystal/lactose systems caused by a greater extent of water migration. In co-freeze-dried lactose/WPI systems, however, the movement of amorphous lactose might be disturbed by the presence of protein reflecting on the  $\Delta H$  values increased corresponding to pure lactose at 0.33  $a_w$  at 25 °C. The  $\Delta C_p$  values of both  $\alpha$ - and  $\beta$ -types lactose crystal/lactose systems increased concomitantly with the content of crystals increasing. And the difference of  $\Delta C_p$  in  $\beta$ -type of lactose crystal/lactose was bigger than was found for  $\alpha$ -lactose monohydrates containing systems after equilibrium at 0.33  $a_w$  and 25 °C (Fig. 3.4). However, there was no significant variation of  $\Delta C_p$  measured for the first and second heating scans in lactose/WPI mixtures after storage at 0.33  $a_w$  and 25 °C. The variation of  $\Delta C_p$  implied



that the quantity of amorphous phase (Raine et al., 1945; Saunders et al., 2004) had changed in crystal/lactose systems and probably induced by either migration of water or lactose between crystal and amorphous phase in DSC heating. After equilibrium at 0.33  $a_w$  and 25 °C, the water in amorphous phase could migrate to crystalline phase and attach on the surface of crystals due to its lower water content. Those migrating water dissolved some lactose on crystalline surface in first heating scan and then increased the  $T_{g1}$  of mixtures corresponding to pure lactose. After second heating scan in DSC, however, the  $T_{g2}$  of mixtures decreased and the  $\Delta C_p$  values of mixtures increased which could be induced by of the variation in amorphous and crystalline phase contents. To be specific, the amorphous lactose as well as crystals might be produced by lactose dissolving water during cooling scan with cooling rate of 10 °C/min.

### 7.2.3 ALPHA-RELAXATION AND STRUCTURAL RELAXATION TIMES

DYNAMIC-MECHANICAL PROPERTIES AND  $\alpha$ -RELAXATION Typically, The frequency-dependent  $\alpha$ -relaxation of amorphous sugars in DMA measurements may vary for many reasons such as molecular interactions, degree of crystallinity, and the presence of other components affecting glass transition, e.g., water (Slade and Levine, 1991; Lopez-Diez and Bone, 2004), carbohydrates (Cruz et al., 2001; Potes et al., 2012), and proteins (Faivre et al., 1999; Regand and Goff, 2006). For example, the presence of other food components, such as water, sugar, phase separated components (different type of crystals and proteins), could alter the movement of amorphous lactose molecules, and thus, affect the  $\alpha$ -relaxations and viscous flow characteristics of amorphous sugars. The peak of loss modulus ( $E''$ ) flattened concomitantly with increasing protein contents in lactose/WPI systems at low  $a_w$  and 25 °C (Fig. 4.3). Such effects of protein on lactose retarded diffusion and the  $E''$  results reflected the amorphous lactose content of the mixtures, as the protein existed in separate phases apart from amorphous lactose. As the  $E''$  could be related to the amount of energy converted to heat during relaxations, in the present study, the  $E''$  peaks of amorphous

lactose decreased and broadened concomitantly with increasing water activities (Fig. 3.6). Hence, the  $E''$  of glass forming lactose, trehalose, and lactose/trehalose mixtures could be altered by the presence of water at low water activities ( $a_w \leq 0.44$ ) as the molecular mobility was enhanced by water plasticization as well as the retarded viscous flow characteristics of amorphous sugars. The  $E''$  of lactose/trehalose systems showed a peak at each ratio, whereas a weaker peak was found for pure trehalose at each  $a_w \leq 0.33$ , compared with each lactose containing sugar system (Fig. 5.8). It should be noted that the  $E''$  values of semi-crystalline lactose systems significantly decreased concomitantly with the  $\alpha$ -lactose monohydrate and anhydrous  $\beta$ -lactose content increasing after storage at 0.33  $a_w$  and 25 °C (Fig. 3.6). The water migration, therefore, could enhance viscous flow of lactose by the presence of crystals due to enhanced molecular movement of amorphous lactose. However, the peaks and broadness of  $E''$  for sugars/WPI mixtures were significantly changed concomitantly with the content of WPI increasing, compared with pure amorphous sugars lactose after storage at  $a_w \leq 0.44$   $a_w$  and 25 °C (Fig. 3.6 and 5.8). As expected, the  $E''$  results reflected the amorphous lactose content of the mixtures as the crystalline phase and WPI existed in separate phases apart from the amorphous lactose (Silalai and Roos, 2011b). The  $T_\alpha$  was determined from the peak temperature of  $E''$  in the DMA spectra (Talja and Roos, 2001; Silalai and Roos, 2011ab). Since the physical state of amorphous carbohydrate systems is strongly influenced by water, the  $T_\alpha$  of pure amorphous lactose and trehalose at lower water activities was increased concomitantly with decreasing water activity at a frequency of 0.5 Hz, which agreed with previous studies (Silalai and Roos, 2011; Renzetti et al., 2012). These changes in systems could be explained by the free volume theory (Royall et al., 2005; Meinders and van Vliet, 2009). As water increased the free volume in the system and molecular mobility of the amorphous components, the  $T_\alpha$  values of lactose/trehalose mixtures slightly changed compared to pure trehalose due to the mixtures sorbed similar quantity of water as each individual sugar after storage at each low  $a_w$  at 25 °C. However, the presence of WPI could increase the  $T_\alpha$  values of amorphous sugars/WPI mixtures, which was due to the protein causing physical blocking effects and reduced

the movement of amorphous sugars.

DIELECTRIC PROPERTIES AND  $\alpha$ -RELAXATION Besides DMA, the DEA measurement in Chapter VI also allowed determination of  $\alpha$ -relaxation and its corresponding temperature for amorphous food solids systems at various frequencies. Similarly to mechanical properties, the dielectric properties of the materials were affected by molecular interactions and water plasticization. For example, the magnitude of the  $\varepsilon''$  peak correlated directly to  $a_w$  of amorphous lactose at low water activities ( $0.23 \leq a_w \leq 0.44$ ) as water content increased and plasticization enhanced the mobility of lactose molecules. This agreed with Silalai and Roos (2011) who reported that  $\varepsilon''$  peaks found for skim milk powder increased in magnitude with increasing  $a_w$  (Fig. 6.4 A). The  $\varepsilon''$  describes an energy loss that is used by polar groups in materials under the alternating electric field. The lower levels of WPI containing lactose/WPI mixtures ( $\leq 30\%$ ) showed higher magnitudes of  $\varepsilon''$  peaks than pure lactose after humidification at the same  $a_w$  and 25 °C (Fig. 6.4). Conversely, the  $\varepsilon''$  data followed the amorphous lactose content of the mixtures as WPI and lactose exist in separate phases. The  $T_\alpha$  value of each material in dielectric analysis at 1.0 kHz occurred above the corresponding calorimetric onset  $T_g$  measured by DSC in agreement with Silalai and Roos (2011). The presence of water, in the present study, decreased the  $T_\alpha$  values of amorphous lactose and lactose/WPI mixtures as the peak temperature of  $\varepsilon''$  concomitantly decreased with increasing  $a_w$  (Table 6.2). The  $T_\alpha$  values of amorphous lactose could be significantly increased by WPI in lactose/WPI mixtures (Table 6.2). Lactose can be assumed to exist separated from protein. The frequency-dependent  $T_\alpha$  indicated an apparent relaxation time of lactose in WPI mixtures. Water plasticization enhanced the molecular mobility of lactose molecules which consequently decreased the peak temperature of  $\varepsilon''$ . However, the WPI contained in mixtures hindered the molecular mobility of lactose and increased the apparent relaxation times and  $T_\alpha$ . The presence of other components, i.e., water and protein, affected the structural relaxations, relaxation times and  $T_\alpha$  of glass forming sugars in freeze-dried sugars/protein systems based on DEA measurements.

## 7.3. STRUCTURAL RELAXATION CHARACTERISTICS OF FOOD SOLIDS SYSTEMS

### 7.3.1. WLF CONSTANTS

As noted in Chapter I, we confirmed that the WLF-relationship with “universal” constants ( $-C_1 = -17.44$  and  $C_2 = 51.6$ ) did not fit the experimental data but material-specific constants gave a good fitting performance for water containing amorphous sugar and sugar/WPI mixtures at  $a_w$  below 0.44. Also, we calculated the material-specific WLF constants for amorphous sugar and sugar/protein mixtures based on relaxation times of the DEA and DMA measurements. The material-specific  $C_1$  for amorphous lactose increased concomitantly with  $a_w$  increasing, whereas both

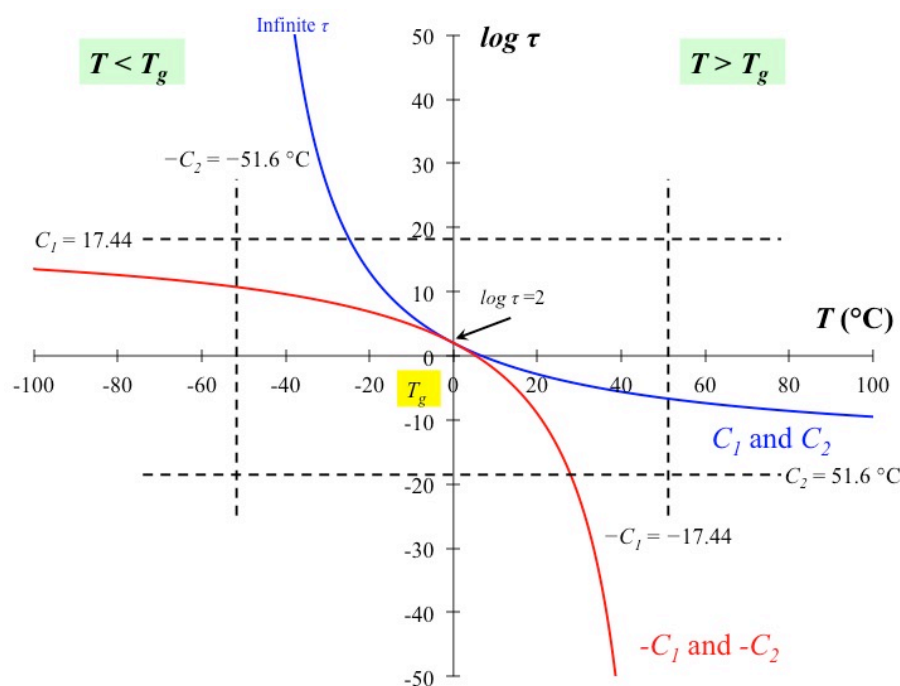


**Fig. 7.2** WLF plots with the universal constants based on Eq. (1.9) and the  $T_g$  as the reference temperature, where the blue line was draw with  $-C_1 = -17.44$  and  $C_2 = 51.6$  and red line was draw with  $C_1 = -17.44$  and  $C_2 = -51.6$ . The structural relaxation times ( $\tau$ ) at  $T_g$  are typically found at  $10^2$  s.

$C_1$  and  $C_2$  decreased by the presence of WPI content at  $a_w$  below 0.44. It is important to note that fitting of the WLF model to experimental relaxation times may result in positive or negative values for the constants  $C_1$  and  $C_2$  (Roos and Drusch, 2015). The  $C_1$  gives the maximum number of log decades for the change in  $\tau$  as anchored to  $T_g$  and  $C_2$  gives  $T$  for infinite  $\tau$  (Fig. 7.2). When the temperature is above  $T_g$ , the structural relaxation time rapidly dropped in several logarithmic decades. Also, the structural relaxation times are not defined at the temperature below  $T_g$  where infinitely long structural relaxation times are approached. Therefore, in the present study, we found that the  $C_1$  and  $C_2$  with negative values determined the downward concavity for WLF relationship, which showed the profiles for the decreases of relaxation times of amorphous lactose at temperatures above calorimetric  $T_g$ . Therefore, the material-specific WLF constants could be used to describe material properties and structural relaxation processes of amorphous lactose at various water activities. The presence of other components, e.g., water and protein, affected the structural overall relaxation processes as well as apparent relaxation times of sugar/protein mixtures.

### 7.3.2. WLF AND STRENGTH

When the storage temperature increases to above  $T_g$ , amorphous materials loose solid characteristics concomitantly with decreasing  $\tau$ , which is reflected on by decreasing viscosity and increasing flowability of the materials (Lillie and Gosline, 1990; Slade et al., 1991). Such loss of solid characteristics results in collapse of wall membranes in porous structures typical of dehydrated foods. As we noted in Chapter I, the  $S$  calculated from numerical values varying with composition ( $C_1$  and  $C_2$ ) in WLF equation could be used to describe solid characteristics, e.g., flow characteristics, of amorphous materials based on time and temperature dependent behavior in amorphous food solids. The strength combines the characterization of material state in

a system and serves as a relaxation times factor to show the critical temperature difference at which a sharp change in properties of the system occurs. Thus, this parameter is simple in use and it describes viscous flow characteristics of glass forming materials.

COMPOSITIONAL EFFECTS ON  $S$  Our study showed that the  $S$  of amorphous sugar containing mixtures could be altered by the presence of other food components such as water, other sugars, and protein. For example, the water could govern the structural strength or viscous flow characteristics of glass forming lactose as the  $S$  value decreased concomitantly with increasing water content (Fig. 3.7). Similarly, as the  $S$  parameter provides a measure of structural transformation, a low  $S$  value referred to a more rapid structural change. Such rapid changes occurred in the presence of water as the structural relaxations of amorphous lactose were enhanced by water plasticization. We found that water could govern the structural strength or viscous flow characteristics of glass forming trehalose. And the trehalose could affect the structural strength of glass forming sugar as the  $S$  value of lactose/trehalose mixtures slightly decreased concomitantly with the quantity of trehalose increasing at 0.33  $a_w$  (Fig. 5.9). That occurred as trehalose could disturb the molecular mobility of amorphous lactose. However, the relatively higher  $S$  exhibited by amorphous sugar/WPI mixtures indicated that the mixes were strengthened against structural deformation as the presence of polymeric components could improve the strength of amorphous sugar because proteins could become a physical barrier for the movement of sugar molecules in system with a contribution to overall strength.

STRENGTH ON SEMI-CRYSTALLINE LACTOSE According to Fig. (3.7), the presence of crystalline phase could affect the strength of semi-crystalline lactose after storage at 0.33  $a_w$  and 25 °C. For example, the  $S$  of  $\alpha$ -lactose monohydrate containing amorphous lactose mixtures showed a greater  $S$ , whereas  $\beta$ -type of lactose crystal/lactose system had a smaller  $S$  value corresponding to pure amorphous lactose. The anhydrous  $\beta$ -lactose might reduce the strength of semi-crystalline lactose and

enhance the flow characteristic of solids due to a high migrating water effects, whereas the  $\alpha$ -lactose monohydrate could keep the whole system strong reflecting on less dramatic structural changes above the glass transition. Moreover, we found that the strength was governed by the fraction of amorphous lactose in  $\alpha$ - and  $\beta$ -type of lactose crystal/lactose mixtures after storage at 0.33  $a_w$  and 25 °C. The strength of  $\beta$ -type of lactose crystal containing mixtures increased concomitantly with the increasing of amorphous lactose content. Therefore, the  $S$  parameter could be considered as an effective approach to quantify the solid characteristics of semi-crystalline sugars and could control processing as well as the quality and stability of crystal containing food and pharmaceutical products.

### 7.3.3 STRENGTH AND CRYSTALLIZATION

STRENGTH AT HIGH  $a_w$  As noted above, the presence of water could affect the structural strength of amorphous lactose containing systems due to increased molecular mobility of the glass former, which was reflected by decreasing  $S$  values. We built on an available non-linear model (Eq. 7.2) to interpret the relationship between  $S$  values and water contents in glass forming sugar and sugar mixtures at  $a_w \leq 0.44$  and achieved a very good fitting performance. As the predicted water contents of non-crystalline sugars at  $a_w \geq 0.56$  could be estimated by GAB model (Eq. 1.1) based on fractional water sorption behavior, the estimated  $S$  values could be calculated for non-crystalline sugar and sugar mixtures. As the water contents of non-crystalline lactose at whole  $a_w$  could be estimated by GAB model, in the present study, we found that the estimated  $S$  and corresponding water content could be calculated for non-crystalline lactose at 25 °C and high  $a_w$  based on Eq. (7.2). Since the predicted  $S$  of glass forming trehalose and lactose/trehalose mixtures decreased following the increases of water content as we noted above, above model (Eq. 7.2) could be considered and used to predict the structural strength of glass-forming sugars using when exposed to high  $a_w$ .

$$S = \frac{w_1 S_{d1} + k w_2 S_{d2}}{w_1 + w_2} \quad (7.2)$$

Where  $w_1$  and  $w_2$  respectively refer to the weight fraction of dry solid and water;  $k$  is a constant;  $S_1$  and  $S_2$  refer to structural strength for anhydrous solids (or solid mixtures) and strength value of pure water. It should be noted that the strength of water is very low and the  $S$  value of water is around 6 °C based on the viscosity data (Maidannyk et al., 2017).

CRYSTALLIZATION AND STRENGTH CONCEPT Crystallization during food storage often results from an exposure of amorphous sugars to high  $a_w$  condition due to the water plasticization depressed  $T_g$  and increased molecular mobility of noncrystalline sugar in systems (Roos and Karel, 1991; Biliaderis et al. 2002).  $S$  value estimates for amorphous trehalose and lactose/trehalose mixtures significantly decreased after storage at 0.65 and 0.76  $a_w$  and the occurring of crystallization was observed in water sorption testing. Furthermore, the  $S$  values of trehalose/WPI system increased with increasing protein quantity and reduced crystallization by protein was observed in our study. Therefore, we believed that the  $S$  concept could be applied to reduce or accelerate crystallization of glass forming sugars as well as for quality and stability control of food solids. The relationship between crystallization temperatures ( $T_{cr1}$  and  $T_{cr2}$ ) and strength of amorphous lactose was also shown on Fig. (4.5) with a high correlation coefficient. The crystallization temperature was decreased with the decreasing of  $S$  values and the low structural strength represented a rapid molecular mobility in amorphous lactose (Fig. 4.5). However, as the presence of other components, i.e., WPI, increased the  $S$  value of lactose/WPI systems, the lactose crystallization temperature was increased even high water content existed in systems. Therefore, the present study showed that WPI could play an important role in enhancing structural strength and preventing sugar crystallization. And the crystallization behavior of amorphous lactose could be controlled by structural strength in processing as well as to improve quality and stability of food and



pharmaceutical materials. According to DDI measurements, similarly, there was a linear relationship between  $a_w^{(cr)}$  and  $S$  with high correlation for lactose and lactose/WPI mixtures (Fig. 6.6). The pure lactose had a lower  $a_w^{(cr)}$  and  $S$  value than WPI containing systems. This result indicated that the structural strength could be related to water-induced crystallization of amorphous sugars during isothermal water sorption. Therefore, we believe the  $S$  could be used to estimate time-dependent water sorption-induced solid properties of amorphous food mixtures during storage at various water activities, i.e., structural transformations and crystallization. Moreover, proteins as commonly used components could be used to increase structural strength of food and pharmaceutical systems, and thus, control water sorption properties as well as structural relaxation rates and crystallization.

## 7.4 APPLICATIONS OF THE REASERCH OUTCOMES

### 7.4.1. FORMULATION AND DESIGN OF HONEY TO POWDER

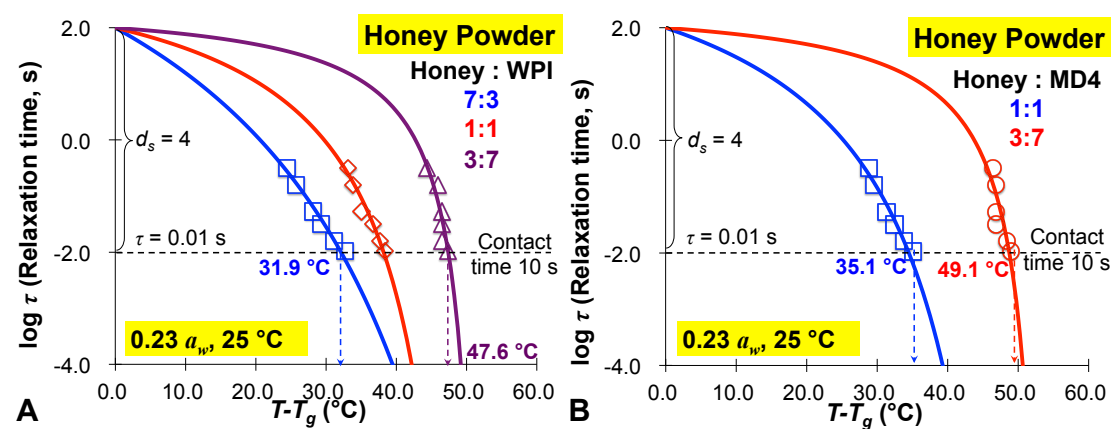


**Fig. 7.3.** Strength parameters ( $S$ ) of freeze-dried honey/WPI (7:3, 1:1, and 3:7 mass ratios) and honey/MD4 (1:1 and 3:7 mass ratios) powder after storage at 0.23  $a_w$  and 25 °C.

Honey is rich in sugars dominated by fructose and glucose that show easy to crystallize properties during storage. Due to the low  $T_g$  value and high viscosity of liquid honey, it is difficult to dry honey alone to powder without adding any of the drying aids. Formulation and design of honey powder structure for improved

dehydration properties, stabilization of active components, and controlled structure deterioration require materials science characterization of components and mixtures. Maltodextrin and whey proteins are common drying aid materials that were used in drying of honey to powder. Therefore, we applied the  $S$  concept for the use in studies of freeze-dried honey/MD4 and honey/WPI mixtures (different mass ratios) and their properties after storage at various water activities ( $0 \sim 0.76 a_w$ ) in room temperature ( $\sim 23^\circ\text{C}$ ) where a component or miscible components within powder structure may experience the glass transition. DSC, DMA, and SSM were used in mapping powder characterization based on  $T_g$ ,  $T_a$  and corresponding  $\tau$  of above two honey powder mixtures. As we noted above, the WLF relationship was used to model the  $\tau$  and  $T_a - T_g$  relationships of two honey powders, where its material-special constants  $C_1$  and  $C_2$  were used to define  $S$  value. Our unpublished results showed that the  $S$  values of two formulation of honey powder increased with by the presence of MD4 and WPI (Fig. 7.3). And the crystallization and structural collapse of honey powder occurred when  $a_w > 0.44$  but was delayed in the presence of MD4 and protein due to physicochemical interactions with inverted sugars in honey powder mixtures (Fig. 7.4). This unpublished results indicated that the  $S$  values could be use to give a quantitative measure to estimate compositional effects on  $\tau$  and the control of solids characterization in the stability in honey powder storage, such as crystallization and collapse. Also, this result is important in understanding glass transition approach to produce honey powder by simple freeze-drying method and using  $S$  concept approaches for assessing the stability of honey powder. Moreover, the  $S$  concept could also be applied to diversify honey products and finally could increase the added value of honey.

#### **7.4.2. POTENTIAL APPLICATIONS IN FOOD INDUSTRY**

Amorphous food solids, such as those of sugars and proteins, are common in the food and pharmaceutical industries. Thus, understanding the physical transition and physicochemical properties of glass forming food solids has a great importance in the

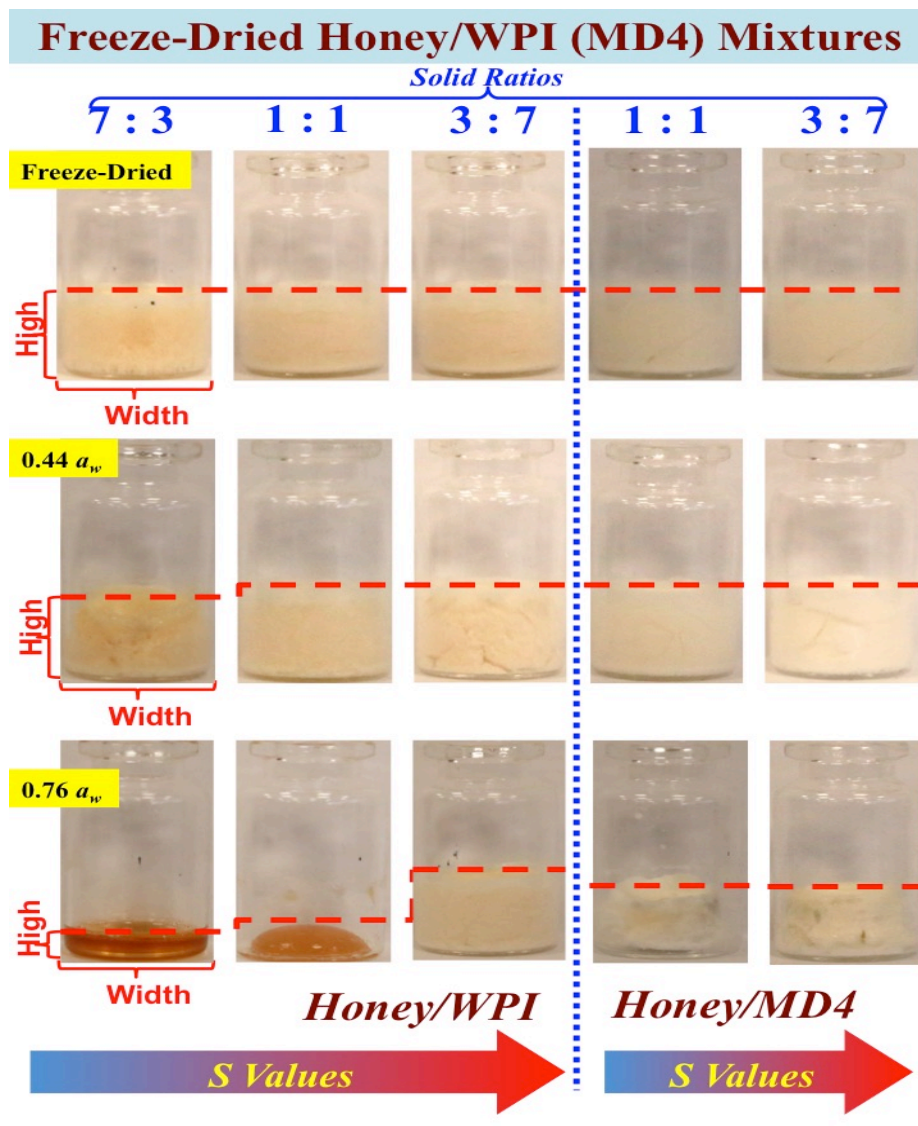


**Fig. 7.4.** Structural changes of freeze-dried honey/WPI and honey/MD4 mixtures after storage from 0 ~ 0.76  $a_w$  up to 240 h at room temperature. The collapse phenomenon in high honey containing mixtures was observed at water activity above 0.44  $a_w$ .

development of processing and shelf life control procedures for such ingredients and relevant products. Data on water sorption, time-dependent crystallization, calorimetric glass transition and crystallization temperatures, and mechanical/dielectric properties in the present study can be used to understand and predict structural changes during processing and storage of relevant foods. Relaxation times derived from  $\alpha$ -relaxation refer to the time factor corresponding to material response to a change in internal or

external thermodynamic conditions such as temperature and  $a_w$ , which can provide a new approach for the description of process-structure-function relationships to foods and food constituents. While the “fragility” concept developed by Angell (1991) may predict some properties of single glass-forming food components, our WLF-derived  $S$  concept was superior for the description of structure deterioration and solids characterization, and therefore, stability and industrial applicability of relevant foods and pharmaceutical materials. For example, the  $S$  value as a new food property can be used to formulate materials in order to improve material performance during drying and powder handling. Moreover, it also can be used to control and predict the physicochemical properties and performance of food solids during storage.

## 7.5. OVERALL CONCLUSIONS

The present thesis provides physicochemical information and reports investigations of water sorption behavior, crystallization, structural, thermal, and mechanical/dielectric changes, and flow characteristic of amorphous food solids system. The overall conclusions could be found as follows:

- (i) The presence of nonfat food components, e.g., trehalose and WPI could affect the water sorption behavior of amorphous lactose and the multi-compositional food solids systems show fractional water sorption properties at various storage temperature (25 °C, 35 °C, and 45 °C) based on both SSM and DDI measurements.
- (ii) The isotherm sorption data for non-crystalline sugars (lactose and trehalose) could be calculated up to 0.76  $a_w$  according to the fractional water sorption data derived from sugars/protein mixtures.
- (iii) The water-induced crystallization of freeze-dried lactose is initial at 0.381  $a_w$  and most rapid between 0.65  $a_w$  and 0.76  $a_w$ , whereas the calorimetric  $T_{cr}$ , rate of the loss of sorbed water (or crystallization kinetics) of lactose is increased

by the addition and increasing quantity of trehalose and WPI;

- (iv) The mechanism of protein inhibition of amorphous sugars (lactose and trehalose) crystallization kinetics involved steric factors, which delayed both nucleation and crystal-growth, and then, affected the number of species of crystalline forms and recrystallization of sugars based on XRD studies.
- (v) Amorphous sugars partly crystallized in sugar/protein systems after storage at high  $a_w$  due to the protein-derived physicochemical blocking effects.
- (vi) The recrystallization of amorphous lactose were observed in XRD patterns after storage above 0.65  $a_w$  at 25 °C and 35 °C as high storage temperature (45 °C) decreased the content of residual water in crystalline lactose.
- (vii) Structural collapse of amorphous lactose/trehalose was observed when storage  $a_w$  above 0.56 and 25 °C after 240 hours of storage but hindered by the presence of WPI.
- (viii) Water can significantly decrease the glass transition of amorphous sugars, while protein only showed slight effects on the calorimetric  $T_g$  of amorphous sugars as phase separation occurred in systems.
- (ix) The water molecules could migrate between crystalline and amorphous phase in semicrystalline systems during storage at 0.33  $a_w$  and 25 °C based on DSC data and anhydrous  $\beta$ -lactose could enhance the extent of water migration across each component in semicrystalline lactose.
- (x) Protein and different types of lactose crystals could affect the enthalpy relaxation of amorphous lactose containing systems after storage at 0.33  $a_w$  and 25 °C due to protein-derived physicochemical blocking effect and water migration.
- (xi) The degree of crystallinity and presence of other components (water, trehalose and WPI) could affect the dynamic-mechanical and dielectric properties of amorphous lactose based on DMA and DEA spectra, such as loss modulus, dielectric loss.
- (xii) The combination of mechanical and dielectric properties offers a new approach in understanding glass transition-related structural relaxations

occurring in food formulation and storage through mapping of structural relaxation times of food components and their mixes.

- (xiii) Relaxation times and  $T_\alpha-T_g$  of amorphous sugars and sugar containing solid systems derived from DMA and DEA measurements could be fitted using WLF relationship with materials-specific constants ( $C_1$  and  $C_2$ ).
- (xiv) The WLF-derived structural strength, using the information of the non-crystalline state of food materials in systematic manner, of amorphous sugar containing food solids systems is dominated by sugar and the presence of other food components (water, crystals, other sugars, and protein) could alter the strength of such systems.
- (xv) Structural strength provided an innovative approach to measure the compositional effects and control solids properties, i.e., crystallization and structural collapse, in food processing as well as for storage stability control of powdered food products in practical applicability, e.g., honey powder.

# *BIBLIOGRAPHY*

- Acevedo NC, Schebor C, Buera P (2008) Non-enzymatic browning kinetics analysed through water–solids interactions and water mobility in dehydrated potato. *Food Chemistry* 108(3): 900-06.
- Adam G, Gibbs JH (1965) On the temperature dependence of cooperative relaxation properties in glass-forming liquids. *Journal of Chemical Physics* 43(1): 139-46.
- Adhikari B, Howes T, Bhandari BR, Langrish TAG (2009) Effect of addition of proteins on the production of amorphous sucrose powder through spray drying. *Journal of Food Engineering* 94(2), 144-53.
- Aguilar CA, Hollender R, Ziegler GR (1994) Sensory Characteristics of Milk Chocolate with Lactose from Spray-Dried Milk Powder. *Journal of Food Science* 59(6): 1239-43.
- Aguilera JM, Chiralt A, Fito P (2003) Food dehydration and product structure. *Trends in Food Science & Technology* 14(10): 432-37.
- Al-Muhtaseb AH, McMinn WAM, Magee TRA (2002) Moisture sorption isotherm characteristics of food products: a review. *Food Bioprocessing Process* 80(2): 118-28.
- Anderson SL, Grulke EA, DeLassus PT, Smith PB, Kocher CW, Landes BG (1995) A model for antiplasticization in polystyrene. *Macromolecules* 28(8): 2944-54.
- Angell CA (1991) Relaxation in liquids, polymers and plastic crystals-strong/fragile patterns and problems. *Journal of Non-Crystalline Solids*, 131-33.
- Angell CA (1997) Why  $C_1 = 16-17$  in the WLF equation is physical-and the fragility of polymers. *Polymer* 38(26): 6261-66.
- Angell CA (2002) Liquid fragility and the glass transition in water and aqueous solutions. *Chemical Review* 102, 2627-50.
- Angell CA, Ngai KL, McKenna GB, McMillan PF, Martin SW (2000) Relaxation in glass forming liquids and amorphous solids. *Journal of Applied Physics* 88(6): 3113.
- Angell CA, Poole PH, Shao J (1994) Glass-forming liquids, anomalous liquids, and polyamorphism in liquids and biopolymers. *II Nuovo. Cimento. D* 16(8):



993-1025.

- Anglea SA, Wang J, Karel M (1993) Quality changes of eggplant due to drying regime. Presented at *Annual Meeting of International Food Technology Chicago* Pap: 192.
- Arvanitoyannis I, Blanshard J (1994) Rates of crystallization of dried lactose-sucrose mixtures. *Journal of Food Science* 59(1): 197-205.
- Avaltroni F, Bouquerand PE, Normand V (2004) Maltodextrin molecular weight distribution influence on the glass transition temperature and viscosity in aqueous solutions. *Carbohydrate Polymer* 58(3): 323-34.
- Babu NJ, Nangia A (2011) Solubility advantage of amorphous drugs and pharmaceutical cocrystals. *Crystal Growth & Design* 11(7): 2662-79.
- Baik MY, Kim KJ, Cheon KC, Ha YC, Kim WS (1997) Recrystallization kinetics and glass transition of rice starch gel system. *Journal of Agriculture and Food Chemistry* 45(11): 4242-48.
- Baird JA, Taylor LS (2012) Evaluation of amorphous solid dispersion properties using thermal analysis techniques. *Advanced Drug Delivery Reviews* 64(5): 396-421.
- Batzer H, Kreibich UT (1981) Influence of water on thermal transitions in natural polymers and synthetic polyamides. *Polymer Bullets* 5(11-12): 585-90.
- Bellows RJ, King CJ (1973) Product collapse during freeze drying of liquid foods. *AIChE Symposium Series* 132(69): 33-41.
- Beristain CI, Garcia HS, Azuara E (1996) Enthalpy-Entropy compensation in food vapor adsorption. *Journal of Food Engineering* 30, 405-15.
- Berlin E, Anderson BA, Pallansch MJ (1968) Water vapour sorption properties of various dried milks and whey. *Journal of Dairy Science* 51(9), 1339-44.
- Bhandari BR, Howes T (1999) Implication of glass transition for the drying and stability of dried foods. *Journal of Food Engineering* 40(1): 71-79.
- Biliaderis CG (1991) The structure and interactions of starch with food constituents. *Canadian Journal of Physiology and Pharmacology* 69(1): 60-78.
- Biliaderis CG, Lazaridou A, Mavropoulos A, Barbayiannis N (2002) Water

- plasticization effects on crystallization behavior of lactose in a co-lyophilized amorphous polysaccharide matrix and its relevance to the glass transition. *International Journal of Food Properties* 5(2): 463-82.
- Borde B, Bizot H, Vigier G, Buleon A (2002) Calorimetric analysis of the structural relaxation in partially hydrated amorphous polysaccharides I. Glass transition and fragility. *Carbohydrate Polymers* 48: 83-96.
- Buckton G, Darcy P (1995) The use of gravimetric studies to assess the degree of crystallinity of predominantly crystalline powders. *International Journal of Pharmaceutics* 123(2): 265-71.
- Buera MDP, Levi G, Karel M (1992) Glass transition in poly (vinylpyrrolidone): effect of molecular weight and diluents. *Biotechnology Progress* 8(2): 144-48.
- Buera P, Schebor C, Elizalde B (2005) Effects of carbohydrate crystallization on stability of dehydrated foods and ingredient formulations. *Journal of Food Engineering* 67(1): 157-65.
- Buma TJ, Wiegers GA (1967) X-ray powder patterns of lactose and unit cell dimensions of beta-lactose. *Netherlands Milk and Dairy* 21(3-4): 208.
- Burin L, Jouppila K, Roos YH, Kansikas J, Buera MP (2004) Retention of  $\beta$ -galactosidase activity as related to Maillard reaction, lactose crystallization, collapse and glass transition in low moisture whey systems. *International Dairy Journal* 14(6): 517-25.
- Cao N, Yang X, Fu Y (2009) Effects of various plasticizers on mechanical and water vapor barrier properties of gelatin films. *Food Hydrocolloids* 23(3): 729-35.
- Cardona S, Schebor C, Buera MP, Karel M, Chirife J (1997) Thermal stability of invertase in reduced-moisture amorphous matrices in relation to glassy state and trehalose crystallization. *Journal of Food Science*, 62(1): 105-12.
- Carullo A, Vallan A (2012) Measurement uncertainty issues in freeze-drying processes. *Measurement* 45(7): 1706-12.
- Champion D, Le Meste M, Simatos D (2000) Towards an improved understanding of glass transition and relaxations in foods: molecular mobility in the glass transition range. *Trend in Food Science and Technology* 11: 41-55.

- Chang YP, Karim AA, Seow CC (2006) Interactive plasticizing–antiplasticizing effects of water and glycerol on the tensile properties of tapioca starch films. *Food Hydrocolloids* 20(1): 1-8.
- Chernov AA (1984) *Modern Crystallography III: Crystal Growth*. Springer, Berlin.
- Chung HJ, Chang HI, Lim ST (2004) Physical aging of glassy normal and waxy rice starches: Effect of crystallinity on glass transition and enthalpy relaxation. *Carbohydrate Polymers* 58(2): 101-07.
- Chung HJ, Lee EN, Lim ST (2002) Comparison in glass transition and enthalpy relaxation between native and gelatinized rice starches. *Carbohydrate Polymers* 48, 287-98.
- Clark Z, Paterson AHJ, Joe R, Mcleod JS (2016). Amorphous lactose crystallisation kinetics. *International Dairy Journal* 56, 22-28.
- Clerjon S, Daudin JD, Damez JL (2003) Water activity and dielectric properties of gels in the frequency range 200 MHz–6 GHz. *Food Chemistry* 82(1): 87-97.
- Cocero AM, Kokini JL (1991) The study of the glass transition of glutenin using small amplitude oscillatory rheological measurements and differential scanning calorimetry. *Journal of Rheology* 35(2): 257-70.
- Cohen MH, Turnbull D (1959) Molecular transport in liquids and glasses. *Journal of Chemical Physics* 31(5): 1164-69.
- Crowe JH, Crowe LM, Jackson SA (1983) Preservation of structural and functional activity in lyophilized sarcoplasmic reticulum. *Archives of Biochemistry and Biophysics* 220(2): 477-84.
- Crowley KJ, Zografi G (2001) The use of thermal methods for predicting glass former fragility. *Thermochim Acta* 380(2): 79-93.
- Cruz IB, Oliveira JC, MacInnes WM (2001) Dynamic mechanical thermal analysis of aqueous sugar solutions containing fructose, glucose, sucrose, maltose and lactose. *International Journal of Food Science & Technology* 36(5): 539-50.
- Darcy P, Buckton G (1997) The influence of heating/drying on the crystallisation of amorphous lactose after structural collapse. *International Journal of Pharmaceutics* 158(2): 157-64.

- Das D, Langrish TAG (2012a) Activated-rate theory: Effect of protein inhibition and the temperature dependence of crystallization kinetics for lactose-protein mixtures. *Food Research International* 48(2): 367-73.
- Das D, Langrish TAG (2012b) An activated-state model for the prediction of solid-phase crystallization growth kinetics in dried lactose particles. *Journal of Food Engineering* 109(4): 691-700.
- Das D, Lin S, Sormoli ME, Langrish TAG (2013) The effects of WPI and Gum Arabic inhibition on the solid-phase crystallisation kinetics of lactose at different concentrations. *Food Research International* 54(1): 318-23.
- Davis KJ, Dove PM, De Yoreo JJ (2000) The role of  $Mg^{2+}$  as an impurity in calcite growth. *Science* 290(5494), 1134-37.
- De Gusseme A, Carpentier L, Willart JF, Descamps M (2003) Molecular mobility in supercooled trehalose. *The Journal of Physical Chemistry B*, 107(39): 10879-86.
- De Yoreo JJ, Vekilov P (2003) Principles of crystal nucleation and growth. Biom mineralization. Washington, DC: Mineralogical society of America.
- Debenedetti PG, Stillinger FH (2001) Supercooled liquids and the glass transition. *Nature* 410(6825): 259-67.
- Dilworth SE, Buckton G, Gaisford S, Ramos R (2004) Approaches to determine the enthalpy of crystallisation, and amorphous content, of lactose from isothermal calorimetric data. *International Journal of Pharmaceutics* 284(1): 83-94.
- Donth EJ (2013) *The glass transition: relaxation dynamics in liquids and disordered materials*. Springer Science & Business Media.
- Downton GE, Flores-Luna JL, King CJ (1982) Mechanism of stickiness in hygroscopic, amorphous powders. *Industrial & Engineering Chemistry Fundamentals* 21(4): 447-51.
- Drapier-Beche N, Fanni J, Parmentier M, Vilasi M (1997) Evaluation of Lactose Crystalline Forms by Nondestructive Analysis. *Journal of Dairy Science* 80(3): 457-63.
- Duckworth RB (1981) Solute mobility in relation to water content and water activity.

- In: Rockland, L.B., Stewart, G.F. (Eds.), *Water Activity: Influences on Food Quality*. Academic Press, New York, NY: 295-317.
- Elbein AD, Pan YT, Pastuszak I, Carroll D (2003) New insights on trehalose: a multifunctional molecule. *Glycobiology* 13(4): 17-27.
- Enrione JI, Díaz PC, Matiacevich SB, Hill SE (2012) Mechanical and structural stability of an extruded starch-protein-polyol food system. *Journal of Food Research* 1(2): 224.
- Eyring H (1936) Viscosity, plasticity, and diffusion as examples of absolute reaction rates. *Journal of Chemical Physics* 4(4): 283-91.
- Faivre A, Niquet G, Maglione M, Fornazero J, Jal JF, David L (1999) Dynamics of sorbitol and maltitol over a wide time-temperature range. *The European Physical Journal B* 10: 277-86.
- Fan F, Roos YH (2016) Structural relaxations of amorphous lactose and lactose-whey protein mixtures. *Journal of Food Engineering* 173: 106-15.
- Ferry JD (1980) *Viscoelastic properties of polymers*. John Wiley & Sons.
- Fitzpatrick JJ, Barry K, Cerqueira PSM, Iqbal T, O'Neill J, Roos YH (2007) Effect of composition and storage conditions on the flowability of dairy powders. *International Dairy Journal* 17(4): 383-92.
- Foster KD, Bronlund JE, Paterson AHJ (2006). Glass transition related cohesion of amorphous sugar powders. *Journal of Food Engineering* 77(4): 997–1006.
- Fox Jr. TG, Flory PJ (1950) Second-order transition temperatures and related properties of polystyrene. I. Influence of molecular weight. *Journal of Applied Physics* 21(6): 581-91.
- Frick B, Richter D (1995) The microscopic basis of the glass transition in polymers from neutron scattering studies. *Science* 267(5206): 1939.
- Gabarra P, Hartel RW (1998) Corn Syrup Solids and Their Saccharide Fractions Affect Crystallization of Amorphous Sucrose. *Journal of Food Science* 63(3): 523-28.
- Gänzle MG, Haase G, Jelen P (2008) Lactose: crystallization, hydrolysis and value-added derivatives. *International Dairy Journal* 18(7): 685-94.

- Garti N, Leser ME (2001) Emulsification Properties of Hydrocolloids. *Polymer of Advanced Technologies* 12(1-2), 123-35.
- Gibbs JH, DiMarzio EA (1958) Nature of the glass transition and the glassy state. *Journal of Chemistry* 28(3): 373-83.
- Gonnet JM, Guillet J, Sirakov I, Fulchiron R, Seytre G (2002) “In-situ” monitoring of the non-isothermal crystallization of polymers by dielectric spectroscopy. *Polymer Engineering & Science* 42(6): 1159-70.
- Gordon M, Taylor JS (1952) Ideal copolymers and the second-order transitions of synthetic rubbers. i. non-crystalline copolymers. *Journal of Applied Chemistry*, 2(9): 493-500.
- Gowen AA, Abu-Ghannam N, Frias J, Oliveira J (2008) Modelling dehydration and rehydration of cooked soybeans subjected to combined microwave-hot air-drying. *Innovative Food Science & Emerging Technologies* 9(1), 129-37.
- Green JL, Angell CA (1989) Phase relations and vitrification in saccharide-water solutions and the trehalose anomaly. *The Journal of Physical Chemistry* 93(8): 2880-82.
- Greenspan L (1977) Humidity fixed points of binary saturated aqueous solutions. *Journal of Research of the National Bureau of Standards* 81(1): 89-96.
- Hallett J (1963) The temperature dependence of the viscosity of supercooled water. *Proceeding of Physical Society* 82:1046-50.
- Hancock BC, Shamblin SL, Zografi G (1995) Molecular Mobility of Amorphous Pharmaceutical Solids Below Their Glass Transition Temperatures. *Pharmaceutical Research* 12(6): 799-806.
- Haque MK, Kawai K, Suzuki T (2006) Glass transition and enthalpy relaxation of amorphous lactose glass. *Carbohydrate Research*, 341(11): 1884-89.
- Haque MK, Roos YH (2005) Crystallization and X-ray diffraction of spray-dried and freeze-dried amorphous lactose. *Carbohydrate Research* 340(2): 293-301.
- Harris M, Peleg M (1996) Patterns of textural changes in brittle cellular cereal foods caused by moisture sorption. *Cereal Chemistry* 73(2): 225-31.
- Hartel RW (2001) *Crystallization in foods*. Aspen Publishers.

- Hartel RW, Shastry AV (1991) Sugar crystallization in food products. *Critical Review in Food Science and Nutrition* 30(1): 49-112.
- Hatley RH, Mant A (1993) Determination of the unfrozen water content of maximally freeze-concentrated carbohydrate solutions. *International Journal of Biological Macromolecules* 15(4): 227-32.
- Hodge IM (1996) Strong and fragile liquids-a brief critique. *Journal of Non-Crystalline Solids* 202: 164-72.
- Ibach A, Kind M (2007) Crystallization kinetics of amorphous lactose, whey-permeate and whey powders. *Carbohydrate Research* 342(10): 1357-65.
- Icoz DZ, Kokini JL (2008) State diagrams of food materials In: *Food Materials Science*. Springer New York.
- Iglesias HA, Chirife J (1978) Delayed crystallization of amorphous sucrose in humidified freeze dried model systems. *Journal of Food Technology* 13, 137-44.
- Imamura K, Nomura M, Tanaka K, Kataoka N, Oshitani J, Imanaka H, Nakanishi K (2010) Impacts of compression on crystallization behavior of freeze-dried amorphous sucrose. *Journal of Pharmaceutical Science* 99(3): 1452-63.
- Jagannath JH, Nanjappa C, Gupta DD, Arya SS (2001) Crystallization kinetics of precooked potato starch under different drying conditions (methods). *Food Chemistry* 75(3): 281-86.
- Jin DH, Zhang YZ, Suzuki Y, Naganuma T, Ogawa T, Hatakeyama E, Muramoto K (2000) Inhibitory Effect of Protein Hydrolysates on Calcium Carbonate Crystallization. *Journal of Agricultural and Food Chemistry* 48, 5450-54.
- Johari GP (1976) Glass transition and secondary relaxations in molecular liquids and crystals. *Annals of the New York Academy of Sciences* 279(1): 117-40.
- Jouppila K, Kansikas J, Roos YH (1997) Glass Transition, Water Plasticization, and Lactose Crystallization in Skim Milk Powder. *Journal of Dairy Science* 80, 3152-60.
- Jouppila K, Kansikas J, Roos YH (1998) Crystallization and X-ray Diffraction of Crystals Formed in Water-Plasticized Amorphous Lactose. *Biotechnology*

*Progress 14*, 347-50.

Jouppila K, Roos YH (1994a). Water Sorption and Time-Dependent Phenomena of Milk Powders. *Journal of Dairy Science* 77: 1798-808.

Jouppila K, Roos YH (1994b) Glass Transitions and Crystallization in Milk Powders. *Journal of Dairy Science* 77: 2907-15.

Jouppila K, Roos YH (1997) Water sorption isotherms of freeze-dried milk products- applicability of linear and non-linear regression analysis in modelling. *International Journal of Food Science and Technology* 32, 459-71.

Kagotani R, Kinugawa K, Nomura M, Imanaka H, Ishida N, Imamura K (2013) Improving the physical stability of freeze-dried amorphous sugar matrices by compression at several hundreds MPa. *Journal of Pharmaceutical Science* 102(7): 2187–97.

Kaletunc GONUL, Breslauer KJ (1993) Glass transitions of extrudates: relationship with processing-induced fragmentation and end-product attributes. *Cereal Chem*, 70: 548-48.

Kalichevsky MT, Blanshard JMV (1992) A study of the effect of water on the glass transition of 1: 1 mixtures of amylopectin, casein and gluten using DSC and DMTA. *Carbohydrate Polymers* 19(4): 271-78.

Karathanos V (1993) Collapse of structure during drying of celery. *Drying Technol* 11(5): 1005-23.

Karel M (1985) Effects of water activity and water content on mobility of food components, and their effects on phase transitions in food systems. *In Properties of water in foods* (pp. 153-69). Springer Netherlands.

Kasapis S (2012) Relation between the structure of matrices and their mechanical relaxation mechanisms during the glass transition of biomaterials: A review. *Food hydrocolloids* 26(2): 464-72.

Kashchiev D (1999) *Nucleation: Basic Theory with Applications*. Butterworths, Heinemann, Oxford.

Kawakami K, Miyoshi K, Tamura N, Yamaguchi T, Ida Y (2006) Crystallization of sucrose glass under ambient conditions: evaluation of crystallization rate and



- unusual melting behavior of resultant crystals. *Journal of Pharmaceutical Science* 95(6): 1354-63.
- Kedward CJ, MacNaughtan W, Mitchell JR (2000) Isothermal and non-isothermal crystallization in amorphous sucrose and lactose at low moisture contents. *Carbohydr Research*: 423-30.
- Kilburn D, Claude J, Mezzenga R, Dlubek G, Alam A, Ubbink J (2004) Water in glassy carbohydrates: opening it up at the nanolevel. *Journal of Physical Chemistry B* 108(33): 12436-41.
- Kim YJ, Hagiwara T, Kawai K, Suzuki T, Takai R (2003) Kinetic process of enthalpy relaxation of glassy starch and effect of physical aging upon its water vapor permeability property. *Carbohydrate Polymers* 53(3): 289-96.
- Kokini JL, Cocero AM, Madeka H, De Graaf E (1994) The development of state diagrams for cereal proteins. *Trends in Food Science & Technology* 5(9): 281-88.
- Kweon M, Slade L, Levine H (2009) Oxidative gelation of solvent-accessible arabinoxylans is the predominant consequence of extensive chlorination of soft wheat flour. *Cereal Chemistry* 86(4): 421-24.
- Labuza TP, Kaanane A, Chen JY (1985) Effect of Temperature on the Moisture Sorption Isotherms and Water Activity Shift of Two Dehydrated foods. *Journal of Food Science* 50: 385-91.
- Lai HM, Schmidt SJ (1990) Lactose crystallization in skim milk powder observed by hydrodynamic equilibria, scanning electron microscopy and <sup>2</sup>H nuclear magnetic resonance. *Journal of Food Science* 55(4): 994-99.
- Lammert AM, Schmidt SJ, Day GA (1998) Water activity and solubility of trehalose. *Food Chemistry* 61(1): 139-44.
- Lauritzen Jr, JI, Hoffman JD (1973) Extension of theory of growth of chain-folded polymer crystals to large undercoolings. *Journal of Applied Physics* 44(10): 4340-52.
- Le Meste M, Champion D, Roudaut G, Blond, G, Simatos D (2002) Glass transition and food technology: a critical appraisal. *J Food Sci* 67(7): 2444-58.

- LeBail A, Boillereaux L, Davenel A, Hayert M, Lucas T, Monteau JY (2003) Phase transition in foods: effect of pressure and methods to assess or control phase transition. *Innovative Food Science & Emerging Technologies* 4(1), 15-24.
- Lee AL, Wand AJ (2001) Microscopic origins of entropy, heat capacity and the glass transition in proteins. *Nature* 411(6836): 501-04.
- Levi G, Karel M (1995) Volumetric shrinkage (collapse) in freeze-dried carbohydrates above their glass transition temperature. *Food Research International* 28(2): 145-51.
- Levine H, Slade L (1989) A food polymer science approach to the practice of cryostabilization technology. *Comments on Agriculture and Food Chemistry* 1(6): 315-96.
- Li RJ, Roos YH, Miao S (2016) Physical and mechanical properties of lactose/WPI mixtures: effect of pre-crystallisation. *International Dairy Journal* 56, 55–63.
- Lievonen SM, Laaksonen TJ, Roos YH (1998) Glass transition and reaction rates: Nonenzymatic browning in glassy and liquid systems. *Journal of Agriculture and Food Chemistry* 46(7): 2778-84.
- Lievonen SM, Roos YH (2002) Water sorption of food models for studies of glass transition and reaction kinetics. *Journal of Food Science* 67, 1758-66.
- Lillie MA, Gosline JM (1990) The effects of hydration on the dynamic mechanical properties of elastin. *Biopolymers* 29(8-9): 1147-60.
- Liu YT, Bhandari B, Zhou WB (2006) Glass Transition and Enthalpy Relaxation of Amorphous Food Saccharides: A Review. *Journal of Agricultural and Food Chemistry* 54, 5701-17.
- Lloyd RJ, Chen XD, Hargreaves JB (1996) Glass transition and caking of spray-dried lactose. *International Journal of Food Science and Technology* 31, 305–11.
- Lodi A, Vodovotz Y (2008) Physical properties and water state changes during storage in soy bread with and without almond. *Food Chemistry* 110(3): 554-61.
- Lopez-Diez EC, Bone S (2000) An investigation of the water-binding properties of protein/sugar systems. *Physics in Medicine and Biology* 45, 3577-88.

- Luk E, Sandoval AJ, Cova A, Müller AJ (2013) Anti-plasticization of cassava starch by complexing fatty acids. *Carbohydrate Polymers* 98(1): 659-64.
- Magoshi J, Becker MA, Han Z, Nakamura S (2002) Thermal properties of seed proteins. *Journal of Thermal Analysis Calorimetry* 70(3): 833-39.
- Magoshi J, Nakamura S, Murakami KI (1992) Structure and physical-properties of seed proteins.1. Glass-transition and crystallization of zein protein from corn. *Journal of Thermal Analysis Calorimetry* 45(11): 2043-48.
- Maidannyk VA, Nuhardi B, Roos YH (2017). Structural strength analysis of amorphous trehalose-maltodextrin systems. *Food Research International* 96: 121-31.
- Makower B, Dye WB (1956) Sugar crystallization, equilibrium moisture content and crystallization of amorphous sucrose and glucose. *Journal of Agricultural and Food Chemistry* 4(1): 72-77.
- Mazzobre MF, Soto G, Aguilera JM, Buera MP (2001) Crystallization kinetics of lactose in sytems co-lyofilized with trehalose. Analysis by differential scanning calorimetry. *Food Research International* 34(10): 903-11.
- Mazzobre, M. F., Soto, G., Aguilera, J. M., & Buera, M. P. (2001). Crystallization kinetics of lactose in sytems co-lyofilized with trehalose. Analysis by differential scanning calorimetry. *Food Research International* 34(10): 903-11.
- McGarvey OS, Kett VL, Craig DQM (2003) An investigation into the crystallization of  $\alpha$ ,  $\alpha$ -trehalose from the amorphous state. *Journal of Physical Chemistry* 107, 6614–20.
- Meinders MB, van Vliet T (2009) Modeling water sorption dynamics of cellular solid food systems using free volume theory. *Food Hydrocolloids* 23(8), 2234-42.
- Meister E, Gieseler H (2009) Freeze-dry microscopy of protein/sugar mixtures: Drying behavior, interpretation of collapse temperatures and a comparison to corresponding glass transition data. *Jouranl of Pharmaceutical Science* 98(9): 3072-87.
- Miao S, Roos YH (2005) Crystallization kinetics and X-ray diffraction of crystals

- formed in amorphous lactose, trehalose, and lactose/trehalose mixtures. *Journal of Food Science* 70(5): 350-58.
- Michaels AS, Van Kreveland A (1966) Influences of additives on growth rates in lactose crystals. *Netherlands Milk and Dairy Journal* 20(3), 163.
- Miller DP, De Pablo JJ (2000) Calorimetric solution properties of simple saccharides and their significance for the stabilization of biological structure and function. *The Journal of Physical Chemistry B* 104(37): 8876-83.
- Moates GK, Noel TR, Parker R, Ring SG (2001) Dynamic mechanical and dielectric characterisation of amylose–glycerol films. *Carbohydrate Polymers* 44(3): 247-53.
- Mullin JW (2001) *Crystallization*. Oxford, UK Butterworth-Heinemann.
- Naoi S, Hatakeyama T, Hatakeyama H (2002) Phase transition of locust bean gum-, tara gum and guar gum-water systems. *Journal of Thermal Analysis Calorimetry* 70, 841.
- Nasirpour A, Landillon V, Cuq B, Scher J, Banon S, Desobry S (2007) Lactose crystallization delay in model infant foods made with lactose,  $\beta$ -lactoglobulin, and starch. *Journal of Dairy Science* 90(8), 3620-26.
- Nickerson TA (1979) Lactose chemistry. *Journal of Agricultural and Food Chemistry* 27(4): 672-77.
- Noel TR, Ring SG, Whittam MA (1993) Relaxations in supercooled carbohydrate liquids. In: Blanshard, J.M.V., Lillford, P.J. (Eds.), *The Glassy State in Foods*. Nottingham University Press, Loughborough, pp: 173-87.
- O'Loughlin IB, Murray BA, Brodkorb A, FitzGerald RJ, Robinson AA, Holton TA, Kelly PM (2013) Whey protein isolate polydispersity affects enzymatic hydrolysis outcomes. *Food Chemistry* 141(3): 2334-42.
- Oetjen GW, Haseley P (2004) *Freeze Drying Second edition*. Federal Republic of Germany: WILEY-VCH Verlag GmbH & Co. KGaA.
- Omatete OO, Kin CJ (1978) Volatiles retention during rehumidification of freeze-dried food models. *Journal of Food Technology* 13: 265.
- Omar AE, Roos YH (2007b) Glass transition and crystallization behaviour of

- freeze-dried lactose–salt mixtures. *LWT-Food Science and Technology* 40(3): 536-43.
- Omar EAM, Roos YH (2007a) Water sorption and time-dependent crystallization behaviour of freeze-dried lactose–salt mixtures. *LWT - Food Science and Technology* 40(3): 520-28.
- Ottenhof MA, MacNaughtan W, Farhat IA (2003) FTIR study of state and phase transitions of low moisture sucrose and lactose. *Carbohydrate Research* 338(21): 2195-202.
- Paes SS, Sun S, MacNaughtan W, Ibbett R, Ganster J, Foster TJ, Mitchell JR (2010) The glass transition and crystallization of ball milled cellulose. *Cellulose* 17(4), 693–709.
- Parks GS, Gilkey WA (1929) Studies on glass IV. Some viscosity data on liquid glucose and glucose-glycerol solutions. *Journal of Physicl Chemistry* 33:1428-37.
- Peng G, Chen X, Wu W, Jiang X (2007) Modelling of water sorption isotherm for corn starch. *Journal of Food Engineering* 80(2): 562-67.
- Perdomo J, Cova A, Sandoval AJ, García L, Laredo E, Müller AJ (2009) Glass transition temperatures and water sorption isotherms of cassava starch. *Carbohydrate Polymers* 76(2), 305-13.
- Perez J (1994) Theories of liquid-glass transition. *Journal of Food Engineering* 22: 89-114.
- Pittia P, Sacchetti G (2008) Antiplasticization effect of water in amorphous foods. A review. *Food Chemistry* 106(4): 1417-27.
- Potes N, Kerry JP, Roos YH (2012) Additivity of water sorption, alpha-relaxations and crystallization inhibition in lactose–maltodextrin systems. *Carbohydrate Polymers*, 89(4): 1050-59.
- Potes, N. 2014. Physico-chemical properties and component interactions in high solids food systems. PhD Thesis, University College Cork.
- Pouplin M, Redl A, Gontard N (1999) Glass transition of wheat gluten plasticized with water, glycerol, or sorbitol. *Journal of Agriculture and Food Chemistry*

47(2): 538-43.

- Price R, Young PM (2004) Visualization of the crystallization of lactose from the amorphous state. *Journal of Pharmaceutical Sciences* 93(1): 155-64.
- Raghavan SL, Ristic RI, Sheen DB, Sherwood JN, Trowbridge L, York P (2000) Morphology of Crystals of  $\alpha$ -Lactose Hydrate Grown from Aqueous Solution. *The Journal of Physical Chemistry B* 104(51): 12256-62.
- Raine HC, Richards RB, Ryder H (1945) The heat capacity, heat of solution, and crystallinity of polythene. *Transactions of the Faraday Society* 41: 56-64.
- Ratti C (2001) Hot air and freeze-drying of high-value foods a review. *Journal of Food Engineering* 49, 311-19.
- Regand A, Goff HD (2006) Ice recrystallization inhibition in ice cream as affected by ice structuring proteins from winter wheat grass. *Journal of Dairy Science* 89(1), 49-57.
- Renzetti S, Voogt JA, Oliver L, Meinders MJB (2012) Water migration mechanisms in amorphous powder material and related agglomeration propensity. *Journal of Food Engineering* 110(2): 160-68.
- Roos YH (1996) Glass transitions in low moisture and frozen foods: Effects on shelf life and quality. *Food Technology*, 95-108.
- Roos YH (2009) Solid and Liquid States of Lactose. In P. L. H. MacSweeney & P. F. Fox (Eds.), *Advanced Dairy Chemistry, vol. Lactose, Water, Salts and Minor Constituents* (pp. 17-33): Springer.
- Roos YH (2010) Glass transition temperature and its relevance in food processing. *Annual Review of Food Science and Technology* 1: 469-96.
- Roos YH (2013) Relaxations, glass transition and engineering properties of food solids *In Advances in food process engineering research and applications*. pp. 79-90. New York: Springer.
- Roos YH, Drusch S (2015) *Phase transitions in foods*, 2nd ed. San Diego: Academic Press, Inc.
- Roos YH, Fryer PJ, Knorr D, Schuchmann HP, Schroën K, Schutyser MAI, Trystram G, Windhab EJ (2016) Food engineering at multiple scales: case studies,

- challenges and the future - a European perspective. *Food Engineering Review* 8(91), 91-115.
- Roos YH, Karel M (1991a) Phase Transitions of Mixtures of Amorphous Polysaccharides and Sugars. *Biotechnology Progress* 7(1): 49-53.
- Roos YH, Karel M (1991b) Water and Molecular Weight Effects on Glass Transitions in Amorphous Carbohydrates and Carbohydrate Solutions. *Journal of Food Science* 56(6): 1676-81.
- Roos YH, Karel M (1991c) Plasticizing Effect of Water on Thermal Behavior and Crystallization of Amorphous Food Models. *Journal of Food Science* 56: 38-56.
- Roos YH, Karel M (1992) Crystallization of amorphous lactose. *Journal of Food Science* 57: 775-77.
- Roos YH, Potes N (2015) Quantification of Protein Hydration, Glass Transitions, and Structural Relaxations of Aqueous Protein and Carbohydrate-Protein Systems. *The Journal of Physical Chemistry B* 119(23): 7077-86.
- Roos YH, Roininen K, Jouppila K, Tuorila H (1998) Glass transition and water plasticization effects on crispness of a snack food extrudate. *International Journal of Food Property* 1: 163-80.
- Roos YH (2012) *Food Materials Science and Engineering: Phase and State Transitions and Related Phenomena in Foods. First Edition*. Edited by Bhesh Bhandari and Yrjö H. Roos. Blackwell Publishing Ltd.
- Roos YH (2016) Strength as a property of food solids. *Formulation and design for food structure and stability*, University College Cork, 16 June.
- Roser B (1991) Trehalose, a new approach to premium dried foods. *Trends in Food Science & Technology* 2, 166-69.
- Roudaut G, Simatos D, Champion D, Contreras-Lopez E, Le Meste M (2004) Molecular mobility around the glass transition temperature: a mini review. *Innovative Food Science & Emerging Technologies* 5(2): 127-34.
- Royall PG, Huang CY, Tang SW, Duncan J, Van-de-Velde G, Brown MB (2005) The development of DMA for the detection of amorphous content in

- pharmaceutical powdered materials. *International Journal of Pharmacy* 301(1-2): 181-91.
- Ruiz-Cabrera MA, Schmidt SJ (2015) Determination of glass transition temperatures during cooling and heating of low-moisture amorphous sugar mixtures. *Journal of Food Engineering* 146, 36-43.
- Saleki-Gerhardt A, Zografi G (1994) Non-isothermal and isothermal crystallization of sucrose from the amorphous state. *Pharmaceutical Research* 11(8), 1166-73.
- Saunders M, Podlun K, Shergill S, Buckton G, Royall P (2004) The potential of high speed DSC (Hyper-DSC) for the detection and quantification of small amounts of amorphous content in predominantly crystalline samples. *International journal of pharmaceutics* 274(1): 35-40.
- Schebor C, Mazzobre MF, del Pilar Buera M (2010) Glass transition and time-dependent crystallization behavior of dehydration bioprotectant sugars. *Carbohydrate Research* 345(2): 303-08.
- Schiraldi C, Di Lernia I, De Rosa M (2002) Trehalose production: exploiting novel approaches. *Trends in Biotechnology* 20(10): 420-25.
- Schmidt SJ, Lee JW (2012) Comparison between water vapor sorption isotherms obtained using the new dynamic dewpoint isotherm method and those obtained using the standard saturated salt slurry method. *International Journal of Food Properties* 15(2): 236-48.
- Schmitt EA, Law D, Zhang GG (1999) Nucleation and crystallization kinetics of hydrated amorphous lactose above the glass transition temperature. *Journal of Pharmaceutical Sciences* 88(3), 291-96.
- Segur JB, Oberstar HE (1951) Viscosity of glycerol and its aqueous solutions. *International Engineering Chemistry* 43(9): 2117-20.
- Shamblin SL Zografi G (1998) Enthalpy Relaxation in Binary Amorphous Mixtures Containing Sucrose. *Pharmaceutical Research* 15(12): 1828-34.
- Shaw NB, Monahan FJ, O'Riordan ED, O'sullivan M (2002) Physical properties of WPI films plasticized with glycerol, xylitol, or sorbitol. *Journal of Food Science* 67(1): 164-67.



- Shawqi Barham A, Kamrul Haque M, Roos YH, Kieran Hodnett B (2006) Crystallization of spray-dried lactose/protein mixtures in humid air. *Journal of Crystal Growth* 295(2): 231-40.
- Shogren RL (1992) Effect of moisture content on the melting and subsequent physical aging of cornstarch. *Carbohydrate Polymers* 19(2): 83-90.
- Silalai N, Hogan S, O'Callaghan D, Roos YH (2009, June) Dielectric relaxations and stickiness of dairy powders influenced by glass transition. In *Proceedings of the 5th International Symposium on Food Rheology and Structure-ISFRS* (pp. 15-18).
- Silalai N, Roos YH (2010) Roles of water and solids composition in the control of glass transition and stickiness of milk powders. *Journal of Food Science* 75(5): 285-96.
- Silalai N, Roos YH (2011a) Coupling of dielectric and mechanical relaxations with glass transition and stickiness of milk solids. *Journal of Food Engineering* 104(3): 445-54.
- Silalai N, Roos YH (2011b) Mechanical alpha-relaxations and stickiness of milk solids/maltodextrin systems around glass transition. *Journal of Science and Food Agriculture* 91(14): 2529-36.
- Sillick M, Gregson CM (2009) Viscous fragility of concentrated maltopolymer/sucrose mixtures. *Carbohydrate Polymers* 78(4): 879-87.
- Sillick M, Gregson CM (2010) Critical water activity of disaccharide/maltodextrin blends. *Carbohydrate Polymers* 79(4): 1028-33.
- Simpson TD, Parrish FW, Nelson ML (1982) Crystalline Forms of Lactose Produced in Acidic Alcoholic Media. *Journal of Food Science* 47: 1948-51.
- Simatos D, Karel M (1988) Characterization of the condition of water in foods-phsico-chemical aspects. In *Food Preservation by Water activity Control* p.1. CC. Seow(Ed.). Elsevier, Amsterdam.
- Sjögren L, Götze W (1994)  $\alpha$ -relaxation spectra in supercooled liquids. *Journal of Non-Crystalline Solids* 172: 7-15.
- Slade L, Levine H (1995) Glass transitions and water-food structure interactions.

*Advances in Food and Nutrition Research* 38(2): 103-79.

- Slade L, Levine H (1995) Water and the glass transition—dependence of the glass transition on composition and chemical structure: special implications for flour functionality in cookie baking. *Journal of Food Engineering* 24(4): 431-509.
- Slade L, Levine H, Reid DS (1991) Beyond water activity: recent advances based on an alternative approach to the assessment of food quality and safety. *Critical Reviews in Food Science & Nutrition*, 30(2-3), 115-360.
- Smythe BM (1967) Sucrose crystal growth. I. Rate of crystal growth in pure solutions. *Australian Journal of Chemistry* 20(6): 1087-95.
- Soderholm S, Roos YH, Meinander N, Steinby K (2000) Temperature dependence of the Raman spectra of amorphous glucose in the glassy and supercooled liquid states. *Journal of Raman Spectroscopy* 31(11): 995-1003.
- Sormoli EM, Das D, Langrish TAG (2013) Crystallization behavior of lactose/sucrose mixtures during water-induced crystallization. *Journal of Food Engineering* 116(4): 873-80.
- Sothornvit R, Krochta JM (2000) Plasticizer effect on oxygen permeability of  $\beta$ -lactoglobulin films. *Journal of Agriculture and Food Chemistry* 48(12): 6298-302.
- Sperling LH (2005) *Introduction to physical polymer science*. John Wiley & Sons.
- Surana R, Abira Pyne A, Suryanarayanan R (2004) Effect of Aging on the Physical Properties of Amorphous Trehalose. *Pharmaceutical Research* 21(5): 867-74.
- Surana R, Pyne A, Rani M, Suryanarayanan R (2005) Measurement of enthalpic relaxation by differential scanning calorimetry-effect of experimental conditions. *Thermochimica Acta* 433(1-2): 173-82.
- Suyatma NE, Tighzert L, Copinet A, Coma V (2005) Effects of hydrophilic plasticizers on mechanical, thermal, and surface properties of chitosan films. *Journal of Agriculture and Food Chemistry* 53(10): 3950-57.
- Talja RA, Roos YH (2001) Phase and state transition effects on dielectric, mechanical, and thermal properties of polyols. *Thermochimica Acta* 380(2): 109-21.

- Tant MR, Wilkes GL (1981) Physical aging studies of semicrystalline poly (ethylene terephthalate). *Journal of Apply Polymer Science* 26(9): 2813-25.
- Tarjus G, Kivelson D (1995) Breakdown of the Stokes–Einstein relation in supercooled liquids. *Journal of Chemical Physics* 103(8): 3071-73.
- Telis VRN, Martínez-Navarrete N (2009) Collapse and color changes in grapefruit juice powder as affected by water activity, glass transition, and addition of carbohydrate polymers. *Food Biophysics* 4(2): 83-93.
- Timmermann EO, Chirife J, Iglesias HA (2001) Water sorption isotherms of foods and foodstuffs BET or GAB parameters. *Journal of Food Engineering* 48, 19-31.
- To EC, Flink JM (1978) Collapse, a structural transition in freeze dried carbohydrates. *International Journal of Food Science & Technology* 13(6): 567-81.
- Torres DPM, Bastos M, Gonçalves MDPF, Teixeira JA, Rodrigues LR (2011) Water sorption and plasticization of an amorphous galacto-oligosaccharide mixture. *Carbohydrate Polymers* 83(2): 831-35.
- Truong V, Bhandari BR, Howes T, Adhikari B (2002) Analytical model for the prediction of glass transition temperature of food systems. In *Amorphous Food and Pharmaceutical Systems*. The Royal Society of Chemistry, Cambridge.
- Turner NJ, Whyte R, Hudson JA, Kaltovei SL (2006) Presence and growth of *Bacillus cereus* in dehydrated potato flakes and hot-held, ready-to-eat potato products purchased in New Zealand. *Journal of Food Protection* 69(5), 1173-77.
- Urbani R, Sussich F, Prejac S, Casaro A (1997) Enthalpy relaxation and glass transition behaviour of sucrose by static and dynamic DSC. *Thermochimica Acts* 304, 359-67.
- Uritani M, Takai M, Yoshinaga K (1995) Protective effect of disaccharides on restriction endonucleases during drying under vacuum. *Journal of Biochemistry* 117(4): 774-79.
- Van Hook A (1961) *Crystallization: Theory and practice* (No. 152). Reinhold Pub.

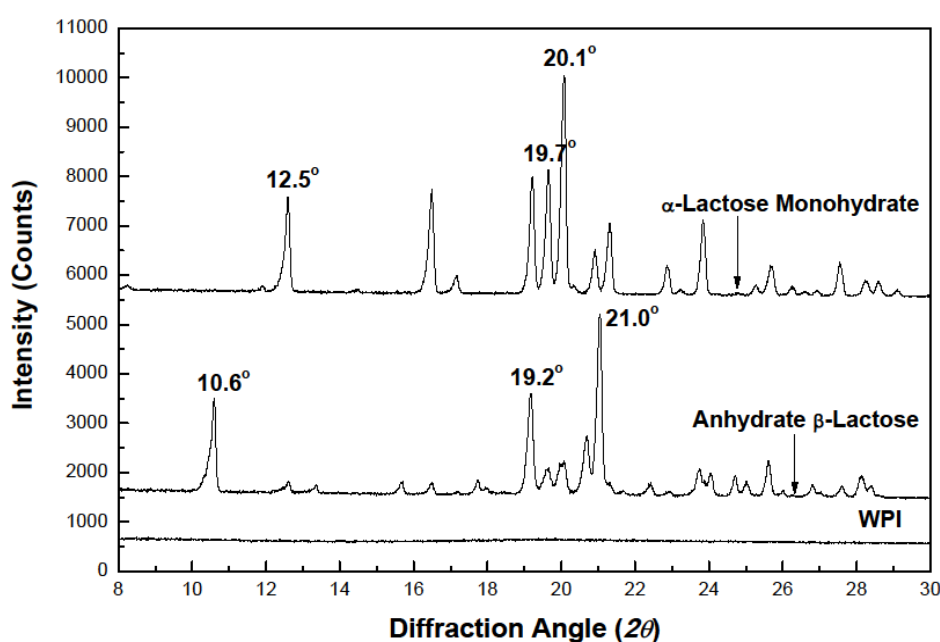
Corp.

- Velikov V, Borick S, Angell CA (2001) The glass transition of water, based on hyperquenching experiments. *Science* 294(5550): 2335-38.
- Verhoeven N, Neoh TL, Furuta T, Yoshii H (2017) Crystallization. In *Engineering Foods for Bioactives Stability and Delivery* (pp. 225-46). Springer New York.
- Wang N, Brennan JG (1995) A mathematical model of simultaneous heat and moisture transfer during drying of potato. *Journal of Food Engineering* 24(1): 47-60.
- Wang S, Langrish T, Leszczynski M (2010) The Effect of Casein as a Spray-Drying Additive on the Sorption and Crystallization Behavior of Lactose. *Drying Technology* 28(3): 422-29.
- Wang W (2005) Protein aggregation and its inhibition in biopharmaceutics. *International Journal of Pharmacy* 289(1-2), 1-30.
- Wang Y, Truong T (2016) Glass transition and crystallization in foods. In *Non-Equilibrium States and Glass Transitions in Foods* pp: 135-68.
- White GW, Cakebread SH (1966) The glassy state in certain sugar-containing food products. *International Journal of Food Science & Technology* 1(1): 73-82.
- Williams ML, Landel RF, Ferry JD (1955) The temperature dependence of relaxation mechanisms in amorphous polymers and other glass-forming liquids. *Journal of the American Chemical Society* 77(14): 3701-07.
- Wunderlich B (2005) *Thermal analysis of polymeric materials*. Springer Science & Business Media.
- Wungtanagorn R, Schmidt SJ (2001a) Phenomenological study of enthalpy relaxation of amorphous glucose, fructose, and their mixture. *Thermochimica Acta* 369(1-2), 95-116.
- Wungtanagorn R, Schmidt SJ (2001b) Thermodynamic properties and kinetics of the physical aging of amorphous glucose, fructose and their mixture. *Journal of Thermal Analysis and Calorimetry* 65, 9-35.
- Yao W, Yu X, Lee JW, Yuan X, Schmidt SJ (2011) Measuring the deliquescence point of crystalline sucrose as a function of temperature using a new automatic

- isotherm generator. *International Journal of Food Properties* 14(4): 882-93.
- Yoshida H (1995) Relationship between enthalpy relaxation and dynamic mechanical relaxation of engineering plastics. *Thermochimica Acta* 266, 119-27.
- You Y, Ludescher RD (2010) The effect of molecular size on molecular mobility in amorphous oligosaccharides. *Food biophysics* 5(2): 82-93.
- Yu KQ, Li ZS, Sun J (2001) Polymer structures and glass transition: A molecular dynamics simulation study. *Macromolecular Theory and Simulations* 10(6): 624-33.
- Yu L (2001) Amorphous pharmaceutical solids: preparation, characterization and stabilization. *Advanced Drug Delivery Reviews* 48, 27-42.
- Yuan X, Carter BP, Schmidt SJ (2011) Determining the critical relative humidity at which the glassy to rubbery transition occurs in polydextrose using an automatic water vapor sorption instrument. *Journal of Food Science* 76(1): 78-89.
- Zhou P, Labuza TP (2007) Effect of water content on glass transition and protein aggregation of whey protein powders during short-term storage. *Food Biophysics* 2(2-3), 108-16.
- Zimeri JE, Kokini JL (2002) The effect of moisture content on the crystallinity and glass transition temperature of inulin. *Carbohydrate Polymers* 48(3): 299-304.

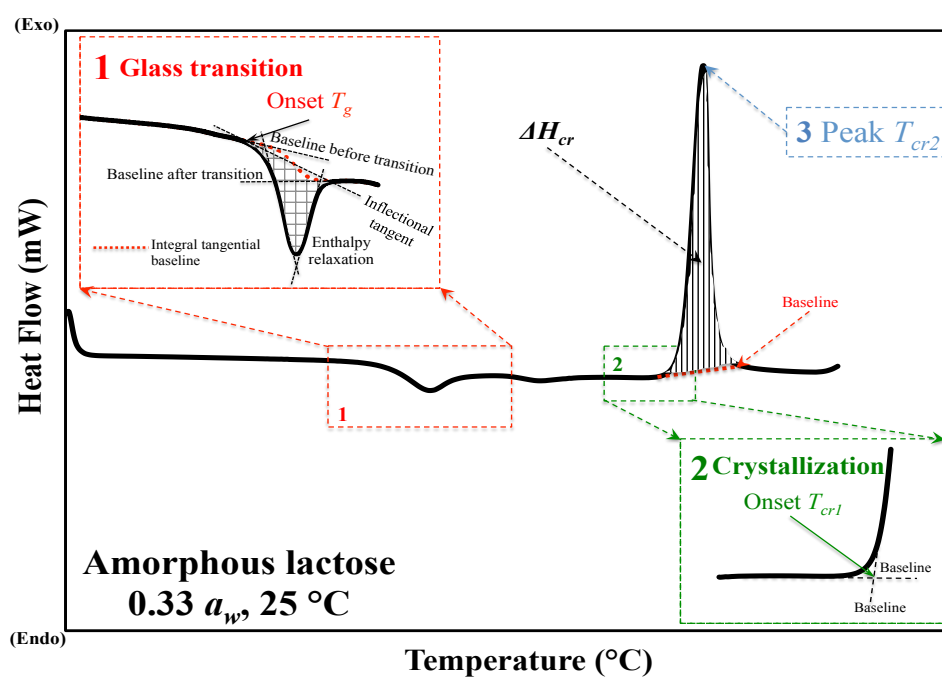
# APPENDIX I

---



Typical XRD Patterns for WPI,  $\alpha$ -Lactose Monohydrate (20.1°), Anhydrous  $\beta$ -Lactose (10.6° and 21.0°) and Anhydrous  $\alpha$ - and  $\beta$ -Lactose Mixture with The Ratios of 5:3 (19.2°) and 4:1 (19.7°) based on Previous References (Jouppila et al., 1997; Haque and Roos, 2005).

## APPENDIX II



DSC thermograms show the onset glass transition temperature ( $T_g$ ), onset ( $T_{cr1}$ ) and peak ( $T_{cr2}$ ) temperature of crystallization for freeze-dried amorphous lactose after storage at 0.33  $a_w$  at 25 °C.

# APPENDIX III

---

## Codes in R Programme

```
#Load in data file
x=data[,2];y=data[,3] #x: water activity, y: water
content
min=range(x)[1];max=range(x)[2]

df1=data.frame(x,y) #set data frame
lw = loess(y ~ x, data=df1,span=11/length(x)) #LOESS
smoothing with a span of 11 points
yy=lw$fitted

sy=spline(x,yy,n=(max-min)*100)$y #smoothing spline
sx=spline(x,yy,n=(max-min)*100)$x #smoothing spline

f=splinefun(sx,sy)
d1=f(sx,deriv = 1) #first derivative

df2=data.frame(sx,d1) #Using the data from the first
derivative as the new dataset
lw = loess(d1 ~ sx, data=df2,span=11/length(sx)) #LOESS
smoothing again
y2=lw$fitted

max=sx[d1==max(d1)]; min=0.1 #Select the targeted region
sxx=sx[sx>=min&sx<=max];yy2=y2[sx>=min&sx<=max]

f=splinefun(sxx,yy2)
d11=f(spline(sxx,yy2,n=round((max-min)*1000))$x,deriv
= 1) #The first derivative is again taken, evaluated at
every 0.001 unit, resulting in the second derivative.

#END
```



# APPENDIX IV

---

## LIST OF PUBLICATIONS

- Fan F, Roos YH (2017) Glass transition, structural relaxations, and structural strength of freeze-dried glucose/fructose mixtures and honey powder. *Manuscript*.
- Fan F, Roos YH (2017) Water sorption, mechanical/dielectric properties, and strength analysis of relaxation times on amorphous food polymers, *Manuscript*.
- Fan F, Roos YH (2017) Structural relaxations, relaxation times and its relevant applications on amorphous food solids: a review. *Food Engineering Reviews*, DOI: 10.1007/s12393-017-9166-6. *In press*.
- Fan F, Mou T, Nurhadi B, Roos YH (2017). Water sorption-induced crystallization, structural relaxations and strength analysis of relaxation times in amorphous lactose/whey protein systems, *Journal of Food Engineering*, 196: 150-58.
- Fan F, Roos YH (2017) Structural strength and crystallization of amorphous lactose in food model solids at various water activities”, *Innovative Food Science & Emerging Technology*, 40: 27-34.
- Fan F, Roos YH (2017) Crystallization and structural relaxation times in structural strength analysis of amorphous sugar/whey protein systems, *Food Hydrocolloids*, 60: 85-97.
- Fan F, Roos YH (2017) Structural relaxations of amorphous lactose and lactose-whey protein mixtures. *Journal of Food Engineering*, 173: 106-15.
- Fan F, Roos YH (2017) X-ray diffraction analysis of lactose crystallization in freeze-dried lactose– whey protein systems. *Food Research International*, 67: 1-11.

## LIST OF CONFERENCES

## Conference paper

Fan F, Roos YH (2017) Structural strength and crystallization in amorphous food models at low water activities. *29th The European Federation of Food Science & Technology (EFFoST) International Conference*, Athens, Greece.

## Oral and poster presentation

Fan, F. Structural Relaxation Times in Food Structural Engineering. [ePoster]. *IFT17, Las Vegas*, 25-28 June 2017

Fan, F. Innovative Uses of Relaxation Times in Formulation and Design for Amorphous Food Solids Structure and Stability. [Oral]. *EFFoST 11th PhD-Work Shop*, Singen, Germany, 28-29 April 2017

Roos YH, Fan F, Nurhadi B. Food Stability Analysis Using Dynamic Dewpoint Isotherms. [Oral, Webinar]. *METER FOOD Webinar – Simplify Your Approach to Product Stability Analysis in Powders*, 12 February 2017.

Fan, F. Food structure engineering and its relevant applications of food solids. [Oral]. *International Forum for Academic and Elites*, Guangzhou, P. R. China, 18-20 December 2016.

Fan F, Roos YH Structural Relaxations, Strength Analysis and Crystallization of Amorphous Lactose/PolyvinylPyrrolidone Mixtures. [Poster]. *Conference of Food Engineering (COFE)*, Columbus, Ohio State University, USA, 12-14 September 2016.

Fan F, Roos YH Water-Induced Relaxation in Amorphous Food Solids: Water Sorption Isotherms, Crystallization and Structural Strength. [Oral]. *International Symposium On the Properties Of Water (ISOPOW XIII)*, Lausanne, Switzerland, 26-29 June 2016.

Fan F, Roos YH Strength and lactose crystallinity. [Oral]. *Formulation and Design for Food Structure and Stability*, Cork, Ireland, 24 June 2016

Fan F, Roos YH Structural Strength and Crystallization in Amorphous Food Models at Low Water Activities. [Oral]. *29th The European Federation of Food Science & Technology (EFFoST) International Conference*, Athens, Greece, 10-12 November 2015.

Fan F, Roos YH X-Ray diffraction and dynamic-mechanical analysis of freeze-dried lactose/trehalose-whey protein systems. [Poster]. *12th International Congress on Engineering and Food*, Quebec City, Canada, 14-18 June 2015.